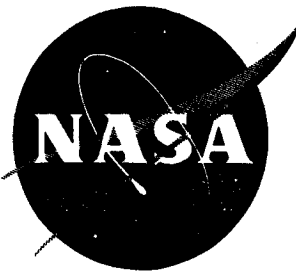


REF ID: A6512687
DE CONFIDENTIAL

NASA TM X-38



GROUP 4
Downgraded at 3 year
intervals; declassified
after 12 years

TECHNICAL MEMORANDUM X - 38 CASE FILE COPY

INVESTIGATION OF THE AERODYNAMIC CHARACTERISTICS OF A

0.067-SCALE MODEL OF THE X-15 AIRPLANE

(CONFIGURATION 3) AT MACH NUMBERS

OF 2.29, 2.98, AND 4.65

By Arthur E. Franklin and Robert M. Lust

Langley Research Center
Langley Field, Va.

DECLASSIFIED - EFFECTIVE 1-15-64
Authority: Memo Geo. Drska 1004 HQ.
Code ATSS-A Dtd. 3-12-64 Subj. Change
in Security Classification Marking

NASA TM X-38

N 65 12687

(THRU)	(CODE)	(CATEGORY)
/	01	
(ACCESSION NUMBER)	(PAGES)	(NASA CR OR TMX OR AD NUMBER)
110		

FACILITY FORM 602

NATIONAL AERONAUTICS AND SPACE ADMINISTRATION
WASHINGTON

November 1959

Hard copy (HC) E5.12

Microfiche (MF) A1.12

DECLASSIFIED

~~CONFIDENTIAL~~

NATIONAL AERONAUTICS AND SPACE ADMINISTRATION

TECHNICAL MEMORANDUM X-38

INVESTIGATION OF THE AERODYNAMIC CHARACTERISTICS OF A
0.067-SCALE MODEL OF THE X-15 AIRPLANE
(CONFIGURATION 3) AT MACH NUMBERS
OF 2.29, 2.98, AND 4.65*

By Arthur E. Franklin and Robert M. Lust

SUMMARY

12687

An investigation was made in the Langley Unitary Plan wind tunnel to determine the drag and the static longitudinal and lateral stability characteristics of a 0.067-scale model of the X-15 airplane (configuration 3). The investigation was made at Mach numbers of 2.29, 2.98, and 4.65. The effect of Reynolds number is shown by results taken at Reynolds numbers of about 0.5×10^6 , 1.85×10^6 , 2.28×10^6 , 3.24×10^6 , 4.0×10^6 , and 4.43×10^6 .

An earlier configuration of this model was investigated in the Langley Unitary Plan wind tunnel in the same range of Mach numbers with results given in NASA Memorandum 4-27-59L.

INTRODUCTION

Arthur

The development of the X-15 research airplane is a coordinated effort between the United States Air Force, the United States Navy, and the National Aeronautics and Space Administration. As part of the development program, the present investigation was made to determine the aerodynamic characteristics of a 0.067-scale model of the X-15 airplane configuration (configuration 3) in the Langley Unitary Plan wind tunnel. A model of an earlier configuration of this model has also been investigated in the Langley Unitary Plan wind tunnel and the results of that investigation are presented in reference 1.

*Title, Unclassified.

DECLASSIFIED - EFFECTIVE 1-15-64
Authority: Memo Geo. Drobka NASA HQ.
Code ATSS-A Dtd. 3-12-64 Subj: Change
in Security Classification Marking.

031912201030

~~CONFIDENTIAL~~

The present configuration differed from the earlier configuration in the distribution of vertical stabilizing surface area, a change in airfoil section of the vertical surfaces, speed-brake area, and the location of the vertical-control-surface hinge line. In addition, the fuselage nose and side fairing were modified from the configuration of reference 1 by decreasing the nose fineness ratio and reducing the length of the fuselage side fairings. The canopy was modified by changing its shape and its location with respect to the nose of the fuselage.

In addition to results obtained in the previous investigation in the Langley Unitary Plan wind tunnel, results obtained at subsonic speeds are presented in reference 2. The results of the present investigation are presented herein without analysis and are supplemented with summaries of the aerodynamic parameters.

SYMBOLS

The longitudinal stability characteristics of the model are referred to the stability system of axes, and the lateral stability characteristics of the model are referred to the body system of axes. The systems of axes used and the positive directions of the forces, moments, and angles are shown in figure 1. The moments of the model are presented about a point located at the 0.16-chord point of the mean aerodynamic chord and on the fuselage reference line (chord plane of the wing mean aerodynamic chord). The symbols used in this paper are defined as follows:

- b span, in.
c chord, in.
 \bar{c} mean aerodynamic chord, in.
 \bar{c}_H mean aerodynamic chord of horizontal tail, in.
 \bar{c}_V mean aerodynamic chord of vertical tail, in.
 C_D drag coefficient, Drag/qS
 $C_{D,b}$ base drag coefficient, Base drag/qS
 C_L lift coefficient, Lift/qS

~~CONFIDENTIAL~~

DECLASSIFIED

~~CONFIDENTIAL~~

3

L 3 5 1	C_m	pitching-moment coefficient, $\frac{\text{Pitching moment}}{qS\bar{c}}$
	C_l	rolling-moment coefficient, $\frac{\text{Rolling moment}}{qSb}$
	C_n	yawing-moment coefficient, $\frac{\text{Yawing moment}}{qSb}$
	C_Y	side-force coefficient, $\frac{\text{Side force}}{qS}$
	$C_{L\alpha}$	lift-curve slope ($\alpha \approx 0^\circ$), $\partial C_L / \partial \alpha$
	$C_m C_L$	pitching-moment-curve slope (C_L at $\alpha \approx 0^\circ$), $\partial C_m / \partial C_L$
	$C_{m_{it}}$	stabilizer effectiveness parameter ($i_t \approx 0^\circ$), $\partial C_m / \partial i_t$
	$C_{l\beta}$	effective dihedral parameter ($\beta \approx 0^\circ$), $\partial C_l / \partial \beta$
	$C_{n\beta}$	directional stability parameter ($\beta \approx 0^\circ$), $\partial C_n / \partial \beta$
	$C_{Y\beta}$	side-force parameter ($\beta \approx 0^\circ$), $\partial C_Y / \partial \beta$
	$C_{l\delta_r}$	roll-control effectiveness parameter ($\delta_r \approx 0^\circ$), $\partial C_l / \partial \delta_r$
	$C_{l\delta_v}$	rolling-moment parameter due to yaw-control deflection ($\delta_v \approx 0^\circ$), $\partial C_l / \partial \delta_v$
	$C_{n\delta_r}$	yawing-moment parameter due to roll-control deflection ($\delta_r \approx 0^\circ$), $\partial C_n / \partial \delta_r$
	$C_{n\delta_v}$	yaw-control effectiveness parameter ($\delta_v \approx 0^\circ$), $\partial C_n / \partial \delta_v$
	$C_{D,\min}$	minimum drag coefficient
	$\frac{\Delta C_D}{C_L^2}$	drag-due-to-lift factor, $\frac{C_D - C_{D,\min}}{C_L^2}$

CONFIDENTIAL

$(L/D)_{\max}$ maximum lift-drag ratio

M free-stream Mach number

q free-stream dynamic pressure, lb/sq ft

R Reynolds number

S wing area (includes body intercept), sq ft

X, Y, Z longitudinal, lateral, and vertical body axes, respectively

X_s, Y_s, Z_s longitudinal, lateral, and vertical stability axes,
respectively

α angle of attack referred to fuselage reference line, deg

β angle of sideslip referred to model plane of symmetry, deg

δ deflection of control surface, deg

δ_v yaw-control angle, positive as shown in figure 1(c) and
movable for that portion of tail panel as shown in figure 5,
deg

δ_r roll-control angle, positive when trailing edge of δ_{H_R} is
down with respect to trailing edge of δ_{H_L} , $\delta_{H_R} - \delta_{H_L}$, deg

i_t pitch-control angle, positive as shown in figure 1(c),

$$\frac{\delta_{H_R} + \delta_{H_L}}{2}$$
, deg

δ_s speed-brake deflection, deg

Subscripts:

H horizontal tail

L left

R right

0 value taken at zero lift coefficient

V vertical tail

min minimum

L
3
5
1

DECLASSIFIED

~~CONFIDENTIAL~~

5

Configuration component designations:

W wing
F fuselage
H horizontal tail
V vertical tail
L ventral fin
3
5
1
S speed brakes open 35° with respect to closed position

APPARATUS AND MODELS

The tests were conducted in the high Mach number test section of the Langley Unitary Plan wind tunnel. This tunnel is a variable-pressure, continuous, return-flow type. The test section is 4 feet square and approximately 7 feet in length. The nozzle leading to the test section is of the asymmetric sliding-block type. Mach numbers may be varied continuously through a Mach number range from approximately 2.29 to 4.65 without tunnel shutdown.

Photographs of the model are presented in figure 2. Details of the test model and model components are shown in figures 3, 4, and 5. Geometric characteristics are given in table I.

The basic model has a wing with 25.6° sweepback of the quarter chord, an aspect ratio of 2.5, a taper ratio of 0.20, 0° dihedral, and a modified NACA 66-005 airfoil section. Trim in roll, sideslip, and pitch is obtained by deflection of the all-moving stabilizing surfaces (horizontal tail, vertical tail, and ventral fin). The vertical tail and ventral fin consisted of a fixed stub with an all-movable tip forming an unbroken vertical-tail and ventral-fin plan form. The horizontal tail, shown in figure 4, has a 45° sweepback of the quarter chord, a panel aspect ratio of 2.833, a taper ratio of 0.21, a dihedral of -15.0° , and a modified NACA 66-005 airfoil section. The vertical tail shown in figure 5(a) has a sweepback of 23.4° at the quarter chord, a panel aspect ratio of 0.516, a taper ratio of 0.741, and a full wedge of 10.0° as an airfoil section. The ventral fin, shown in figure 5(b), has a sweepback of 23.4° at the quarter chord, a panel aspect ratio of 0.429, a taper ratio of 0.783, and a full wedge of 10.0° as an airfoil section.

03181220.1030

~~CONFIDENTIAL~~

The speed brakes shown in figure 5 are formed by wedges which simulate hinged panels of the rear wedge surfaces of both the vertical-tail and ventral-fin surfaces. The speed brake extended vertically the complete width of the fixed stub of the vertical tail and horizontally from the speed-brake hinge line to the trailing edges of the tail surfaces. The speed brakes open 35° relative to their closed position.

Forces and moments for the complete model were measured by means of a six-component, electrical strain-gage balance. This balance was attached, by means of a sting, to the tunnel central support system.

An additional component of the model system was a remotely operated adjustable coupling with which tests can be performed at variable side-slip angles concurrently with variable angles of attack. This coupling was placed between the model sting and the tunnel central support system.

Vertical tail, ventral fin, and both horizontal-tail panels were independently and remotely actuated. Position indication of the control-surface angles on all surfaces was accomplished by a differential transformer attached to the control-surface linkage.

TESTS

Tests were made through an angle-of-attack range from approximately -10° to 20° at angles of sideslip of about 0° and $\pm 60^{\circ}$. Tests were also made through an angle-of-sideslip range from approximately -6° to 10° at angles of attack of about 0° , 8° , and 16° . All basic model tests were made with a stabilizer deflection of 0° .

The test conditions of Mach number, stagnation and dynamic pressure, and Reynolds number are listed in the following table:

M	Stagnation pressure, lb/sq in. abs	Dynamic pressure, lb/sq ft	Reynolds number
2.29	3.92	168	0.51×10^6
	14.42	619	1.87
	25.00	1,074	3.24
2.98	5.58	140	0.50×10^6
	20.69	520	1.87
	45.03	1,131	4.06
4.65	61.51	385	2.28×10^6
	119.38	747	4.43

~~CONFIDENTIAL~~

DECLASSIFIED

~~CONFIDENTIAL~~

7

The Reynolds numbers are based on the mean aerodynamic chord of the wing. The dewpoint temperature for all tests was maintained below -30° F to prevent adverse condensation effects. The stagnation temperature was maintained at 150° F for all Mach numbers except 4.65 where it was 175° F.

CORRECTIONS AND ACCURACY

The calibration of the flow has shown that there is a small upflow in the test section. The results presented herein have been corrected for this flow misalignment. The maximum deviation of local Mach number in the portion of the tunnel occupied by the model was ± 0.015 from the average values listed in the preceding section.

The angles of attack and sideslip of the model have been corrected for the deflection of the model sting and balance under load. The control-surface angles were maintained at the desired deflections during the test by monitoring the calibrated control-surface position indicators. Pretest calibration of the control-surface systems, however, revealed a certain amount of mechanical slop. The slop leads to the angular uncertainty of the control-surface deflections which are the values quoted in the table of accuracy presented at the end of this section.

Pressure measurements were made at the base of the fuselage over the angle-of-attack range and Mach number range investigated. The base pressure has been used to adjust the level of drag coefficients presented herein to a condition of free-stream static pressure at the base of the fuselage. The base drag coefficients used to make the adjustments are shown in figure 6.

The estimated accuracy of the force and moment coefficients and angles based on calibration and repeatability of the data is as follows:

C_L	± 0.0020
C_D	± 0.0020
C_m	± 0.0010
C_l	± 0.0002
C_n	± 0.0005
C_Y	± 0.0015
$^1 \alpha$, deg	± 0.100
β , deg	± 0.100
δ_{HL} and δ_{HR} , deg	± 0.100
δ_v , deg	± 0.100

¹The values quoted for accuracy of α include the effect of test-section flow angularity.

~~CONFIDENTIAL~~

0317122A1030

8

~~CONFIDENTIAL~~

PRESENTATION OF RESULTS

The results of an investigation of the aerodynamic characteristics of an 0.067-scale model of the X-15 airplane (configuration 3) are presented in figures that are organized as follows:

	Figures
Schlieren photographs of model	7 to 8
Longitudinal stability characteristics:	
Effect of various model components	9
Effect of Reynolds number	10 to 12
Effect of various pitch-control deflections of horizontal-tail panels	13 to 16
Effect of various roll-control deflections	17, 18
Summary of longitudinal stability characteristics	19, 20
Lateral stability characteristics:	
Effect of various model components	21 to 26
Effect of Reynolds number	27 to 30
Effect of various deflections of vertical tail	31 to 36
Effect of various roll-control deflections of horizontal-tail panels	37, 38
Effect of angles of sideslip on various configurations	39
Summary of lateral stability characteristics:	
Effect of various model components	40
Effect of Reynolds number	41, 42
Summary of effectiveness of lateral and directional control devices:	
Effect of horizontal-tail deflections on $C_l_{\delta_r}$ and $C_n_{\delta_r}$	43
Effect of vertical-tail deflection	44, 45
Effect of speed brakes	46, 47

Langley Research Center,
 National Aeronautics and Space Administration,
 Langley Field, Va., May 4, 1959.

~~CONFIDENTIAL~~

DECLASSIFIED

~~CONFIDENTIAL~~

9

REFERENCES

1. Franklin, Arthur E., and Silvers, H. Norman: Investigation of the Aerodynamic Characteristics of a 0.067-Scale Model of the X-15 Airplane (Configuration 2) at Mach Numbers of 2.29, 2.98, 3.96, and 4.65. NASA MEMO 4-27-59L, 1959.
2. Boisseau, Peter C.: Investigation of the Low-Speed Stability and Control Characteristics of a 1/7-Scale Model of the North American X-15 Airplane. NACA RM L57D09, 1957.

L
3
5
1

031912301030

~~CONFIDENTIAL~~

TABLE I.- GEOMETRIC CHARACTERISTICS OF THE 0.067-SCALE MODEL OF THE X-15 AIRPLANE (CONFIGURATION 3)

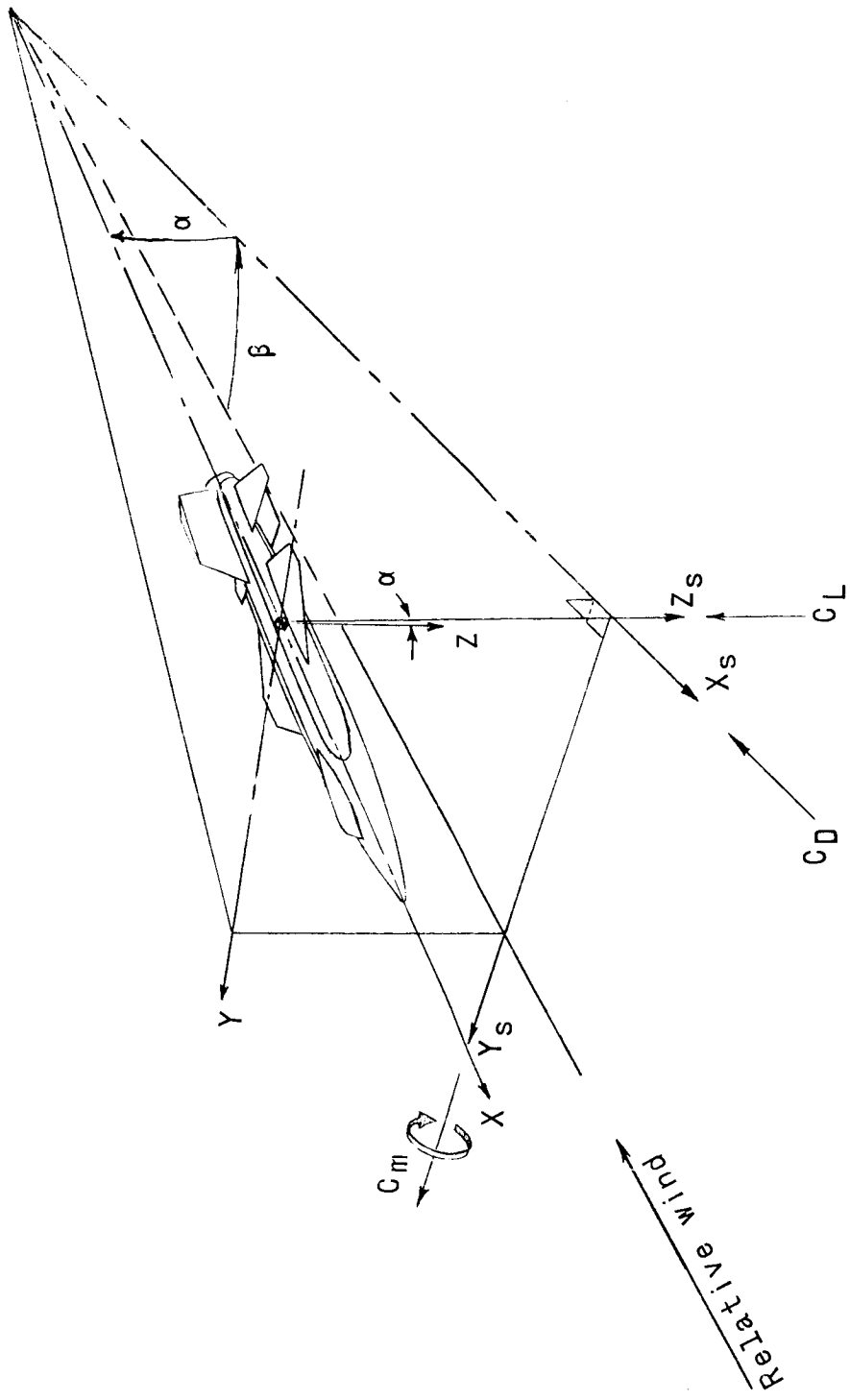
	Total ^a	Exposed ^b
Wing:		
Area, sq ft	0.387	0.364
Span, in.	1,487	11.91
Aspect ratio	3.50	2.19
Taper ratio	0.20	0.21
Sweepback of quarter-chord line, deg	25.63	
Dihedral, deg	0	
Incidence, deg	0	
Geometric twist, deg	0	
Airfoil section:		
Root	NACA 66-005 (modified)	
Tip	NACA 66-005 (modified)	
Root-chord length, in.	11.91	3.77
Tip-chord length, in.	1.35	0.57
Mean aerodynamic chord:		
length, in.	8.21	6.15
Distance from root chord, in.	3.43	2.42
Fuselage:		
Length, in.	39.34	
Width (including side fairing), in.	5.87	
Depth, in.	3.73	
Frontal area, sq in.	10.95	
Overall fineness ratio	10.54	
Side area, sq in.	134.50	
Base area, sq in.	1.01	
Base fairing area, sq in.	2.16	
Horizontal tail:		
Area, sq ft	0.493	0.27 ^c
Span, in.	14.41	9.00
Aspect ratio	2.93	1.41
Taper ratio	0.21	0.30
Mean aerodynamic chord:		
length, in.	5.64	3.99
Distance from root chord, in.	2.93	1.79
Sweepback of quarter-chord line, deg	45.00	
Dihedral, deg	-15.00	
Geometric twist, deg	0	
Incidence, deg	0	
Airfoil section:		
Root	NACA 66-005 (modified)	
Tip	NACA 66-005 (modified)	
Root-chord length, in.	5.18	3.59
Tip-chord length, in.	1.69	1.69
Vertical tail:		
Area, sq ft	0.294	0.181
Span, in.	5.34	3.67
Aspect ratio	0.70	0.51
Taper ratio	0.66	0.74
Airfoil section:		
Root	Full wedge of 10°	
Tip	Full wedge of 10°	
Root-chord length, in.	9.25	5.11
Tip-chord length, in.	6.05	6.05
Ventral fin:		
Area, sq ft	0.269	0.152
Span, in.	4.94	3.07
Aspect ratio	0.65	0.42
Taper ratio	0.69	0.78
Airfoil section:		
Root	Full wedge of 10°	
Tip	Full wedge of 10°	
Root-chord length, in.	9.25	5.11
Tip-chord length, in.	6.40	6.40
Speed brakes:		
Area, sq ft	0.034	

^aSpan and area include fuselage intercept.^bSpan and area do not include fuselage intercept and are based on total exposed surface.~~CONFIDENTIAL~~

DECLASSIFIED

~~CONFIDENTIAL~~

11



(a) Stability axes.

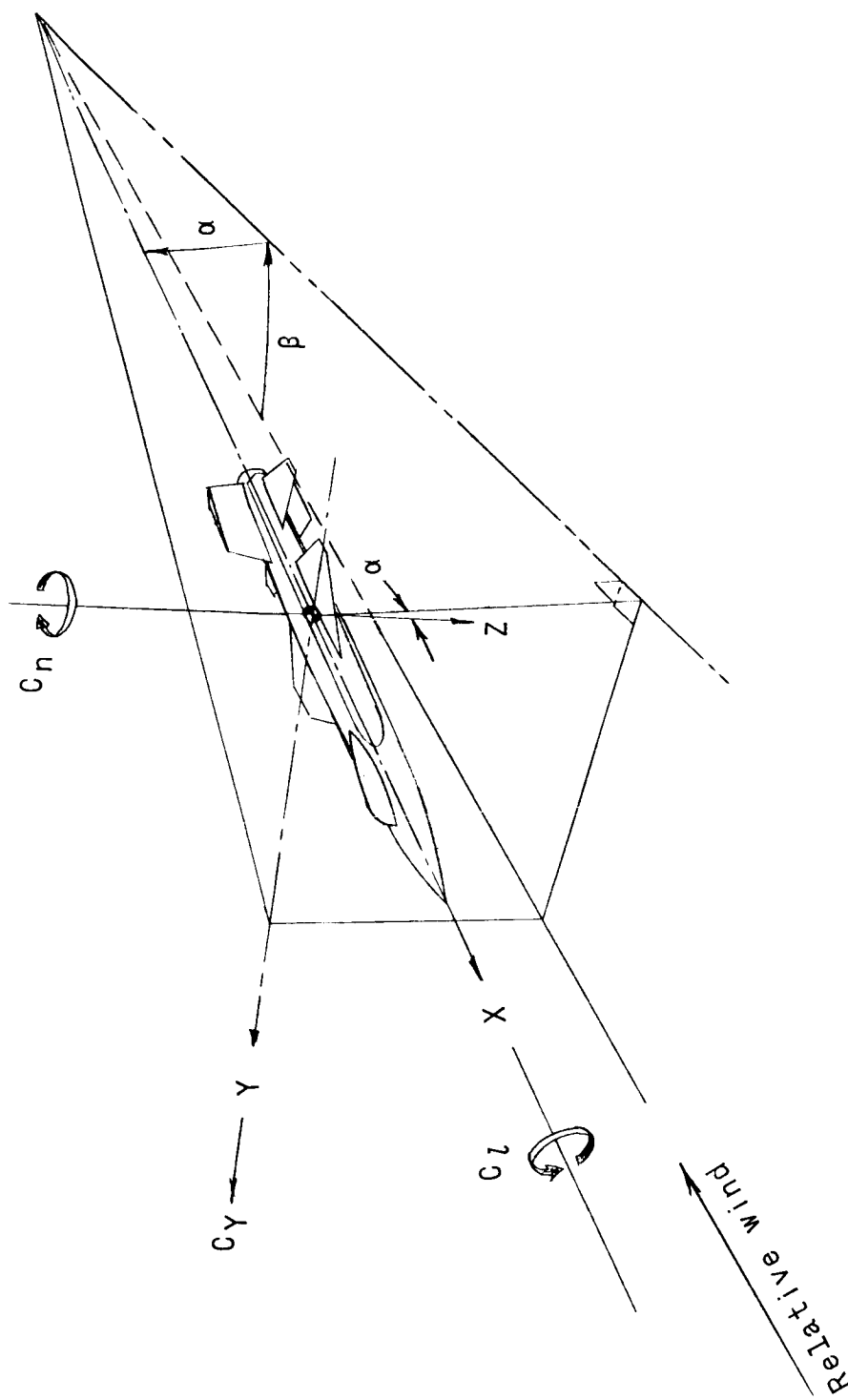
Figure 1.- Axes systems. Positive values of forces, moments, and angles are indicated by arrows.

~~CONFIDENTIAL~~

0319122A1030

~~CONFIDENTIAL~~

12



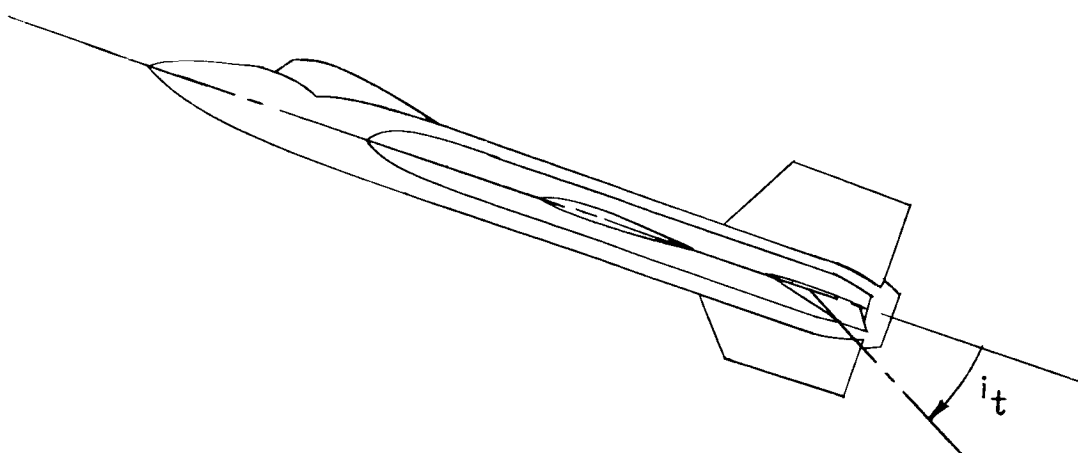
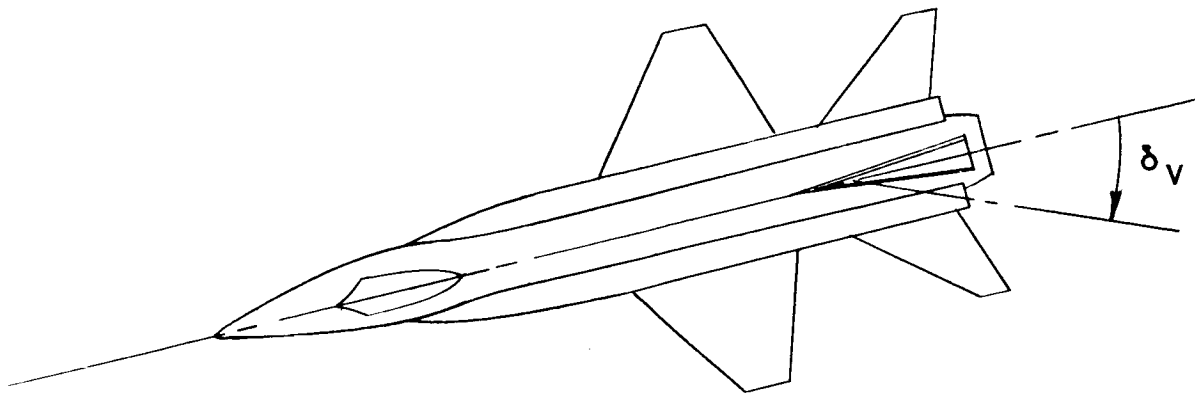
(b) Body axes.

Figure 1.- Continued.

~~DECLASSIFIED~~

~~CONFIDENTIAL~~

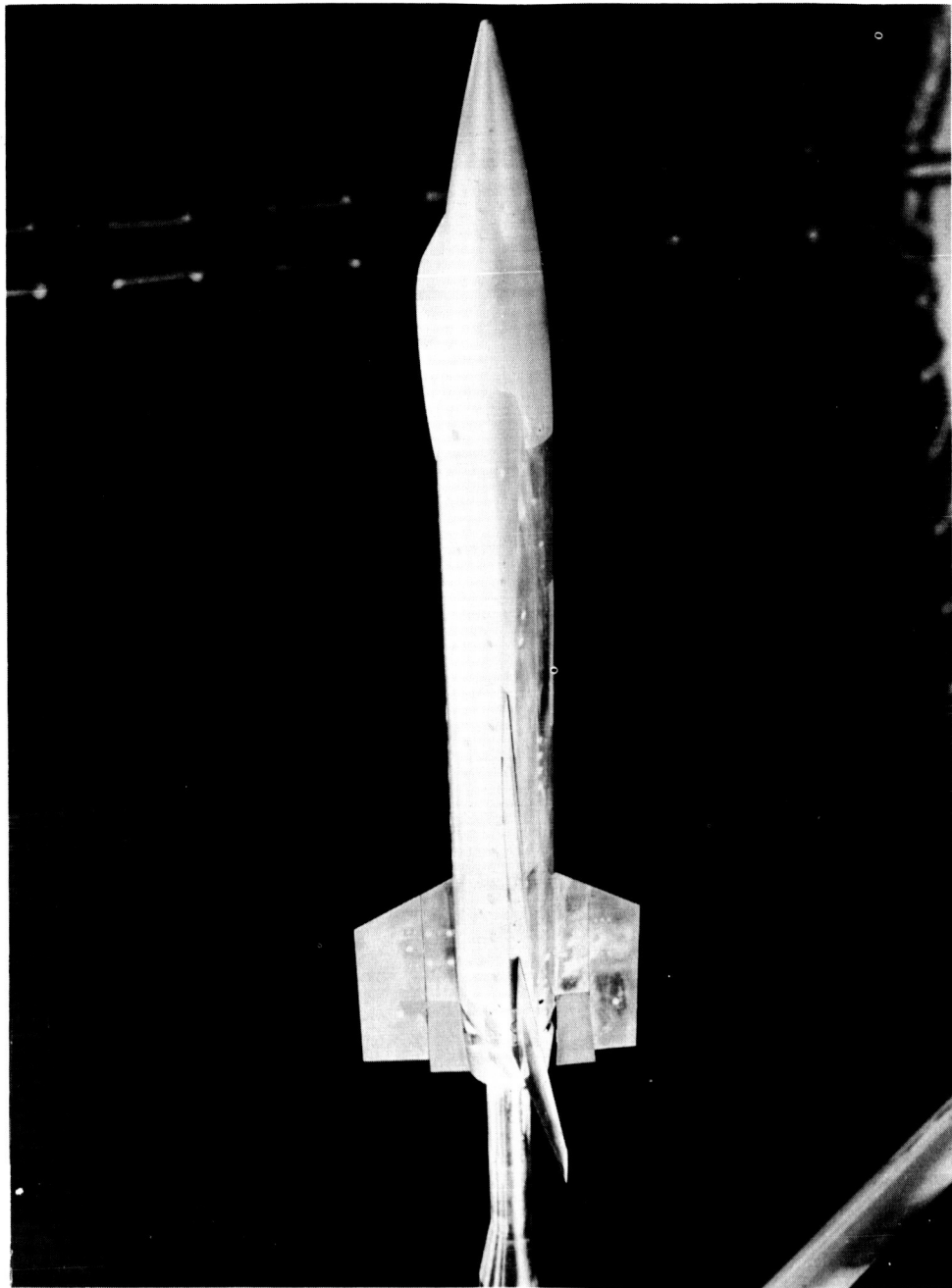
13



(c) Control-surface deflections. $i_t = \frac{\delta_{H_R} + \delta_{H_L}}{2}$

Figure 1.- Concluded.

031312301030



(e) Side view.

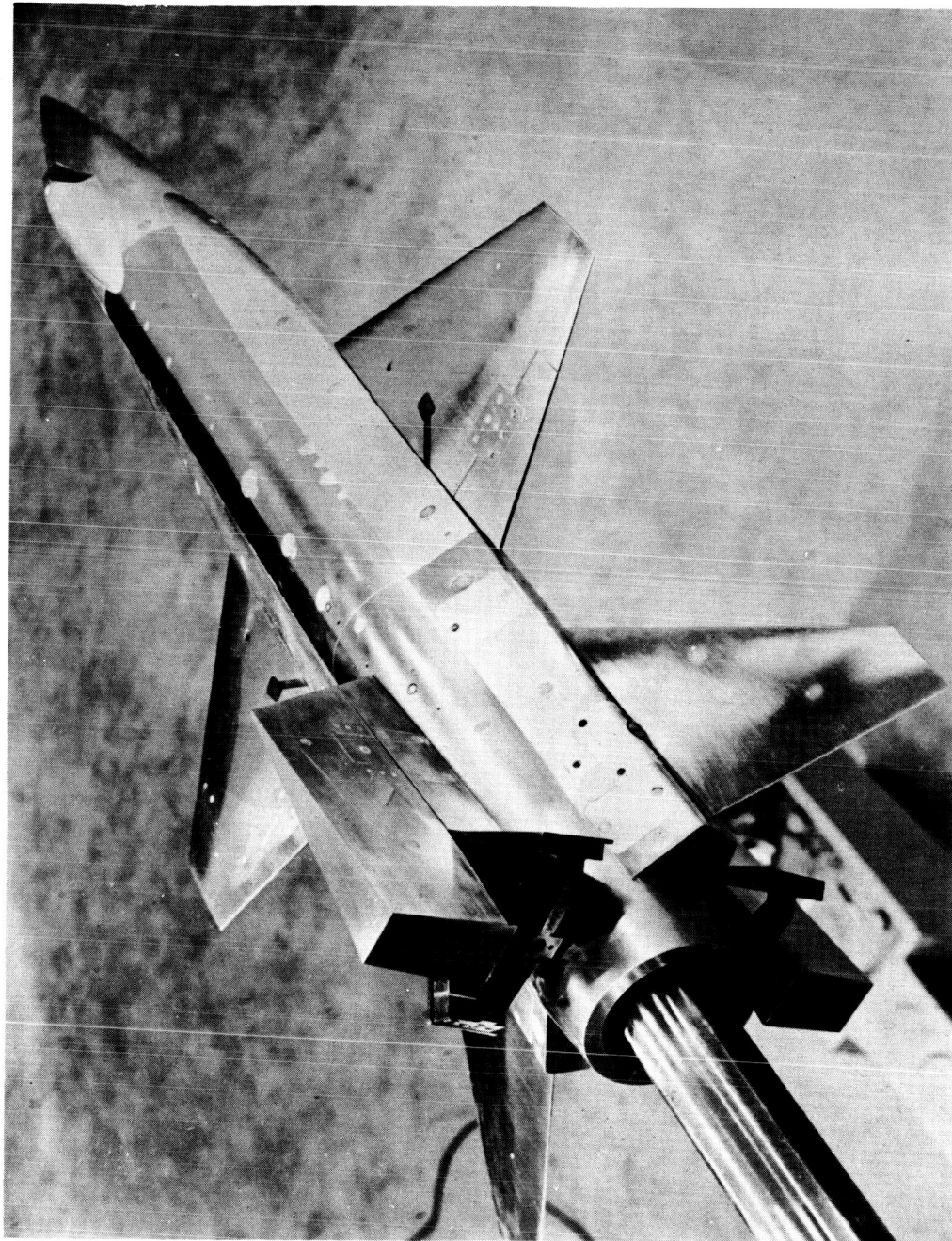
L-57-4350

Figure 2.- Photographs of a 0.067-scale model of the X-15 airplane.

DECLASSIFIED

~~CONFIDENTIAL~~

15



(b) Three-quarter rear view.
L-57-4348

Figure 2.- Continued.

L-351

031712241030

~~CONFIDENTIAL~~

L-57-4349

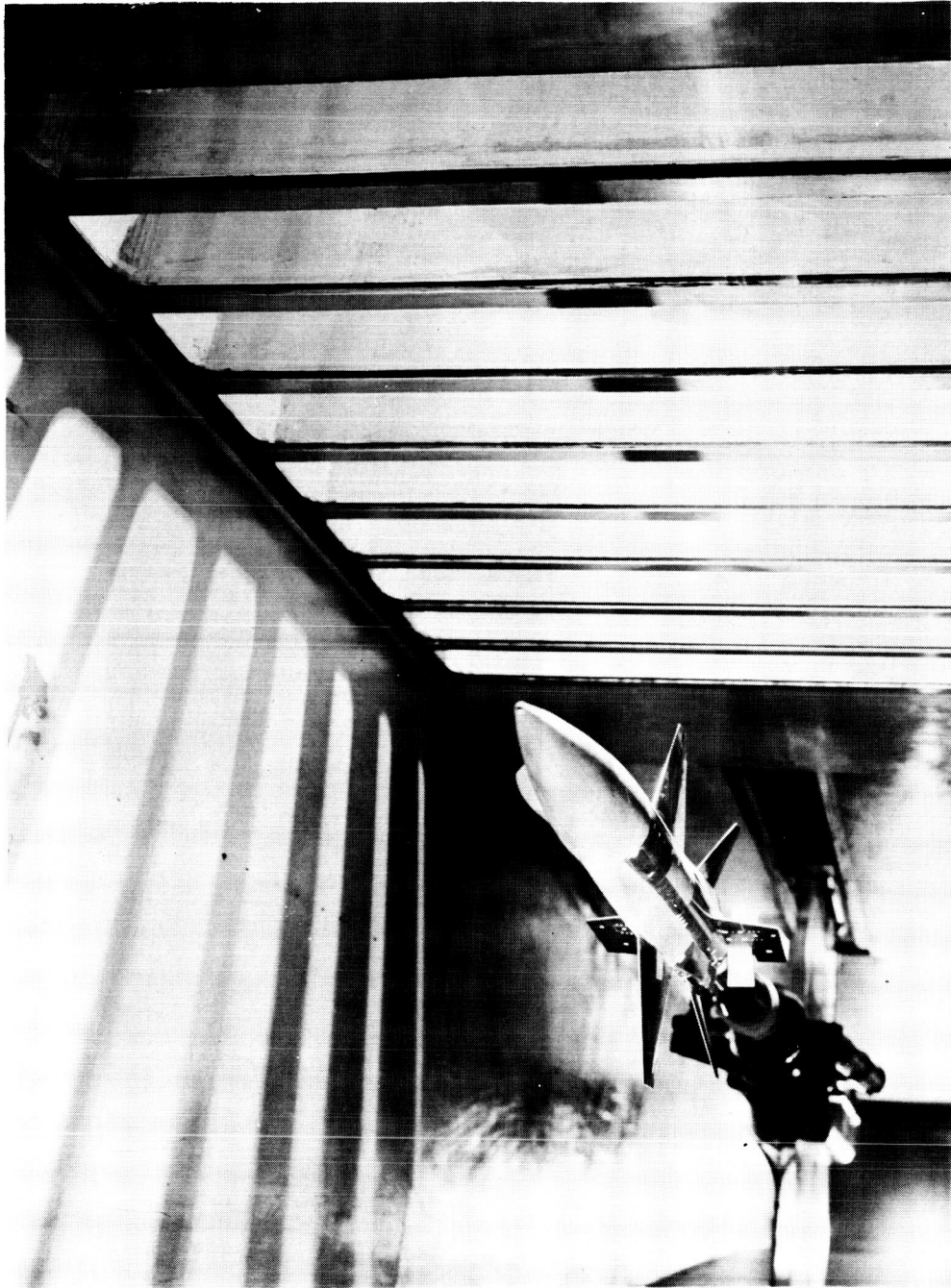
(c) Top view.

Figure 2.- Continued.

~~CONFIDENTIAL~~

DECLASSIFIED

~~CONFIDENTIAL~~



L-57-4537
(d) One-quarter front view.

Figure 2.- Concluded.

03171220 1030

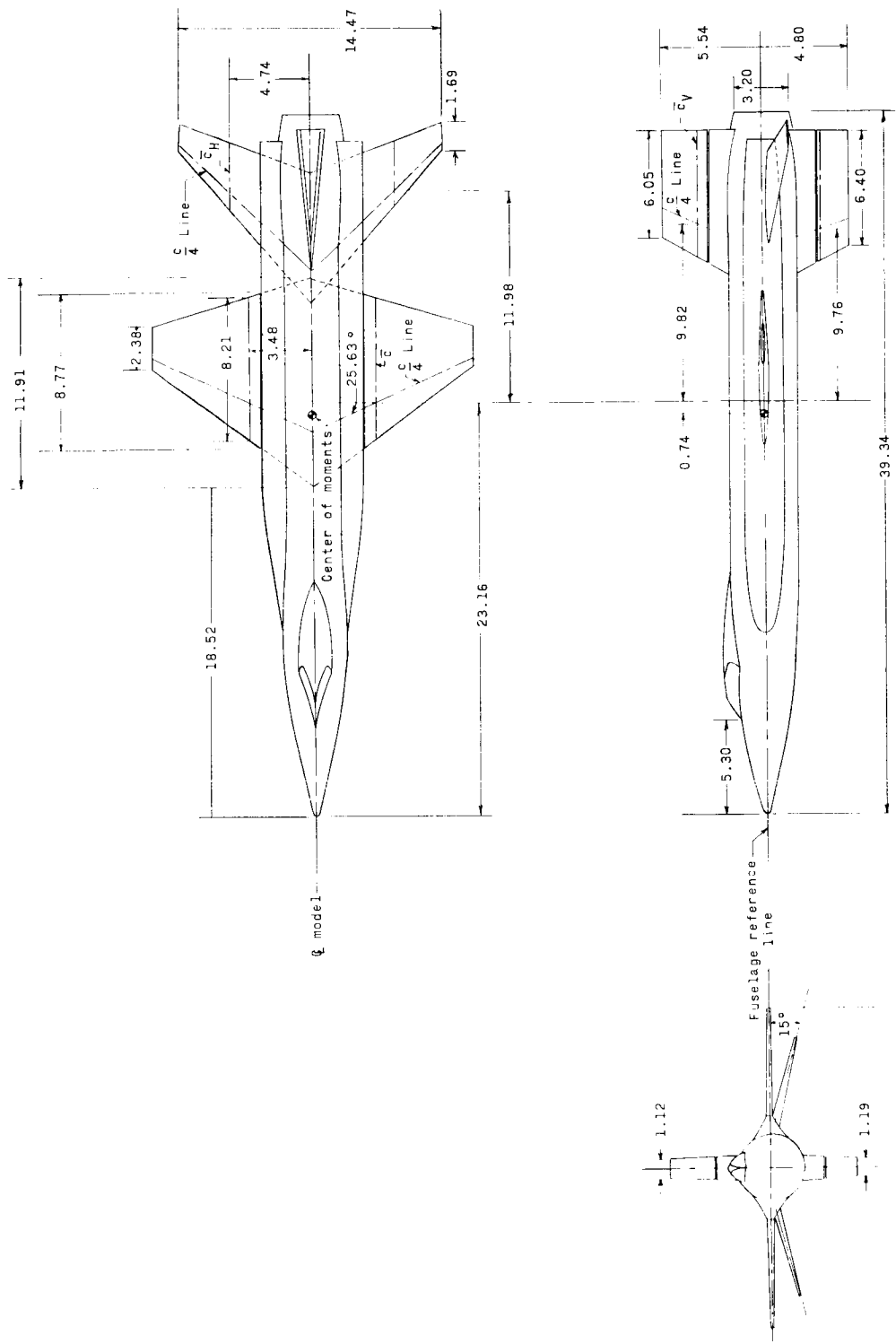


Figure 3.- Details of the 0.067-scale model of the X-15 airplane. Dimensions are in inches unless otherwise noted.

~~CONFIDENTIAL~~ DECLASSIFIED

19

L-351

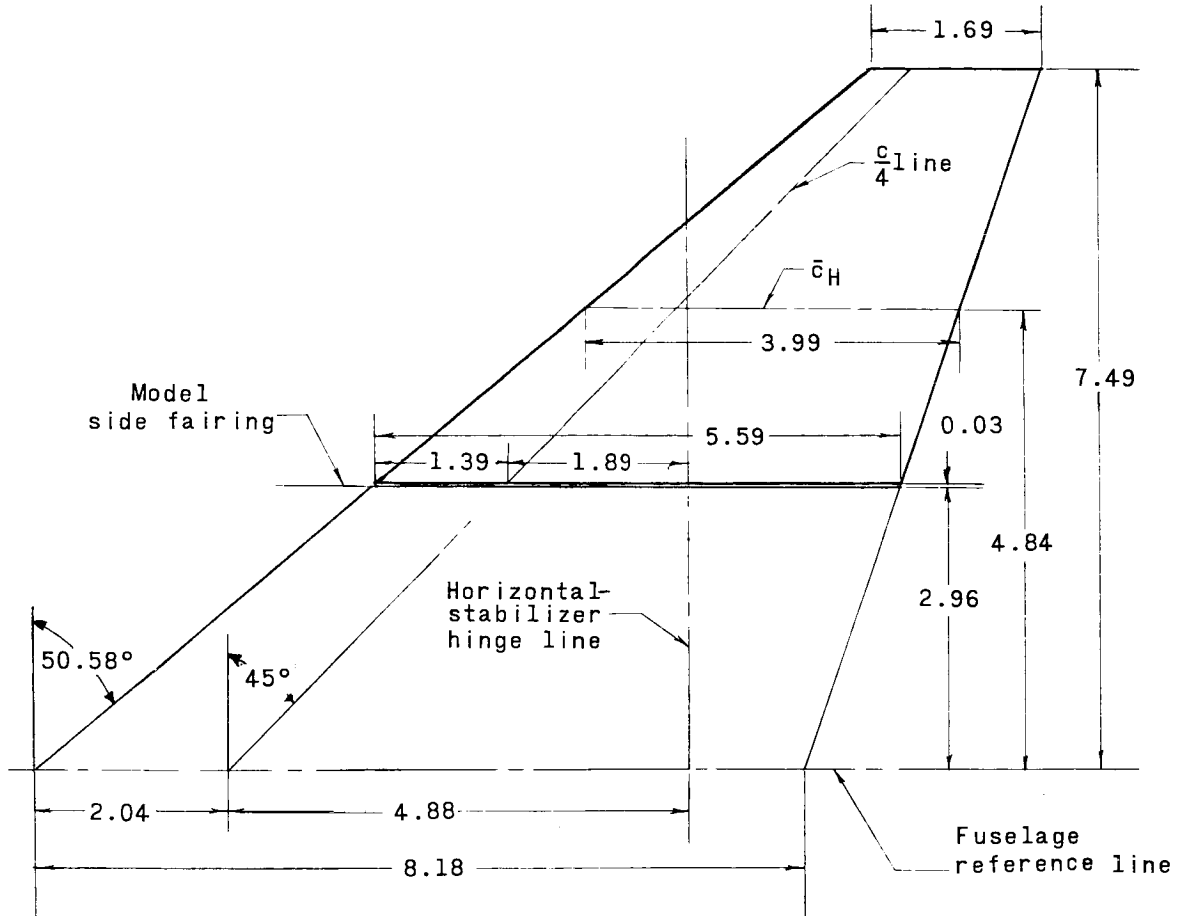
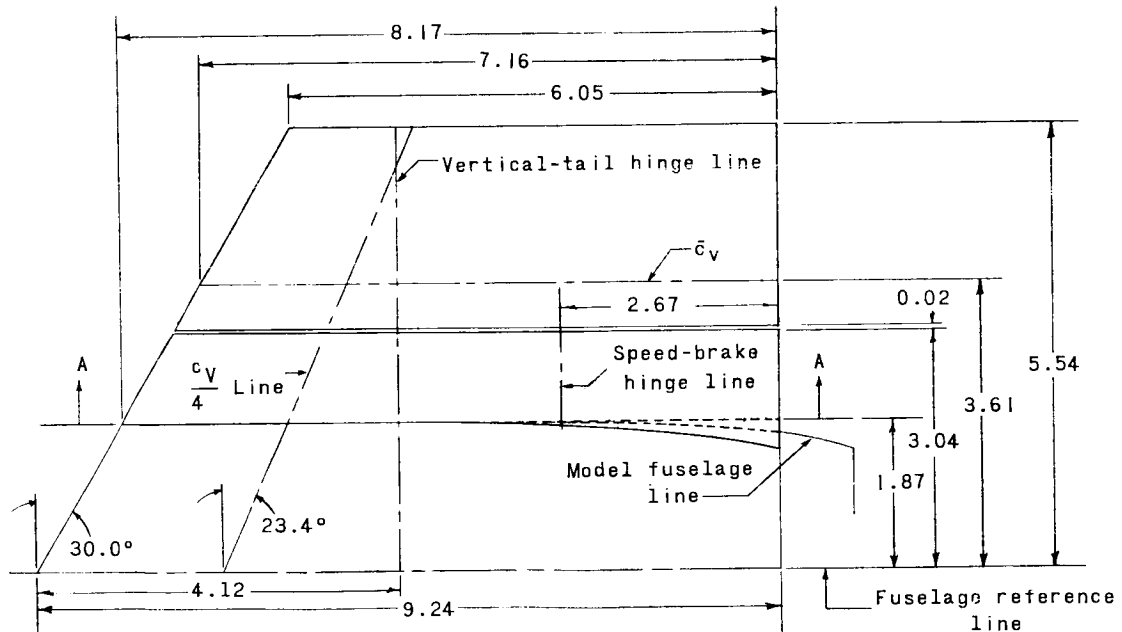
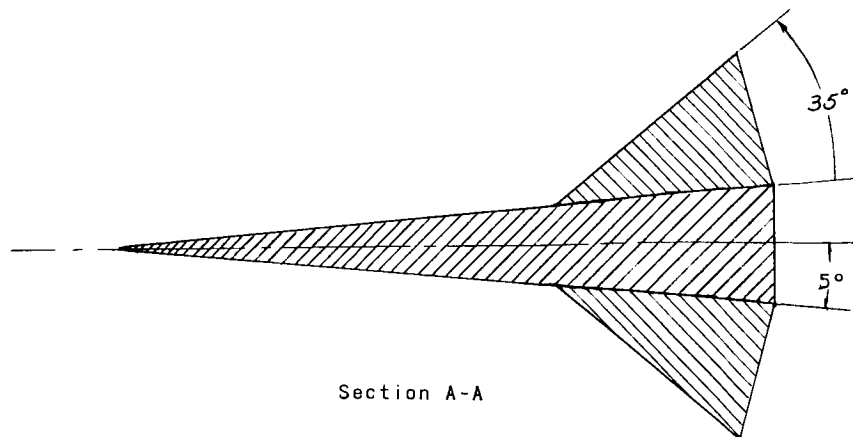


Figure 4.-- Drawing of the horizontal stabilizer. All dimensions are measured in the chord plane of the surface and are in inches unless otherwise noted.

0319122A1030

~~CONFIDENTIAL~~

20



(a) Vertical tail.

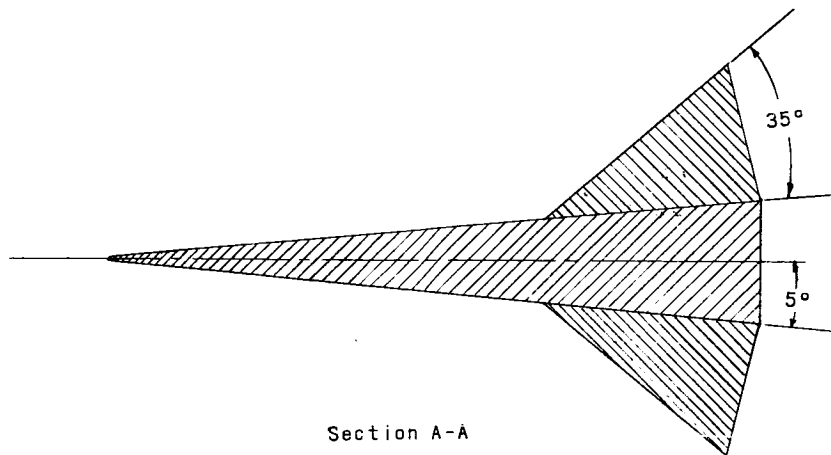
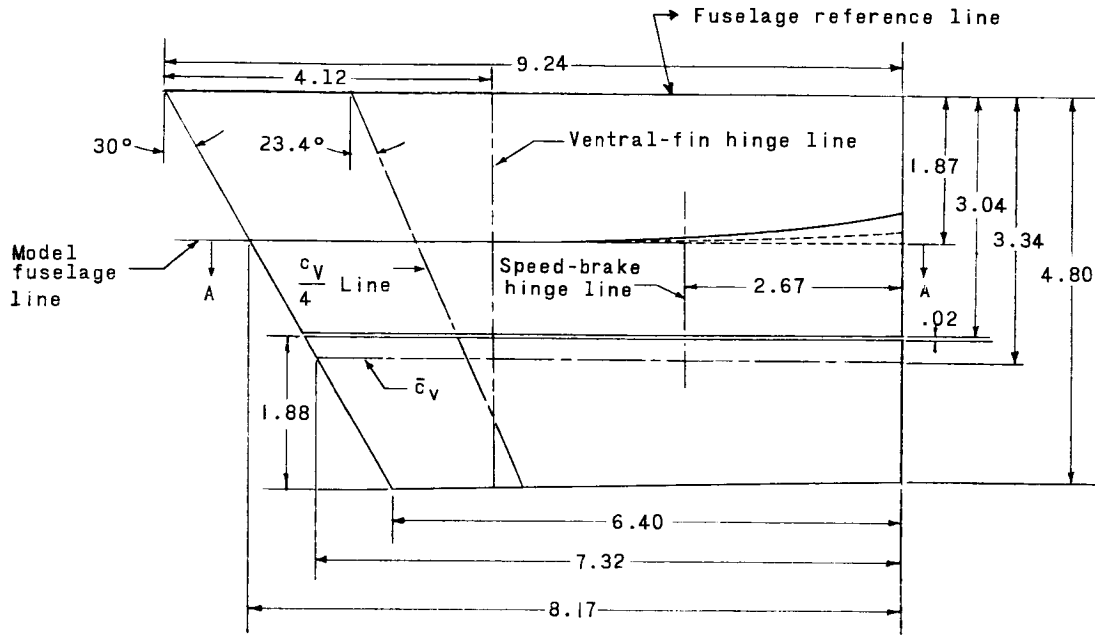
Figure 5.- Drawings of vertical tail and ventral fin. Dimensions are in inches unless otherwise noted.

~~CONFIDENTIAL~~

~~DECLASSIFIED~~

~~CONFIDENTIAL~~

21



(b) Ventral fin.

Figure 5.- Concluded.

031912201030

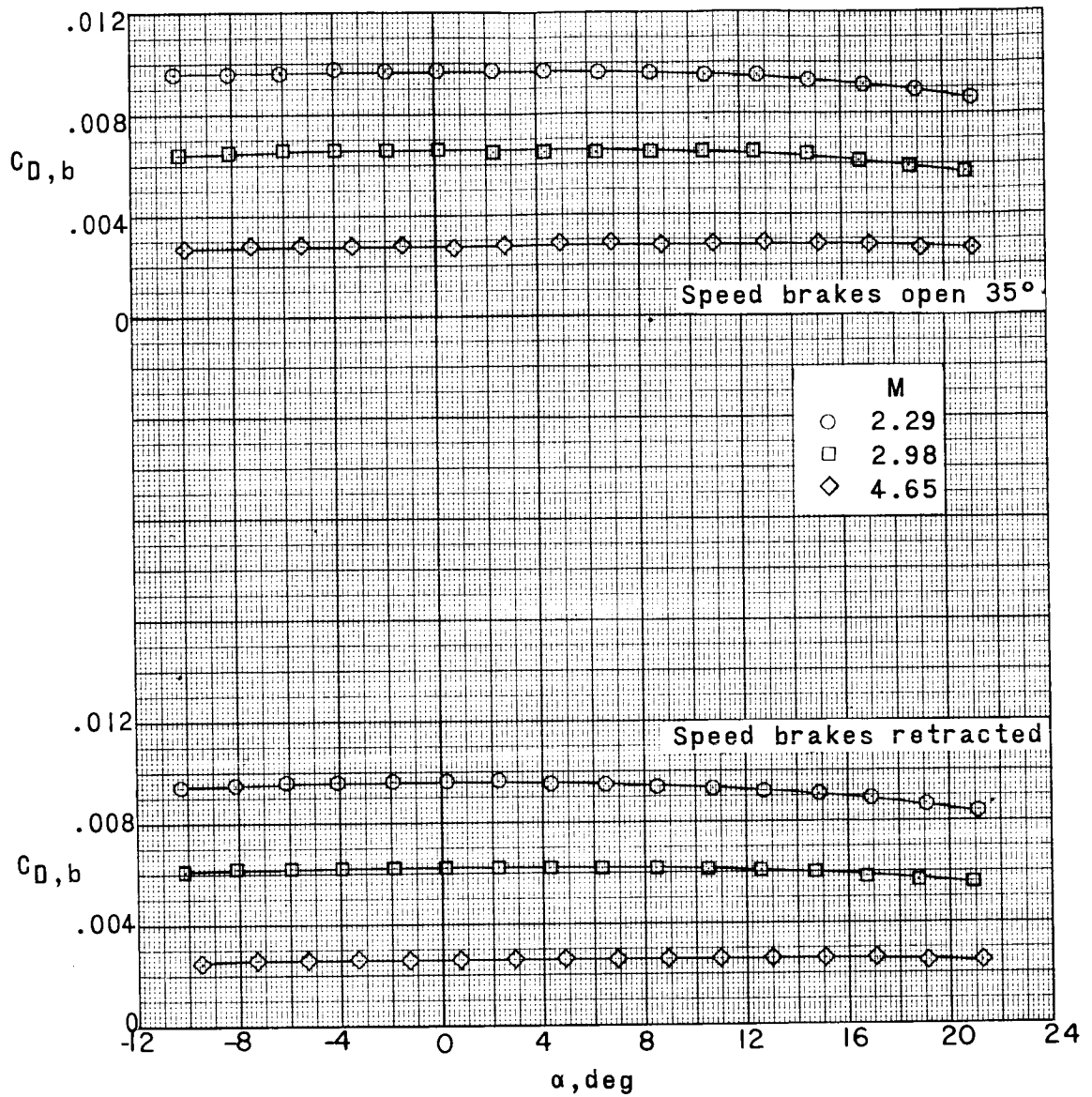
~~CONFIDENTIAL~~

Figure 6.- Fuselage base drag coefficients of a 0.067-scale model of the X-15 airplane at a nominal Reynolds number of 1.87×10^6 .

~~CONFIDENTIAL~~

DECLASSIFIED
~~CONFIDENTIAL~~

23

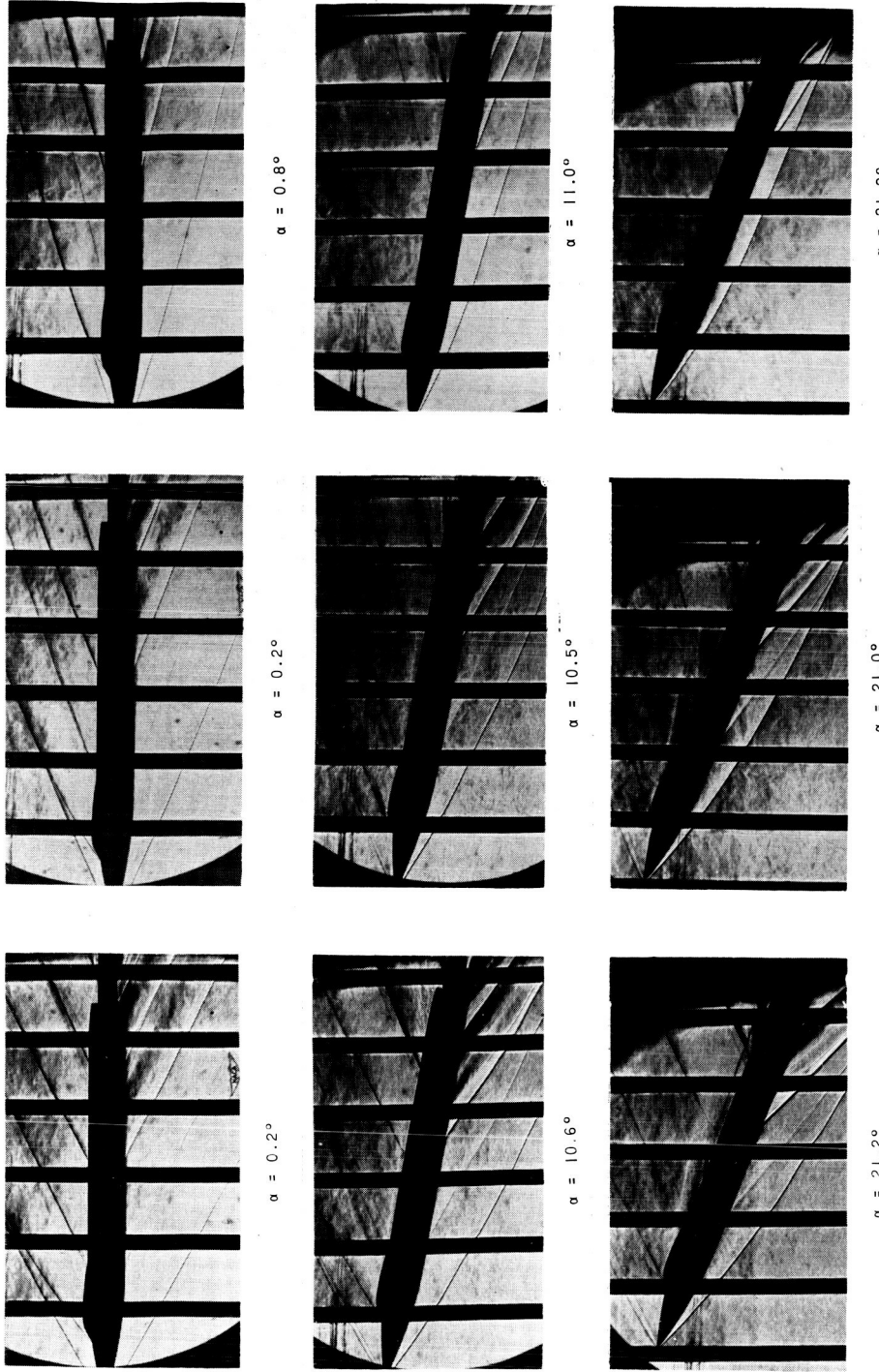


Figure 7.- Schlieren photographs of a 0.067-scale model of the X-15 airplane with vertical tail off in the Langley Unitary Plan wind tunnel.
L-59-1947

031303201030

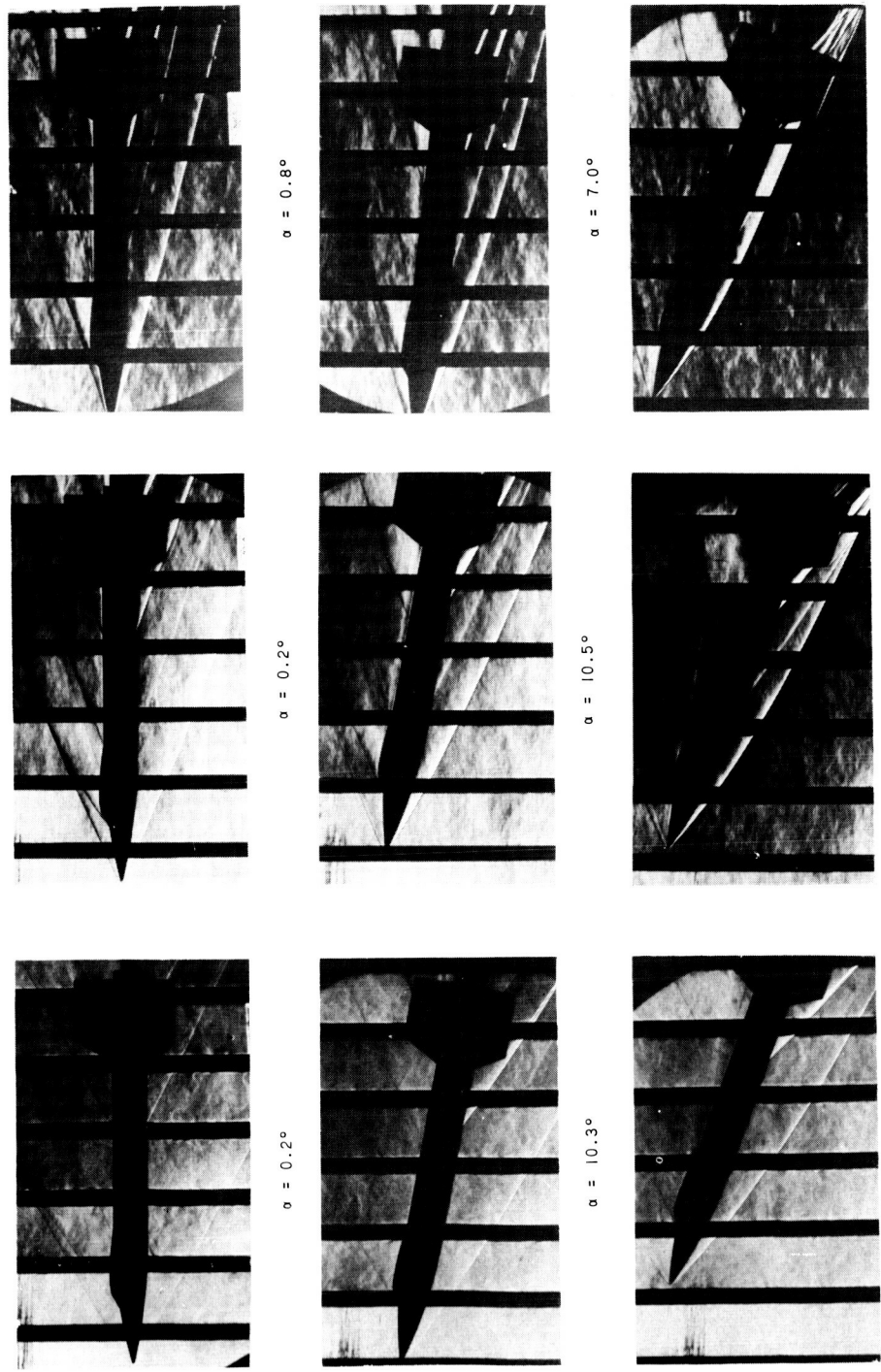


Figure 8.- Schlieren photographs of the complete configuration of a 0.067-scale model of the X-15 airplane with speed brakes retracted in the Langley Unitary Plan wind tunnel.
L-59-1948

DECLASSIFIED

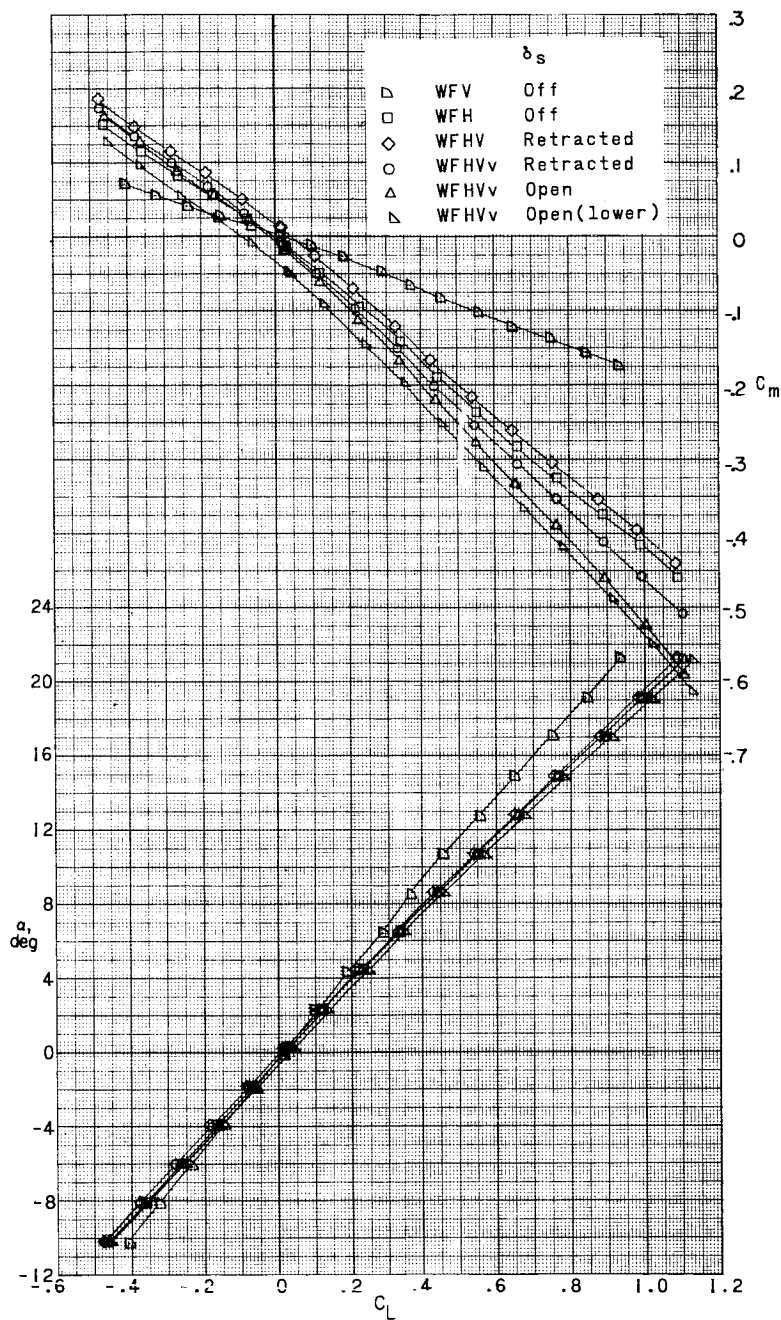
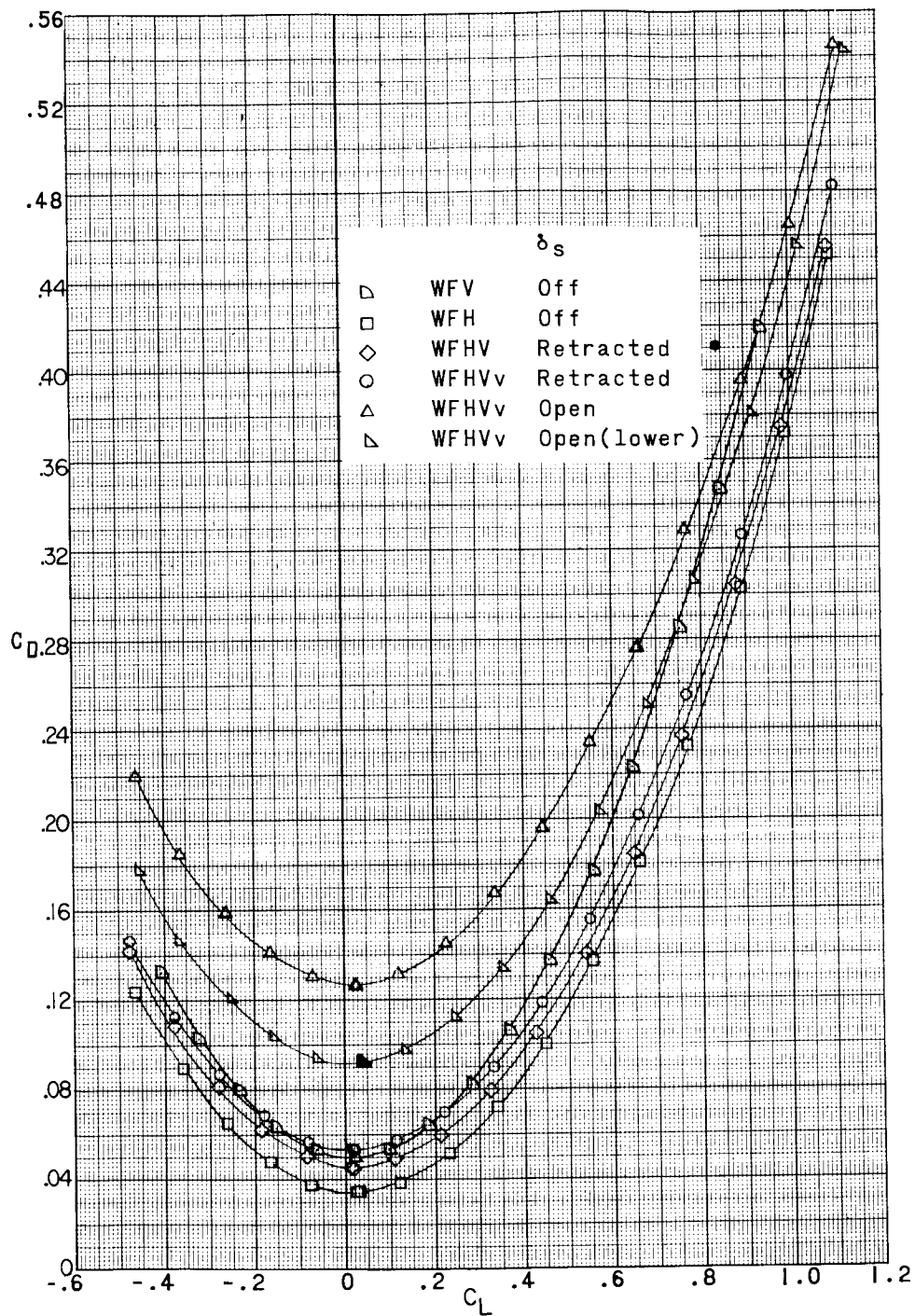
(a) $M = 2.29$.

Figure 9.- Pitch characteristics of a 0.067-scale model of the X-15 airplane with various components of the configuration.

CONFIDENTIAL

03171220.1030
CONFIDENTIAL

(a) Concluded.

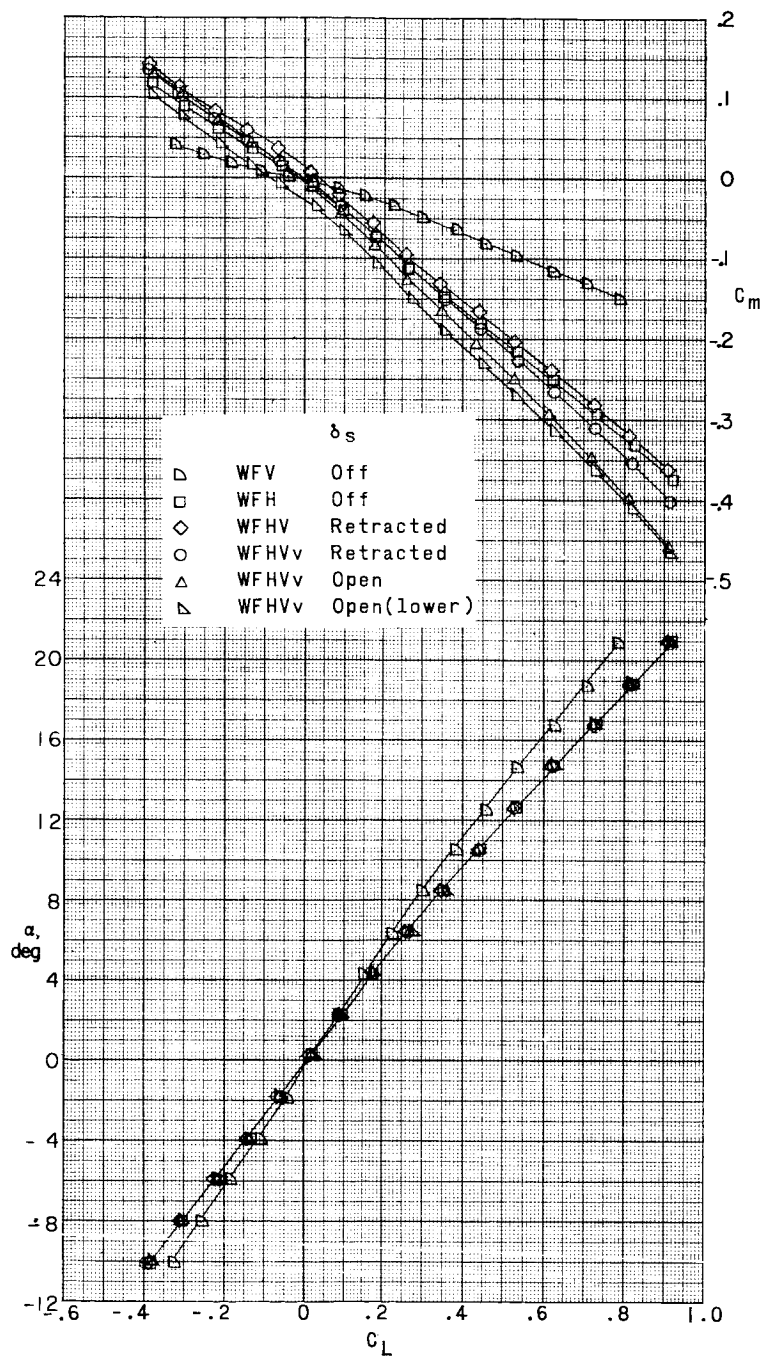
Figure 9.- Continued.

03171220.1030

~~DECLASSIFIED~~

27

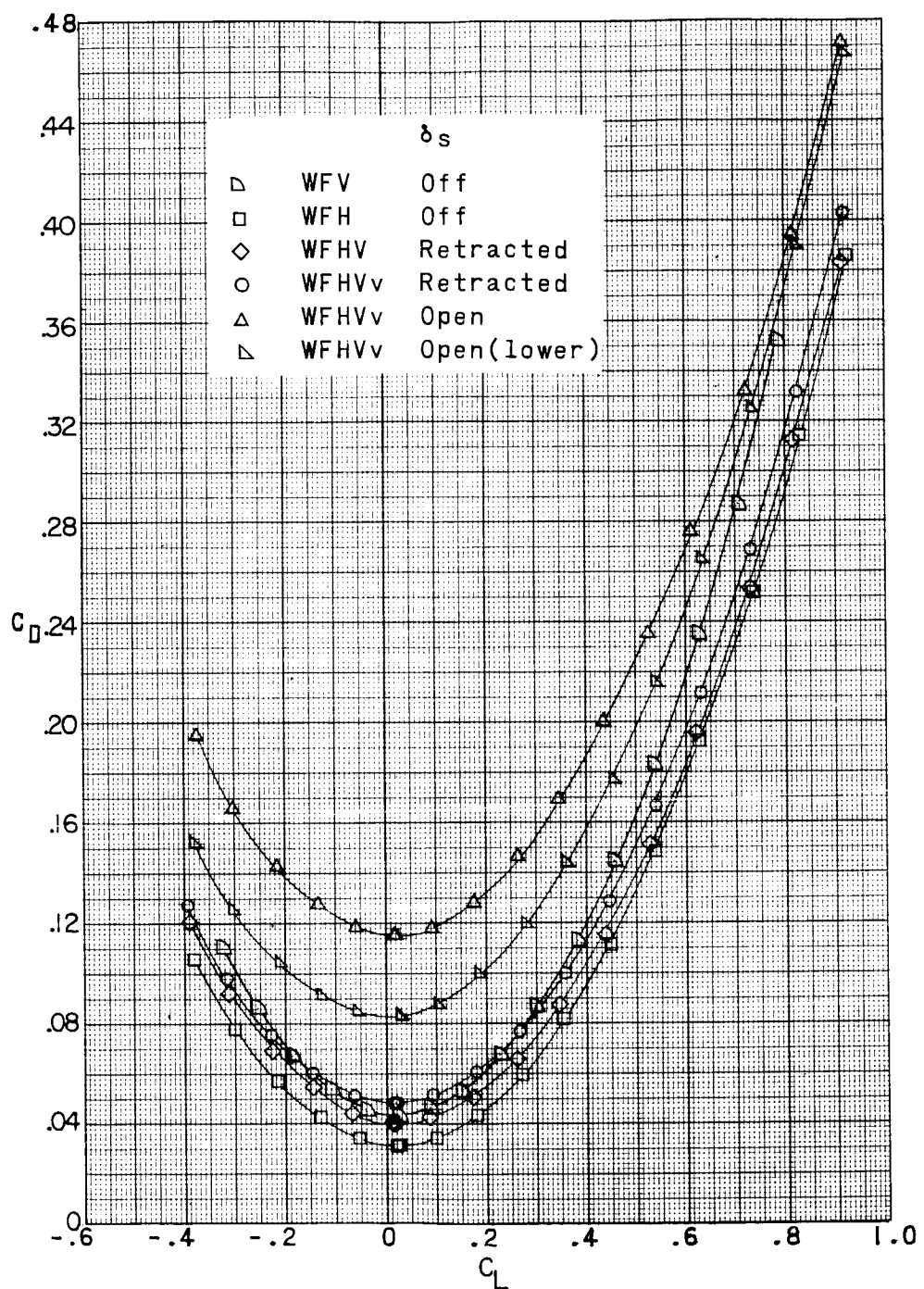
L-351



(b) $M = 2.98$.

Figure 9.- Continued.

CONFIDENTIAL

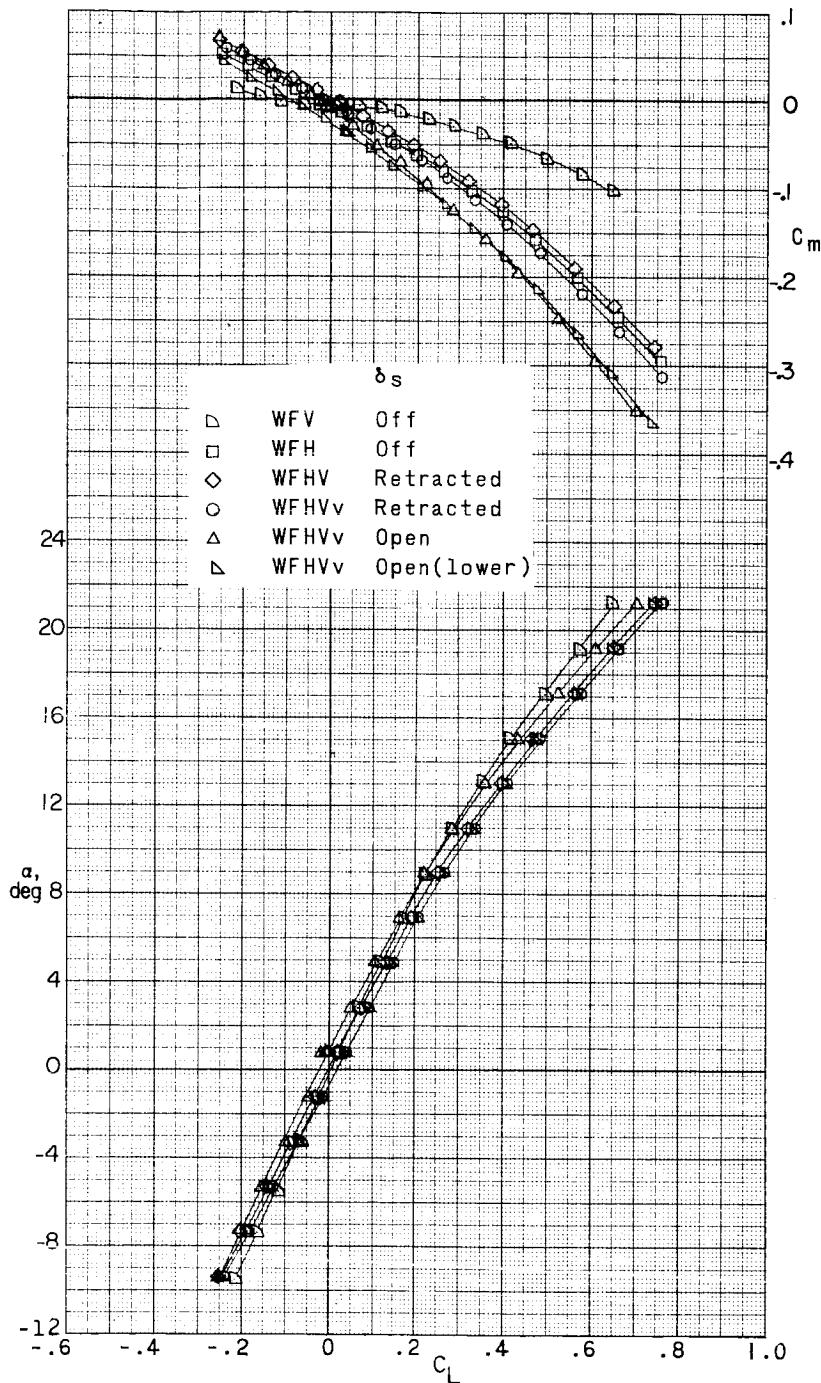


(b) Concluded.

Figure 9.- Continued.

~~DECLASSIFIED~~

29

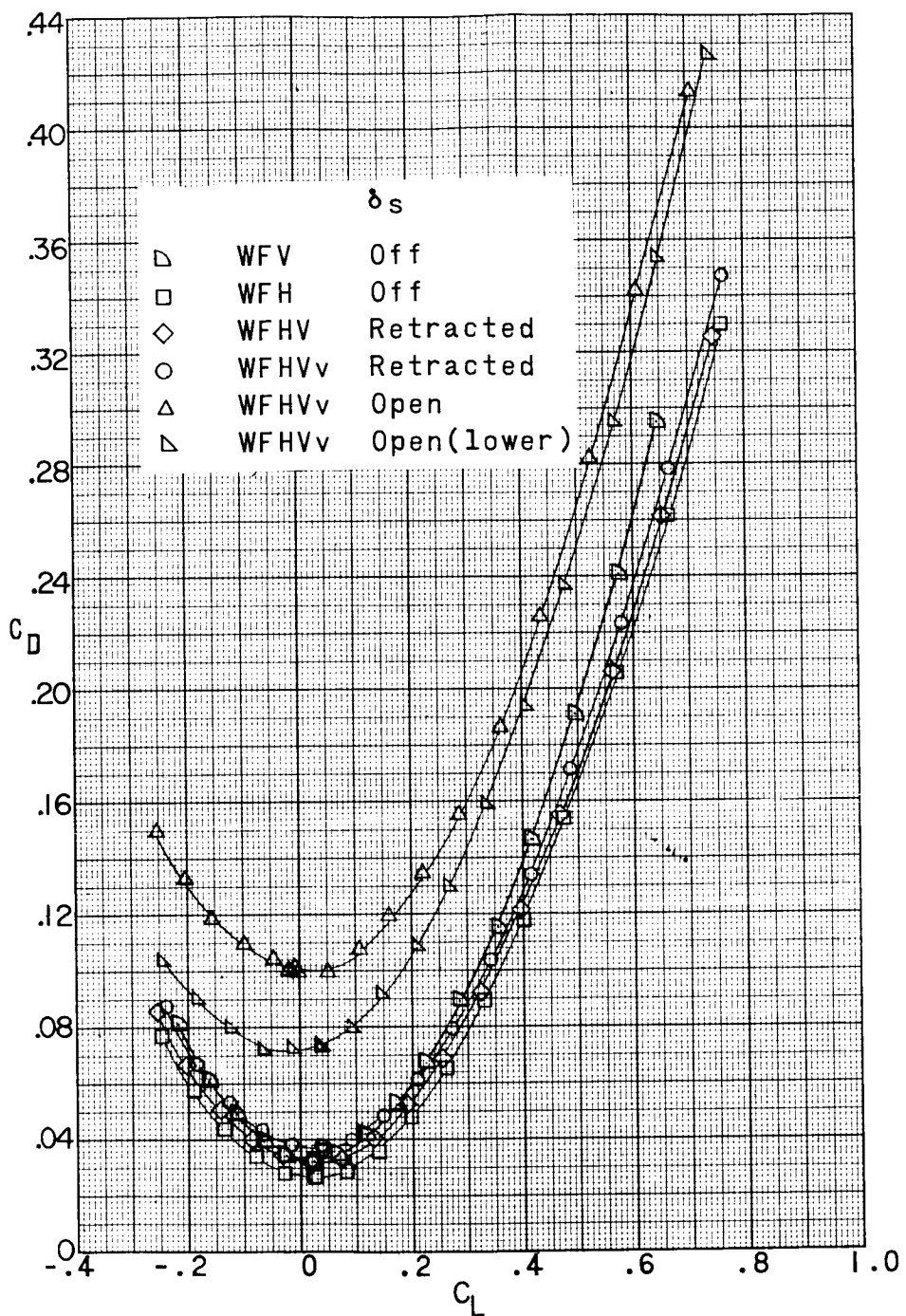


(c) $M = 4.65.$

Figure 9.- Continued.

CONFIDENTIAL

30



(c) Concluded.

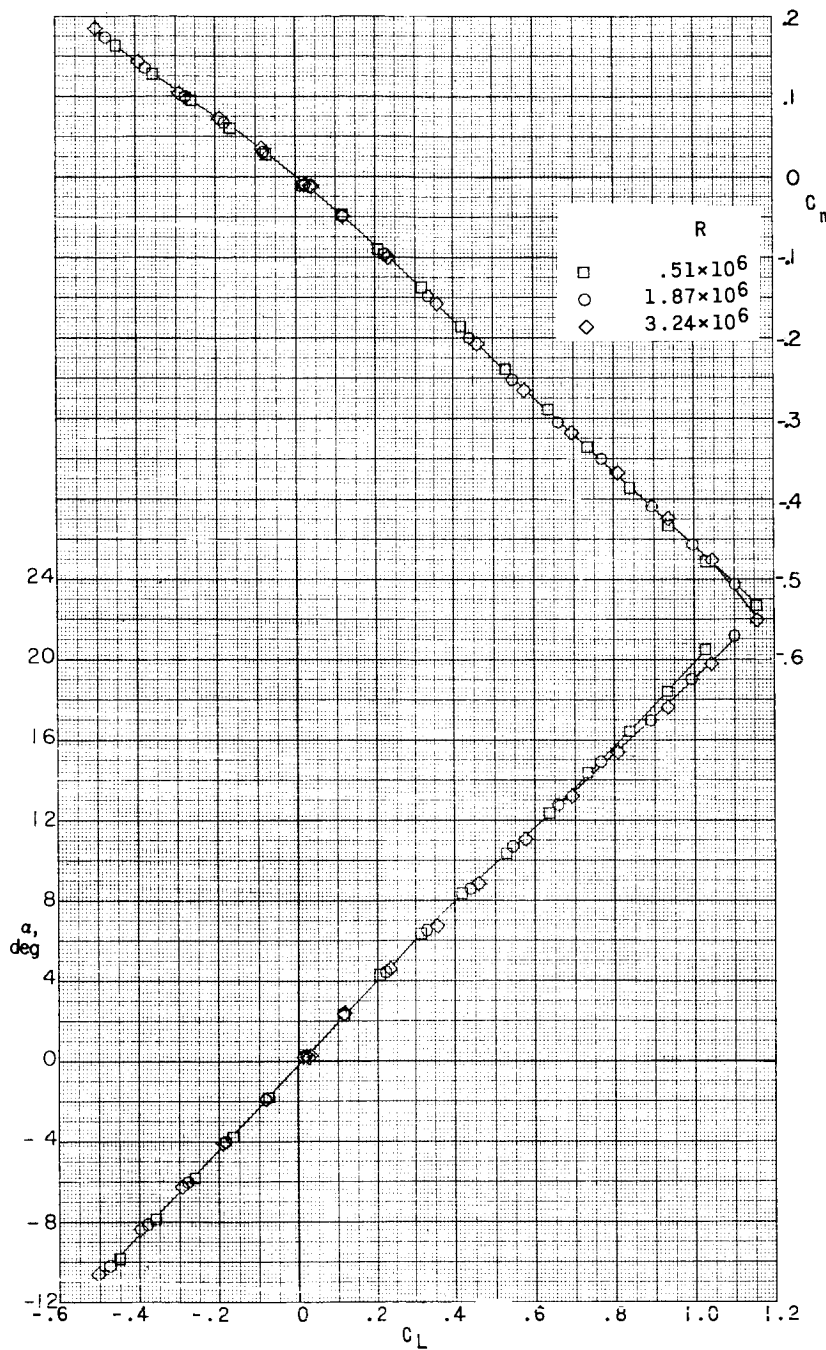
Figure 9.- Concluded.

CONFIDENTIAL

DECLASSIFIED

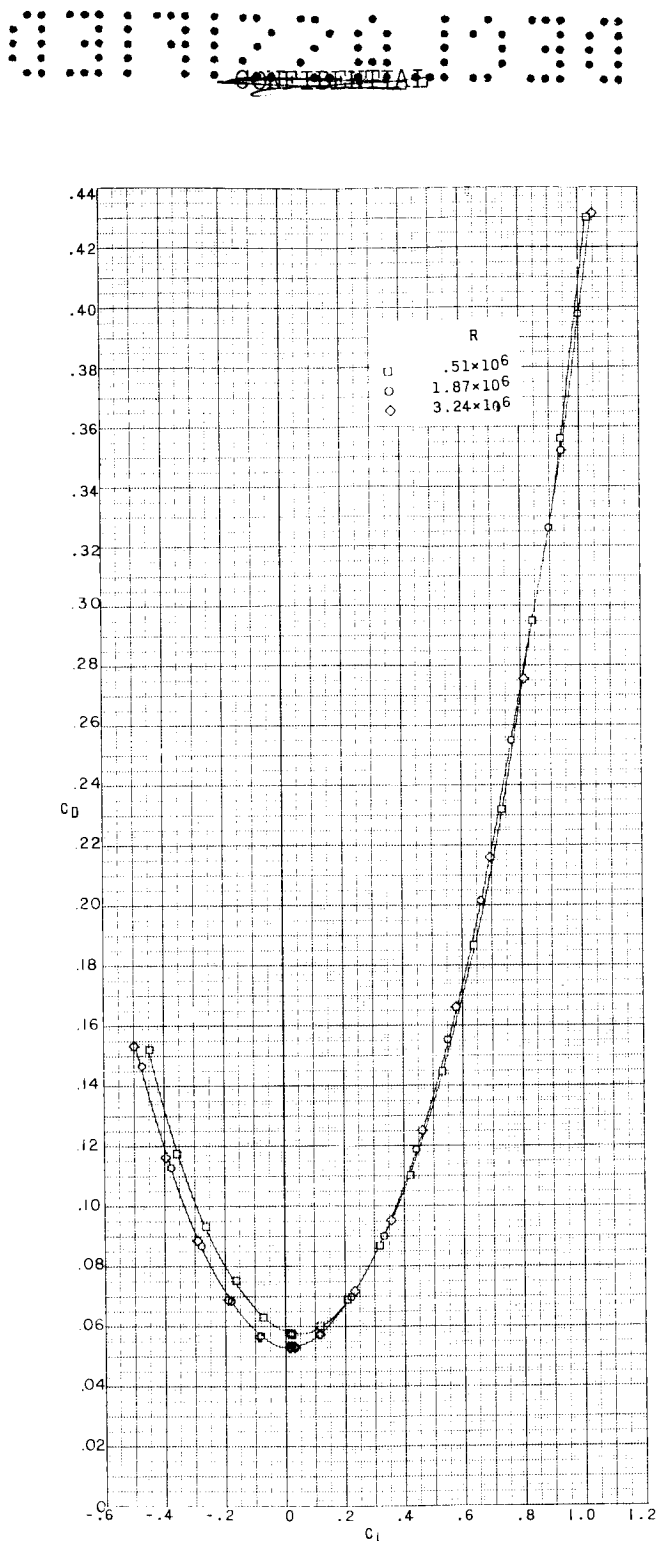
CONFIDENTIAL

31



(a) $M = 2.29$.

Figure 10.- Pitch characteristics of a 0.067-scale model of the X-15 airplane at various Reynolds numbers. Complete model; speed brakes retracted; $\delta_H = 0^\circ$.



(a) Concluded.

Figure 10..- Continued.

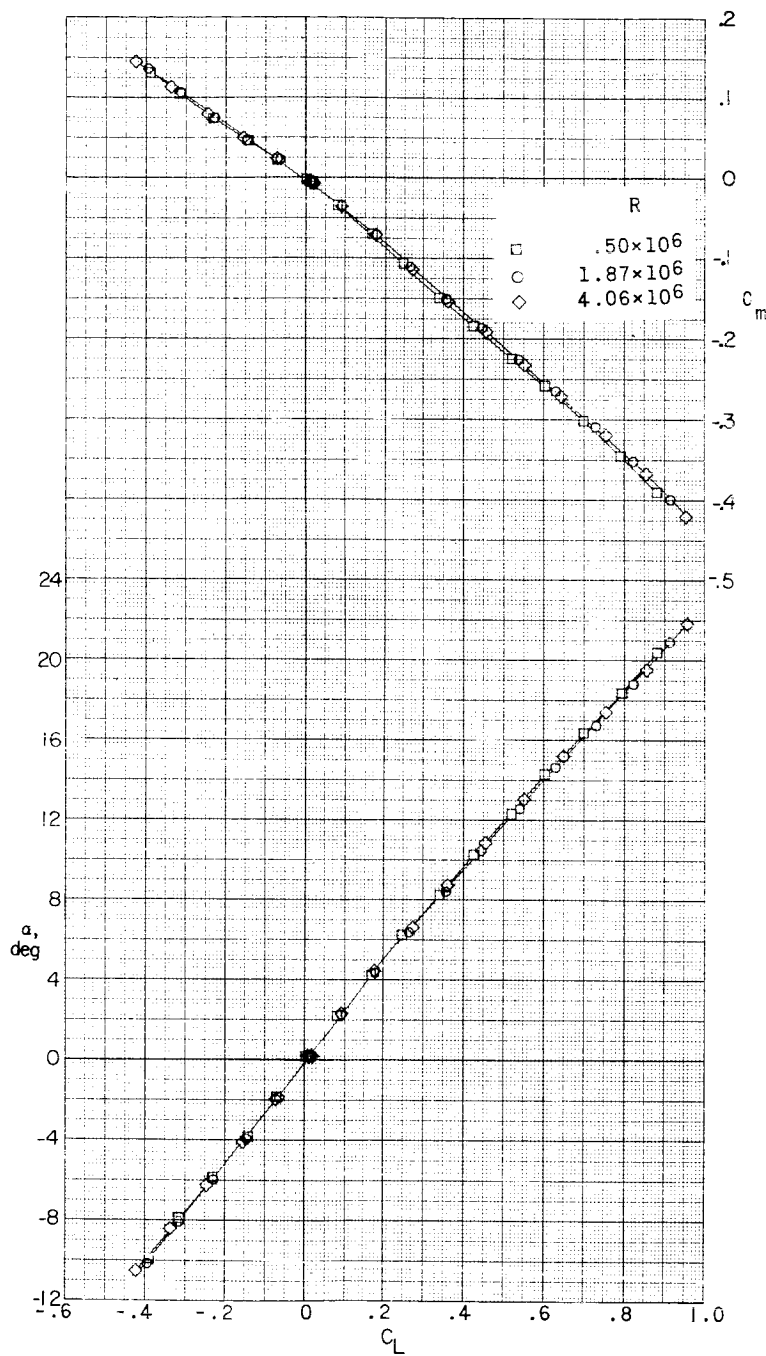
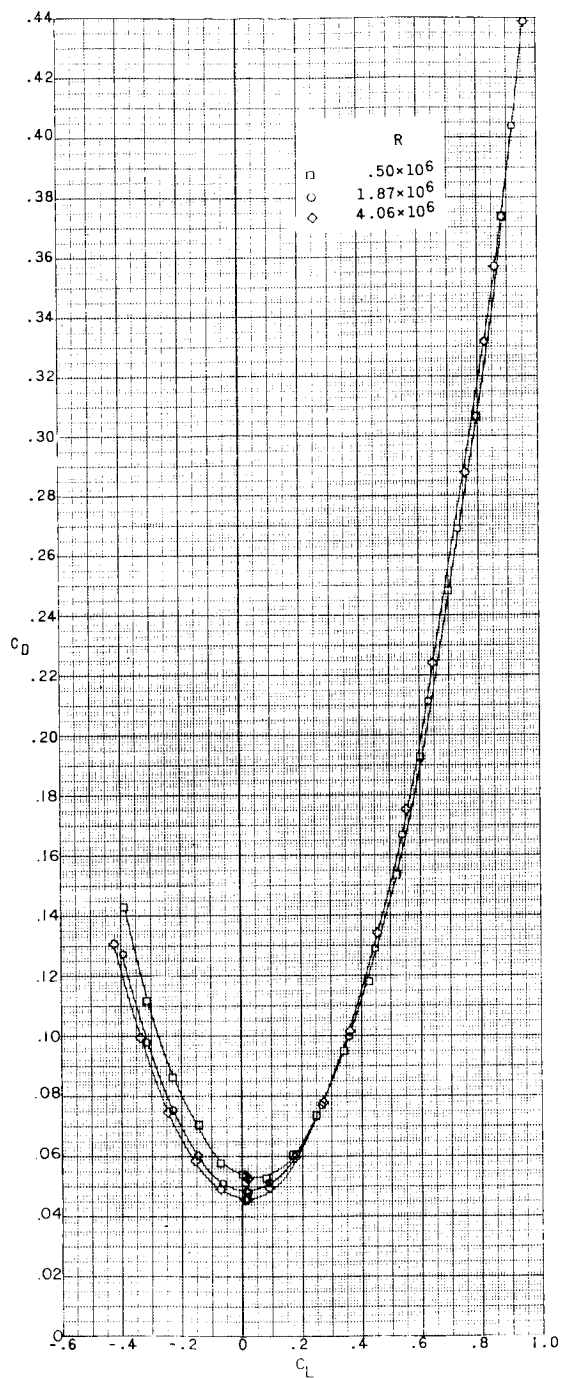
~~DECLASSIFIED~~(b) $M = 2.98$.

Figure 10.- Continued.

~~CONFIDENTIAL~~

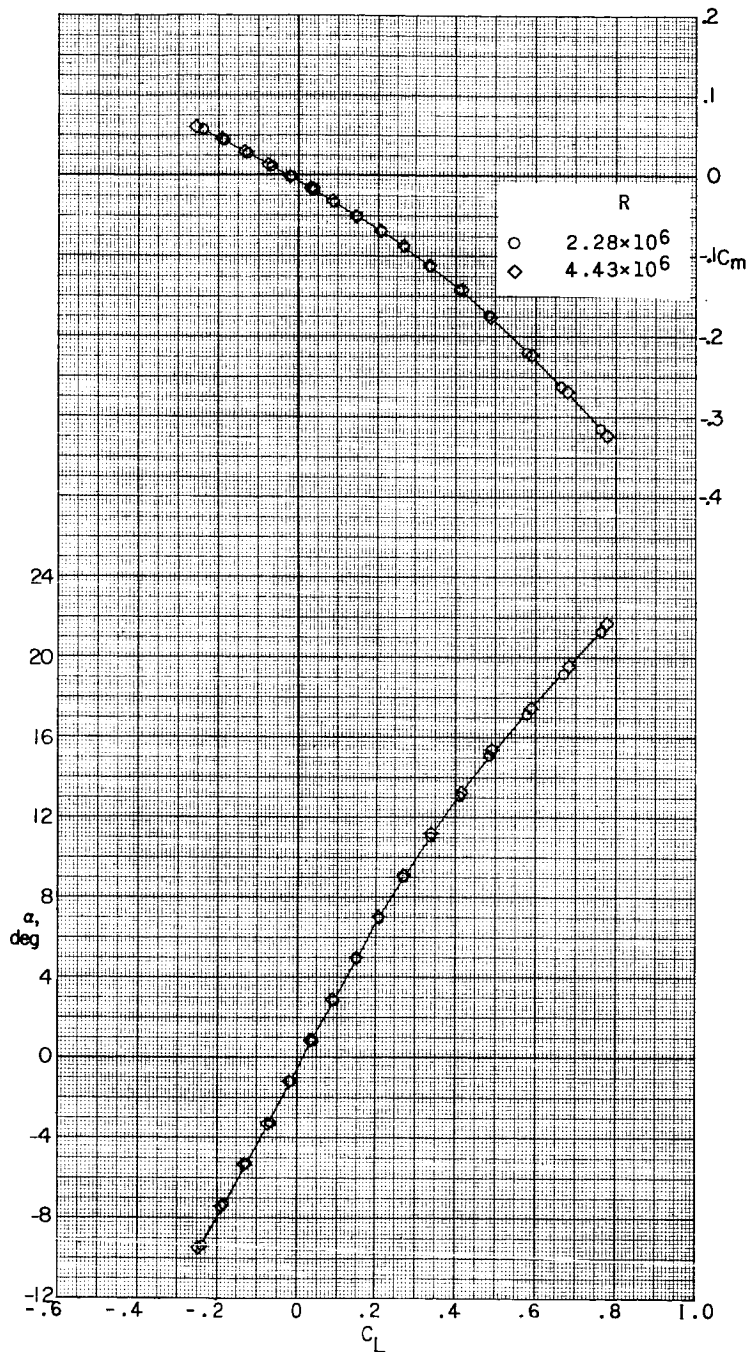
(b) Concluded.

Figure 10.- Continued.

~~CONFIDENTIAL~~

DECLASSIFIED

35

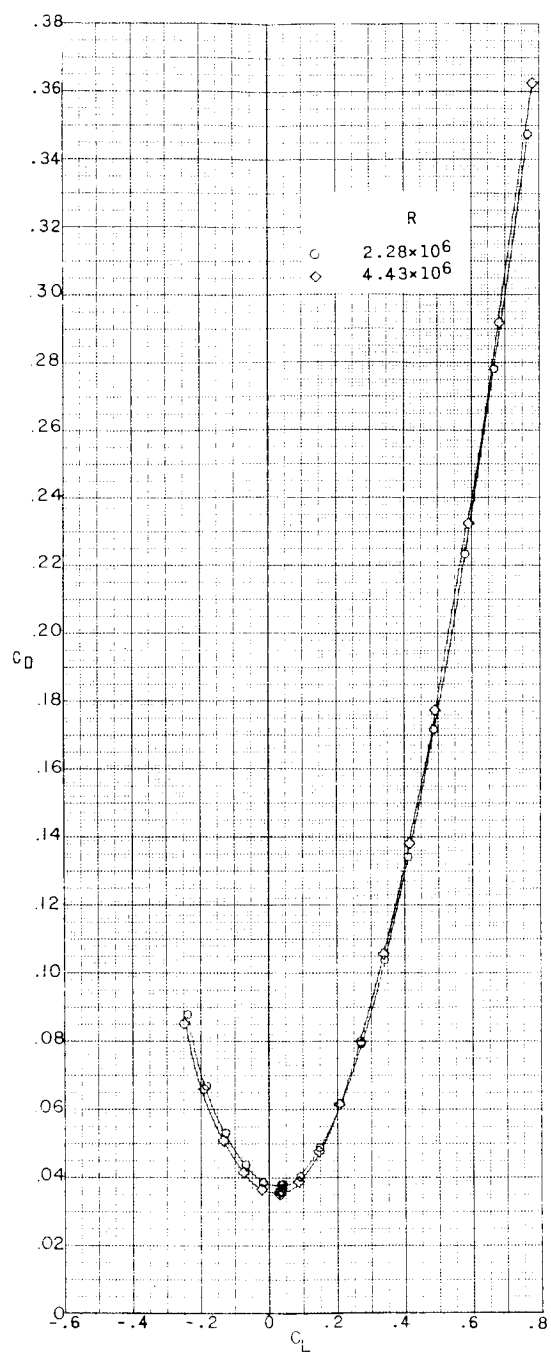


(c) $M = 4.65$.

Figure 10.- Continued.

L-351

CONFIDENTIAL

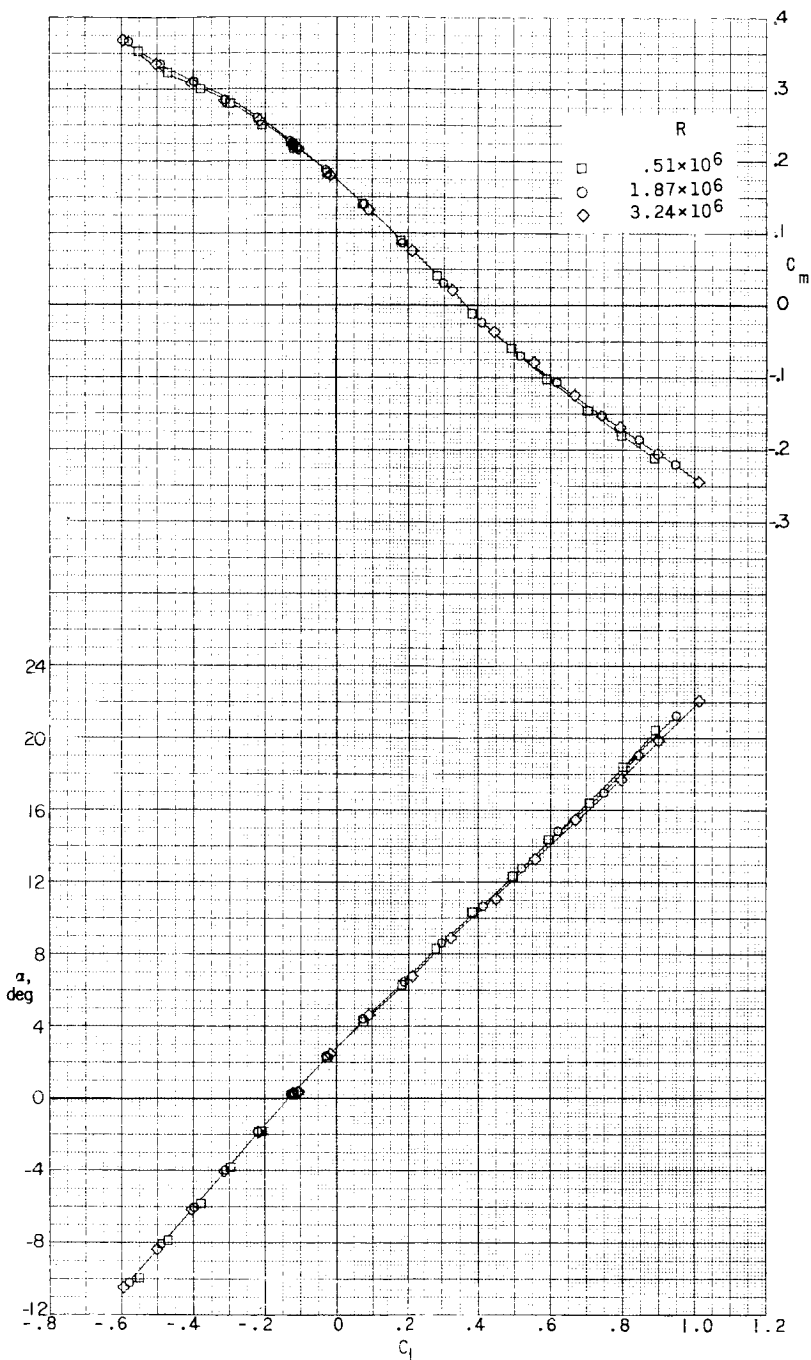


(c) Concluded.

Figure 10.- Concluded.

~~CONFIDENTIAL~~

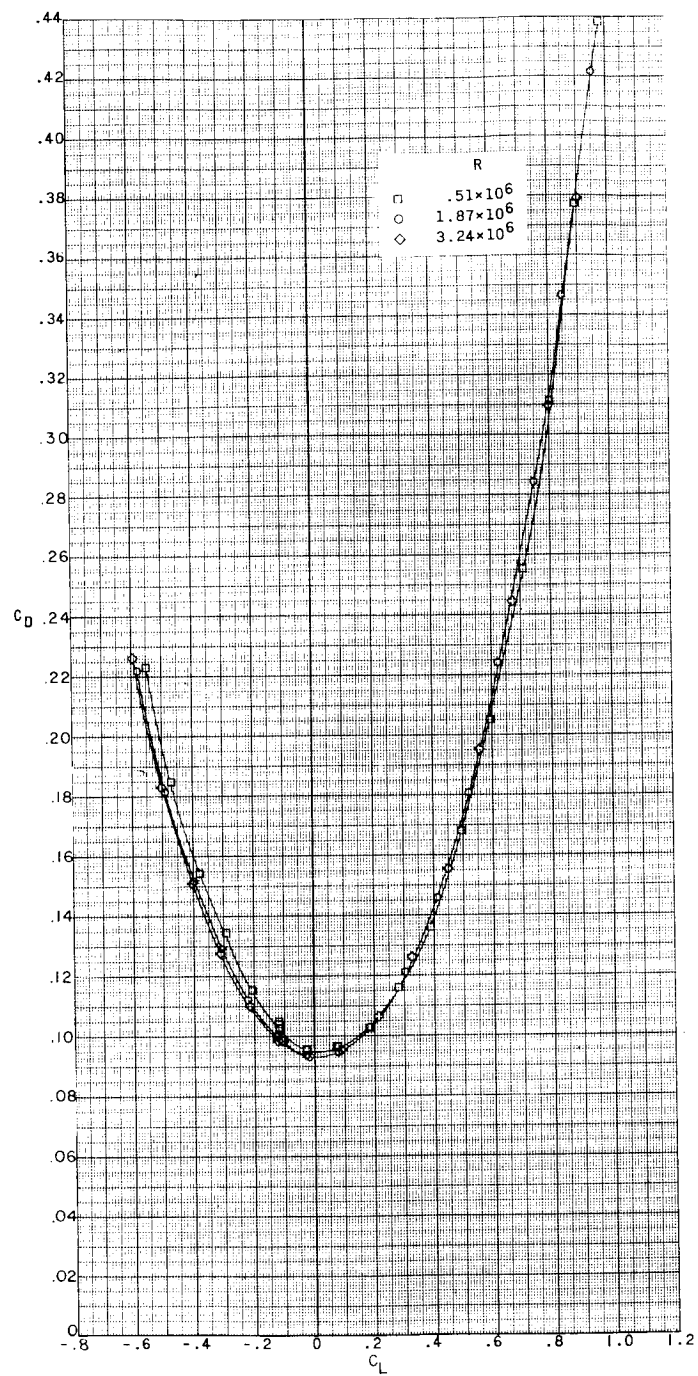
37



(a) $M = 2.29.$

Figure 11-- Pitch characteristics of a 0.067-scale model of the X-15 airplane at various Reynolds numbers. Complete model; speed brakes retracted; $\delta_H = 20^\circ$.

CONFIDENTIAL

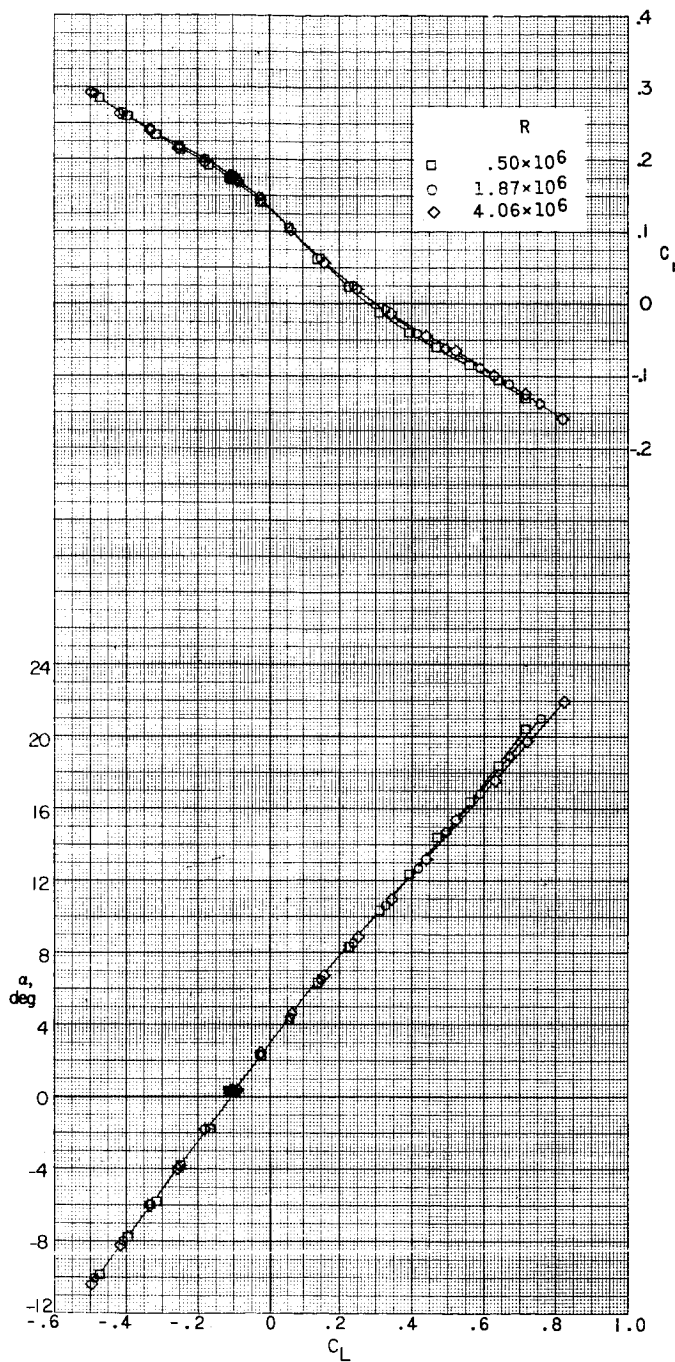


(a) Concluded.

Figure 11.- Continued.

DECLASSIFIED

39

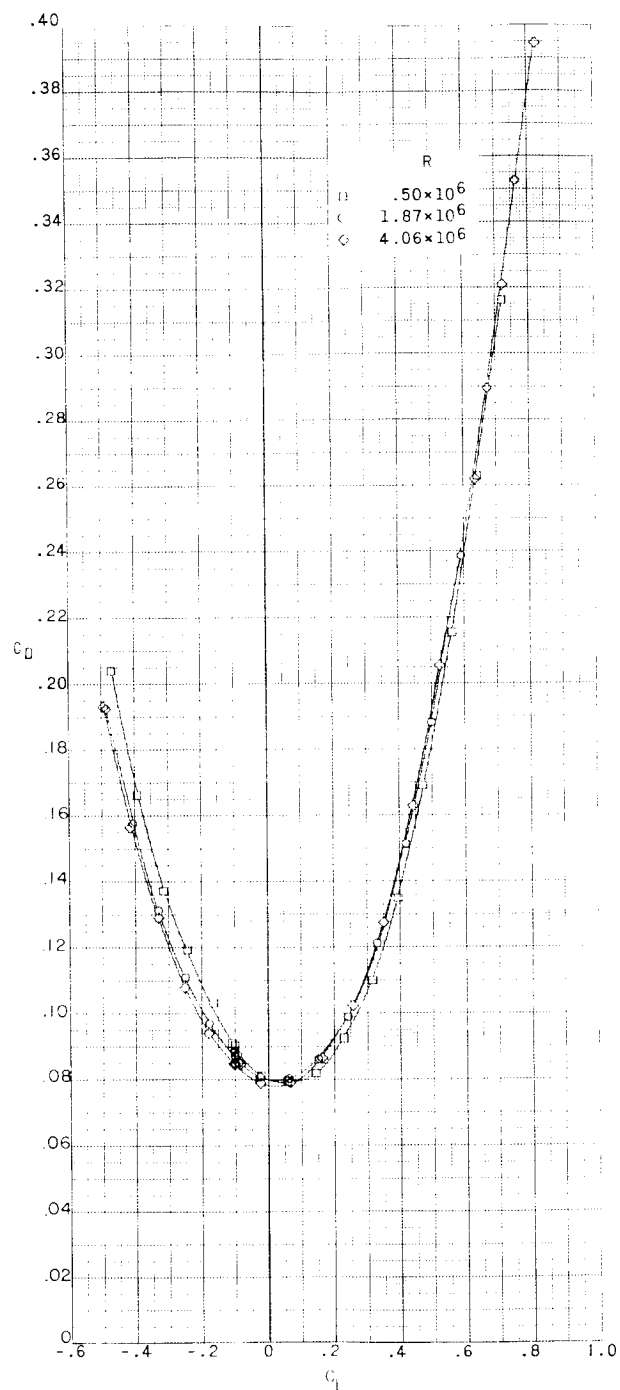


(b) $M = 2.98$.

Figure 11.- Continued.

L-351

00132261030
~~CONFIDENTIAL~~



(b) Concluded.

Figure 11.- Continued.

~~CONFIDENTIAL~~

DECLASSIFIED CONFIDENTIAL

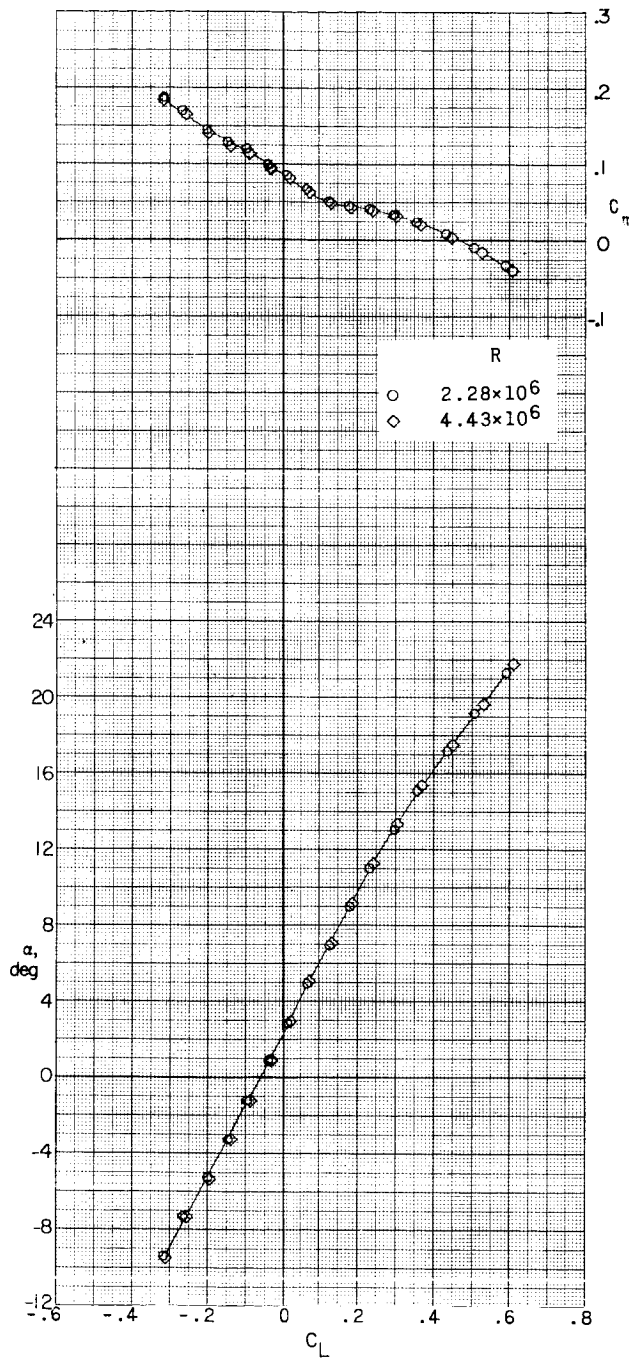
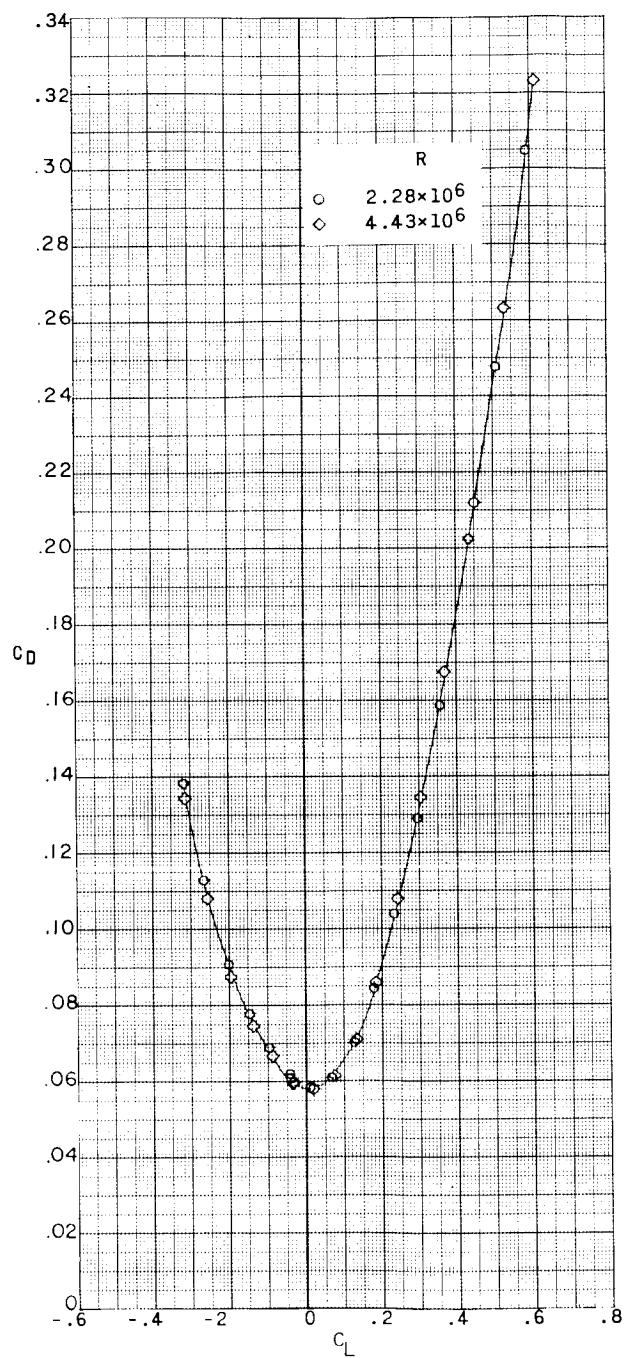
(c) $M = 4.65$.

Figure 11.- Continued.

001912201130
~~CONFIDENTIAL~~

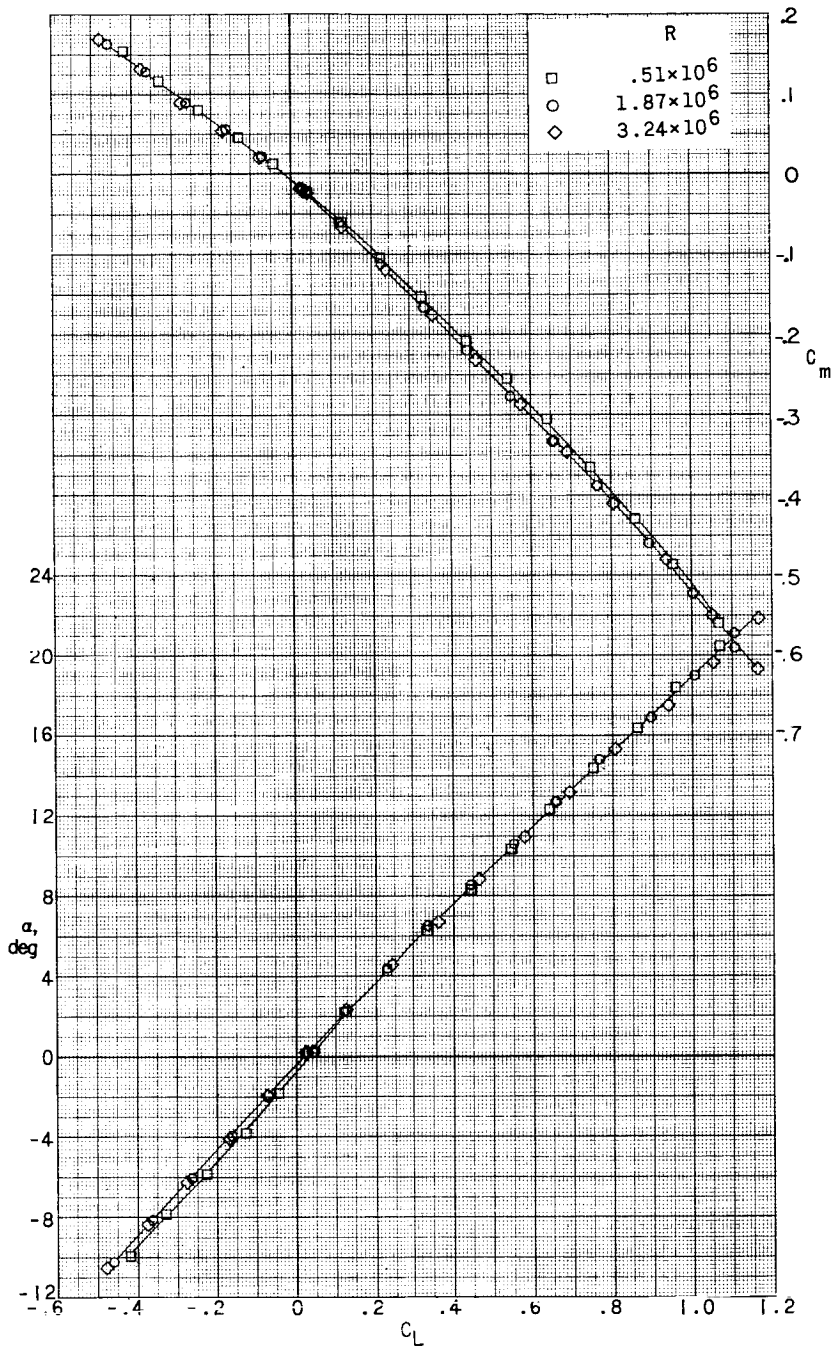
(c) Concluded.

Figure 11.- Concluded.

DECLASSIFIED

CONFIDENTIAL

43



(a) $M = 2.29$.

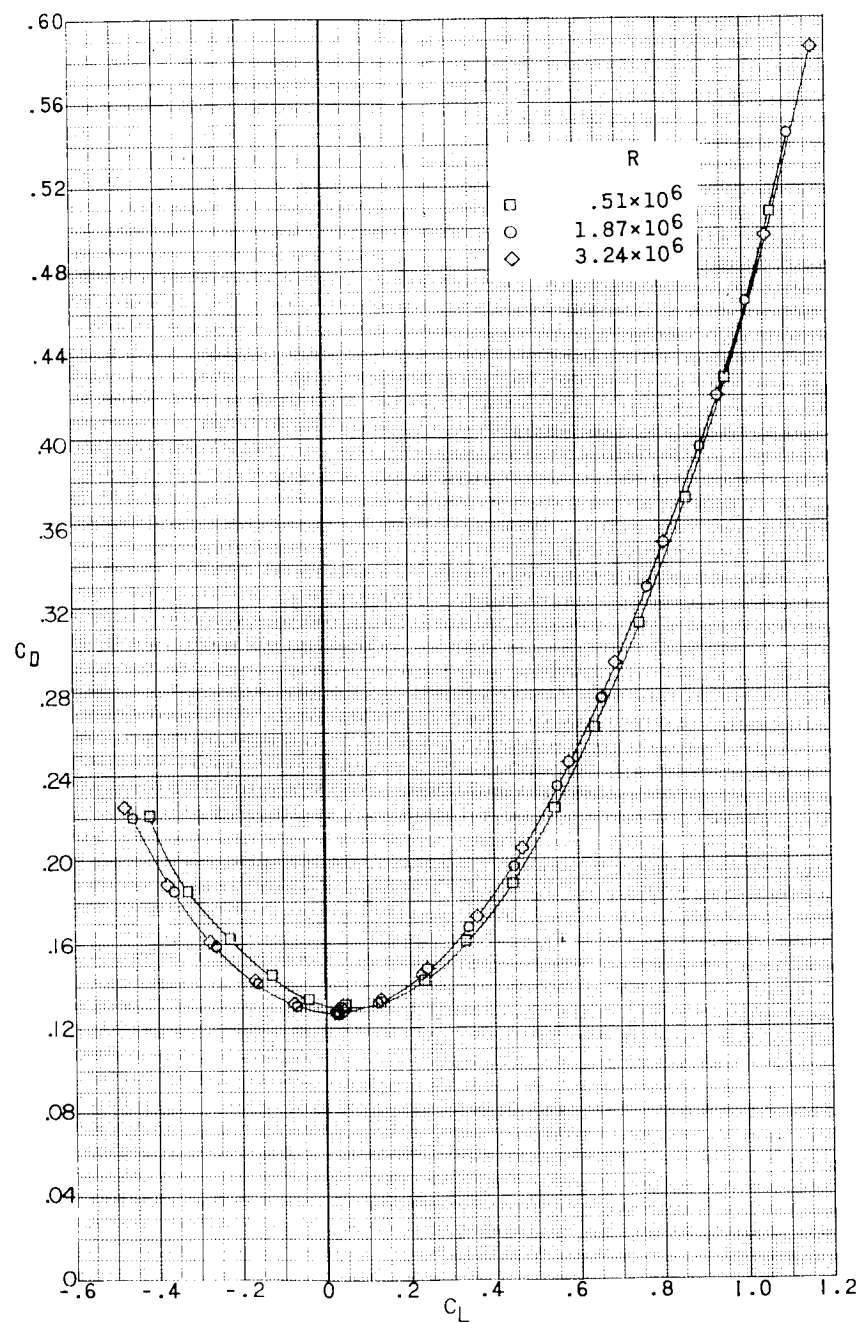
Figure 12-- Pitch characteristics of a 0.067-scale model of the X-15 airplane at various Reynolds numbers. Complete model; speed brakes open 35° .

CONFIDENTIAL

0319132A11030

~~CONFIDENTIAL~~

44

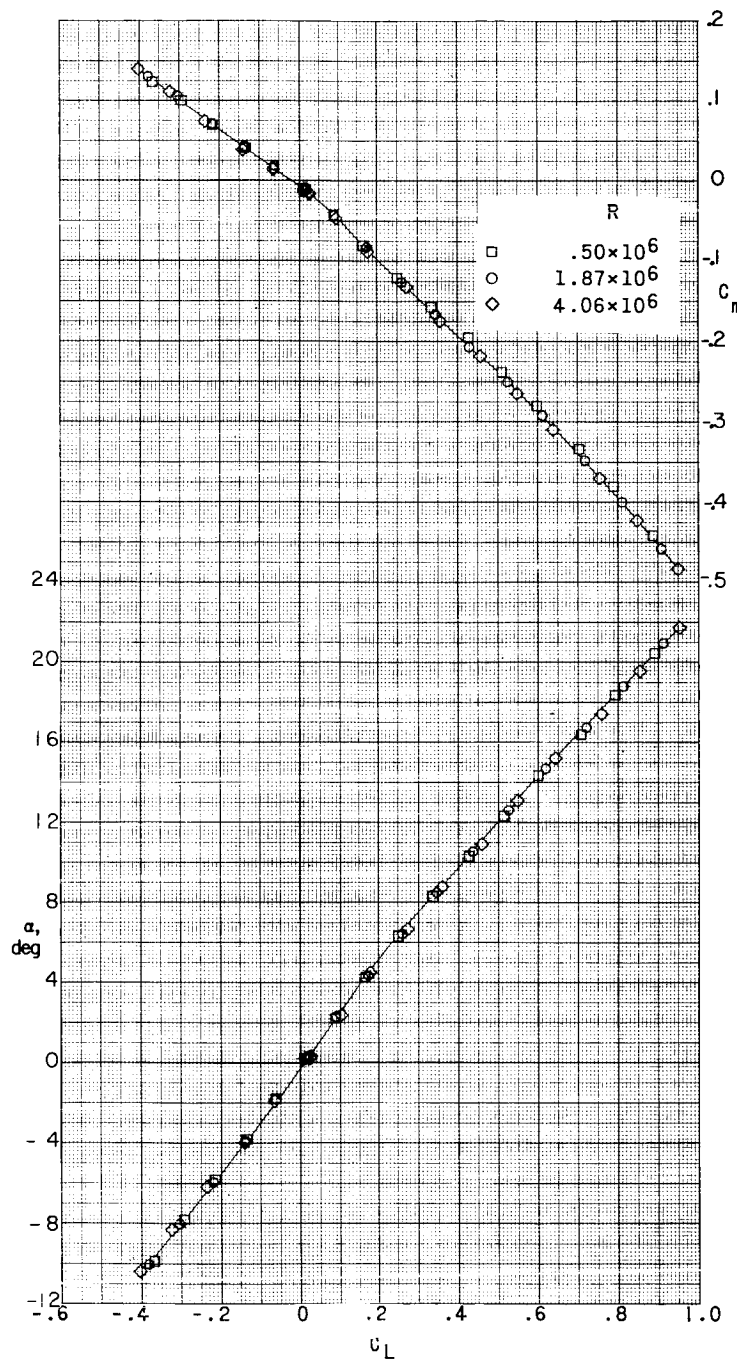


(a) Concluded.

Figure 12.- Continued.

~~CONFIDENTIAL~~

45

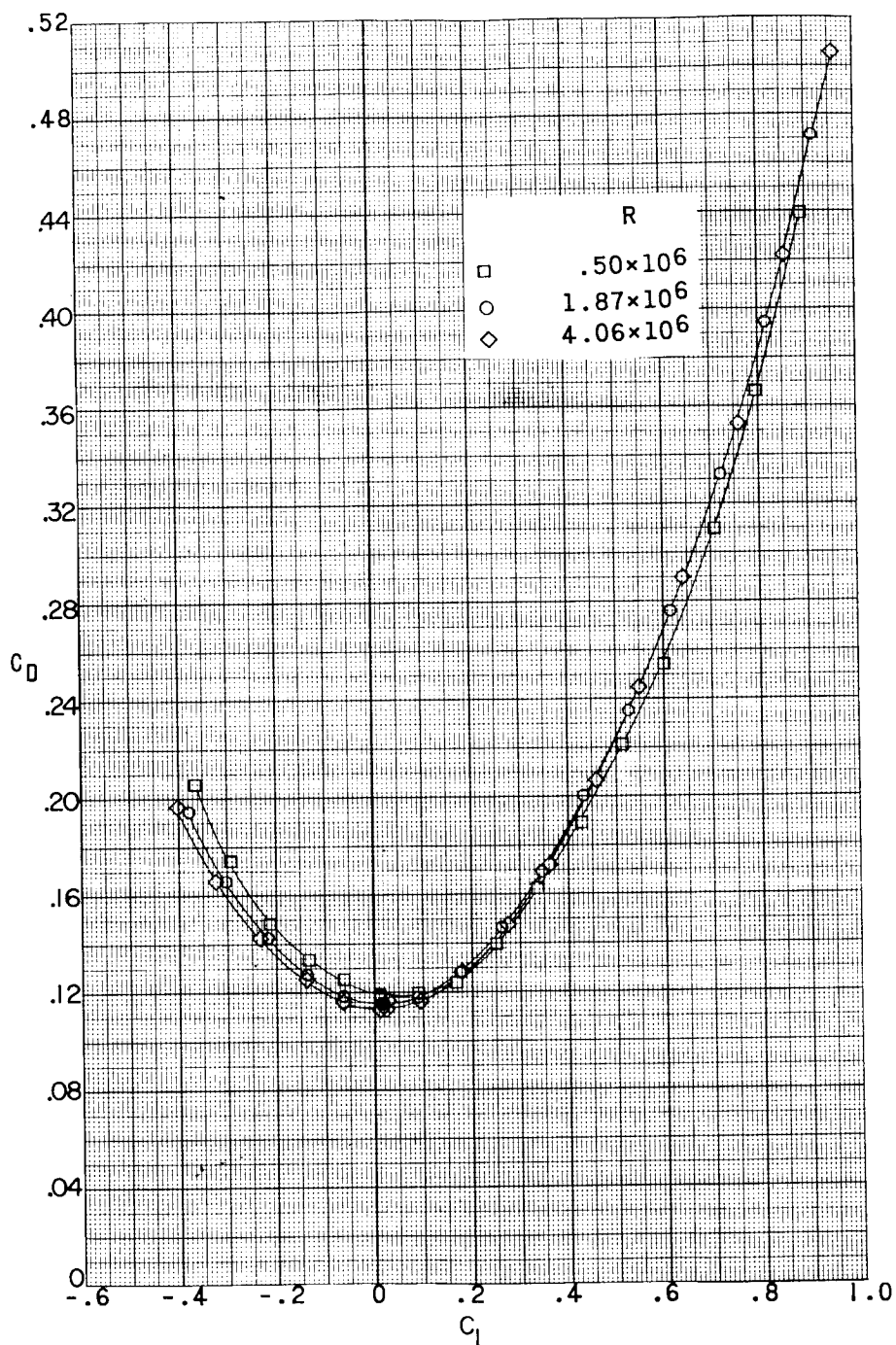


(b) $M = 2.98$.

Figure 12.- Continued.

L-351

CONFIDENTIAL



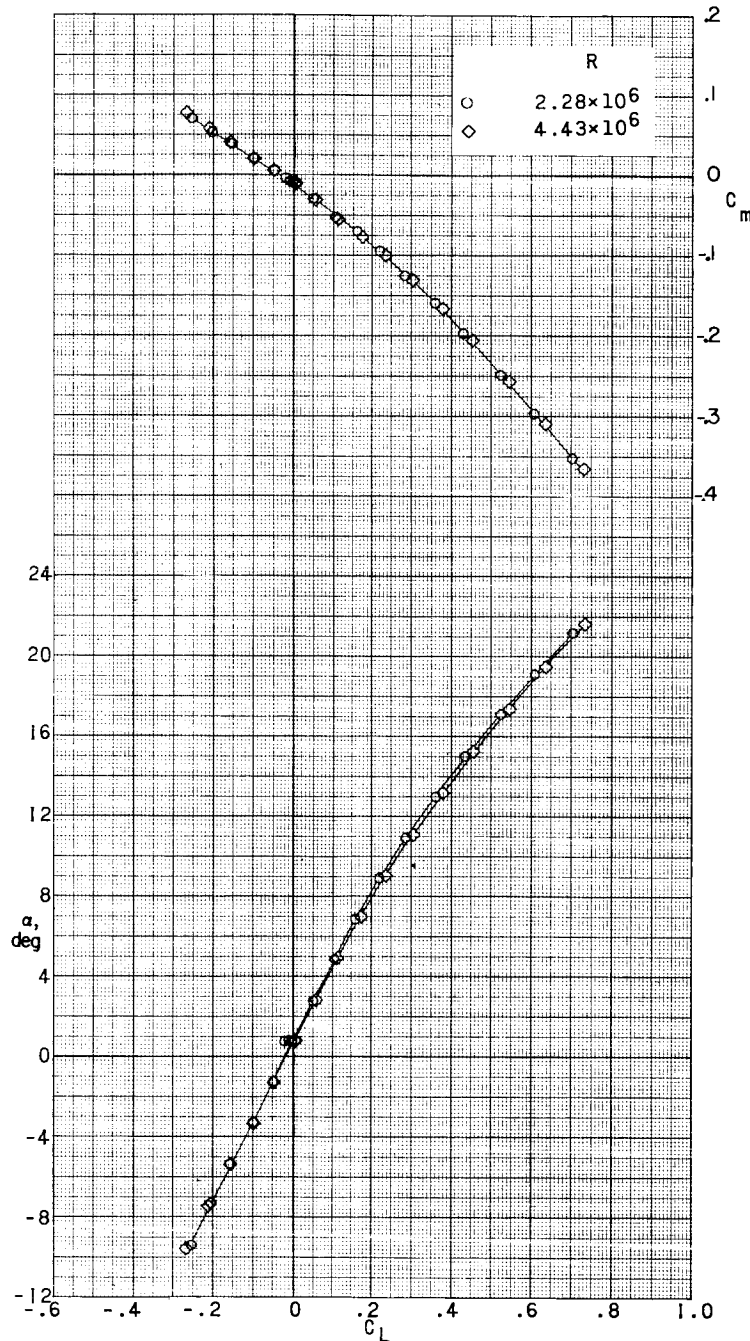
(b) Concluded.

Figure 12.- Continued.

DECLASSIFIED

CONFIDENTIAL

47

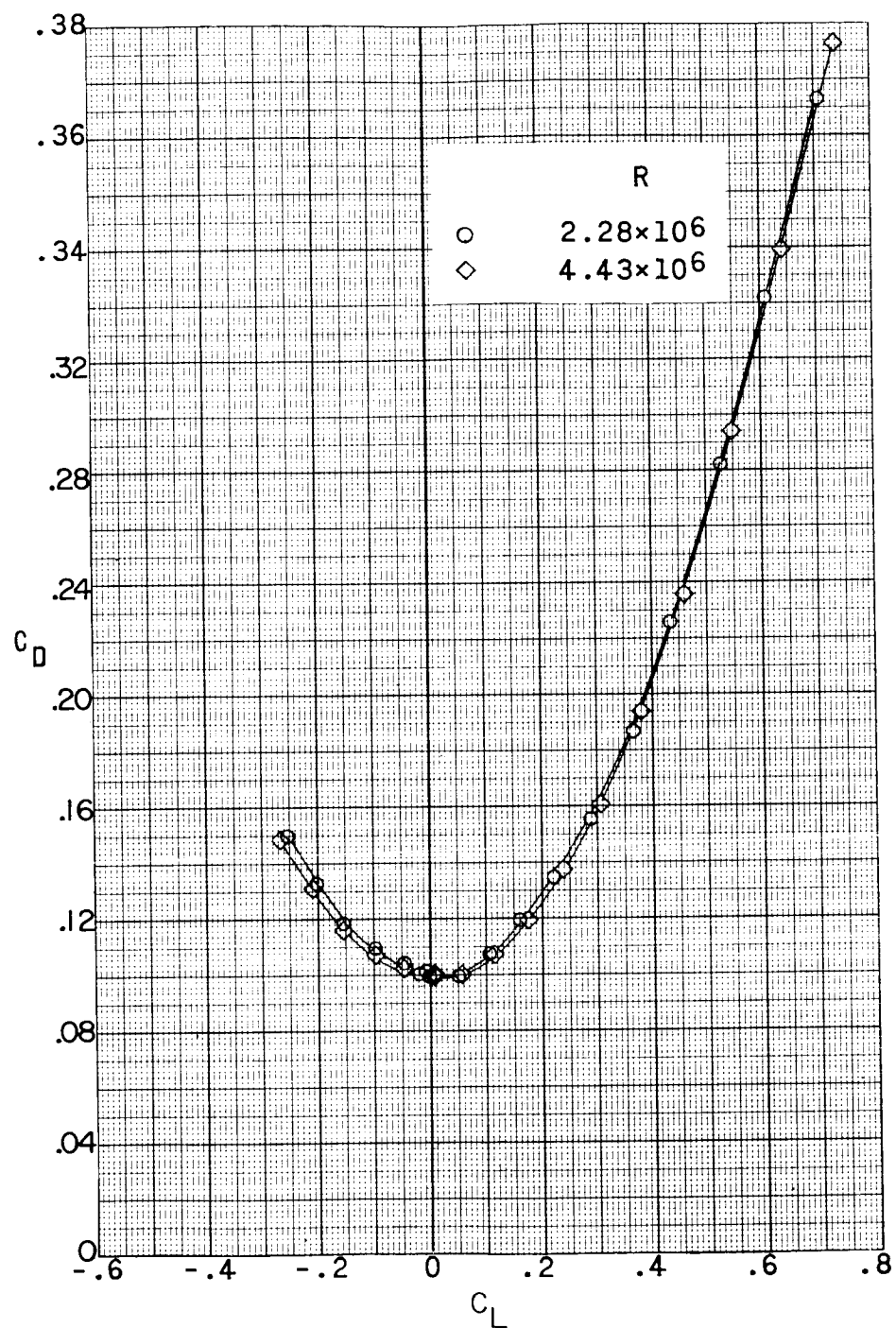


(c) $M = 4.65.$

Figure 12.- Continued.

I-351

CONFIDENTIAL



(c) Concluded.

Figure 12.- Concluded.

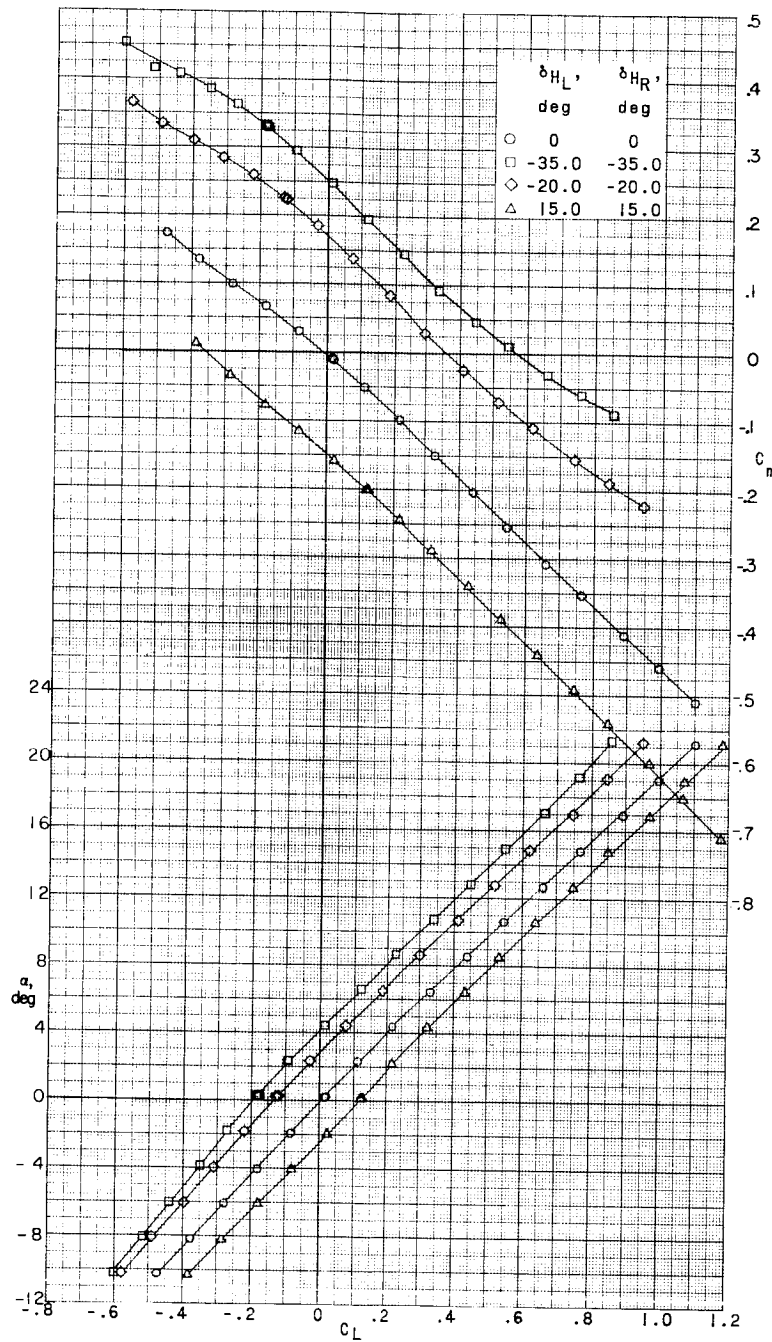
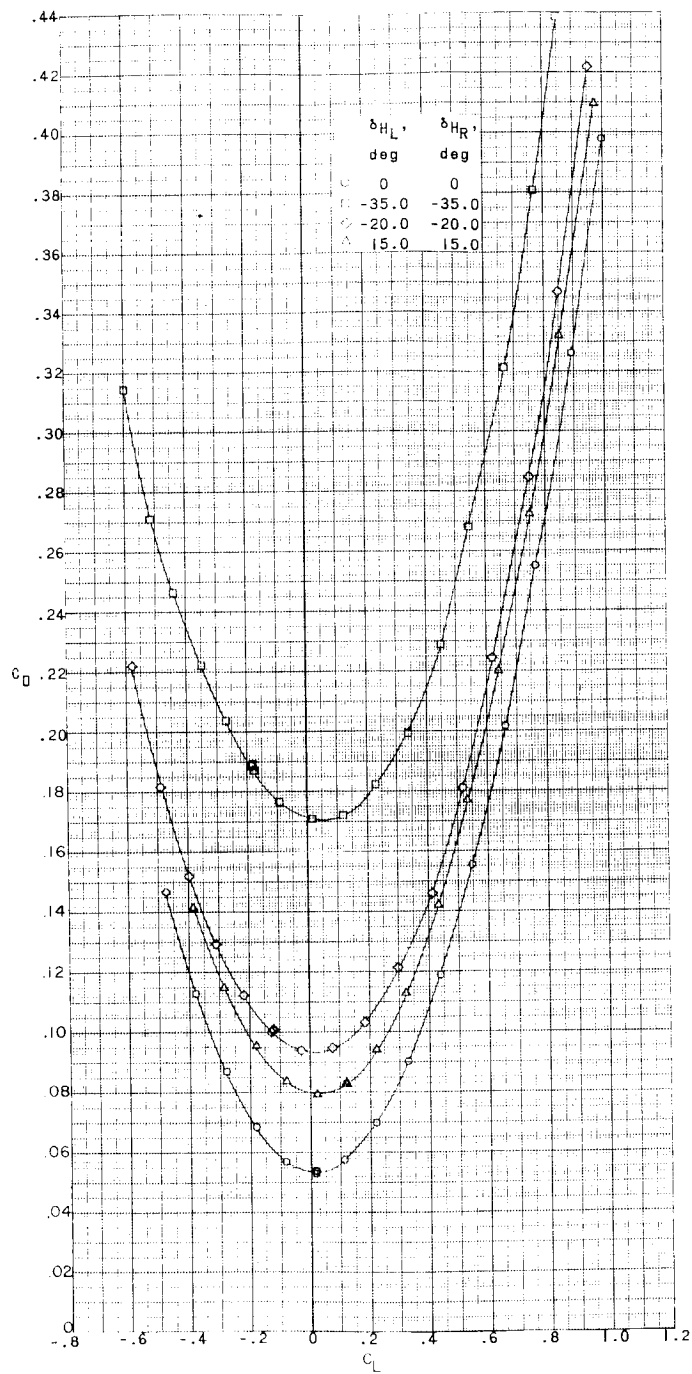
DECLASSIFIED
~~CONFIDENTIAL~~(a) $M = 2.29.$

Figure 13.- Pitch characteristics of a 0.067-scale model of the X-15 airplane with various pitch-control deflections of the horizontal tail. Speed brakes retracted; $\delta_v = 0^\circ$.

031712261030

~~CONFIDENTIAL~~

50



(a) Concluded.

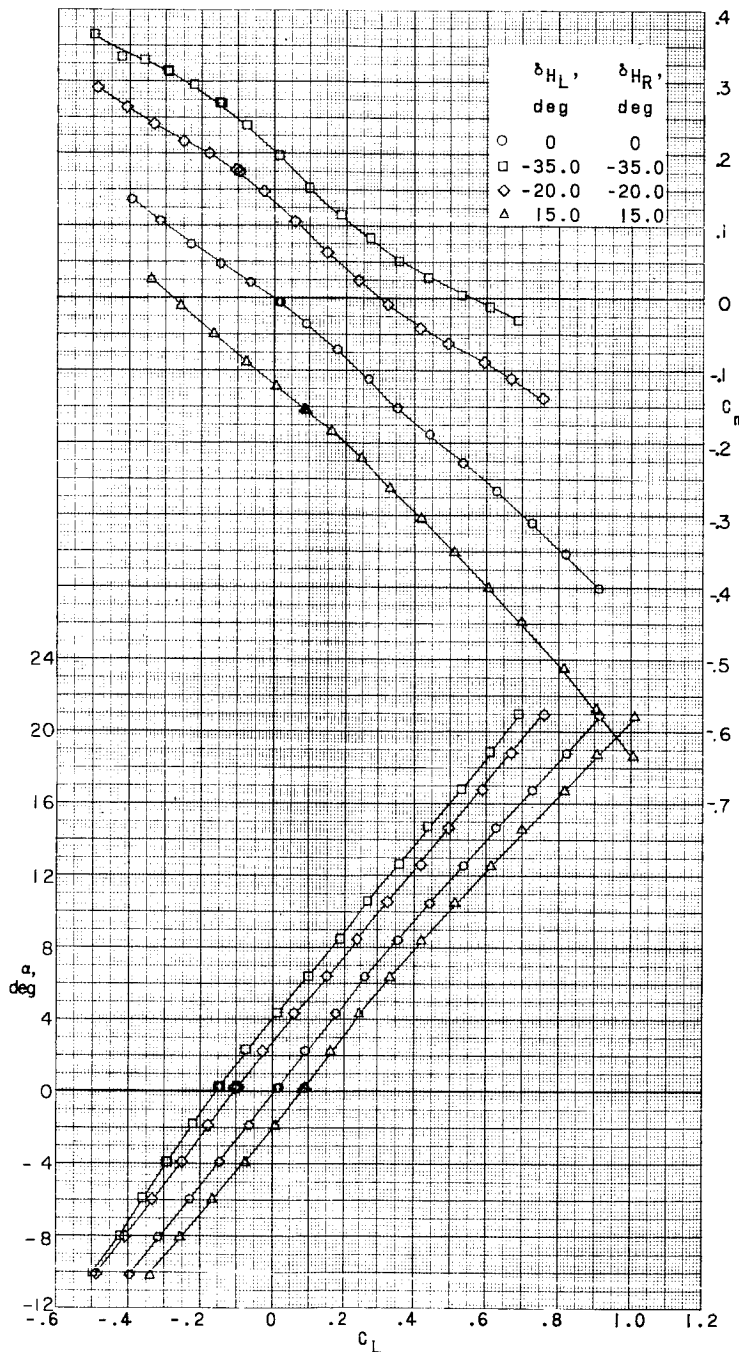
Figure 13.- Continued.

[I-35]

~~CONFIDENTIAL~~

DECLASSIFIED

51

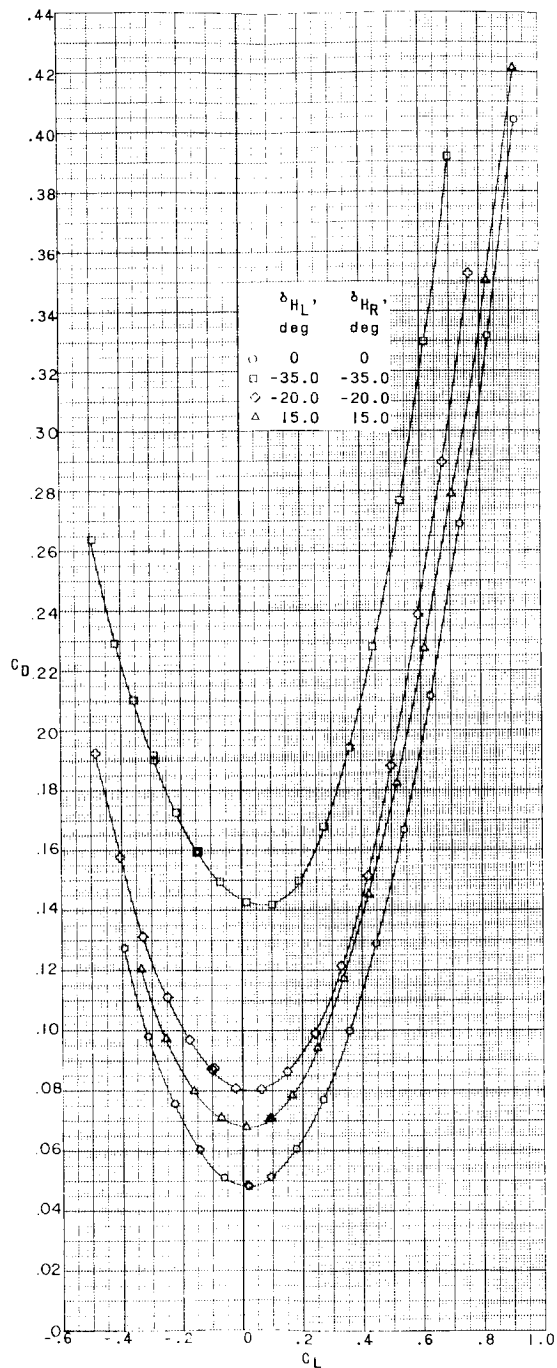


(b) $M = 2.98$.

Figure 13.- Continued.

~~CONFIDENTIAL~~

L-351

031312341030
CONFIDENTIAL

(b) Concluded.

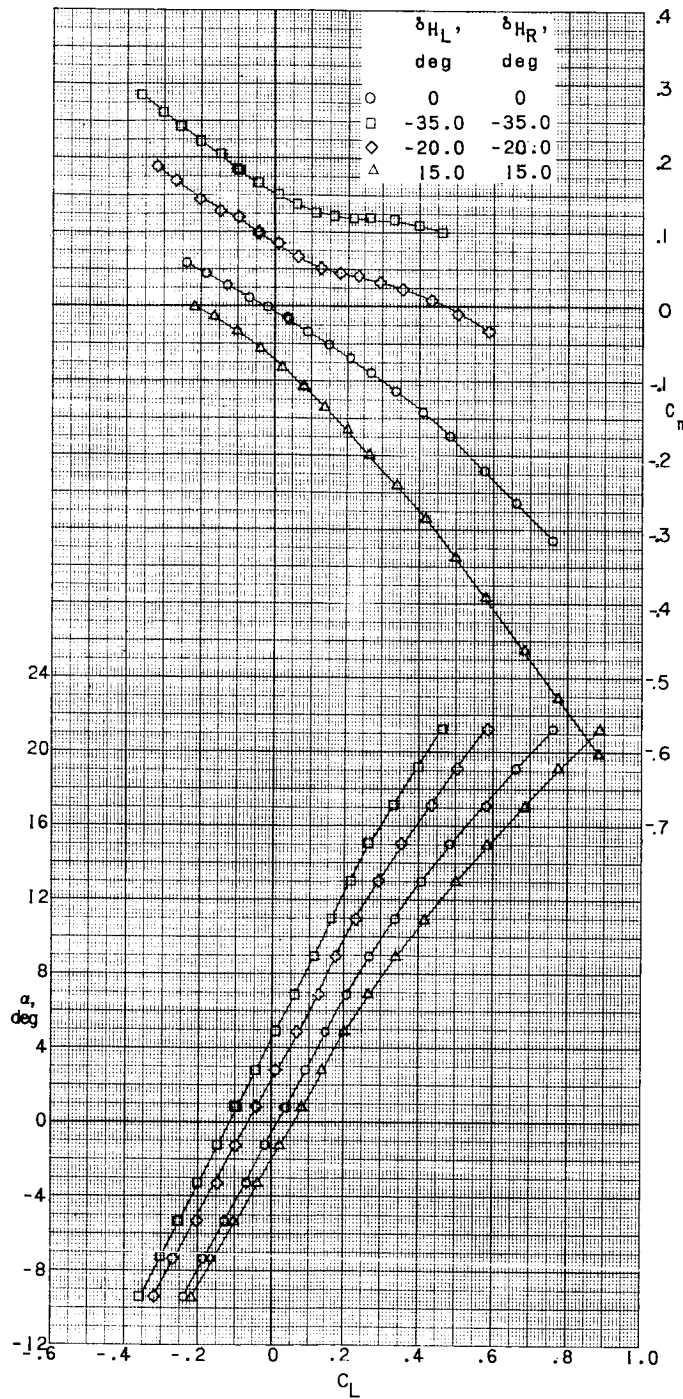
Figure 13.- Continued.

CONFIDENTIAL

DECLASSIFIED

~~CONFIDENTIAL~~

53



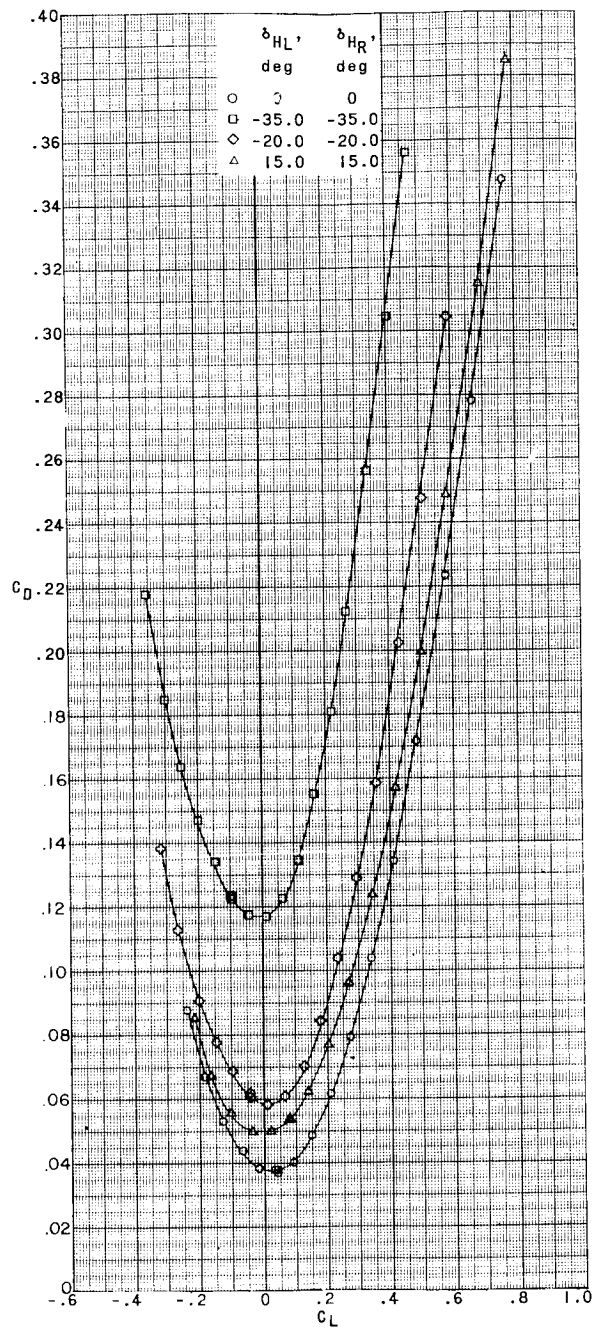
(c) $M = 4.65$.

Figure 13.- Continued.

L-351

0311020 1030

L-351



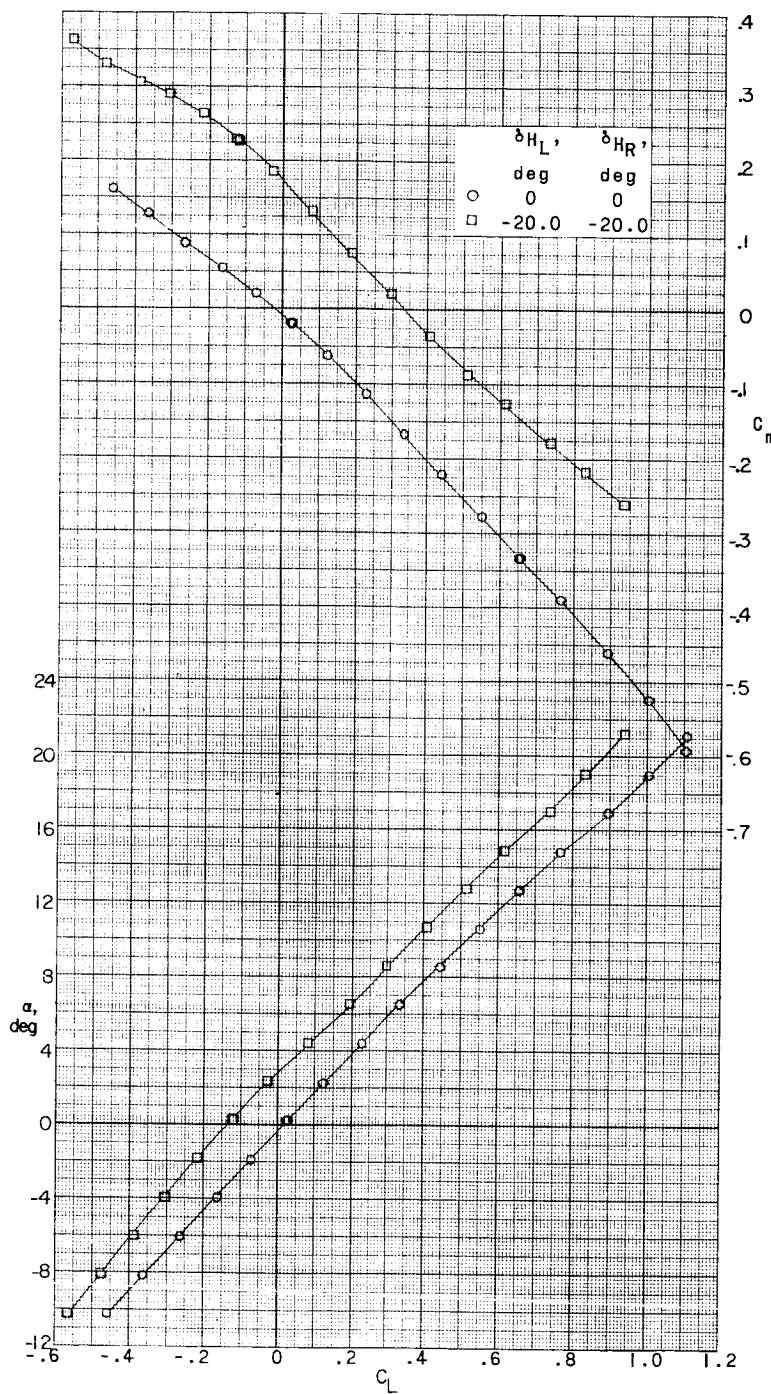
(c) Concluded.

Figure 13.- Concluded.

DECLASSIFIED

~~CONFIDENTIAL~~

55

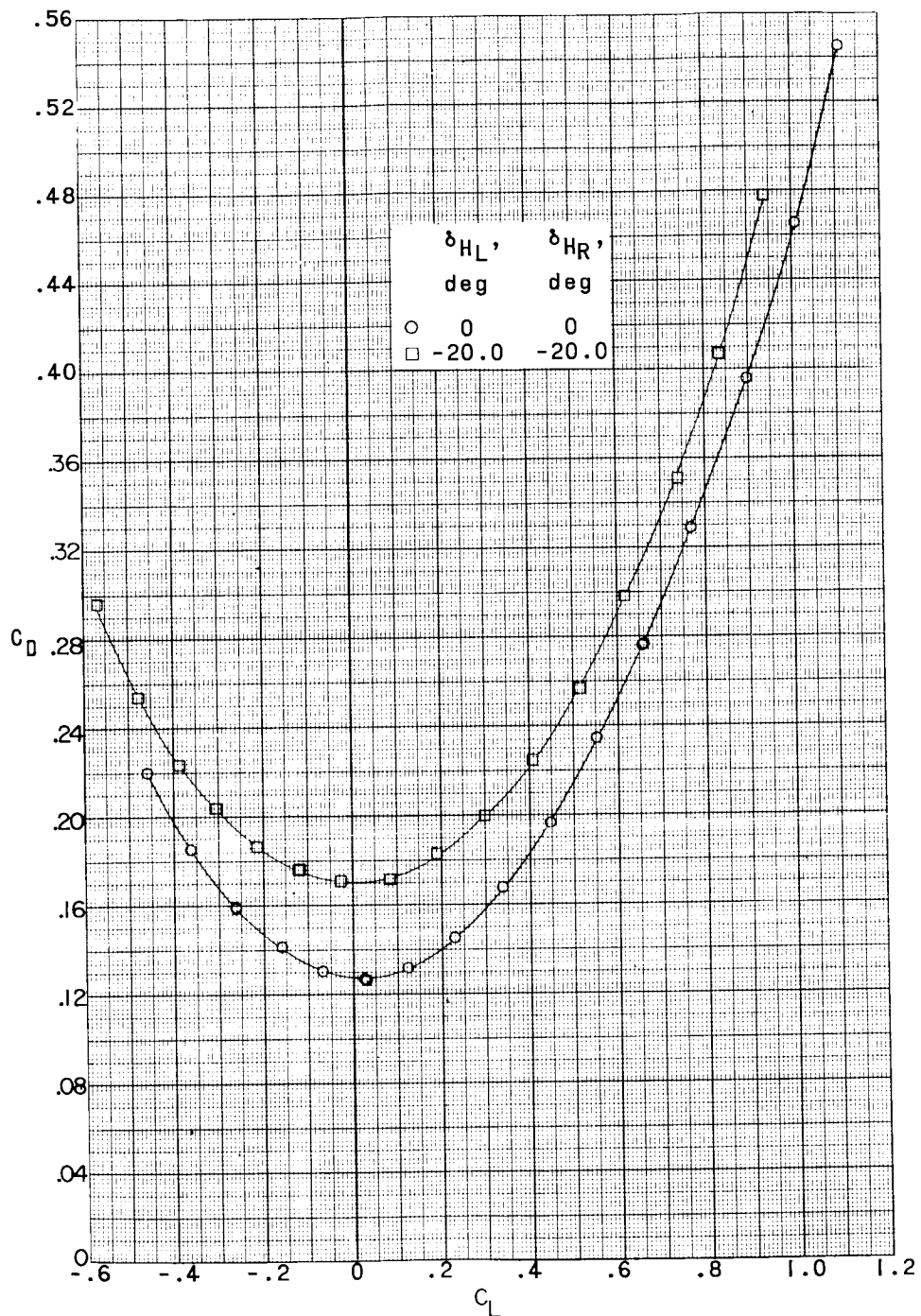


(a) $M = 2.29$.

Figure 14.- Pitch characteristics of a 0.067-scale model of the X-15 airplane with various pitch-control deflections of the horizontal tail. Speed brakes retracted; $\delta_V = 0^\circ$.

O [REDACTED]

L-351

03171820 1030
~~CONFIDENTIAL~~

(a) Concluded.

Figure 14.- Continued.

DECLASSIFIED

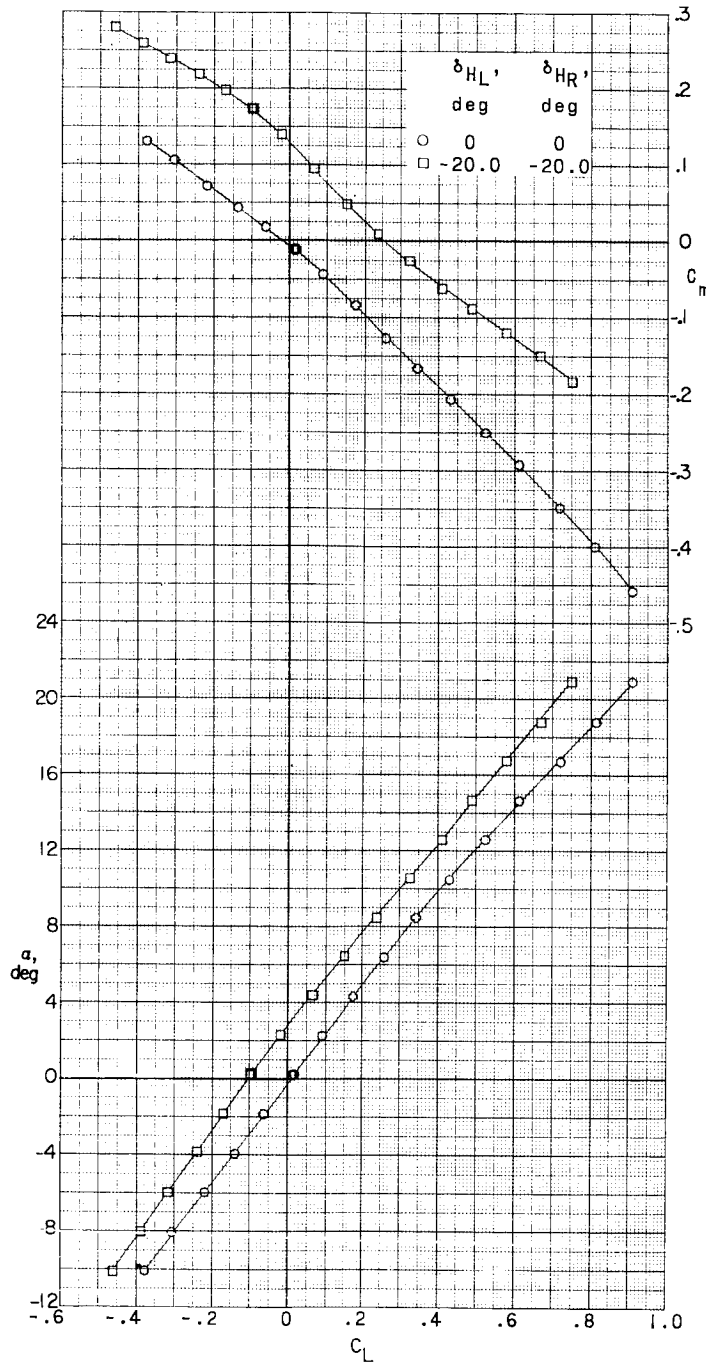
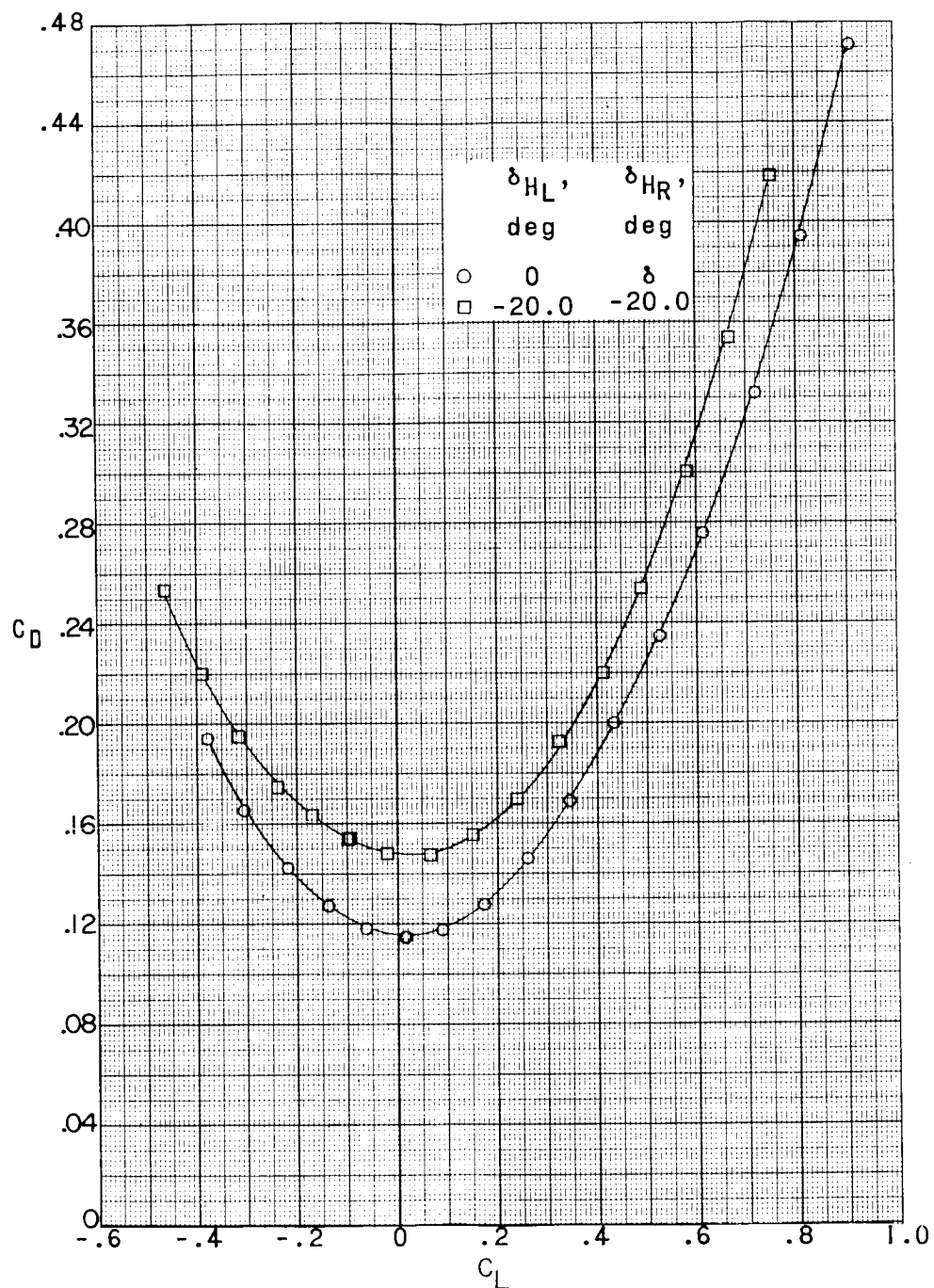
~~CONFIDENTIAL~~(b) $M = 2.98.$

Figure 14.- Continued.

03171220 1030

58



(b) Concluded.

Figure 14.- Continued.

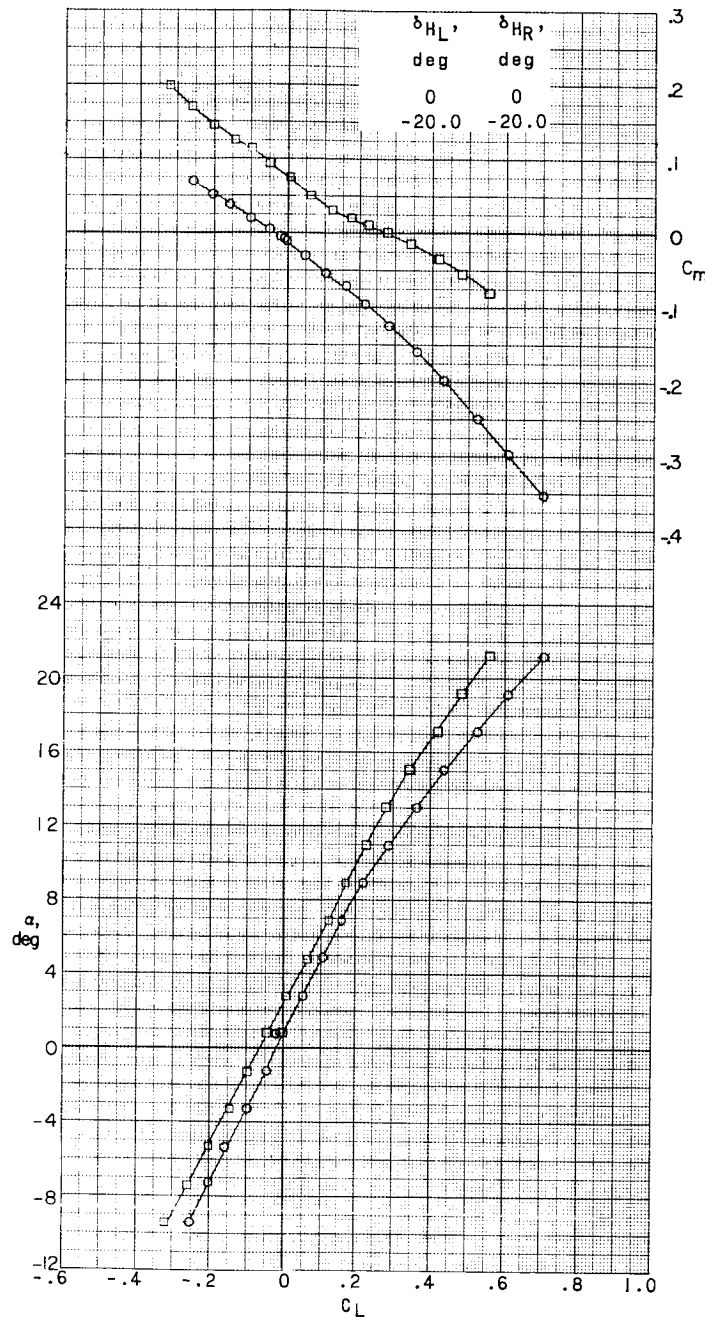
~~CONFIDENTIAL~~

1351

DECLASSIFIED

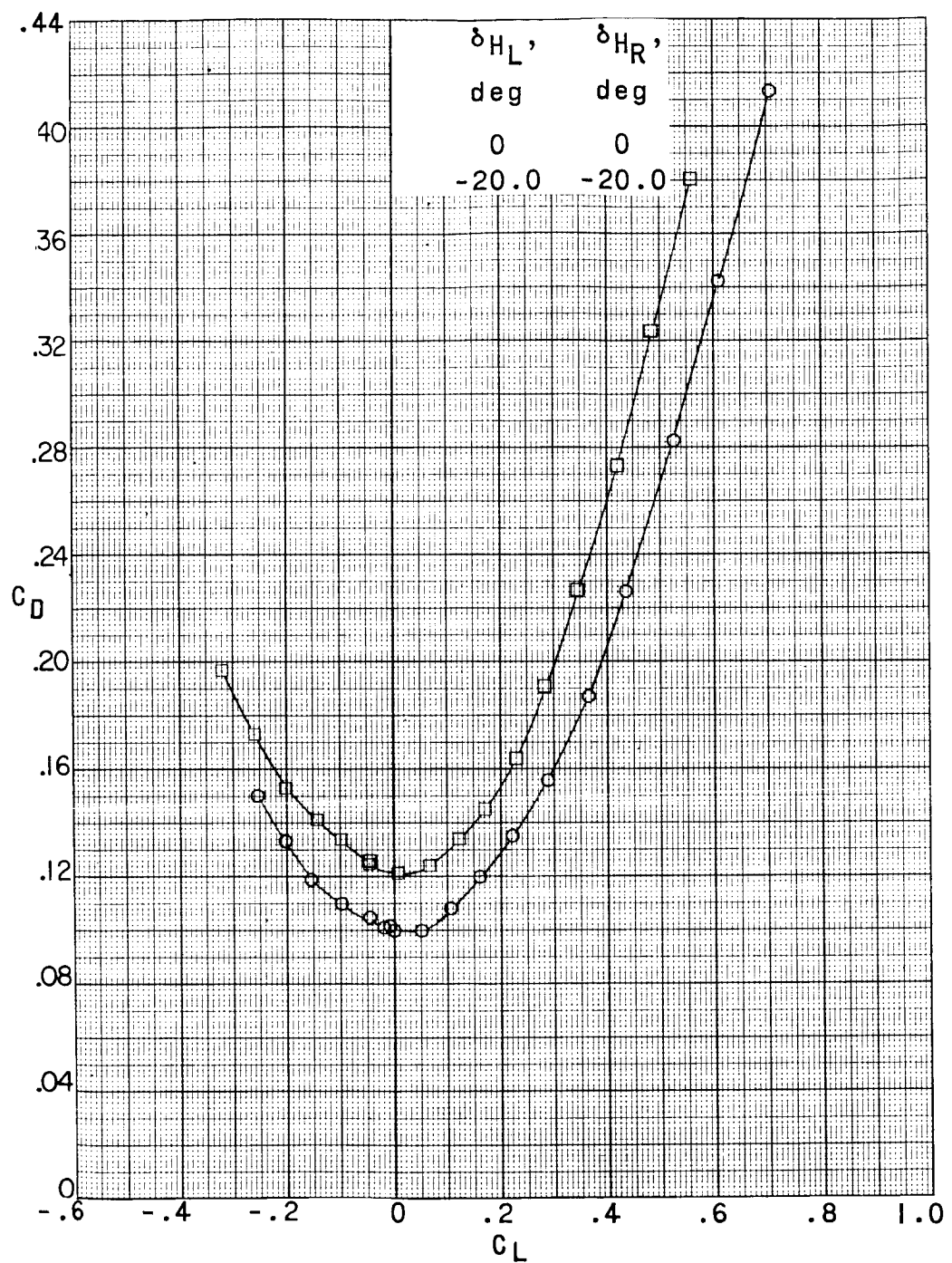
~~CONFIDENTIAL~~

59



(c) $M = 4.65$.

Figure 14.- Continued.

03171820 1030
~~FOR INFORMATION~~

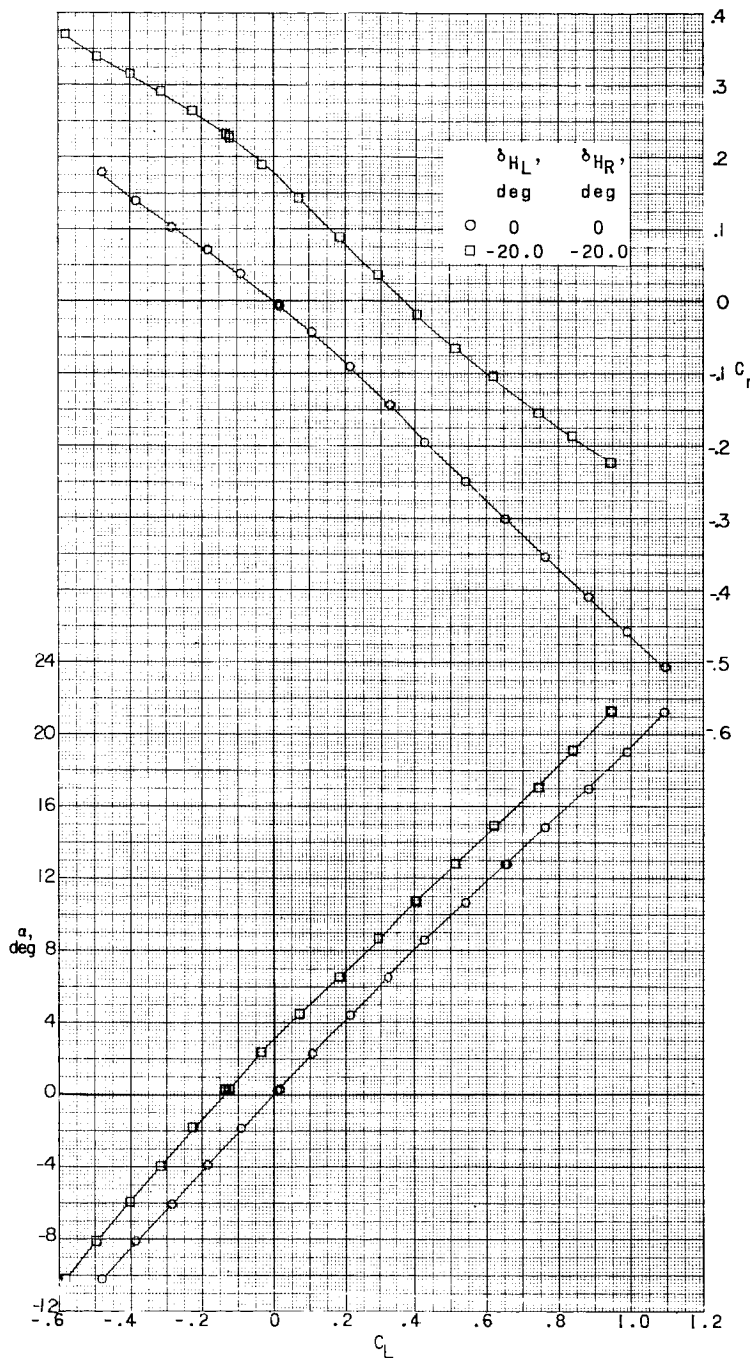
(c) Concluded.

Figure 14.- Concluded.

~~CONFIDENTIAL~~

DECCLASSIFIED

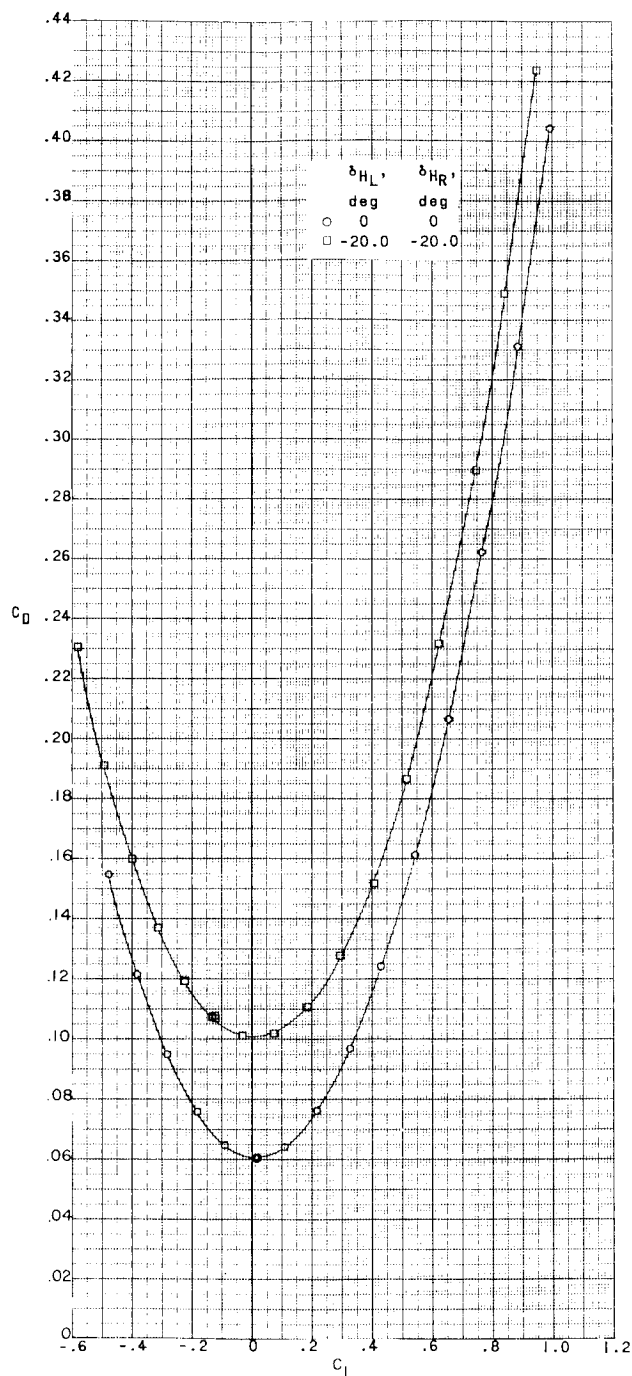
61



(a) $M = 2.29.$

Figure 15.- Pitch characteristics of a 0.067-scale model of the X-15 airplane with various pitch-control deflections of the horizontal tail. Speed brakes retracted; $\delta_v = -7.5^\circ$.

03171820 1030

~~CONFIDENTIAL~~

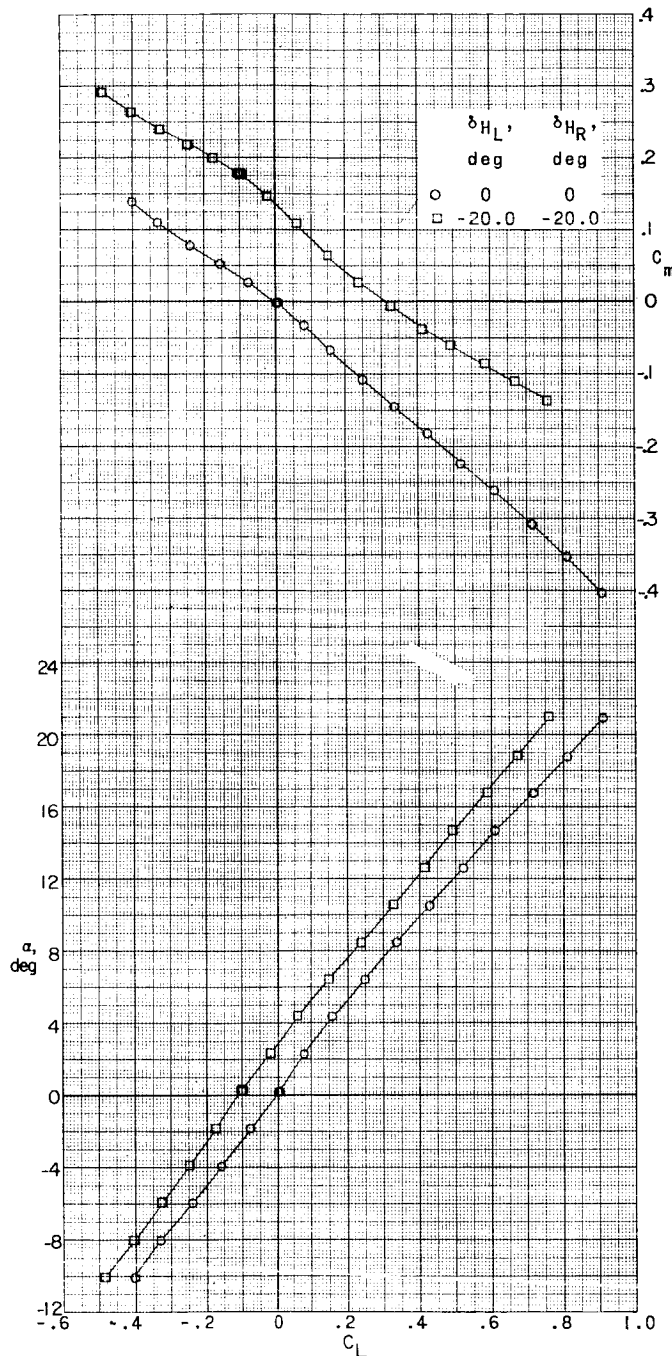
(a) Concluded.

Figure 15.- Continued.

~~CONFIDENTIAL~~

CONFIDENTIAL

63

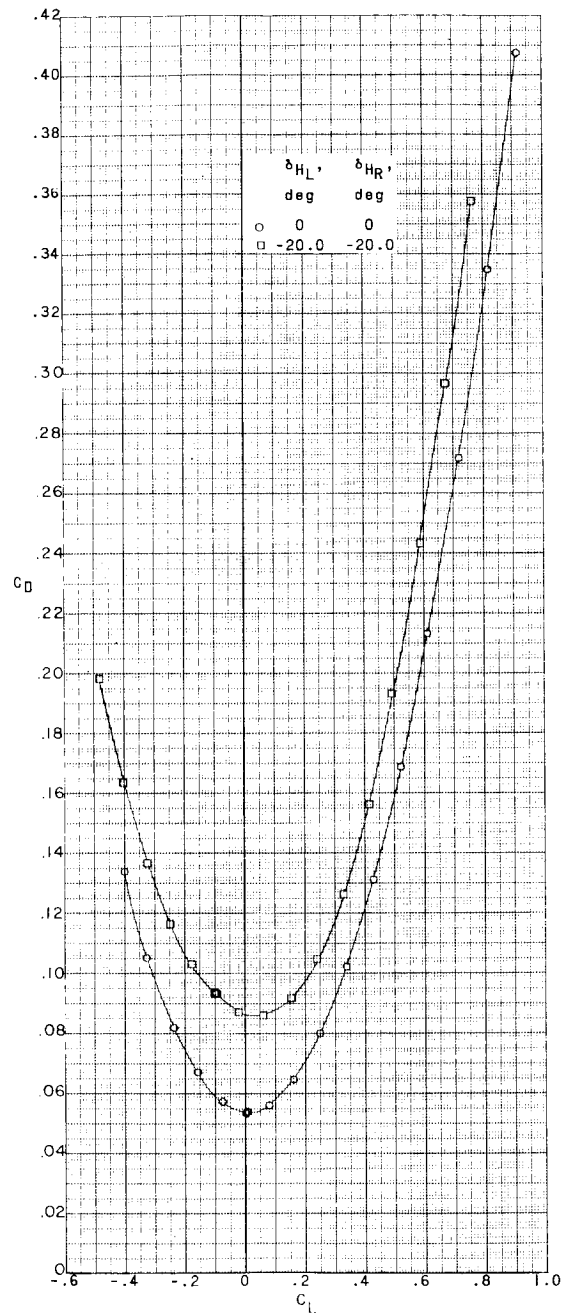


(b) $M = 2.98$.

Figure 15.- Continued.

CONFIDENTIAL

L-551

03171320 1030
~~CONTINUED~~

(b) Concluded.

Figure 15.- Continued.

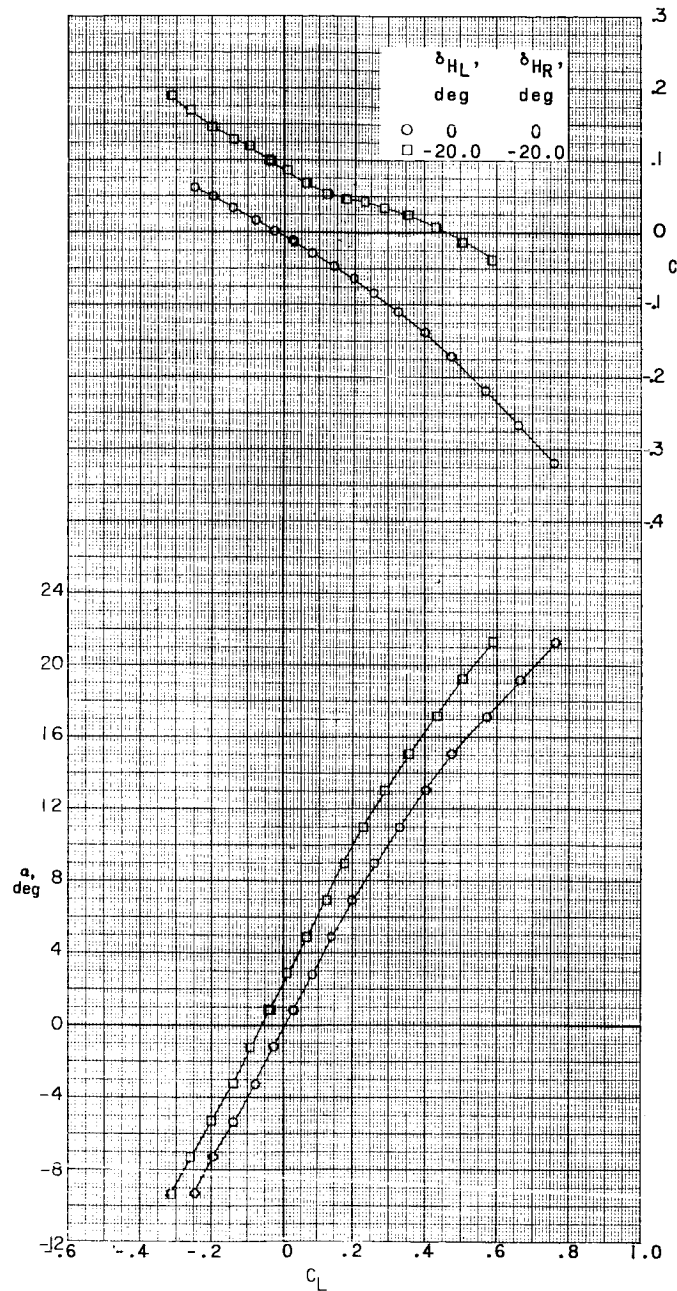
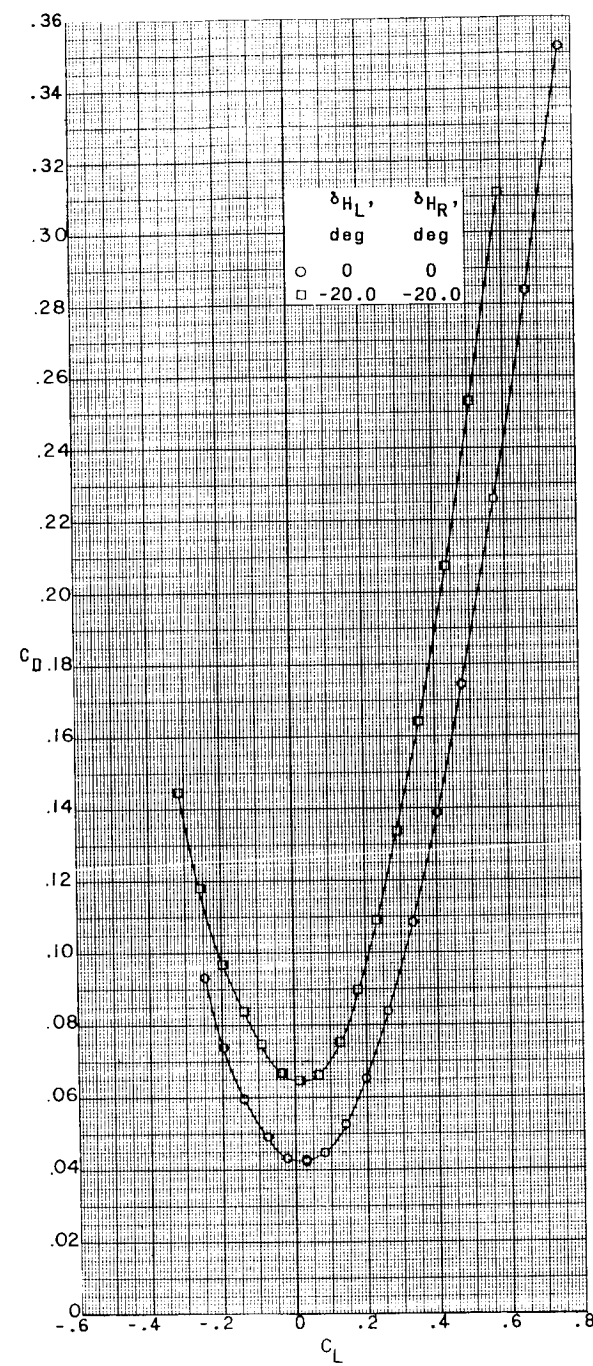
~~CONFIDENTIAL~~(c) $M = 4.65.$

Figure 15.- Continued.

CONFIDENTIAL

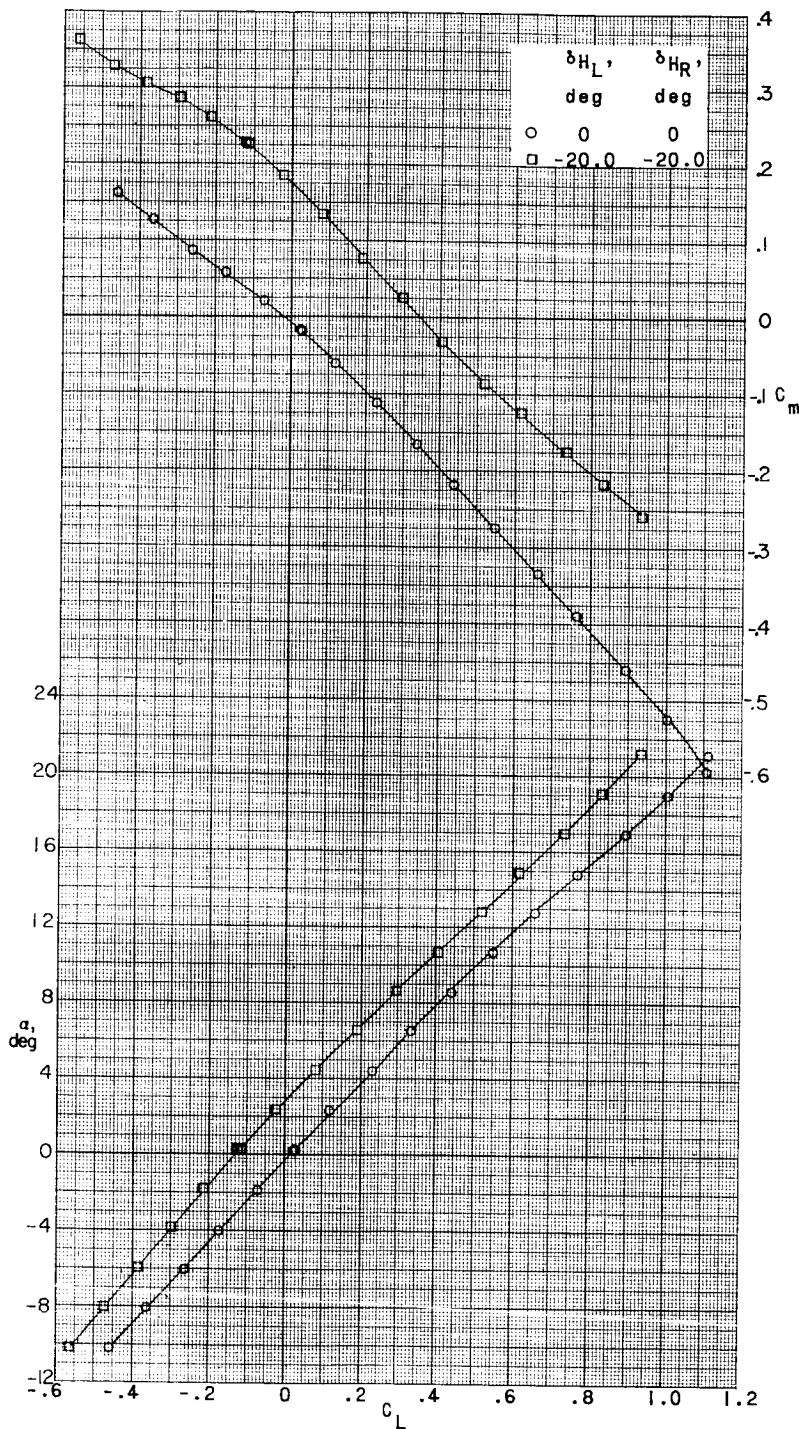


(c) Concluded.

Figure 15.- Concluded.

CONFIDENTIAL

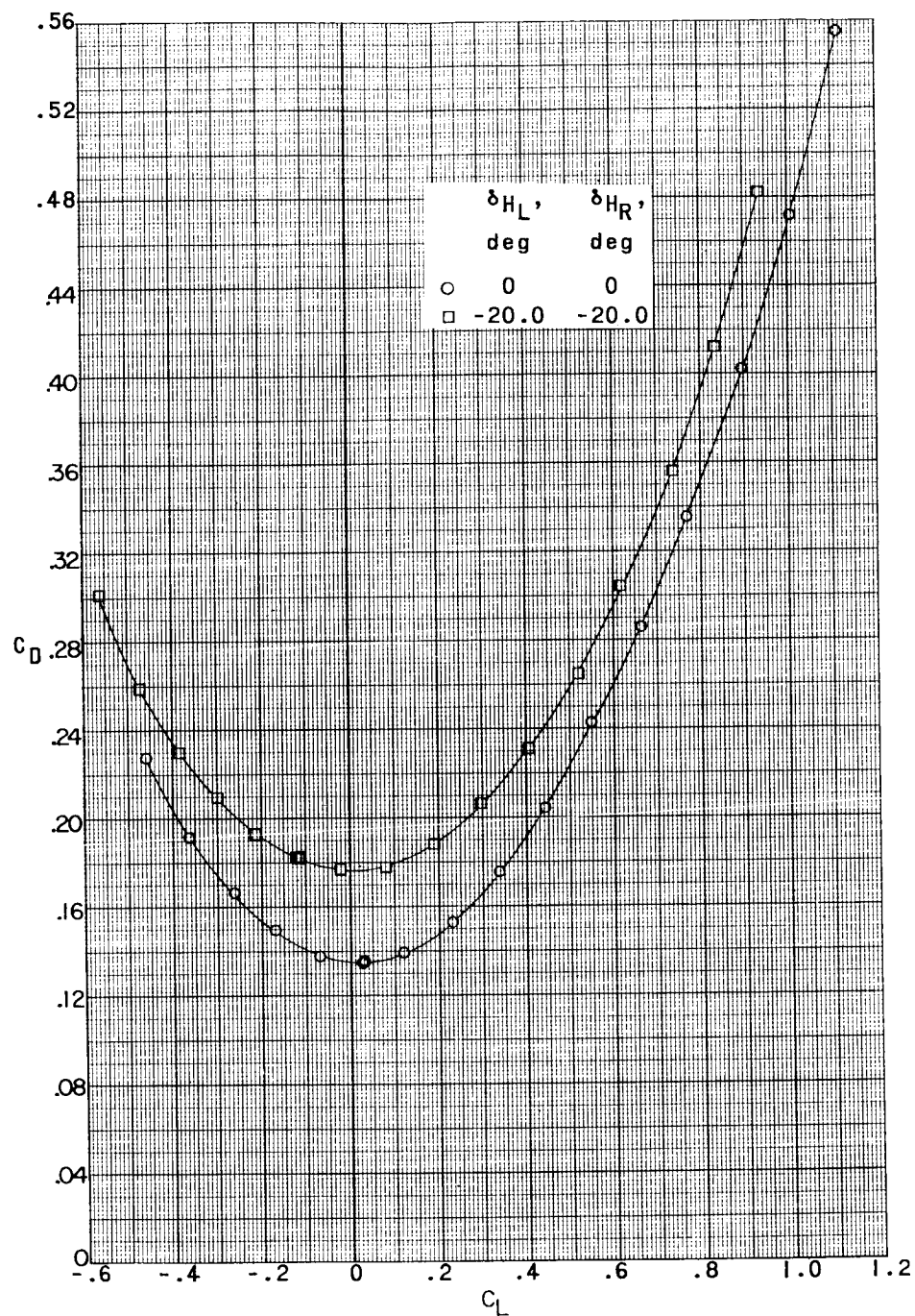
67



(a) $M = 2.29.$

Figure 16.- Pitch characteristics of a 0.067-scale model of the X-15 airplane with various pitch-control deflections of the horizontal tail. Speed brakes open; $\delta_v = -7.5^\circ$.

CONFIDENTIAL

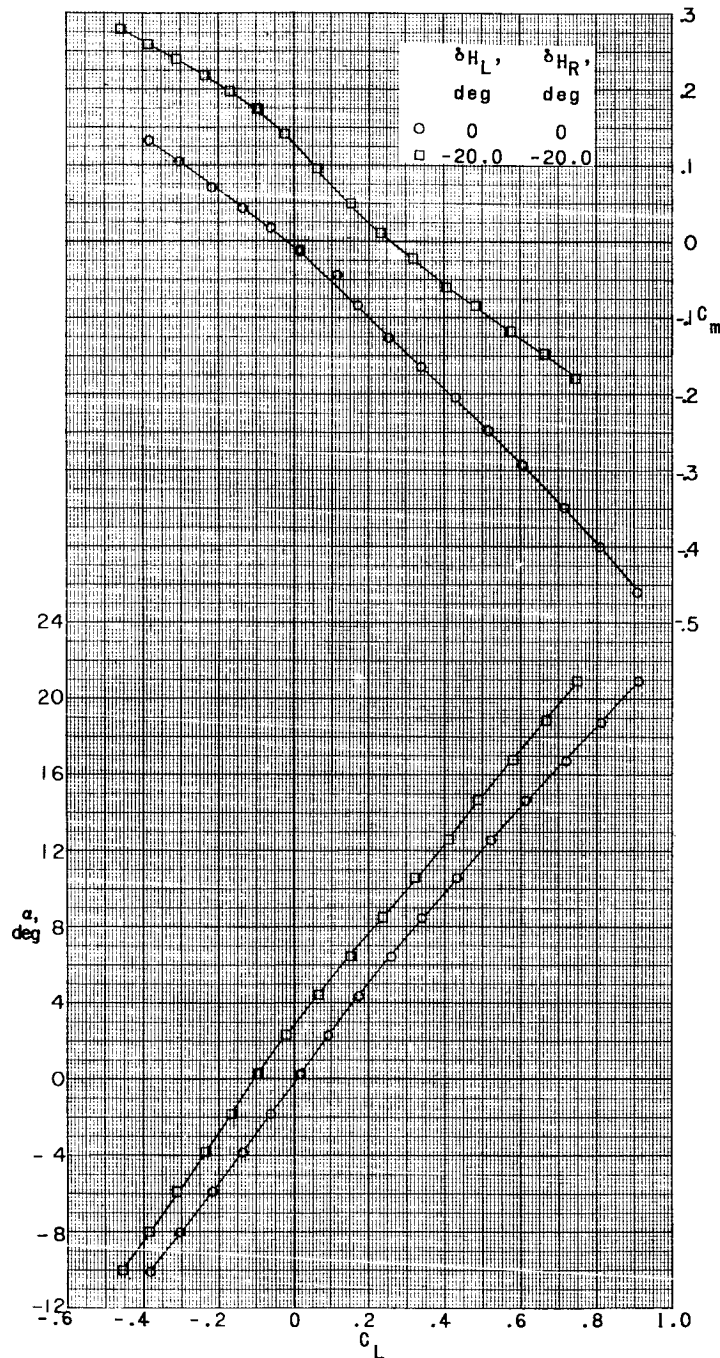


(a) Concluded.

Figure 16.- Continued.

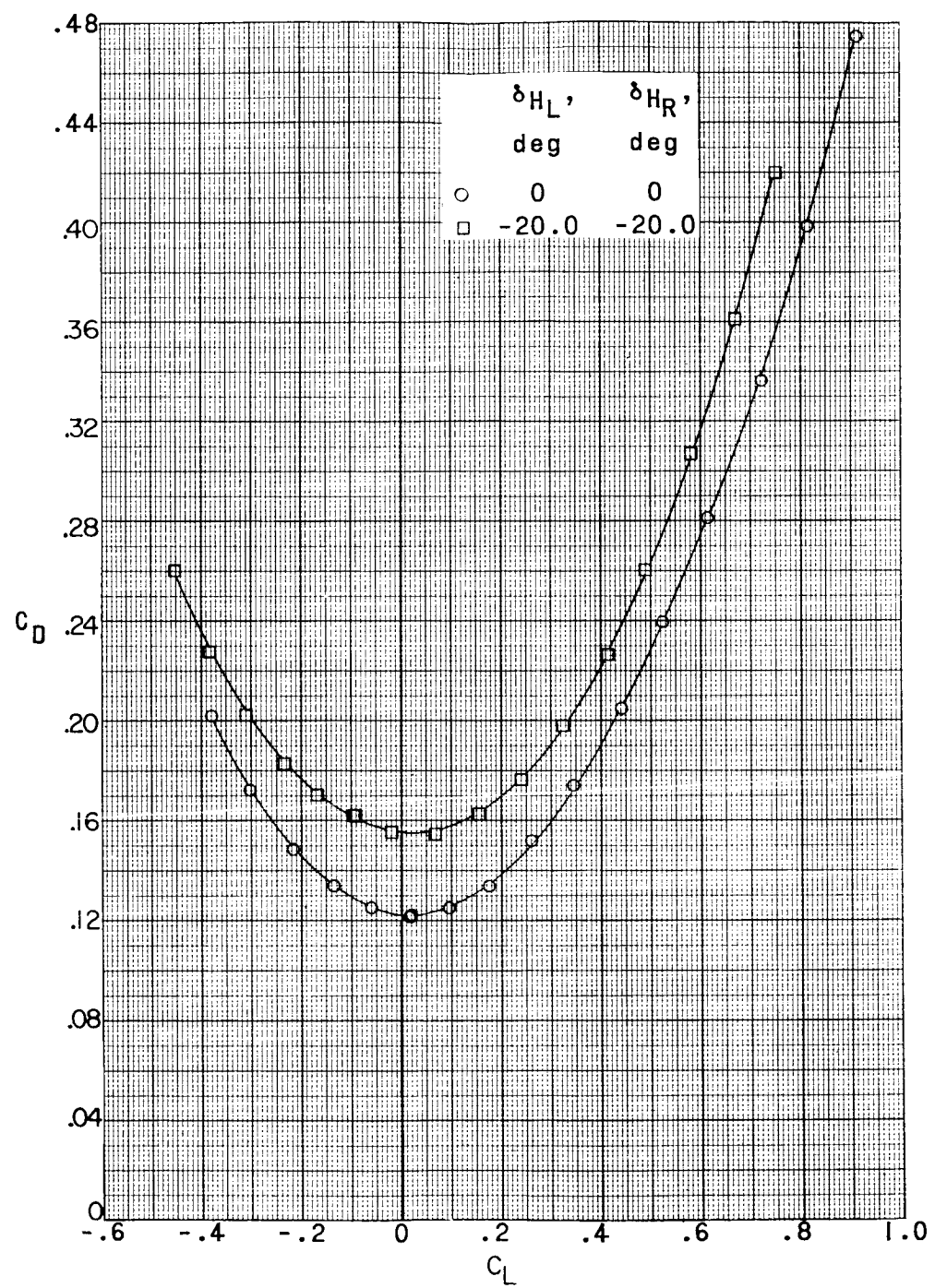
CONFIDENTIAL

69



(b) $M = 2.98$.

Figure 16.- Continued.

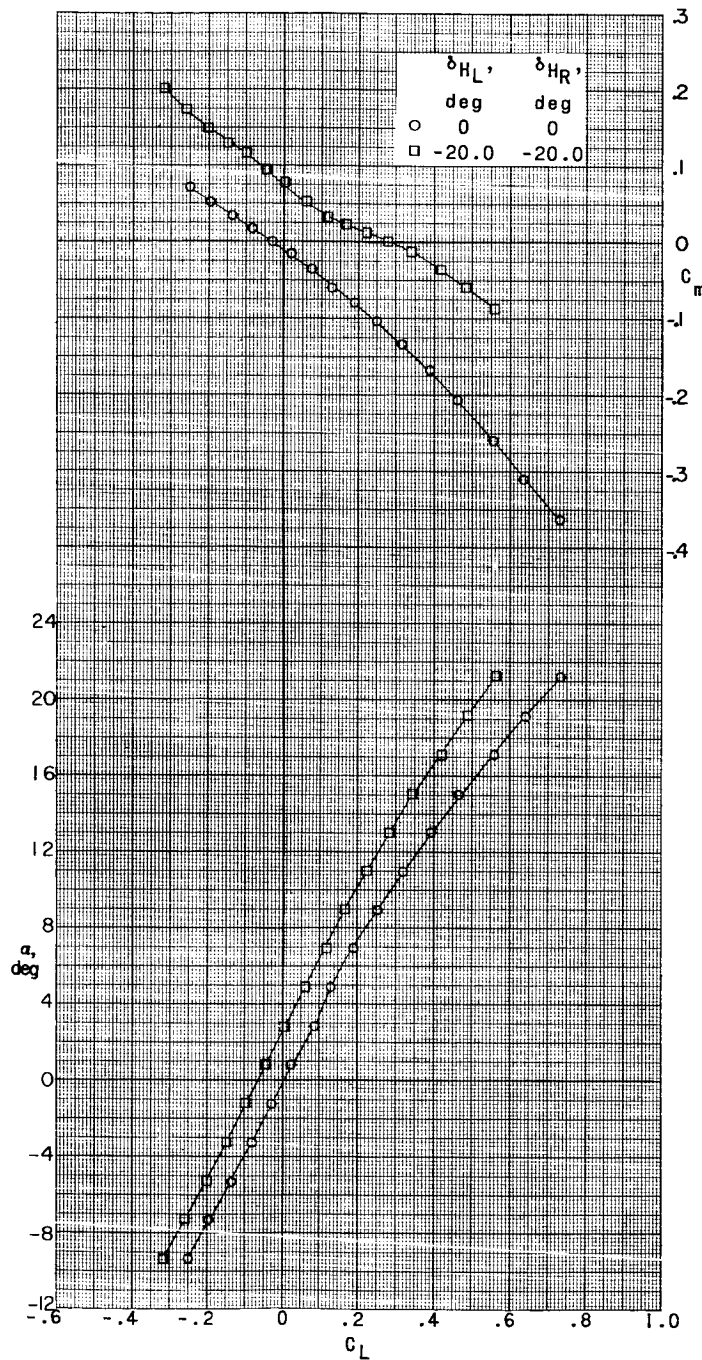


(b) Concluded.

Figure 16.- Continued.

~~CONFIDENTIAL~~

71



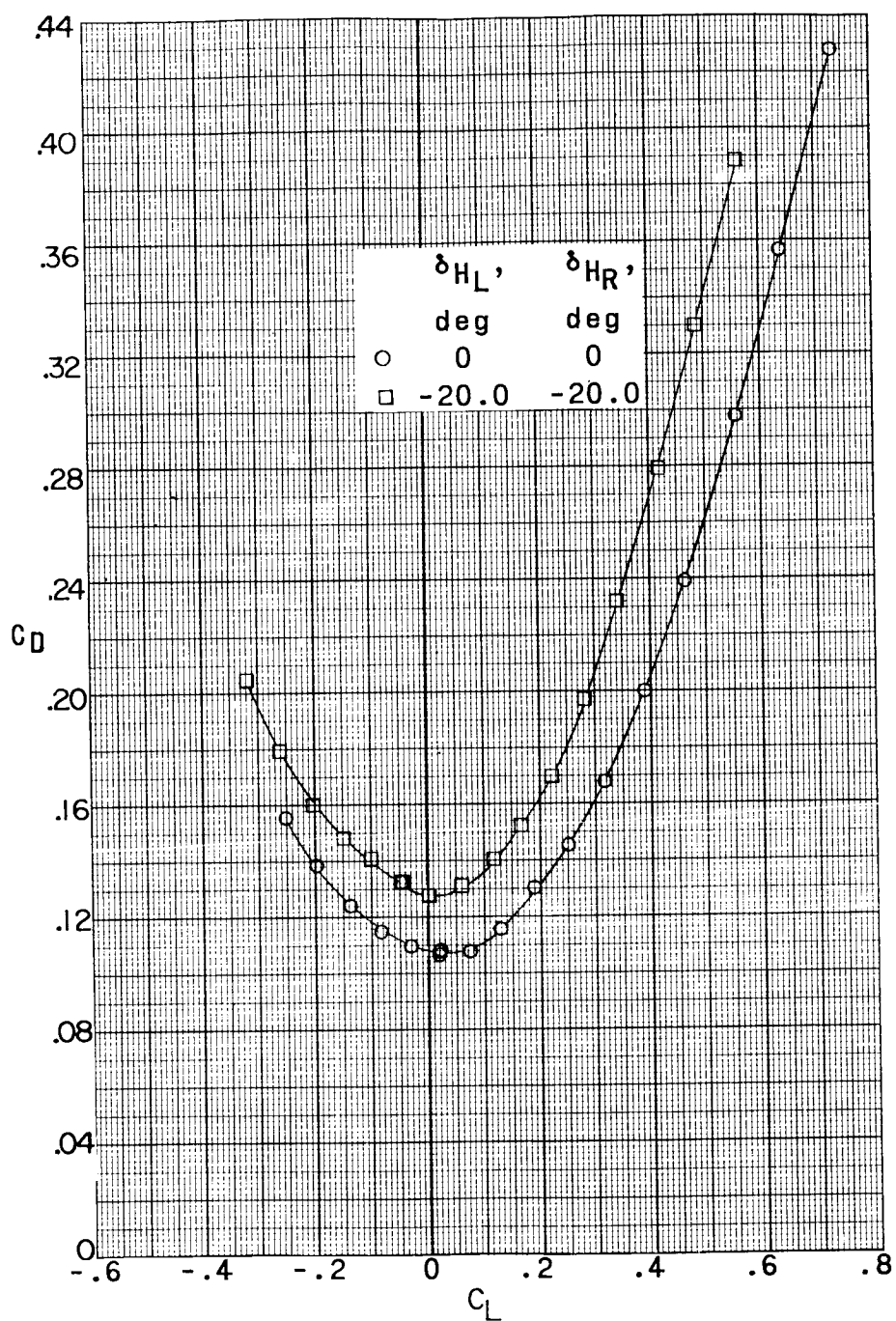
(c) $M = 4.65$.

Figure 16.- Continued.

037022A1030

~~CONFIDENTIAL~~

72



(c) Concluded.

Figure 16.- Concluded.

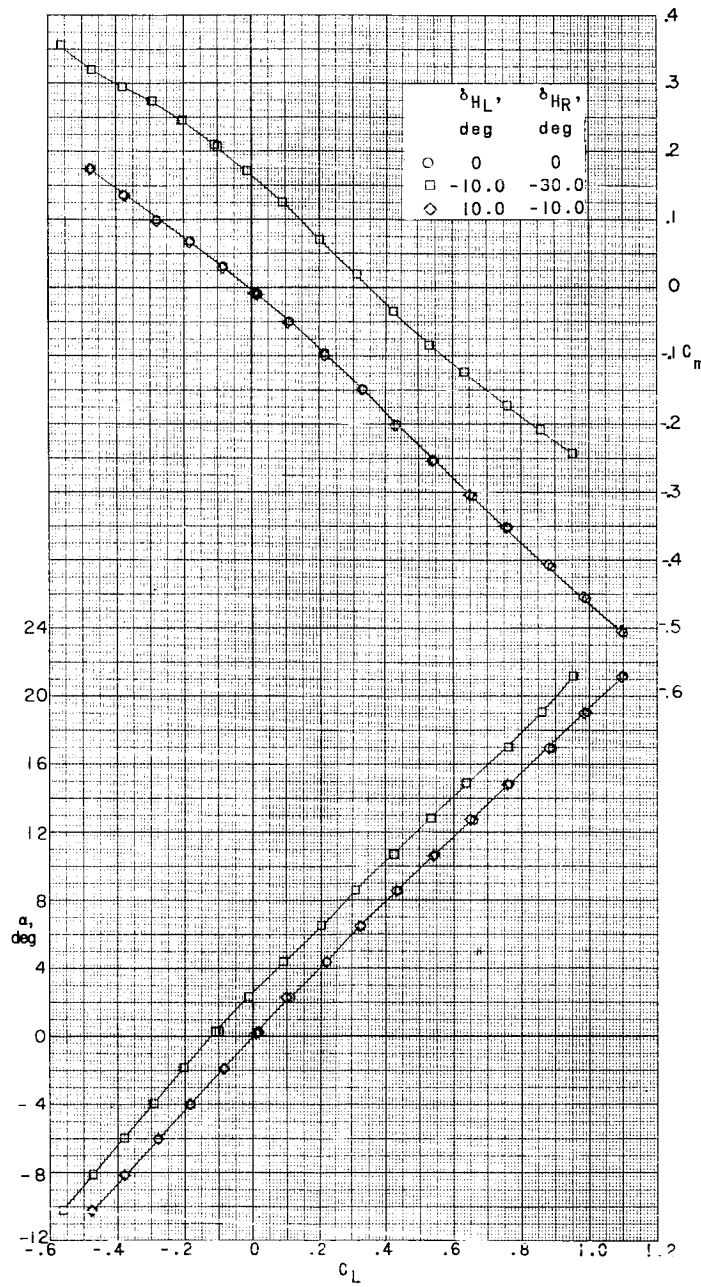
REF ID: A6572
DECLASSIFIED~~CONFIDENTIAL~~(a) $M = 2.29$.

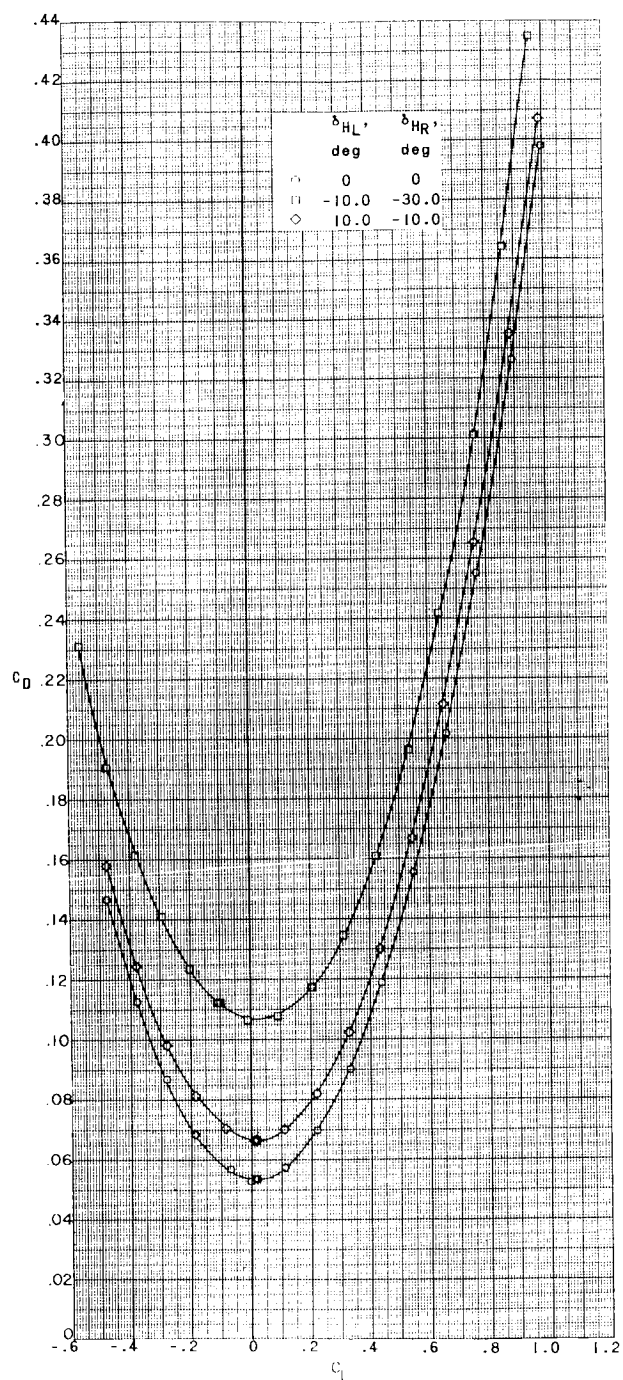
Figure 17.- Pitch characteristics of a 0.067-scale model of the X-15 airplane with various roll-control deflections of the left and right panel of the horizontal tail. Speed brakes retracted; $\delta_V = 0^\circ$.

~~CONFIDENTIAL~~

031928A.1030

~~CONFIDENTIAL~~

74

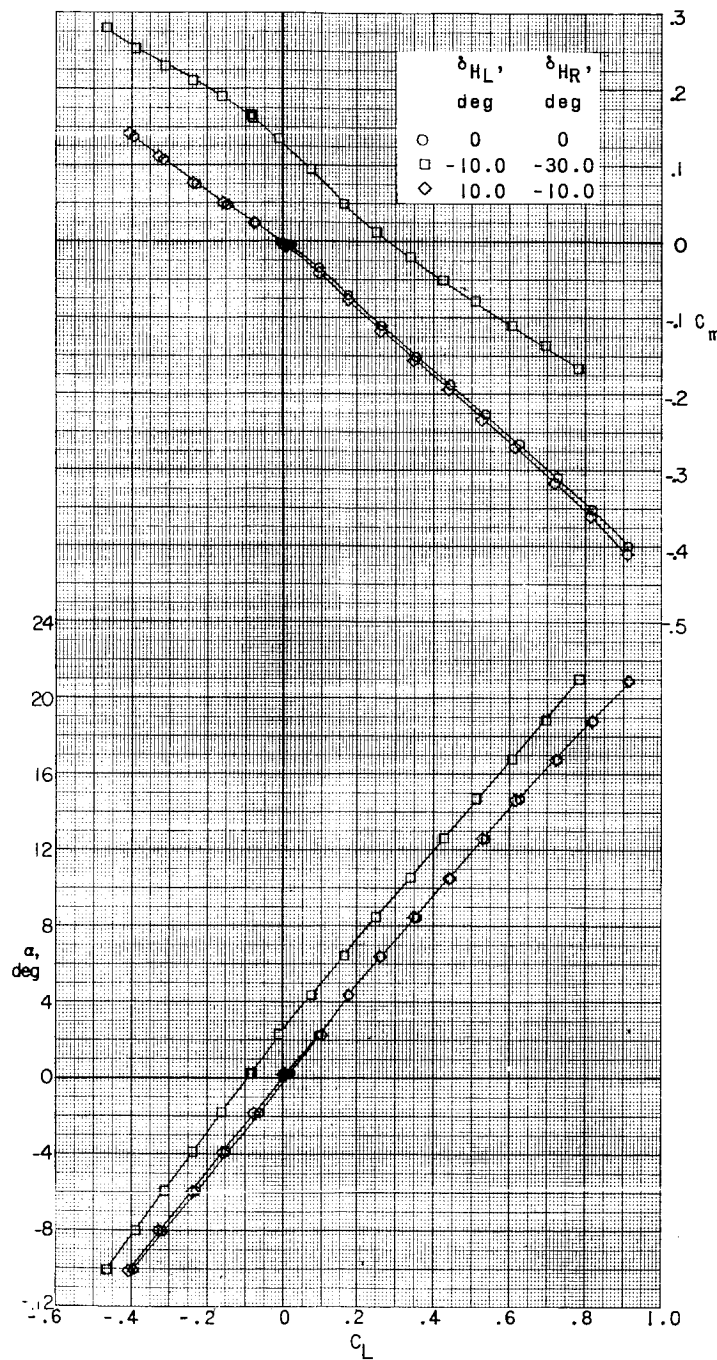


(a) Concluded.

Figure 17.- Continued.

~~CONFIDENTIAL~~

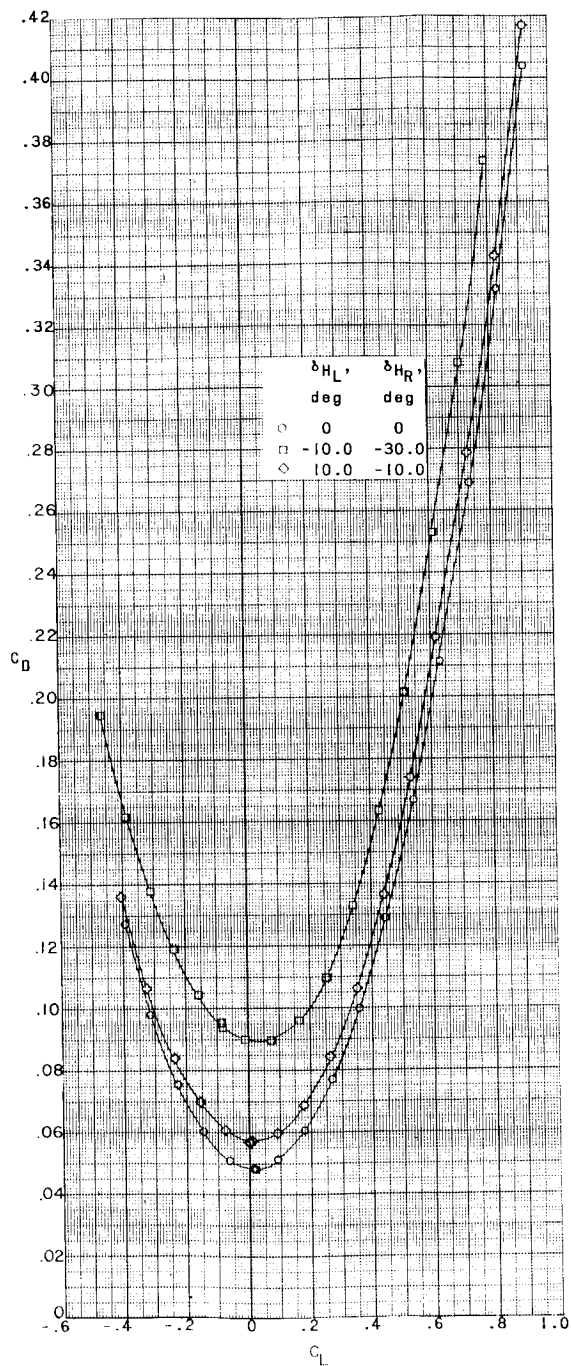
75



(b) $M = 2.98$.

Figure 17.- Continued.

CONFIDENTIAL



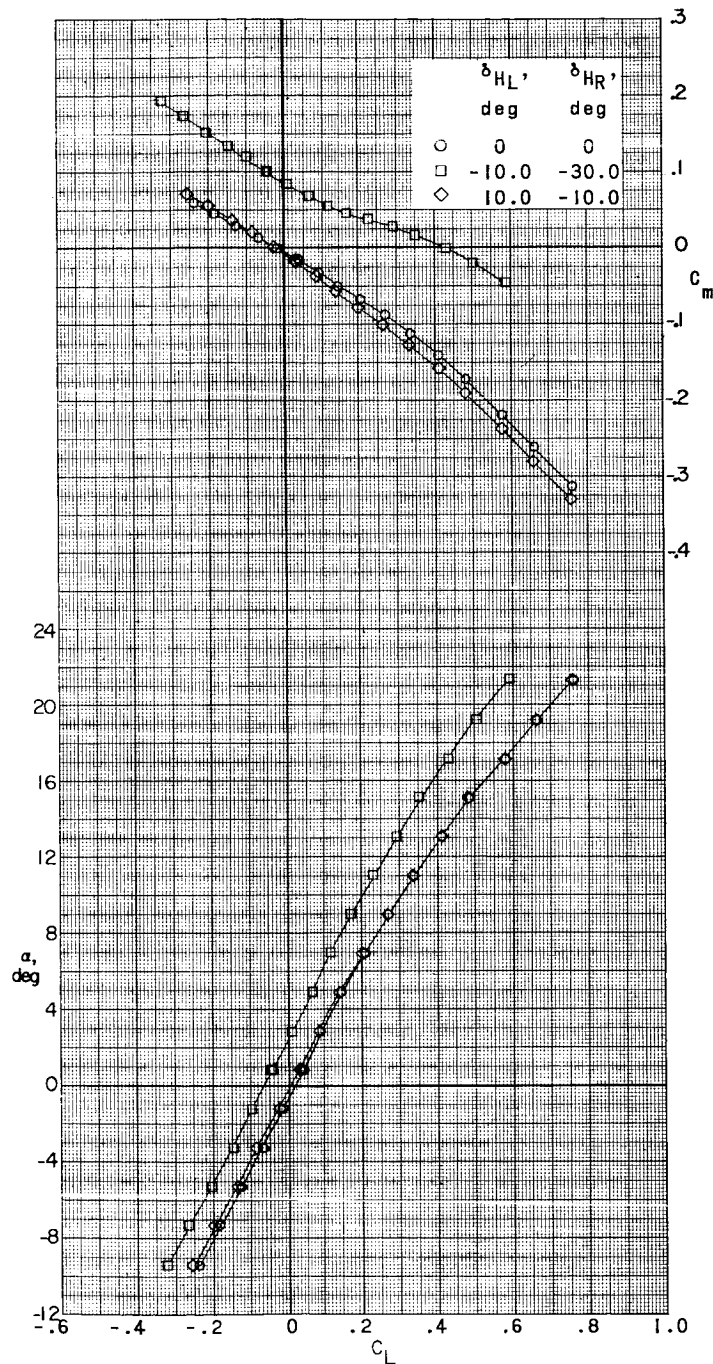
(b) Concluded.

Figure 17.- Continued.

~~CONFIDENTIAL~~

DECIBELS OF FIELD

77



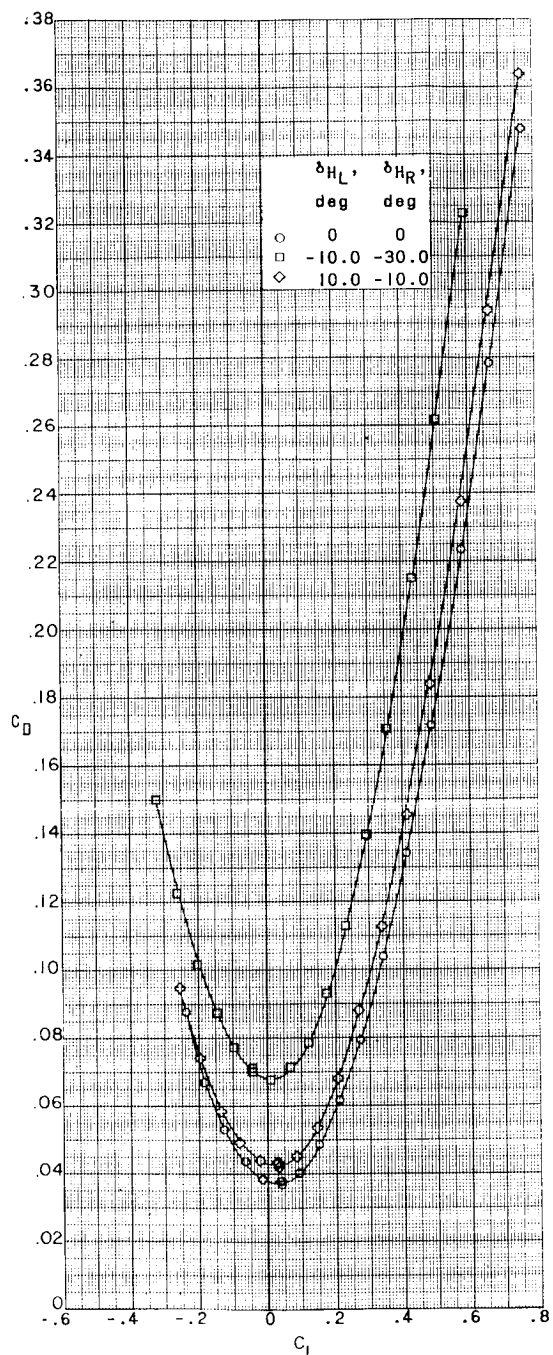
(c) $M = 4.65.$

Figure 17.- Continued.

03171820.1030

~~CONFIDENTIAL~~

78



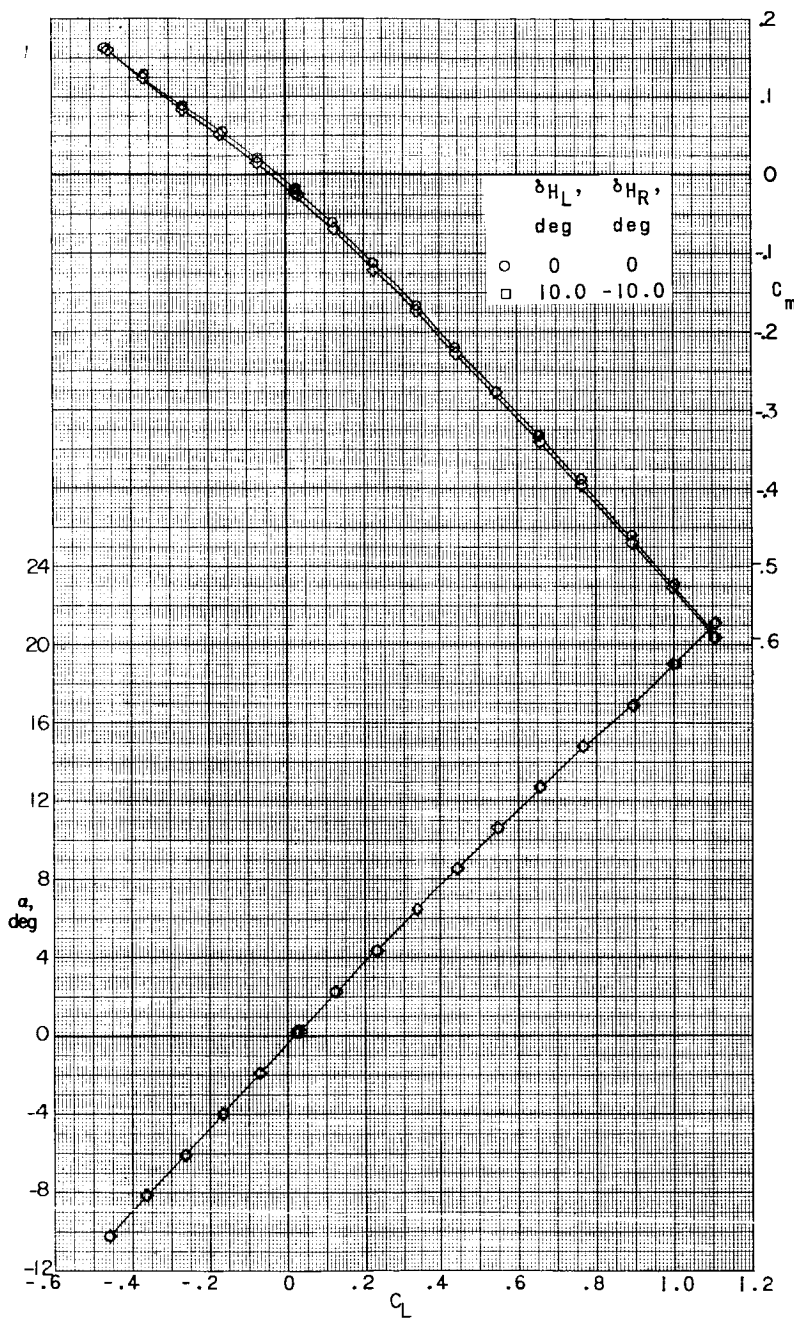
(c) Concluded.

Figure 17.- Concluded.

~~CONFIDENTIAL~~

DECLASSIFIED

79



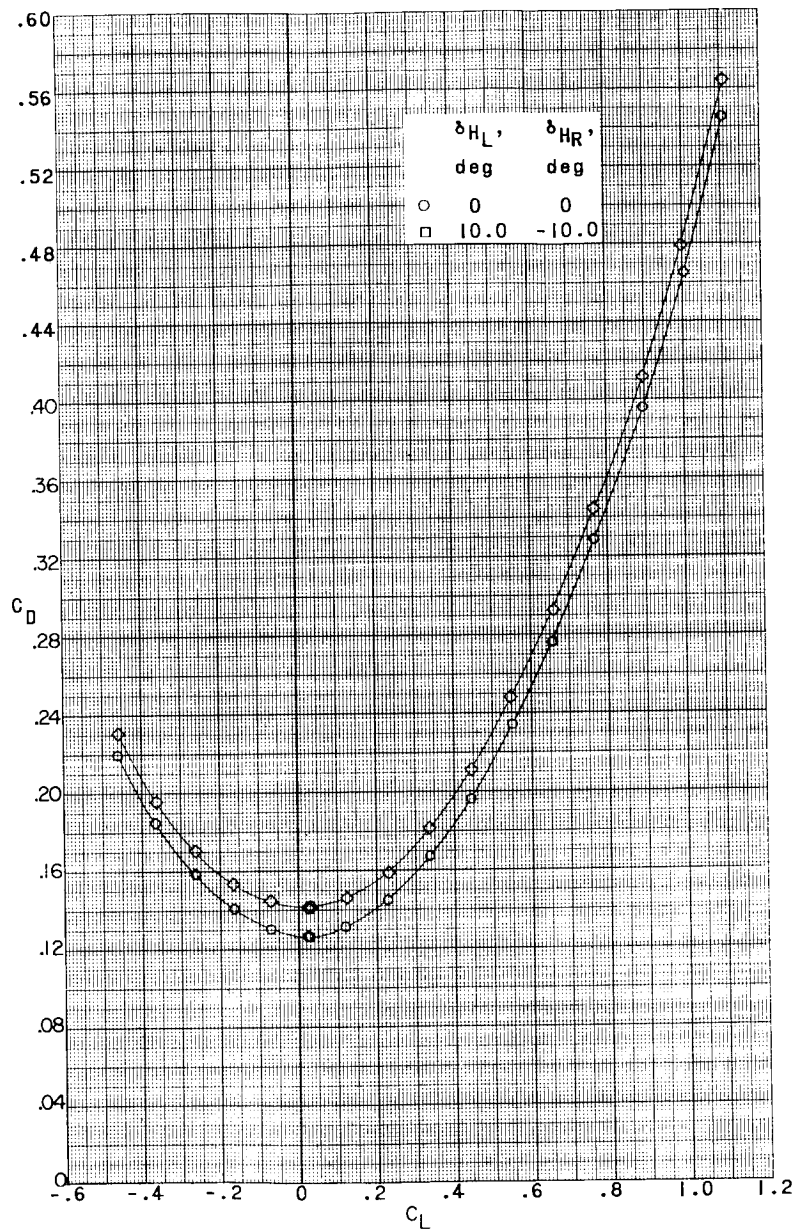
(a) $M = 2.29$.

Figure 18.- Pitch characteristics of a 0.067-scale model of the X-15 airplane with various roll-control deflections of the left and right panel of the horizontal tail. Speed brakes open; $\delta_v = 0^\circ$.

001712201030

~~CONFIDENTIAL~~

80



(a) Concluded.

Figure 18.- Continued.

DECLASSIFIED

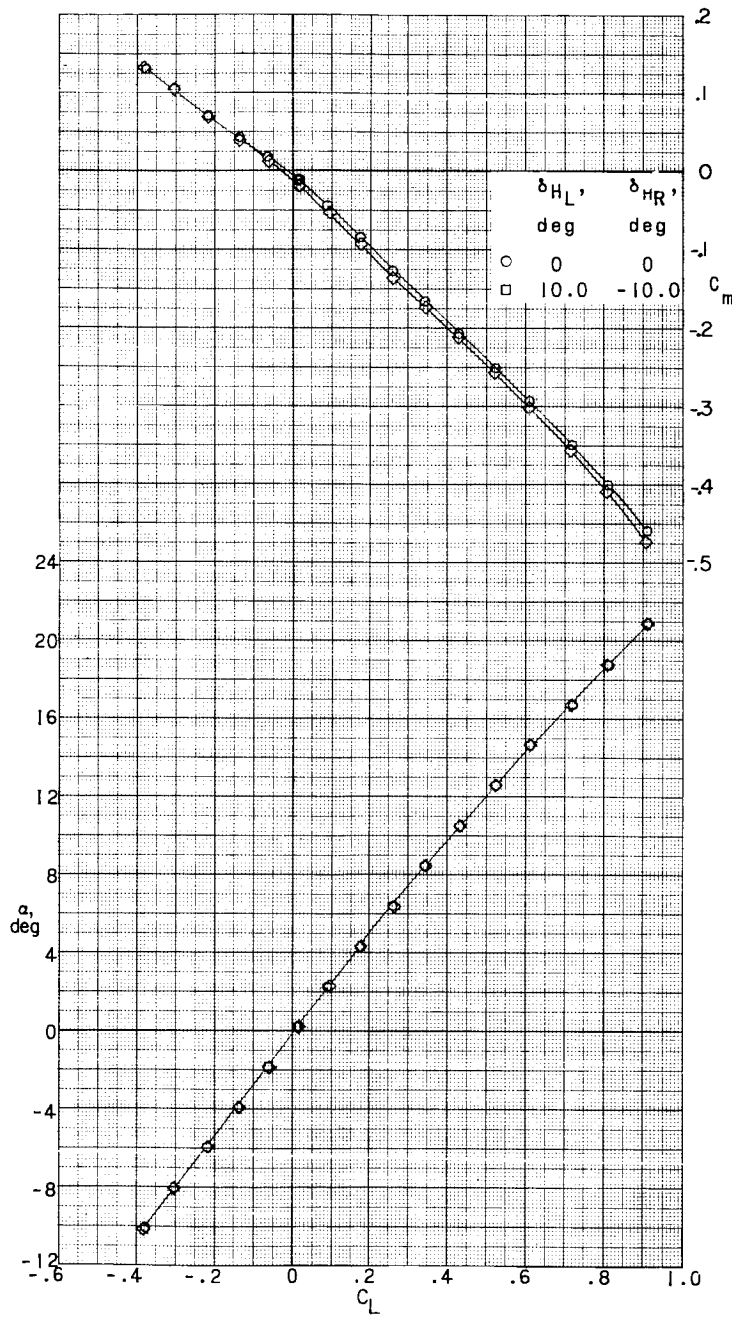
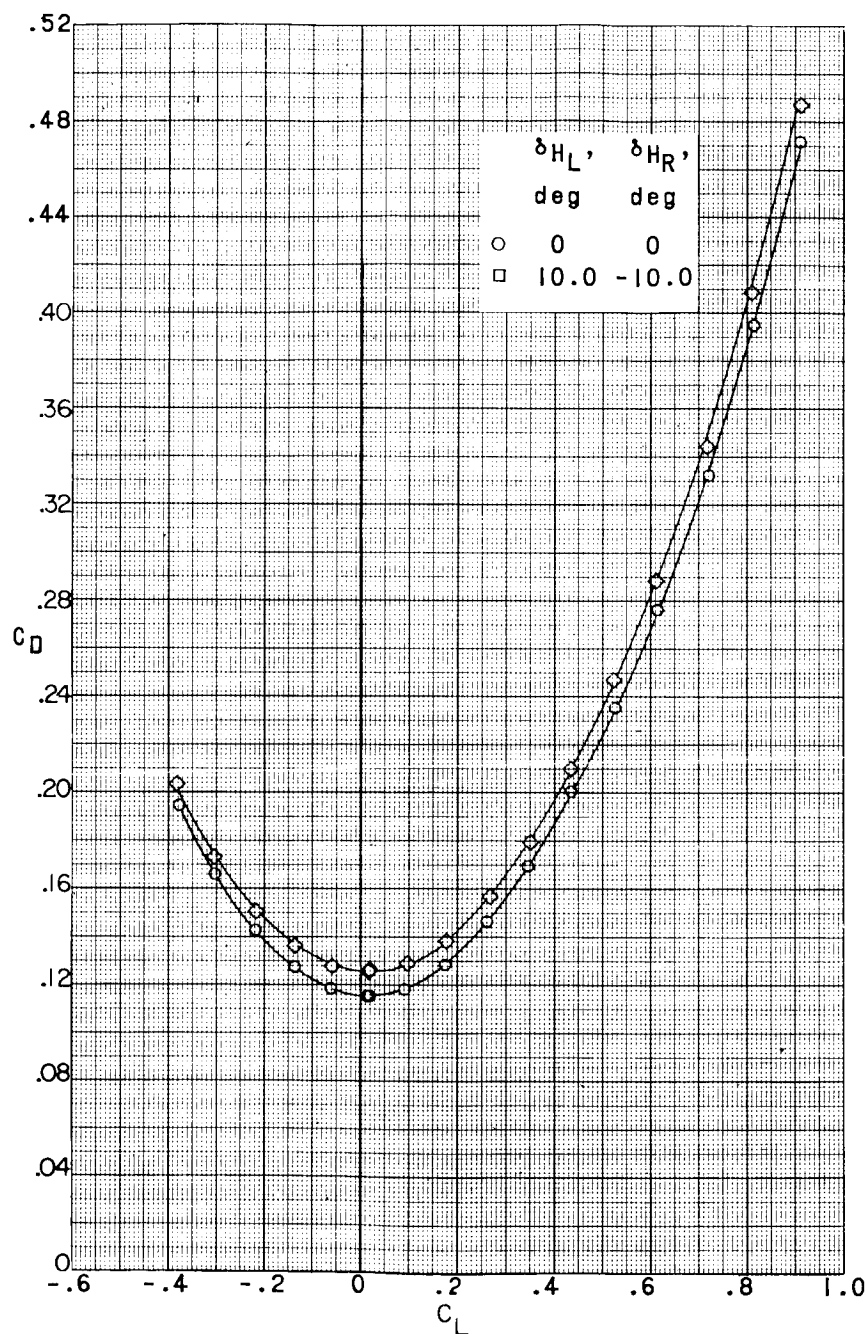
(b) $M = 2.98$.

Figure 18.- Continued.

CONFIDENTIAL

CONFIDENTIAL

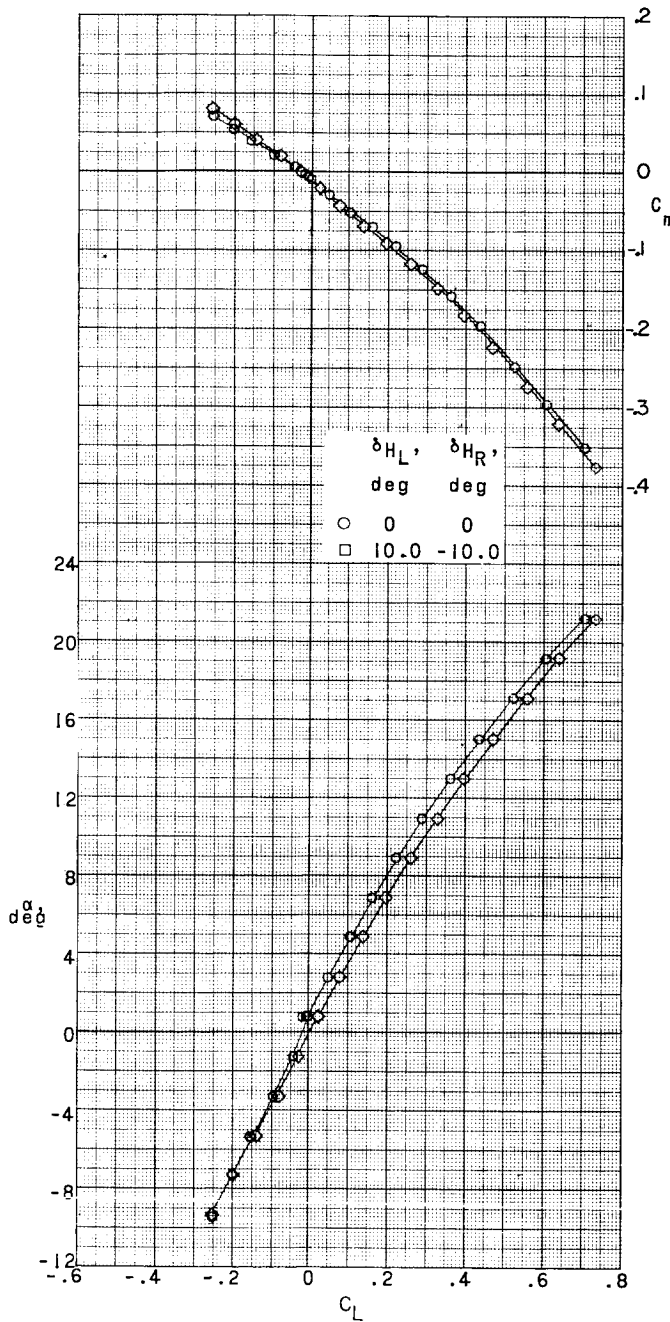


(b) Concluded.

Figure 18.- Continued.

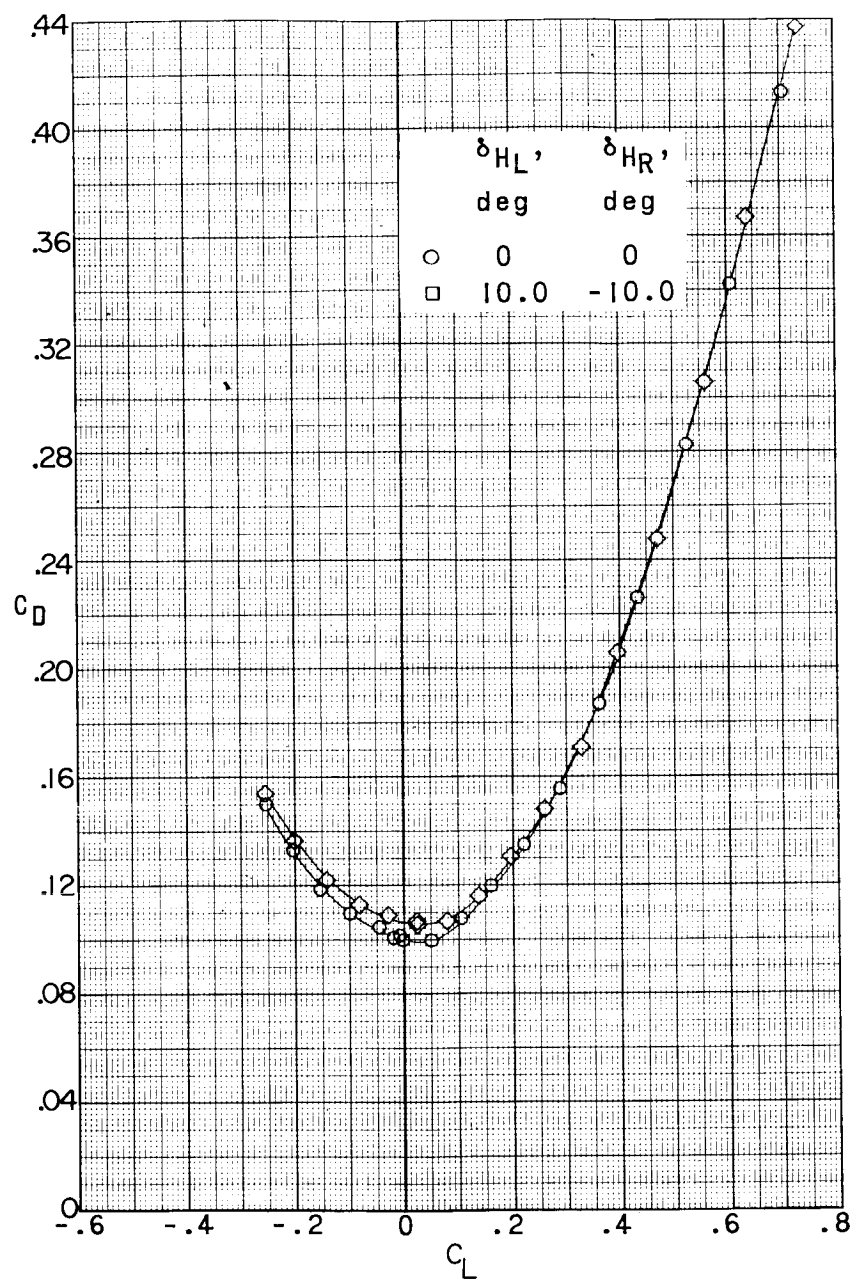
DECLASSIFIED

83



(c) $M = 4.65$.

Figure 18.- Continued.

03171230 1030
CONFIDENTIAL

(c) Concluded.

Figure 18.- Concluded.

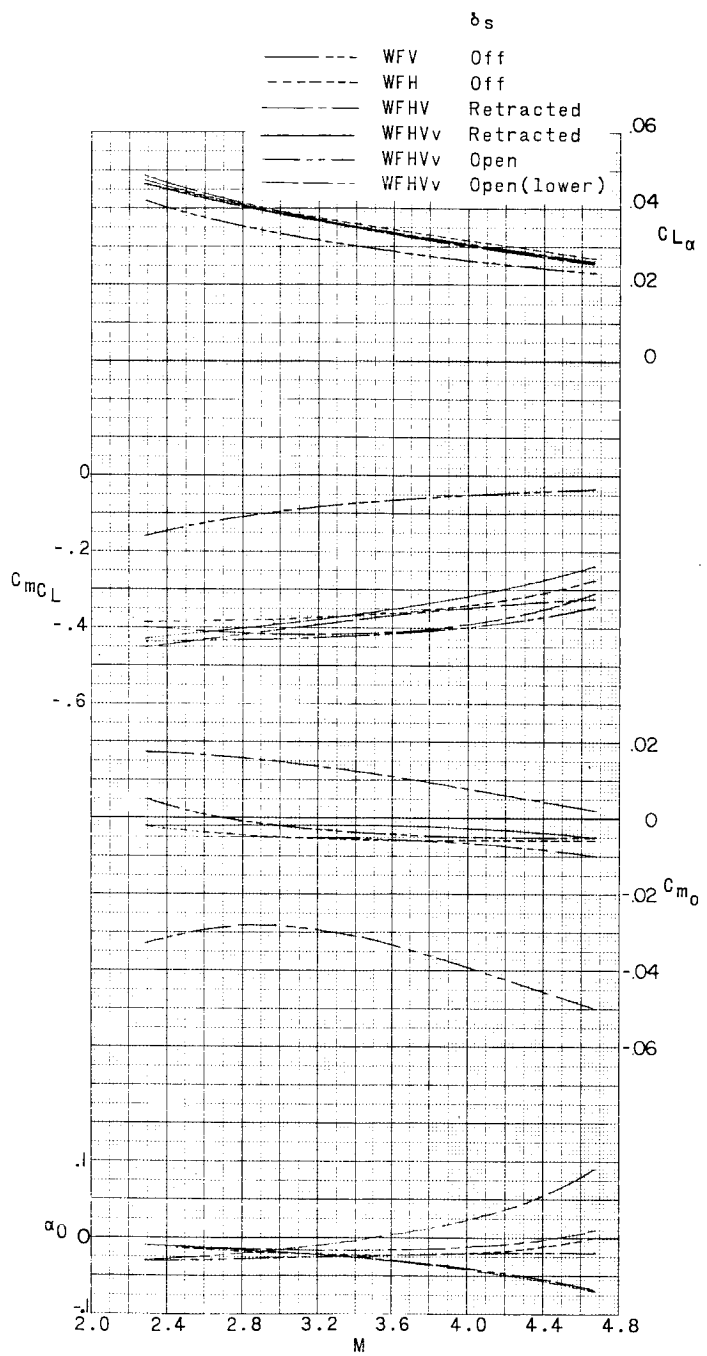


Figure 19.- Summary of longitudinal stability characteristics of a 0.007-scale model of the X-15 airplane.

CONFIDENTIAL

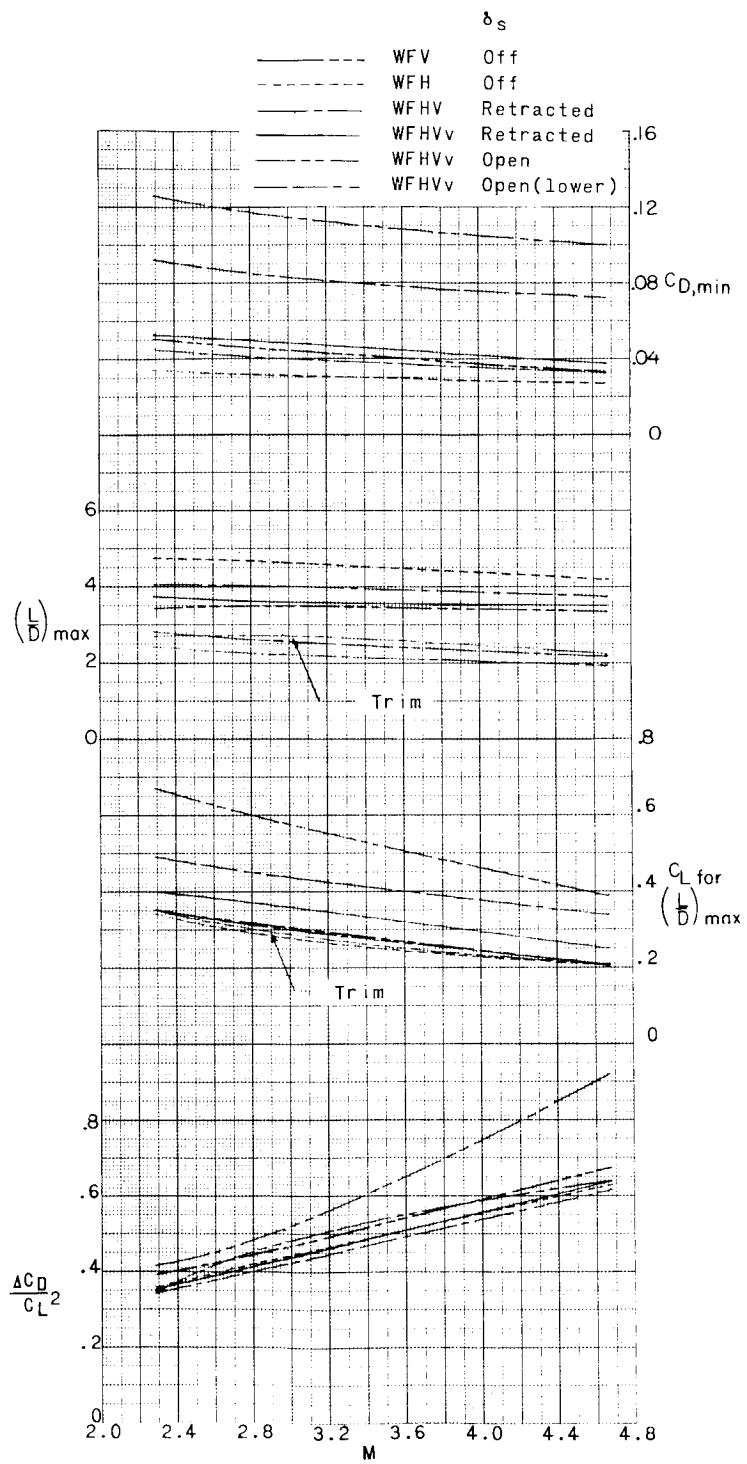


Figure 19.- Concluded.

DECLASSIFIED

CONFIDENTIAL

87

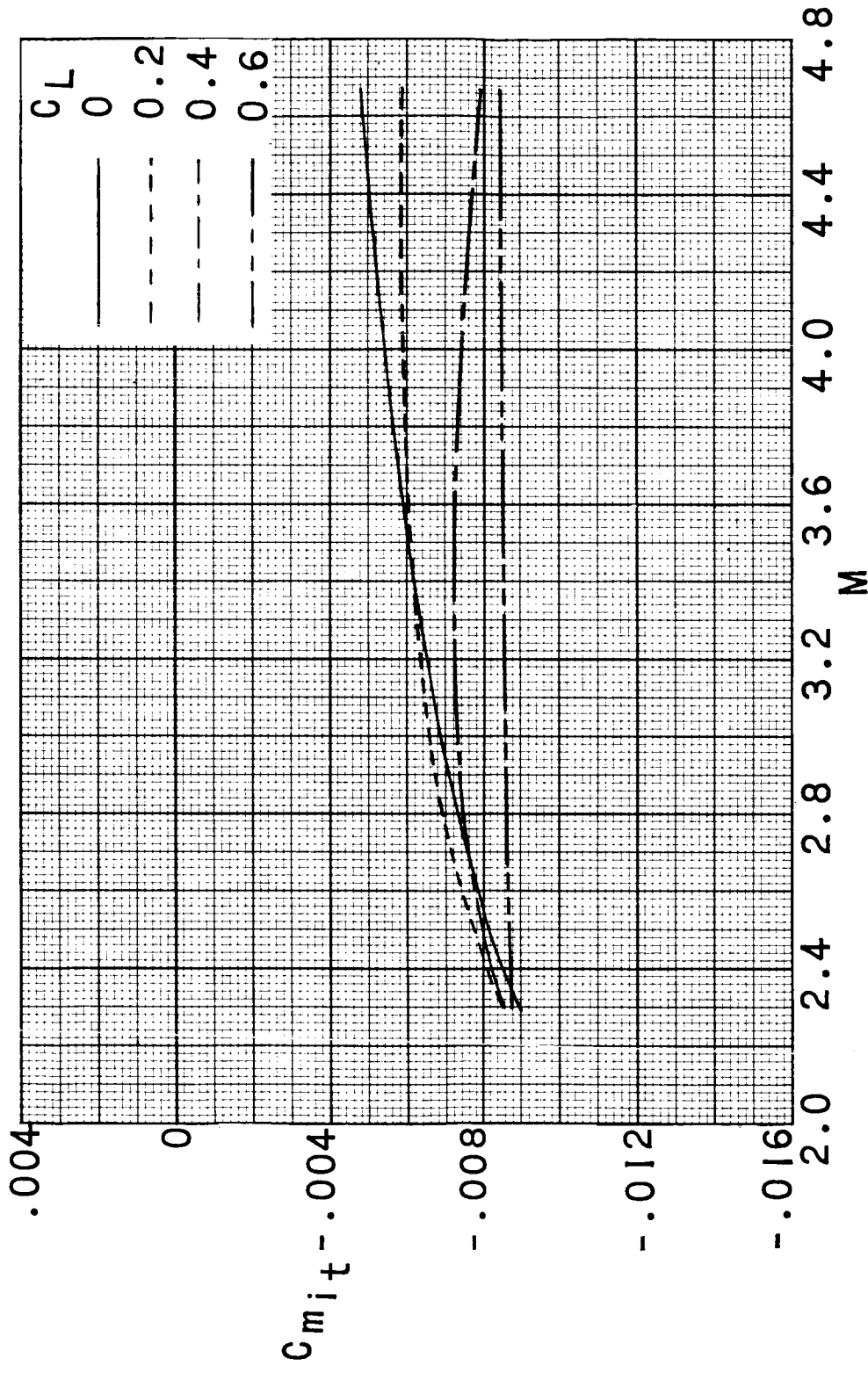


Figure 20.- Summary of stabilizer effectiveness of a 0.067-scale model of the X-15 airplane with symmetrical deflections of the horizontal tail.

0 0 1 3 0 2 0 1 0 3 0

~~CONFIDENTIAL~~

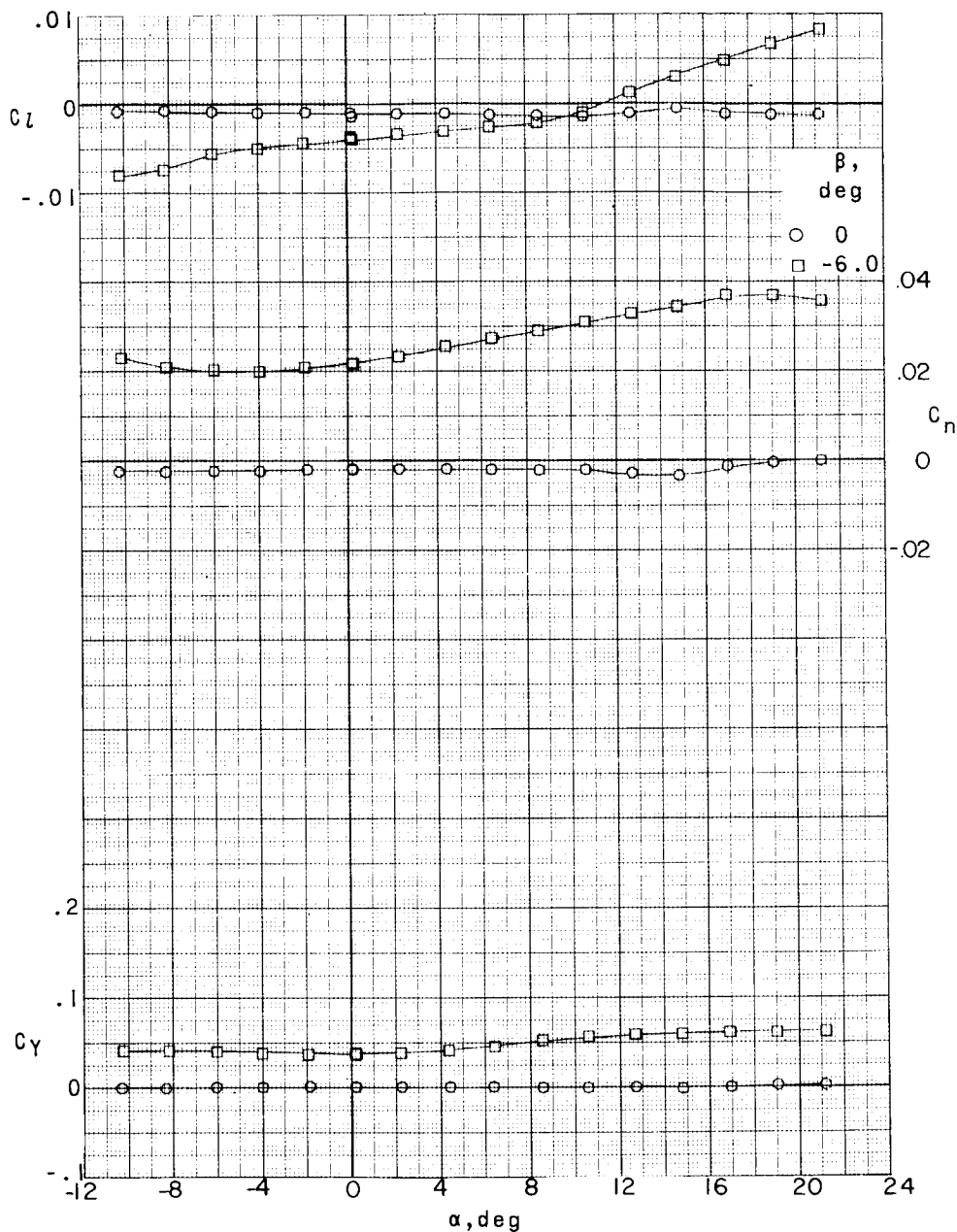
(a) $M = 2.29$.

Figure 21.- Lateral stability characteristics of a WFH configuration of the 0.007-scale model of the X-15 airplane.

~~CONFIDENTIAL~~

DECLASSIFIED

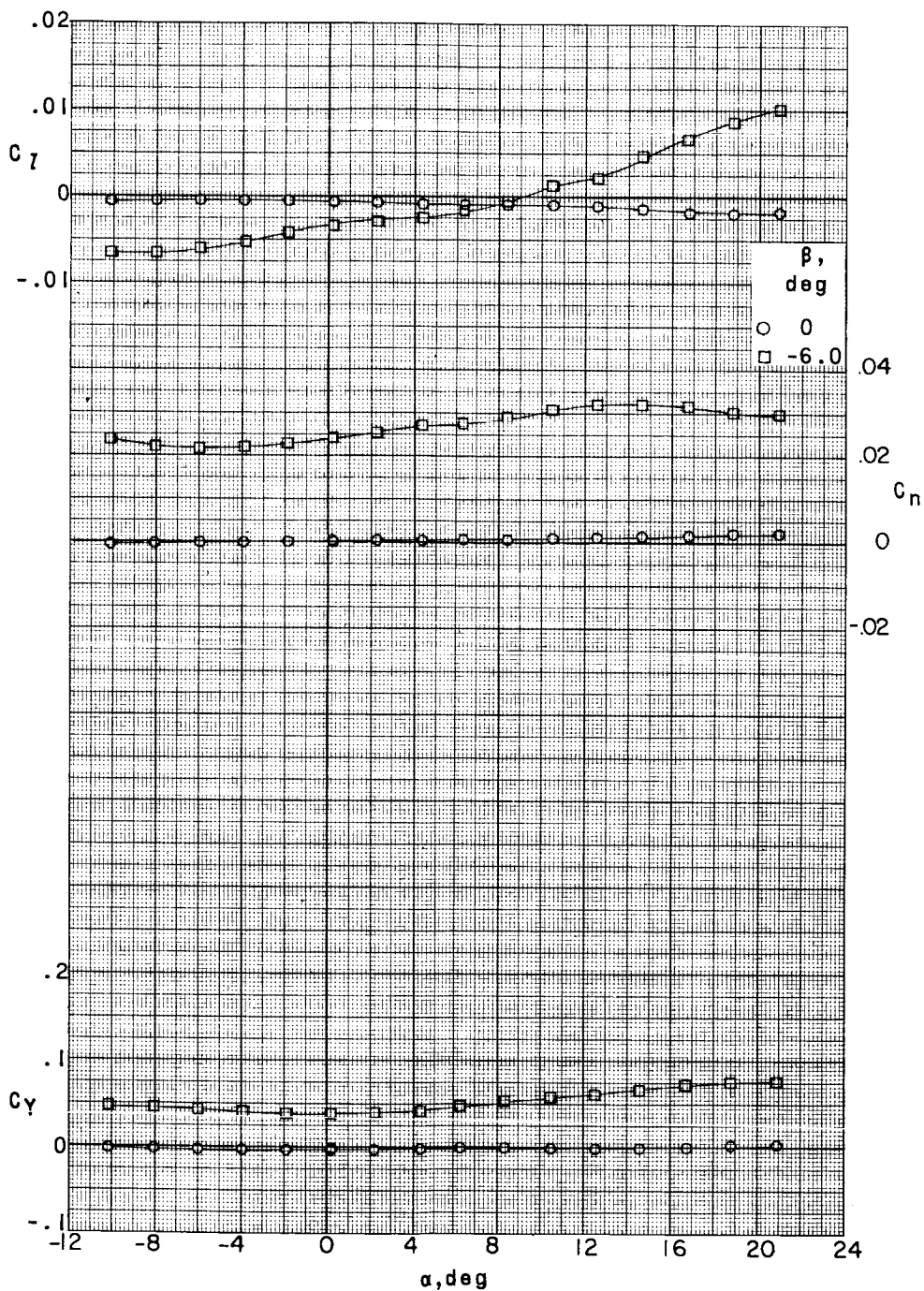
~~CONFIDENTIAL~~(b) $M = 2.98$.

Figure 21.- Continued

031712301030

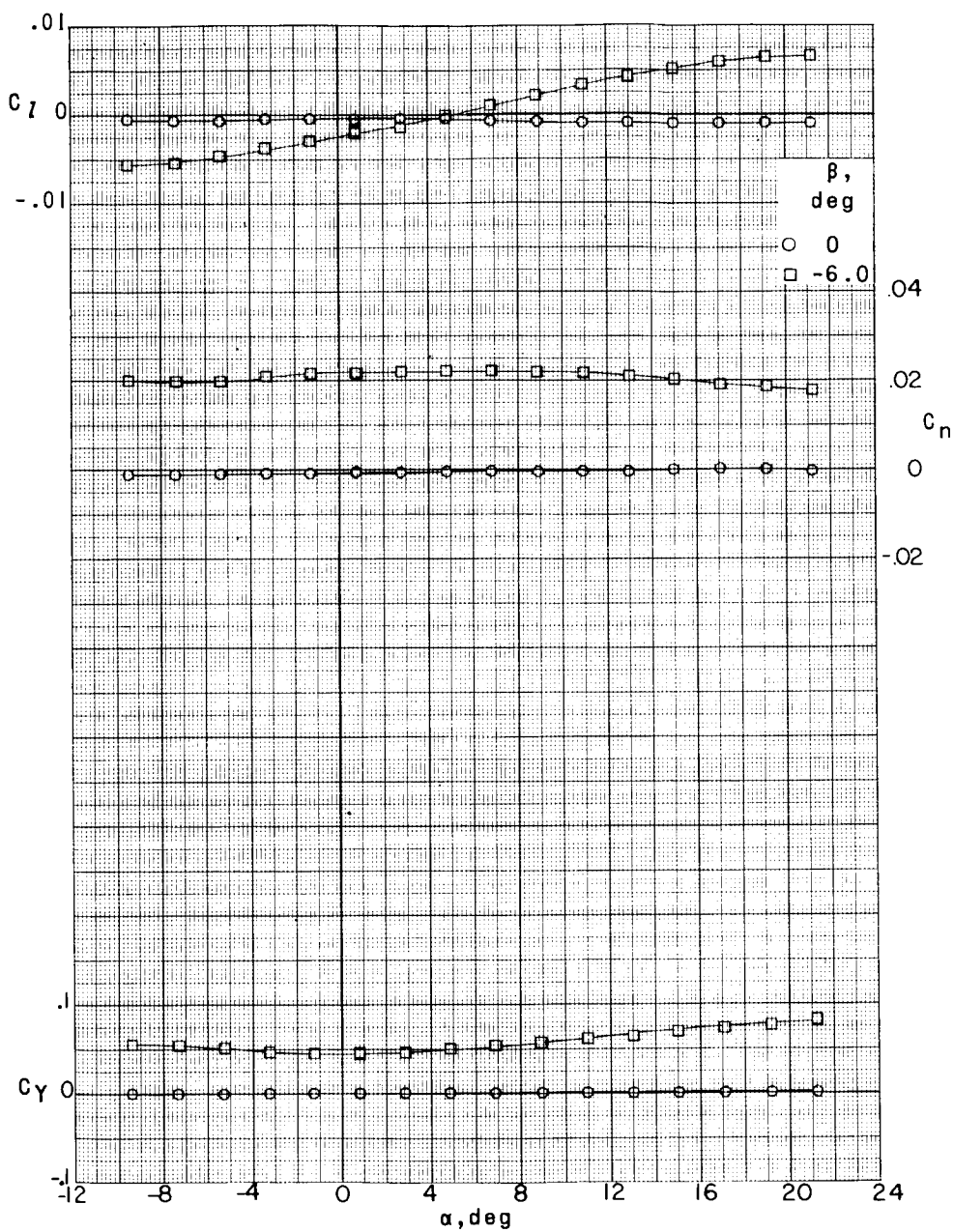
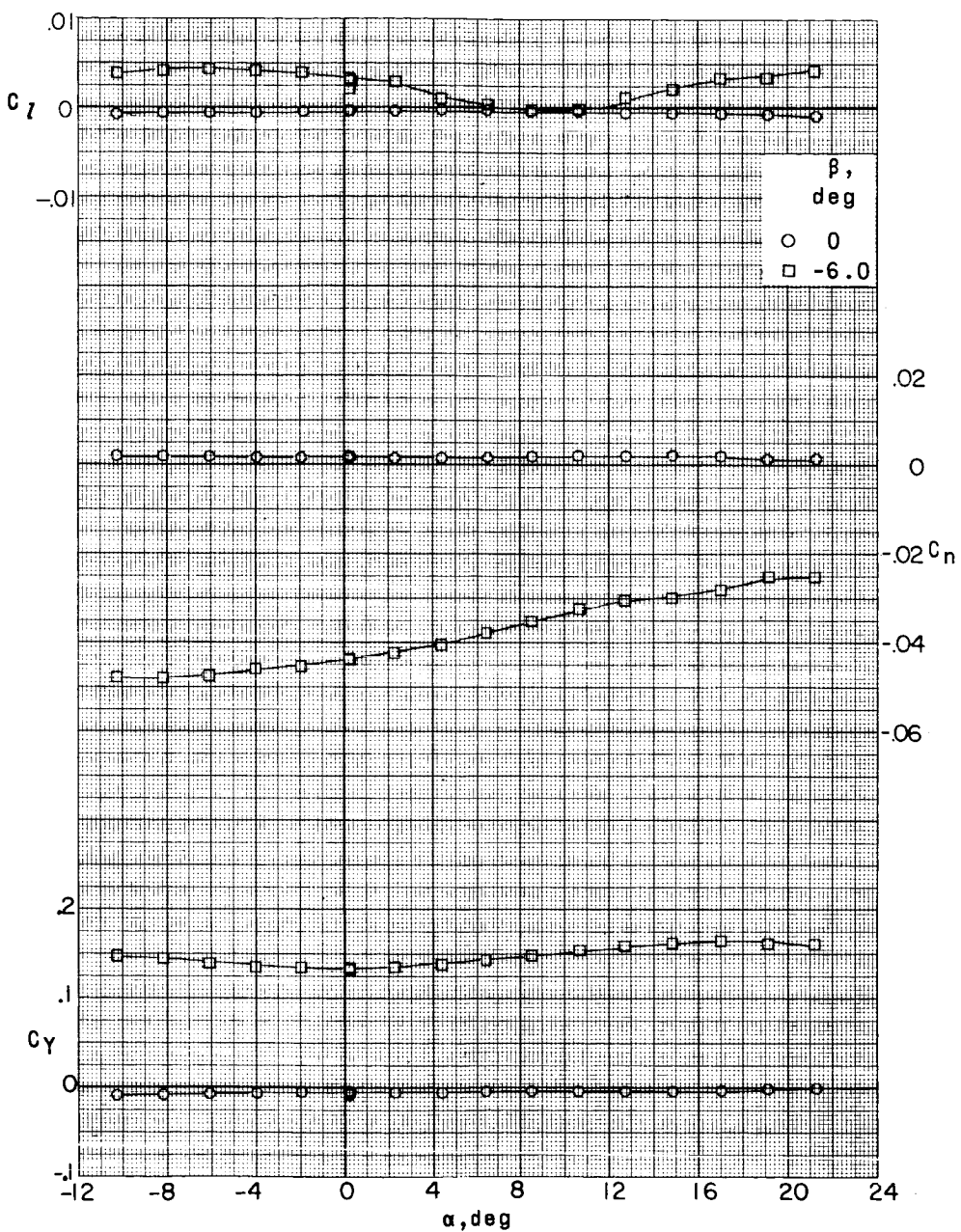
(c) $M = 4.65.$

Figure 21.- Concluded.

~~CONFIDENTIAL~~ DECLASSIFIED

91



(a) $M = 2.29$.

Figure 22.- Lateral stability characteristics of a WFW configuration of the 0.067-scale model of the X-15 airplane.

CONFIDENTIAL

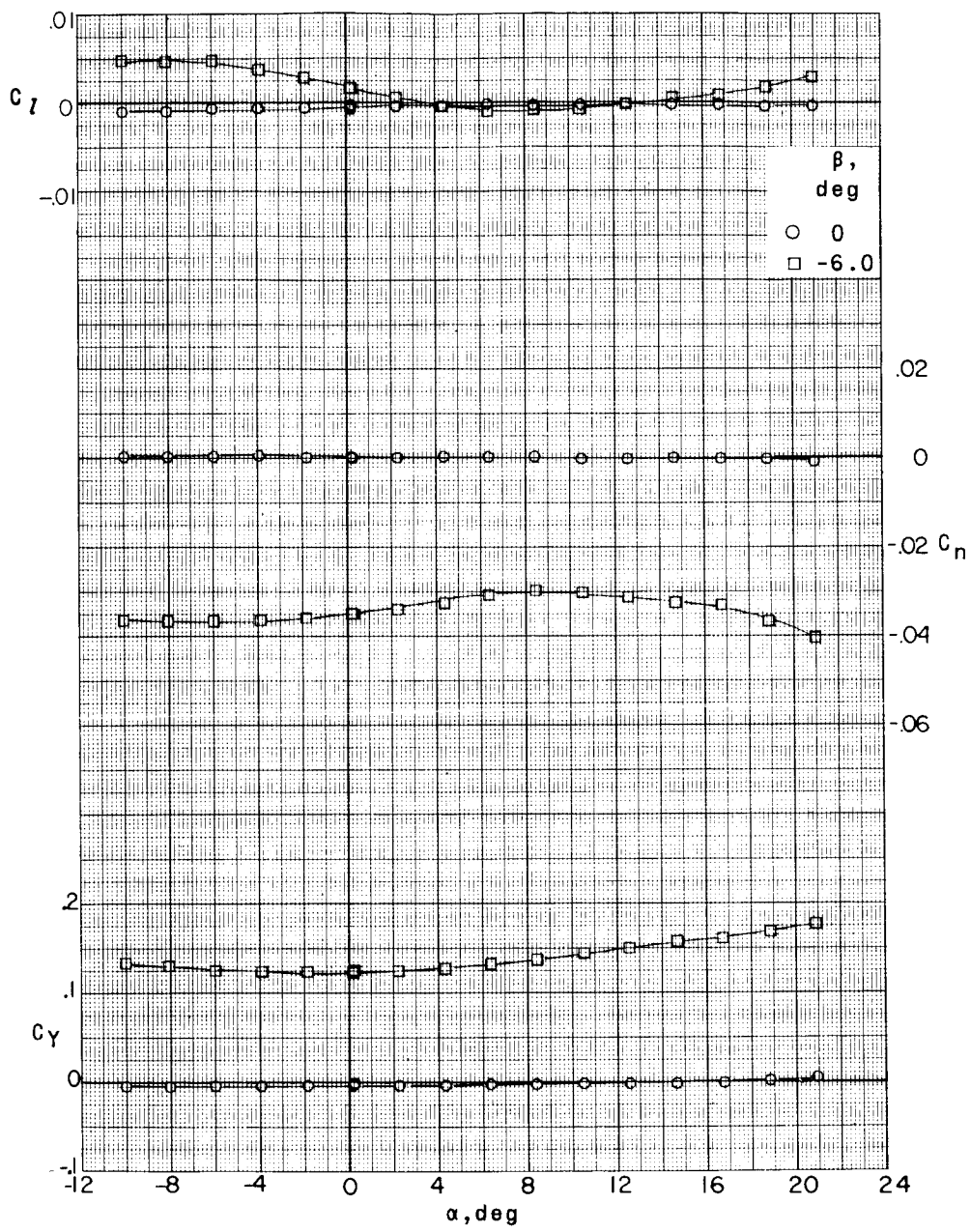
(b) $M = 2.98$.

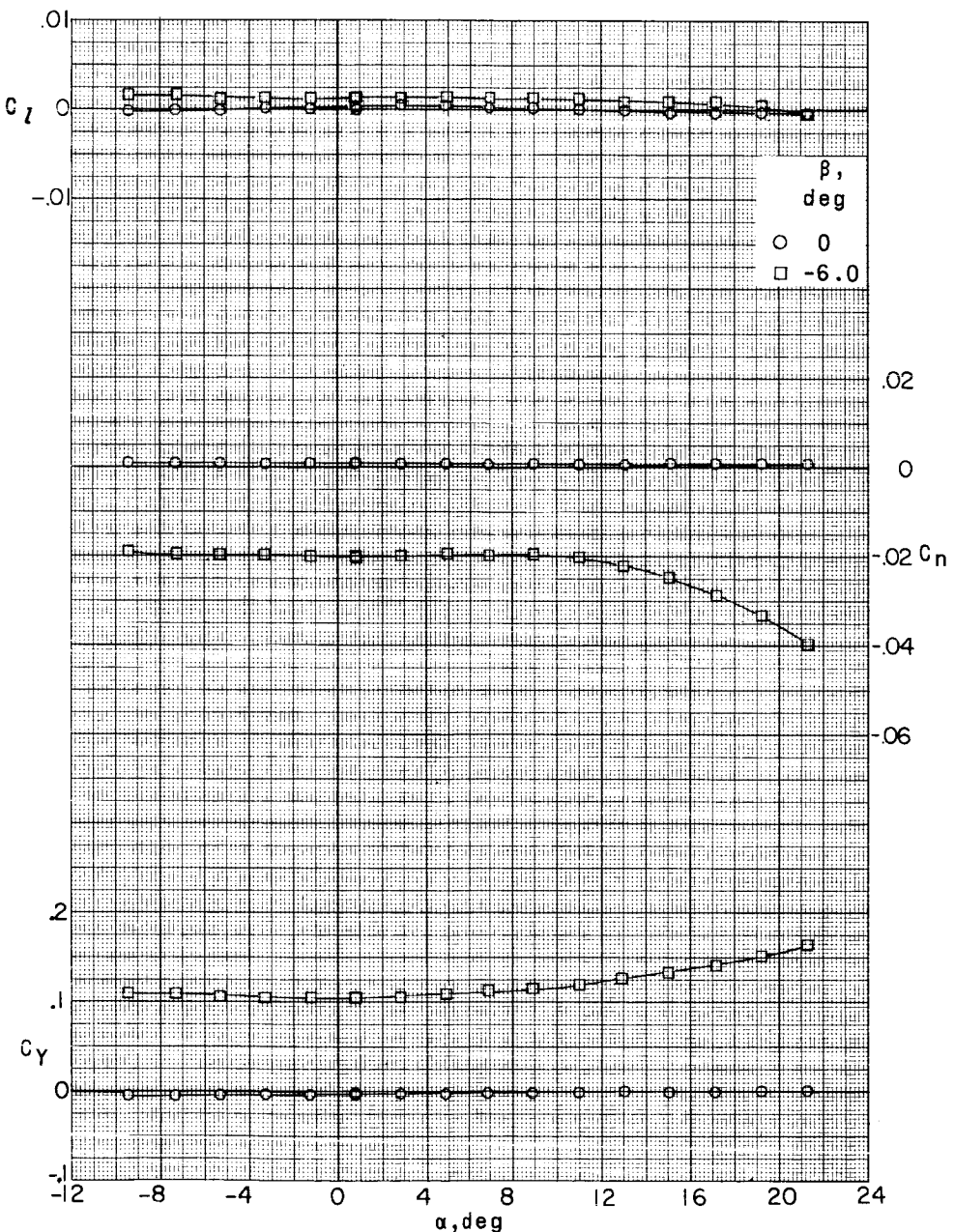
Figure 22.- Continued.

CONFIDENTIAL

L-351

~~DECLASSIFIED~~

93



(c) $M = 4.65.$

Figure 22.- Concluded.

~~CONFIDENTIAL~~

CONFIDENTIAL

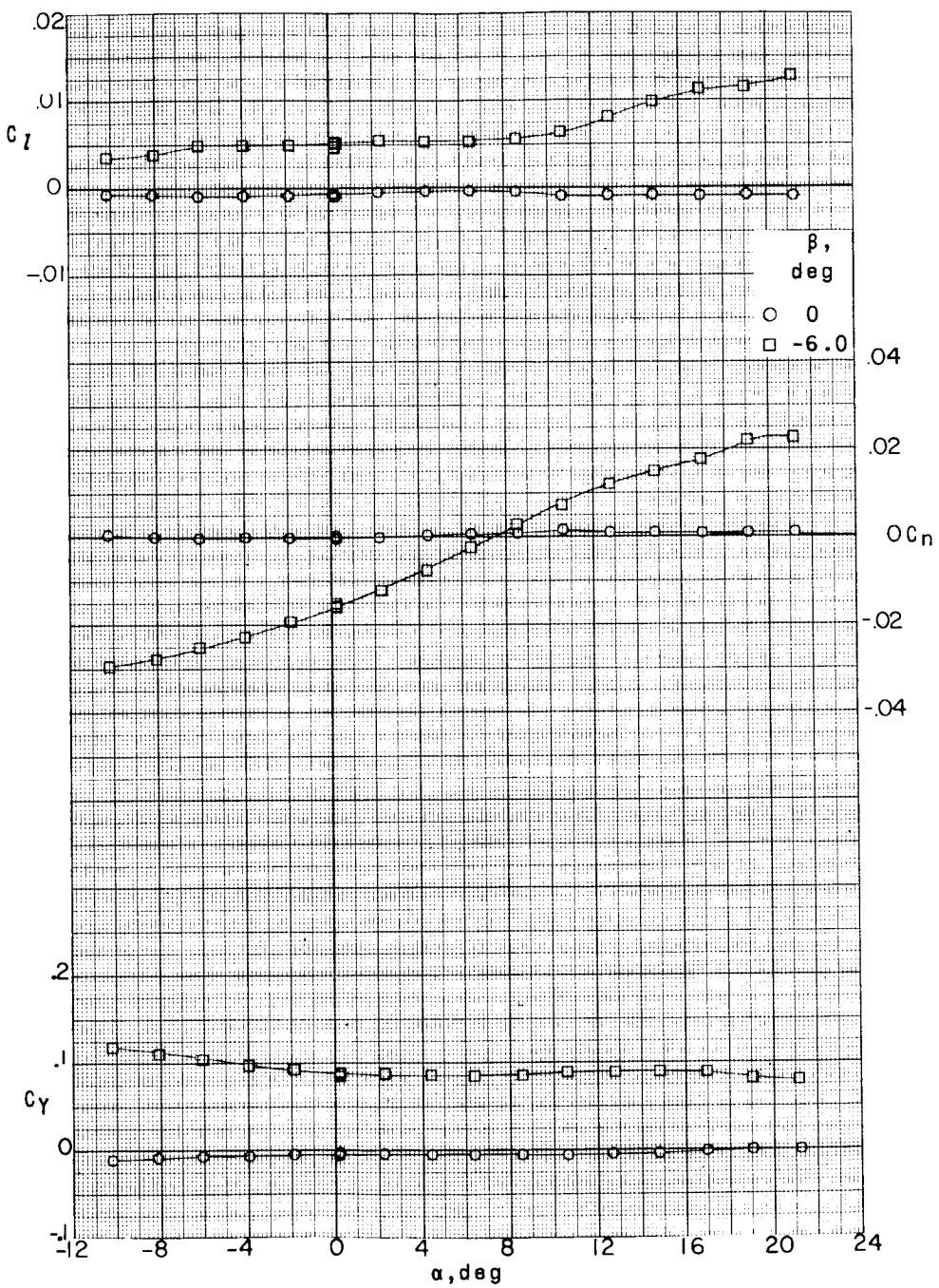
(a) $M = 2.29$.

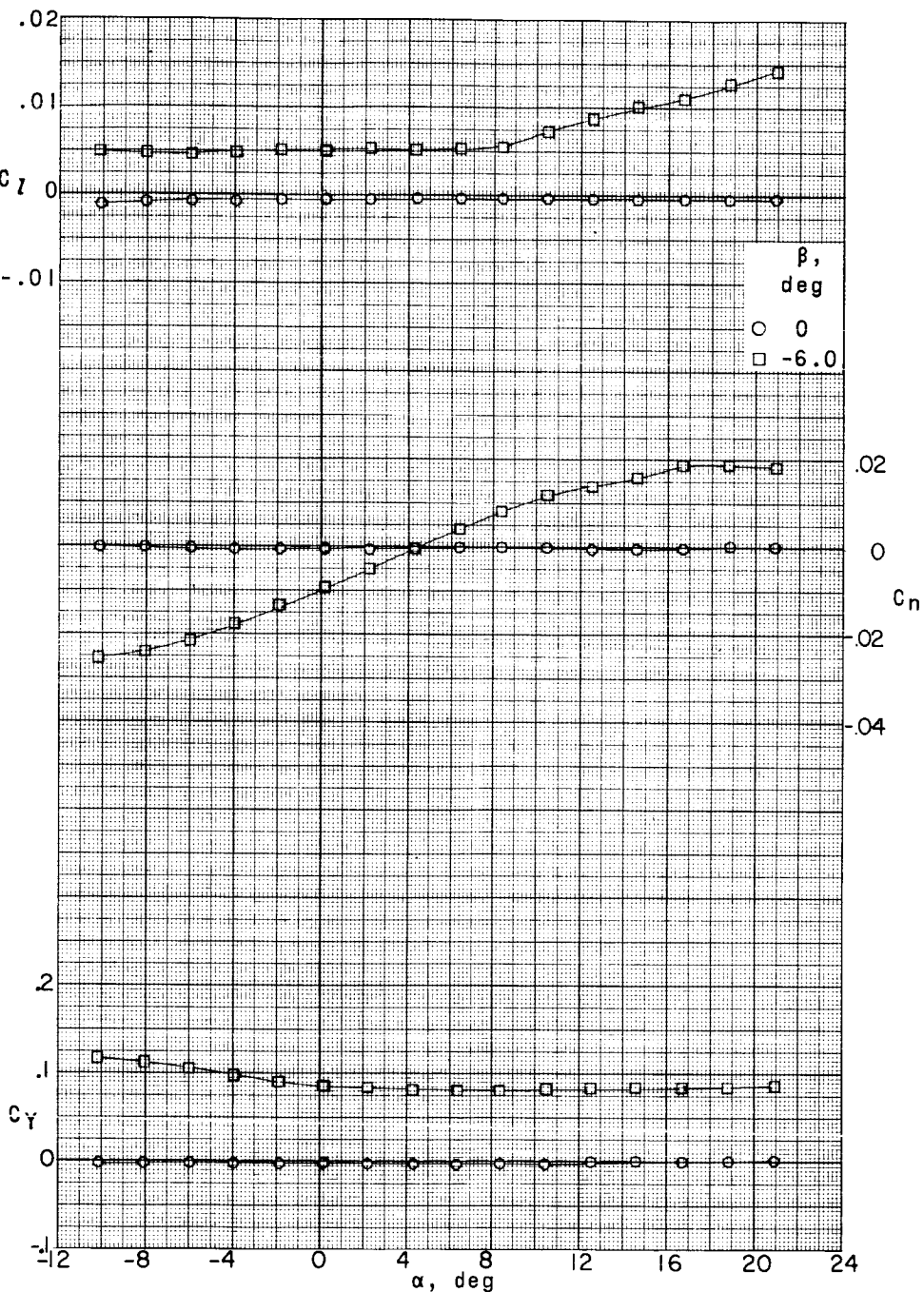
Figure 23.- Lateral stability characteristics of the WFHV configuration of the 0.067-scale model of the X-15 airplane.

CONFIDENTIAL

~~CONFIDENTIAL~~

DECLASSIFIED

95



(b) $M = 2.98.$

Figure 23.- Continued.

031912201030

~~CONFIDENTIAL~~

96

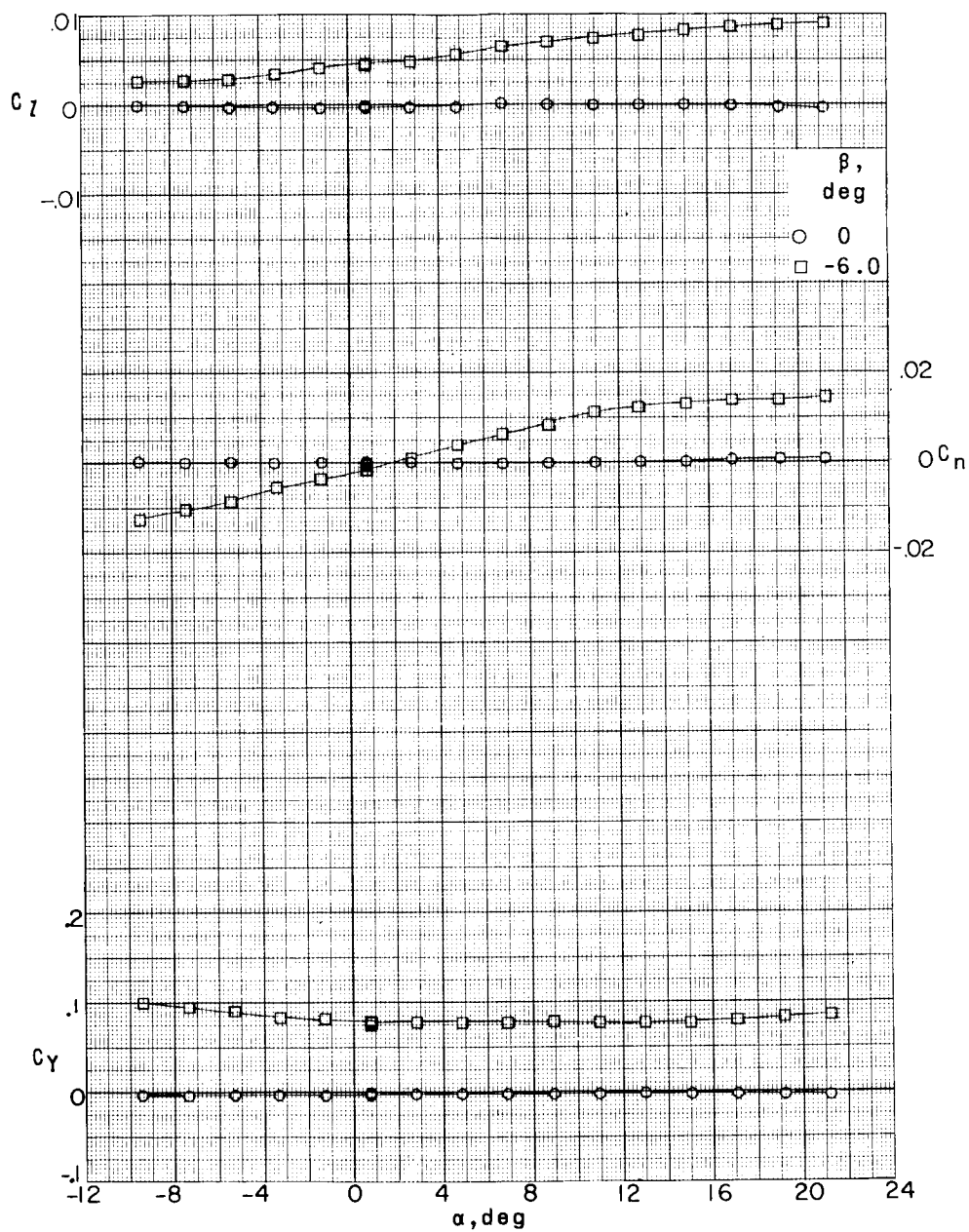
(c) $M = 4.65$.

Figure 23.- Concluded.

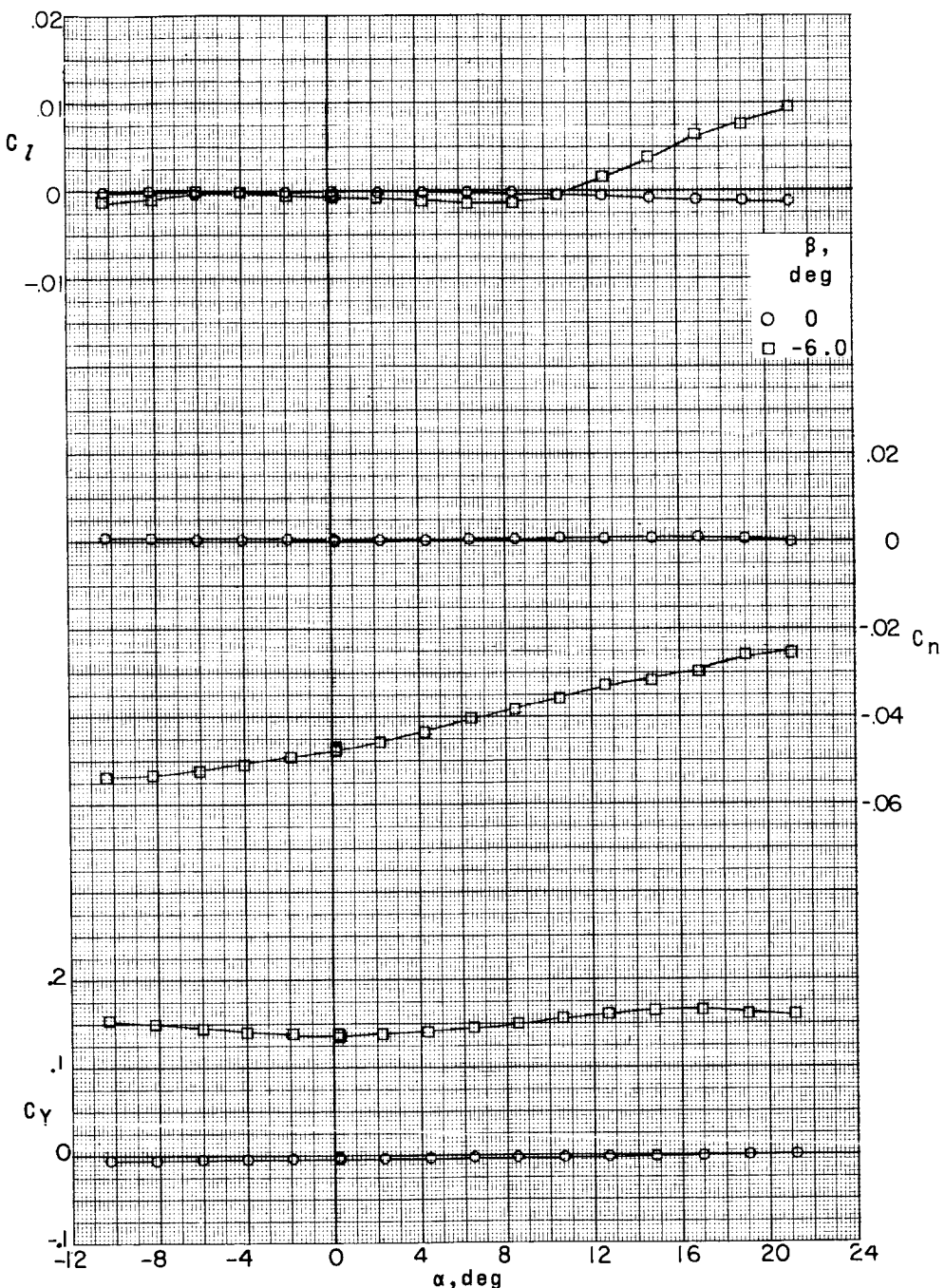
DECLASSIFIED
~~CONFIDENTIAL~~(a) $M = 2.29.$

Figure 24.- Lateral stability characteristics of a 0.067-scale model of the X-15 airplane with speed brakes retracted.

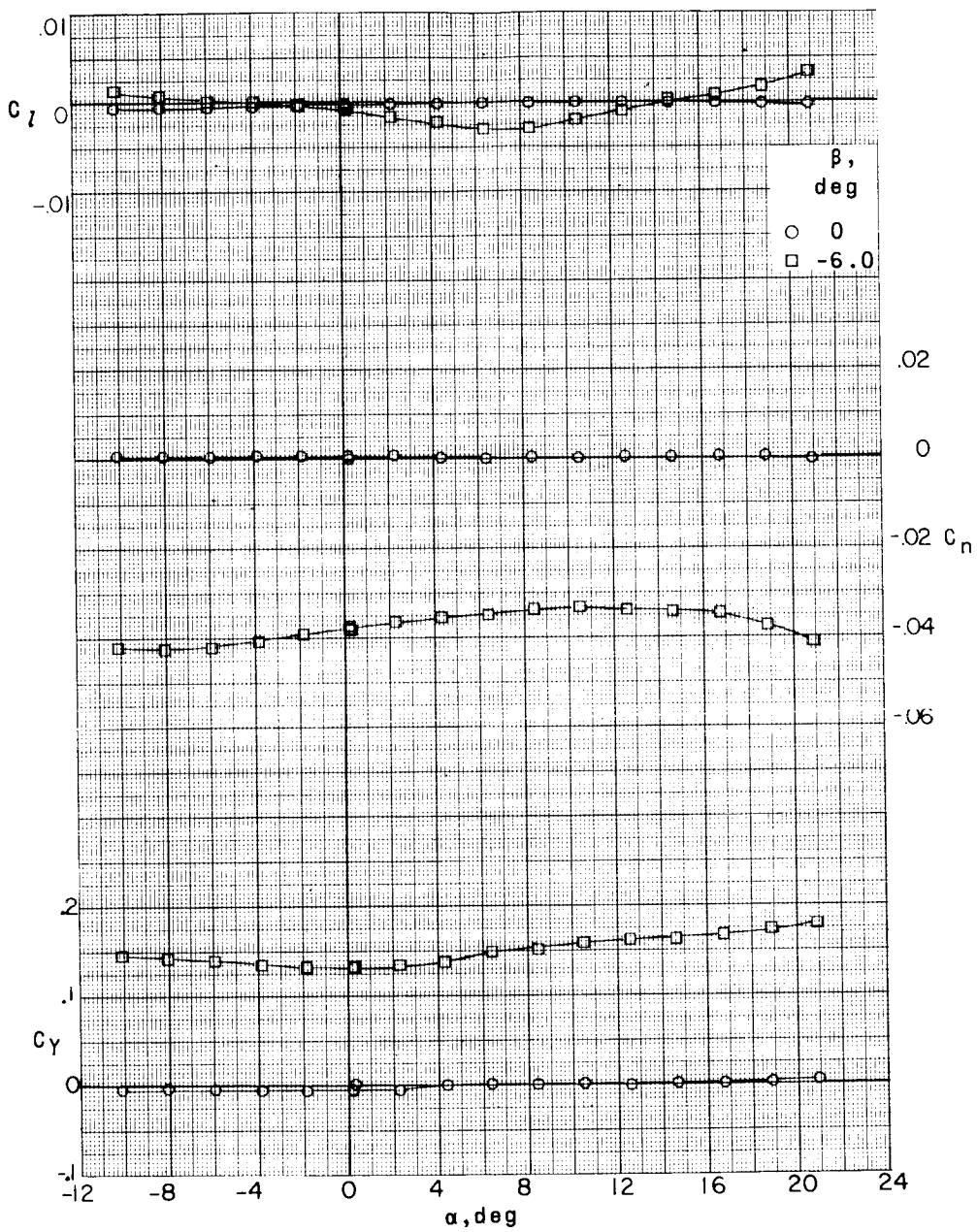
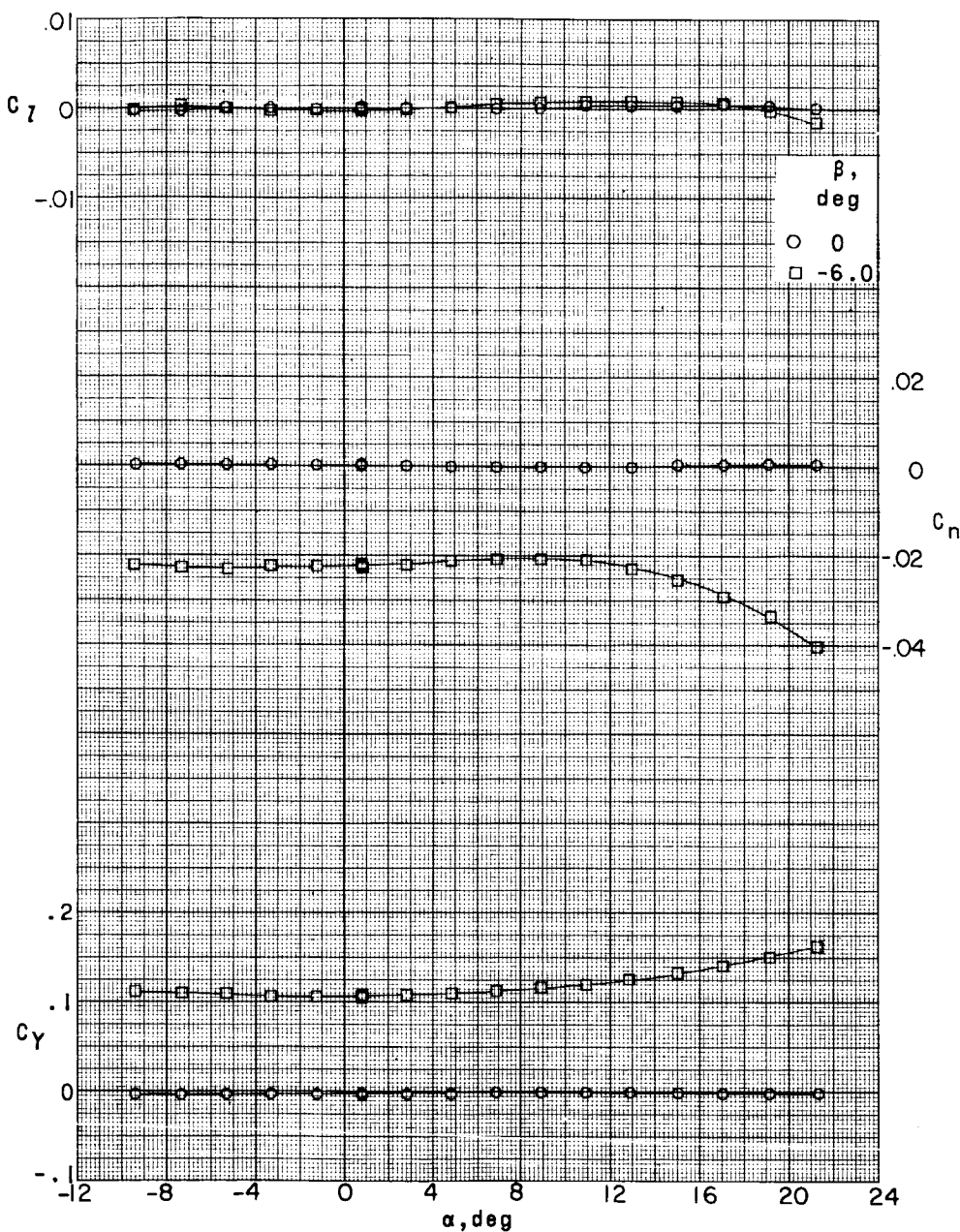
(b) $M = 2.98$.

Figure 24.- Continued.

DECLASSIFIED

~~CONFIDENTIAL~~

99



(c) $M = 4.65$.

Figure 24.- Concluded.

031712261030

~~CONFIDENTIAL~~

100

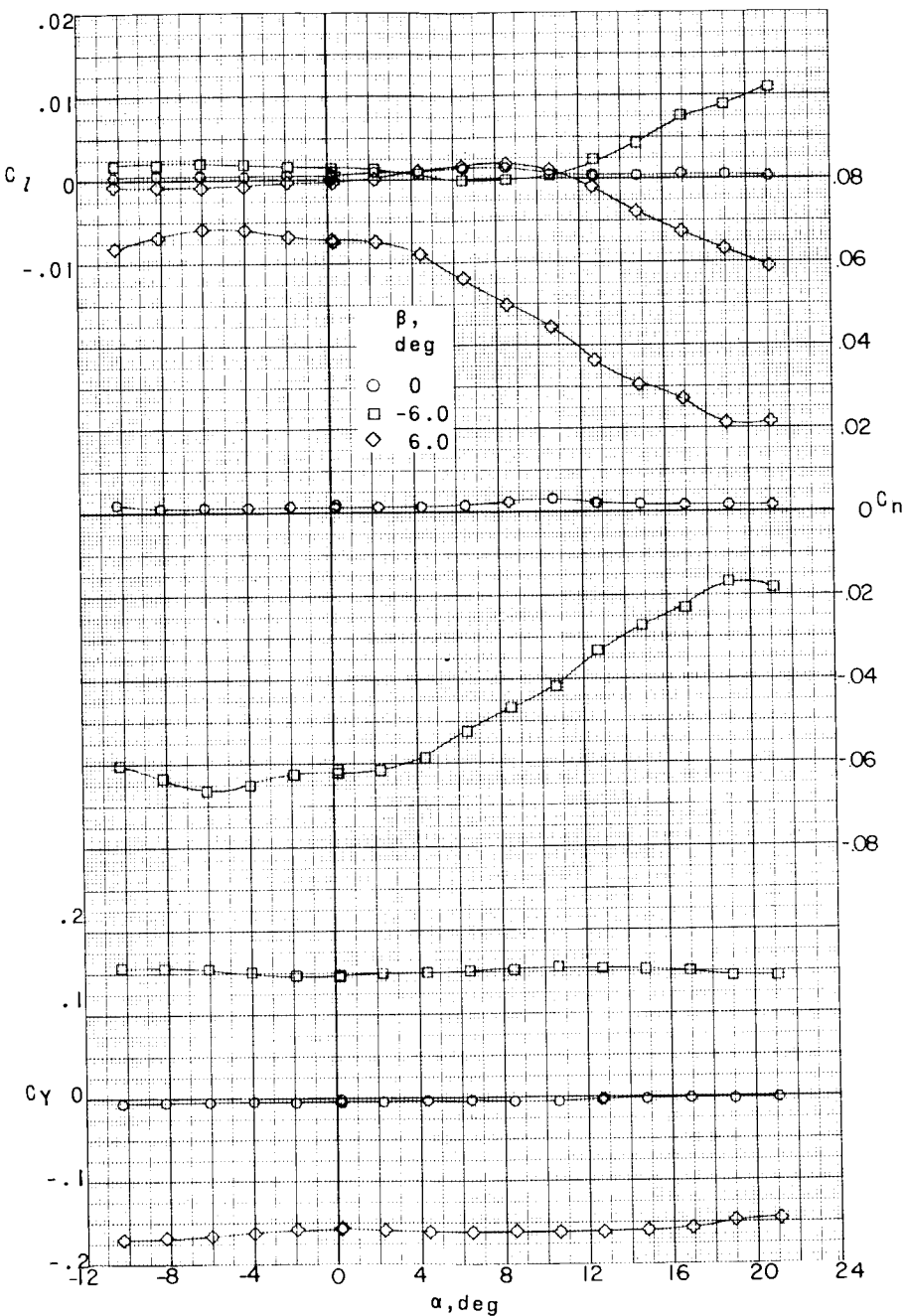
(a) $M = 2.29$.

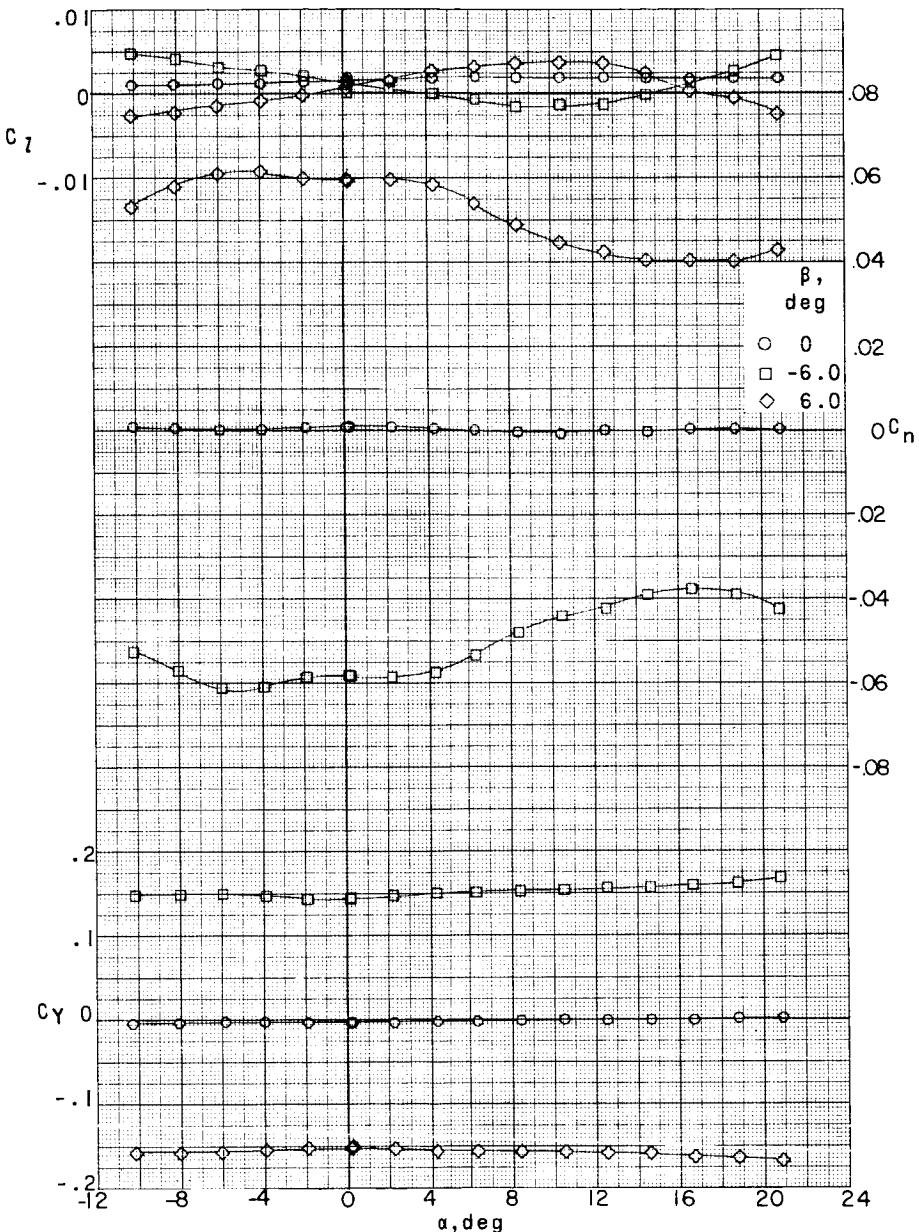
Figure 25.- Lateral stability characteristics of a 0.067-scale model of the X-15 airplane with speed brakes open 35° .

~~CONFIDENTIAL~~

DECLASSIFIED

~~CONFIDENTIAL~~

101



(b) $M = 2.98$.

Figure 25.- Continued.

031312201030

CONFIDENTIAL

102

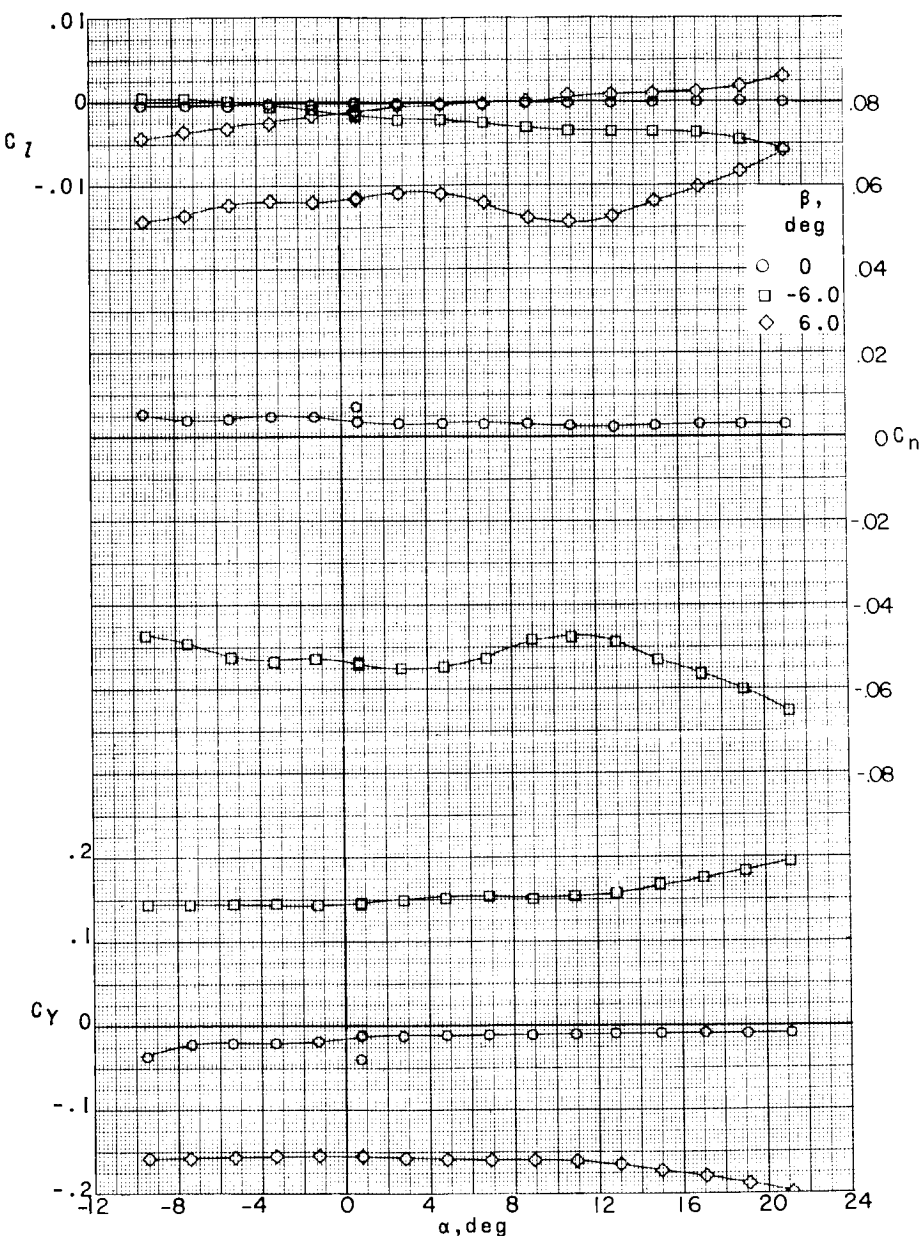
(c) $M = 4.65$.

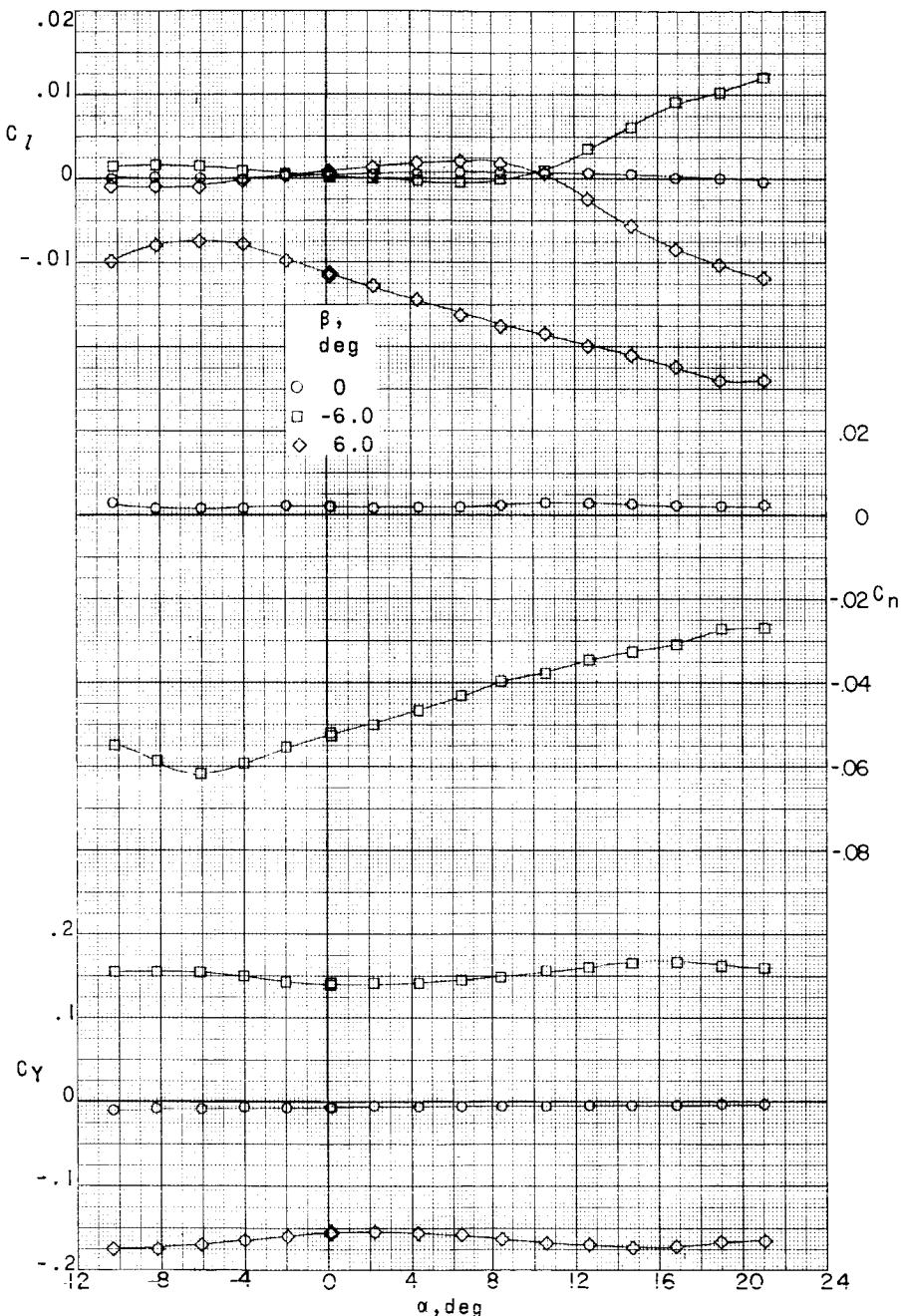
Figure 25.- Concluded.

~~CONFIDENTIAL~~

DECLASSIFIED

103

L-351



(a) $M = 2.29$.

Figure 26.- Lateral stability characteristics of a 0.067-scale model of the X-15 airplane with lower speed brakes open 35°.

~~CONFIDENTIAL~~

03732201030

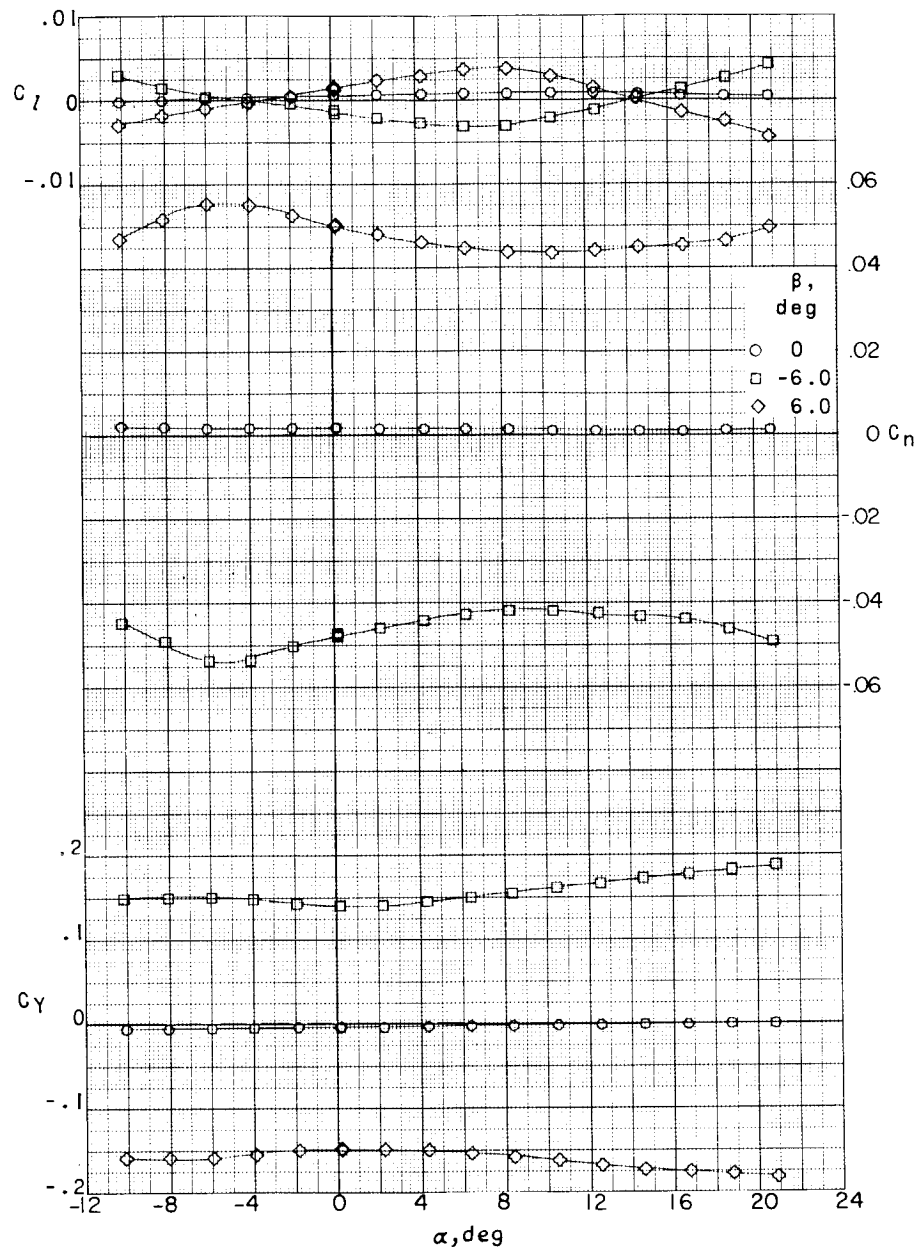
10⁴~~CONFIDENTIAL~~(b) $M = 2.98$.

Figure 26.- Continued.

~~CONFIDENTIAL~~

DECLASSIFIED

~~CONFIDENTIAL~~

105

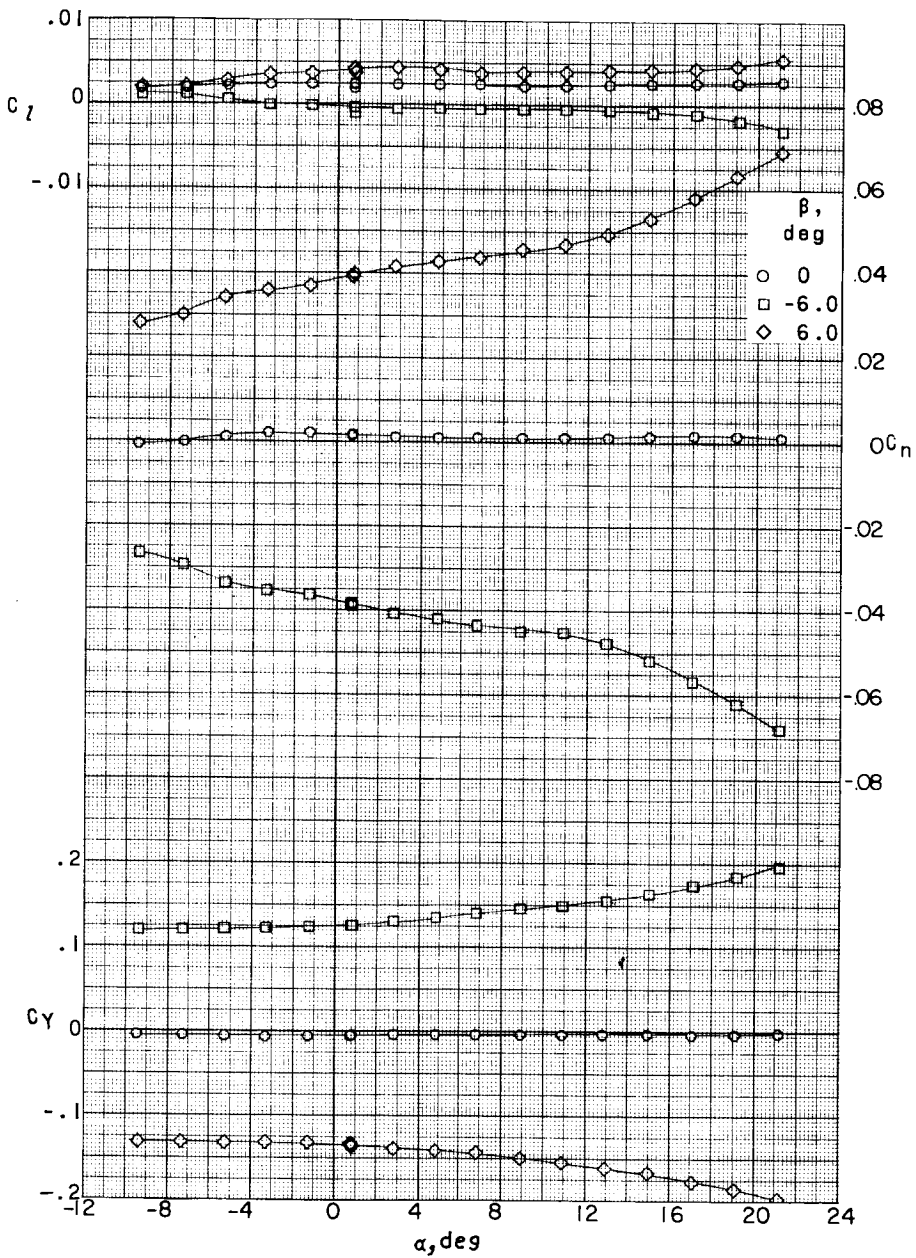
(c) $M = 4.65$.

Figure 26.- Concluded.

~~CONFIDENTIAL~~

03171220.1030

~~CONFIDENTIAL~~

106

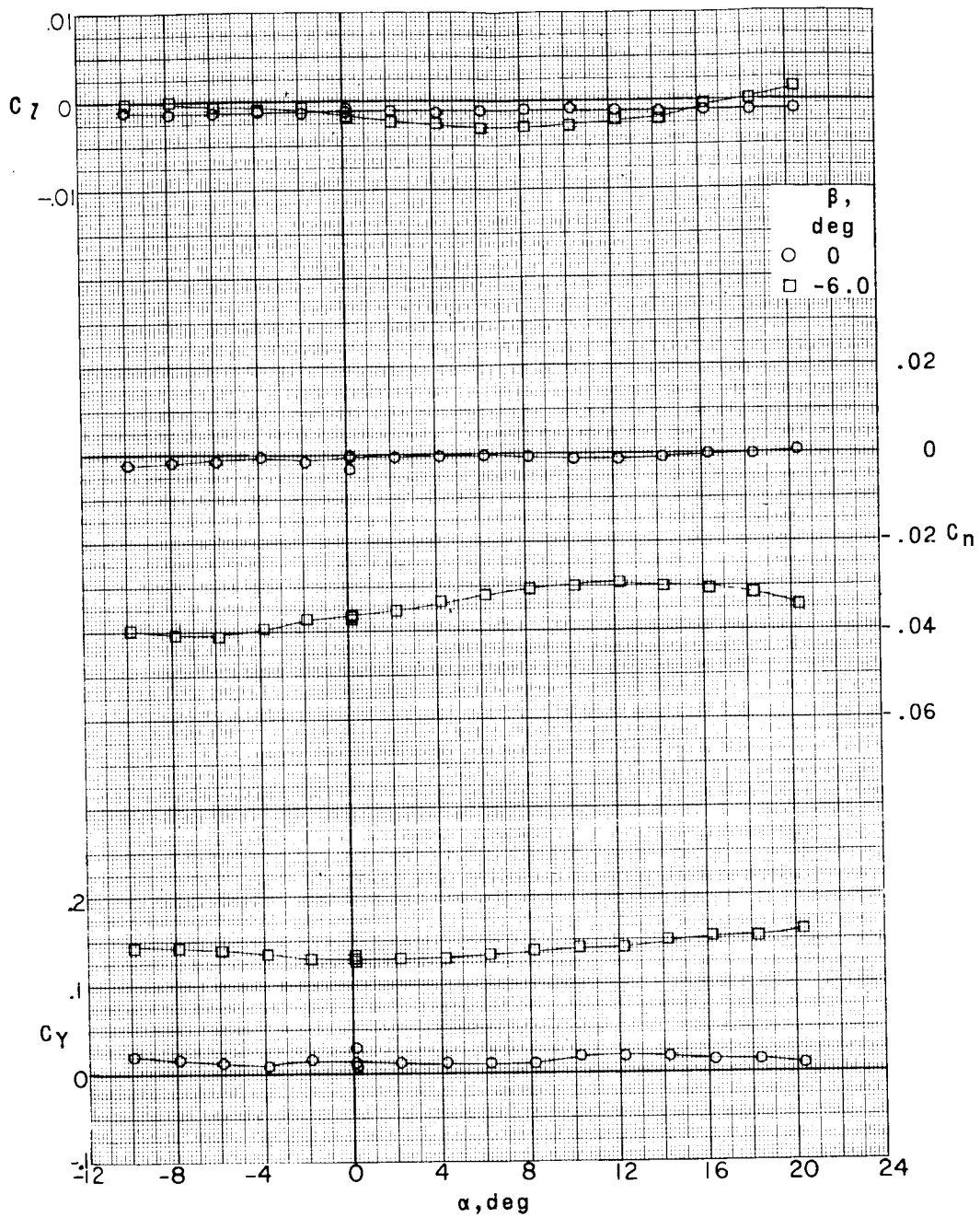
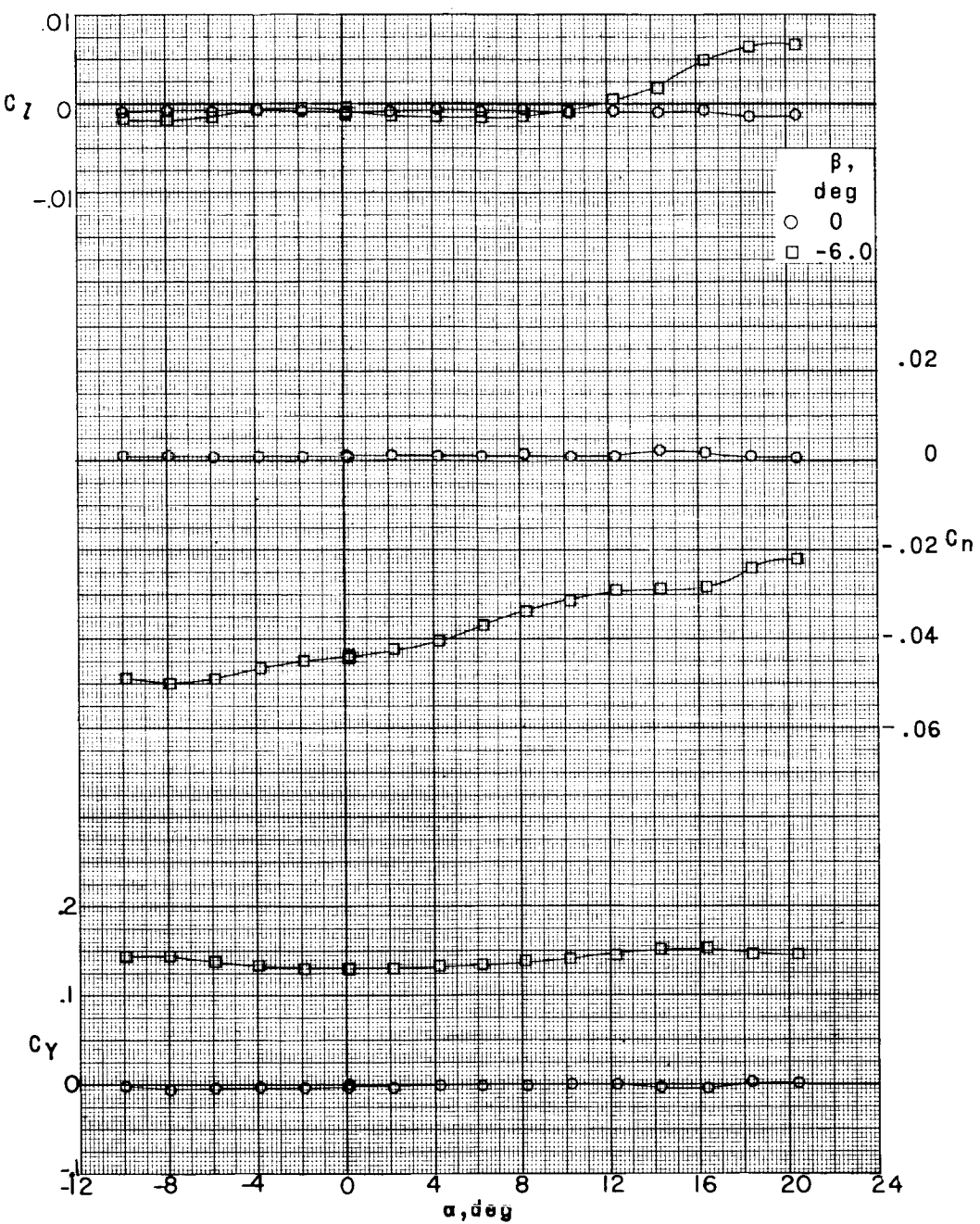
(a) $M = 2.29$.

Figure 27.- Lateral stability characteristics of a 0.067-scale model of the X-15 airplane at a Reynolds number of 0.5×10^6 with speed brakes retracted.

~~CONFIDENTIAL~~
~~DECLASSIFIED~~

107



(b) $M = 2.98$.

Figure 27.- Concluded.

CONFIDENTIAL 031712201030

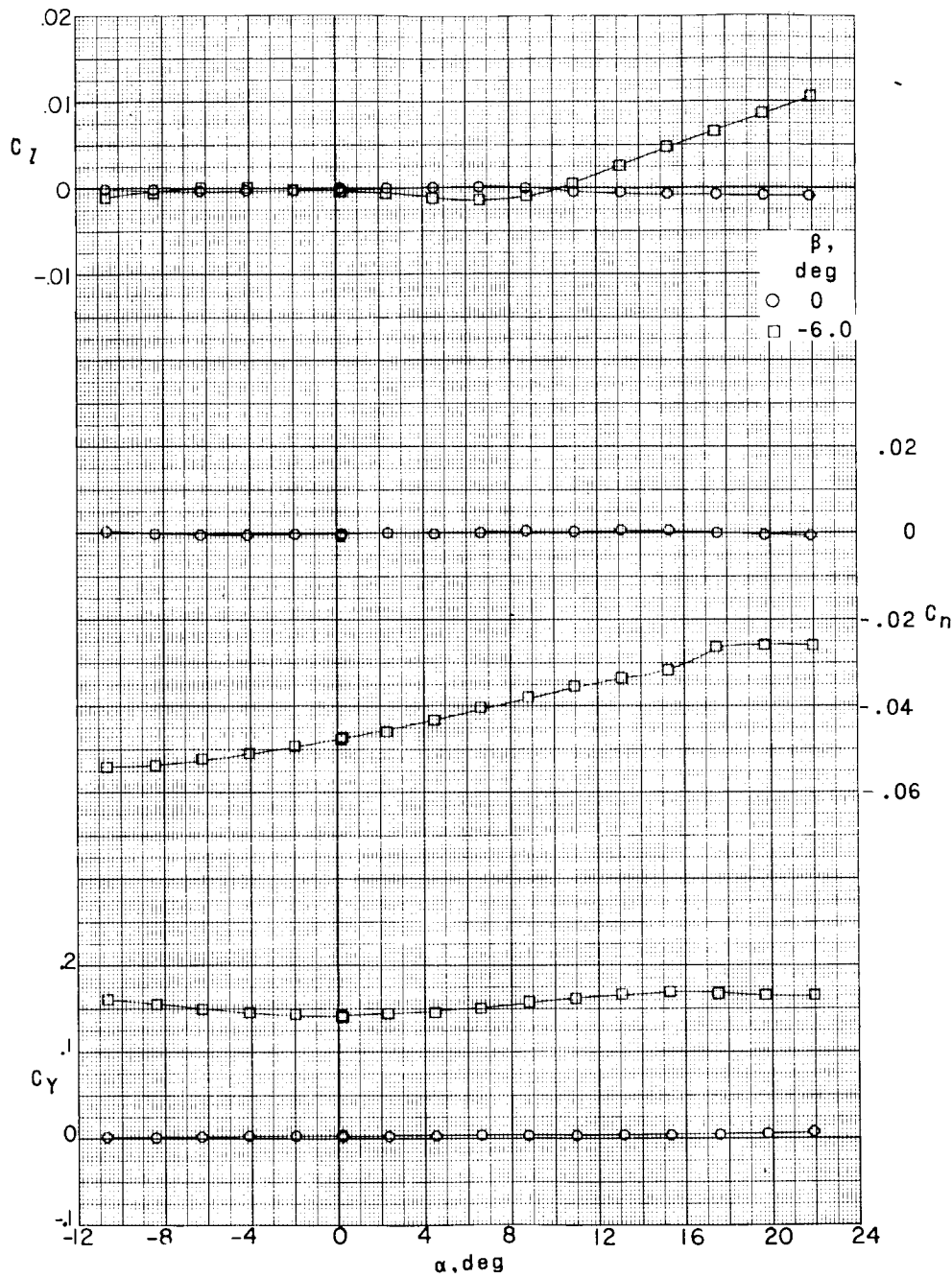
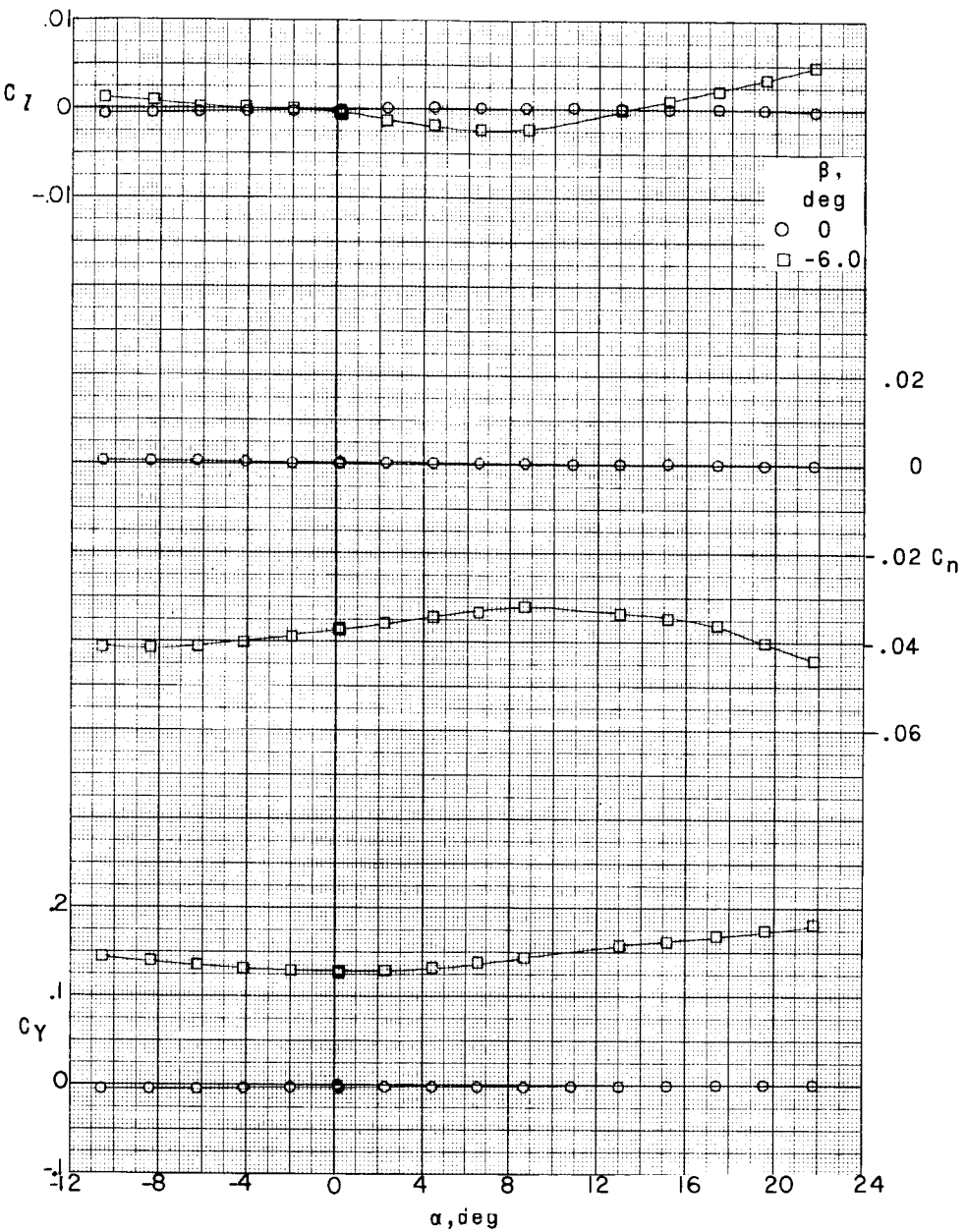
(a) $M = 2.29$; $R = 3.24 \times 10^6$.

Figure 28.- Lateral stability characteristics of a 0.067-scale model of the X-15 airplane with speed brakes retracted.

CONFIDENTIAL

~~CONFIDENTIAL~~
~~DECLASSIFIED~~

109



(b) $M = 2.98; R = 4.06 \times 10^6.$

Figure 28.- Continued.

03/3/2010 3:00

~~CONFIDENTIAL~~

110

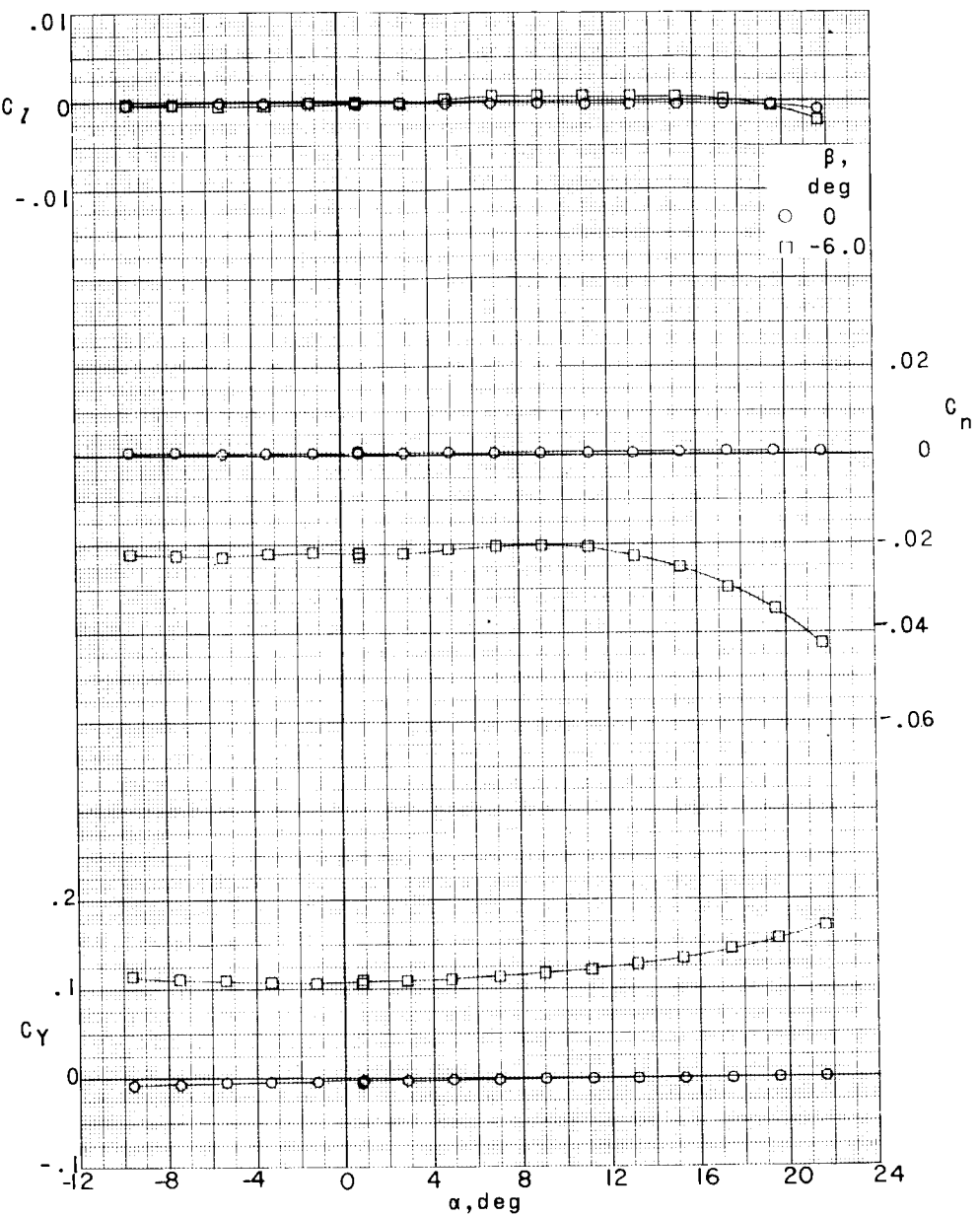
(c) $M = 4.65; R = 4.43 \times 10^6$.

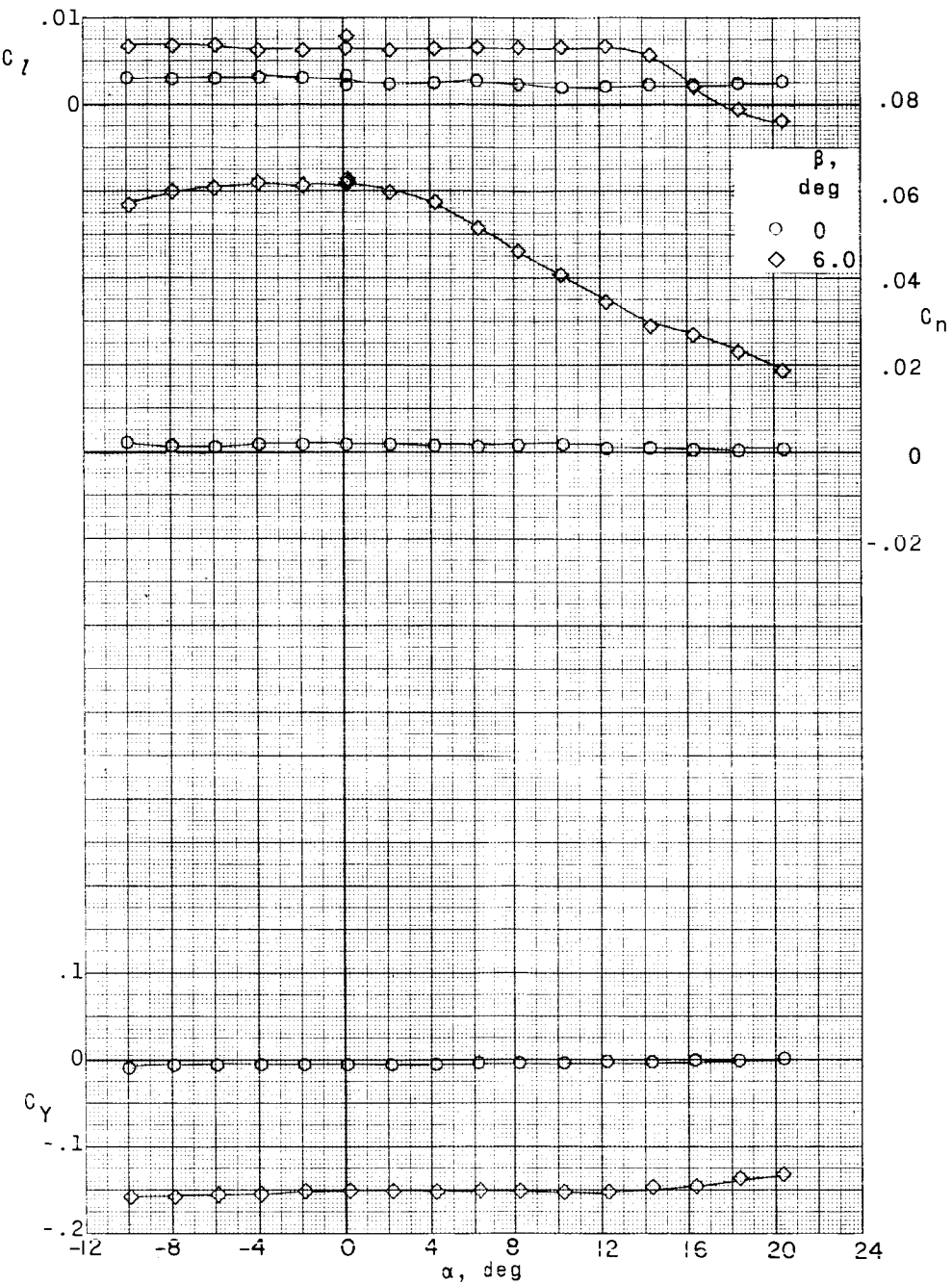
Figure 28.- Concluded.

~~CONFIDENTIAL~~

~~CONFIDENTIAL~~

DECLASSIFIED

111

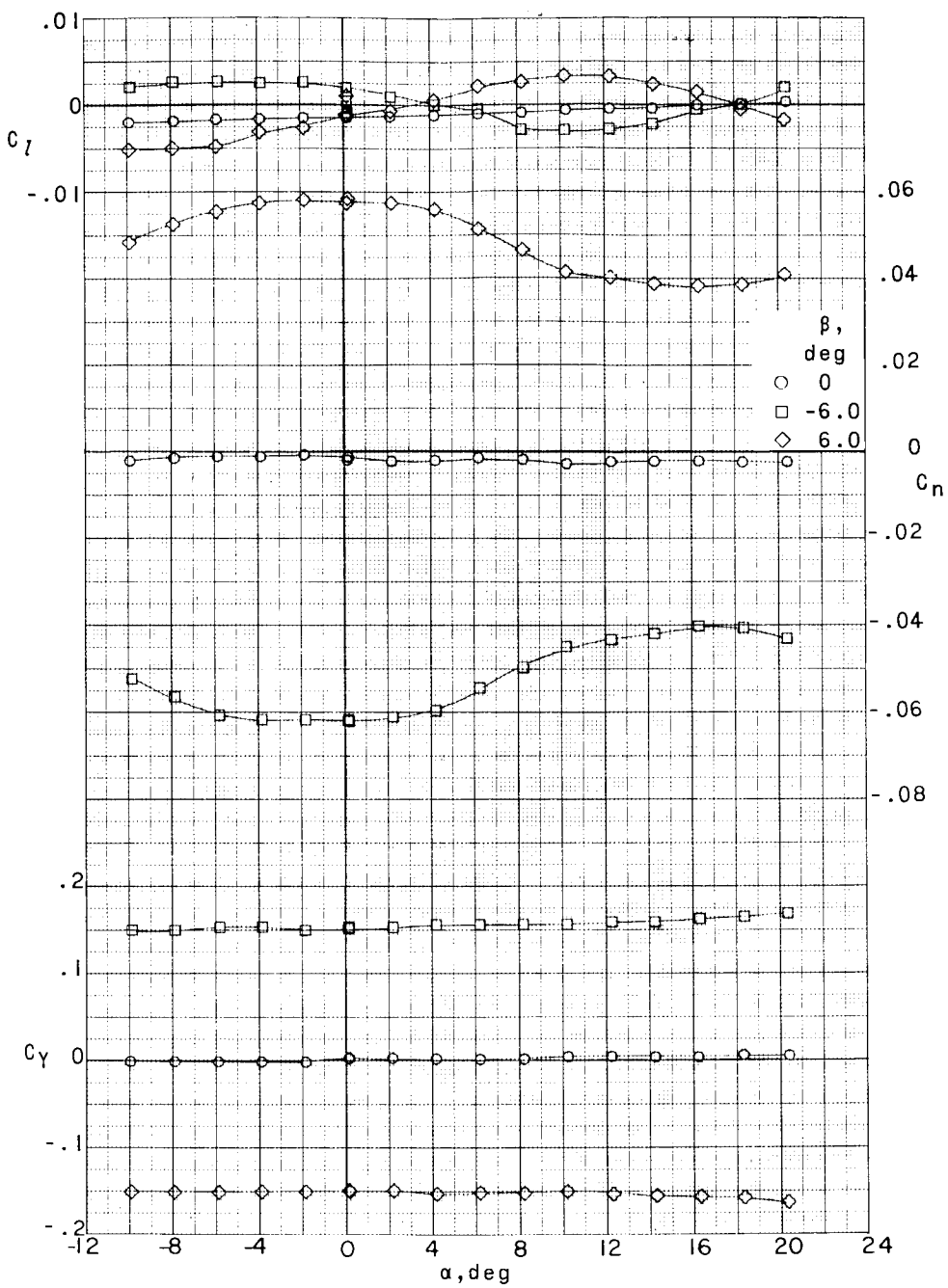


(a) $M = 2.29$

Figure 29.-- Lateral stability characteristics of a 0.067-scale model of the X-15 airplane at a Reynolds number of 0.5×10^6 with speed brakes open 35°.

03/3/2010 03:00

112

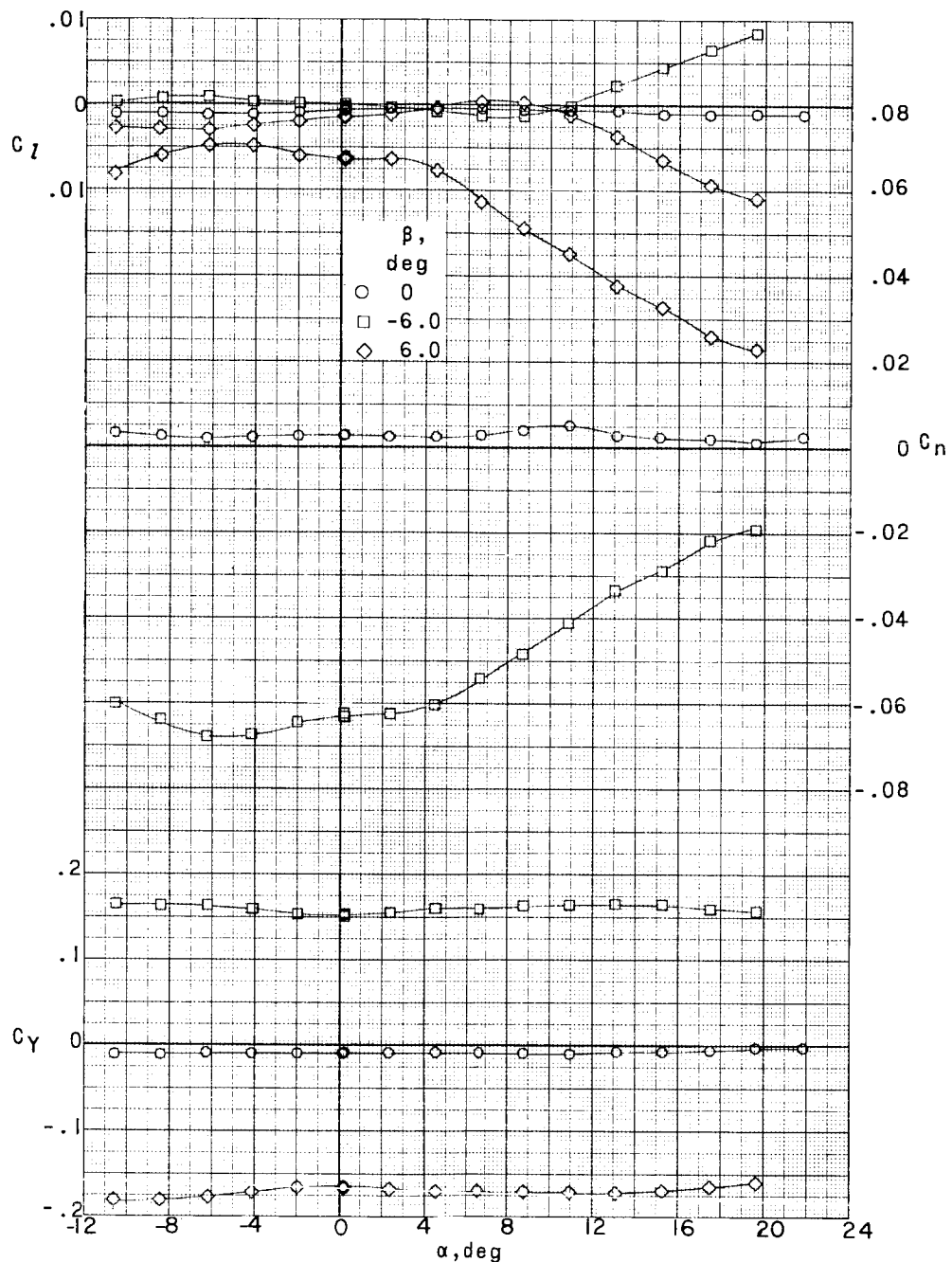


(b) $M = 2.98$.

Figure 29.- Concluded.

CONFIDENTIAL

DECLASSIFIED



(a) $M = 2.29$; $R = 3.24 \times 10^6$.

Figure 30.- Lateral stability characteristics of a 0.067-scale model of the X-15 airplane with speed brakes open 35° .

CONFIDENTIAL

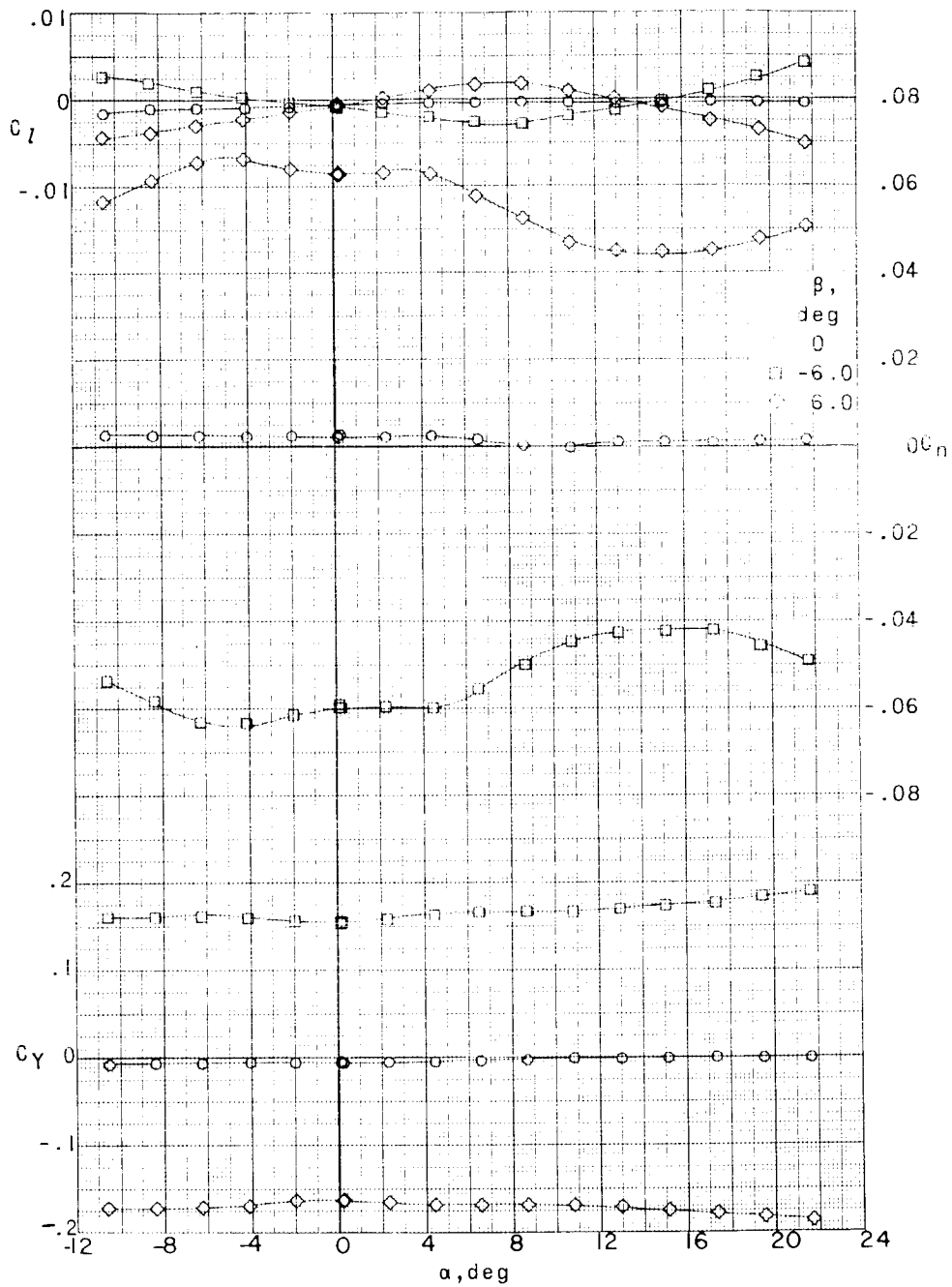
(b) $M = 2.98; R = 4.06 \times 10^6$.

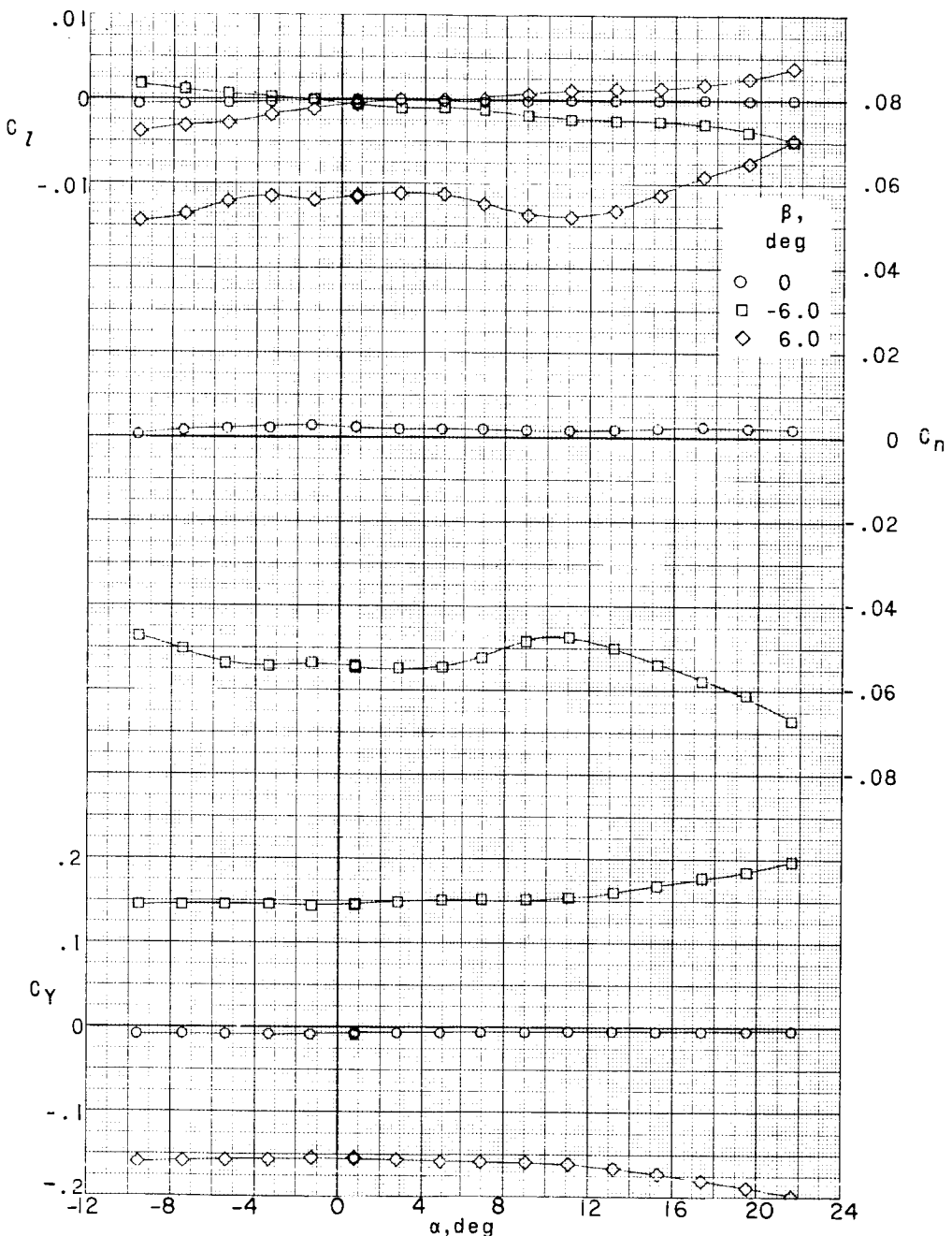
Figure 30.- Continued.

CONFIDENTIAL

L-351

~~CONFIDENTIAL~~

115



(c) $M = 4.65$; $R = 4.43 \times 10^6$.

Figure 30.- Concluded.

031913201030

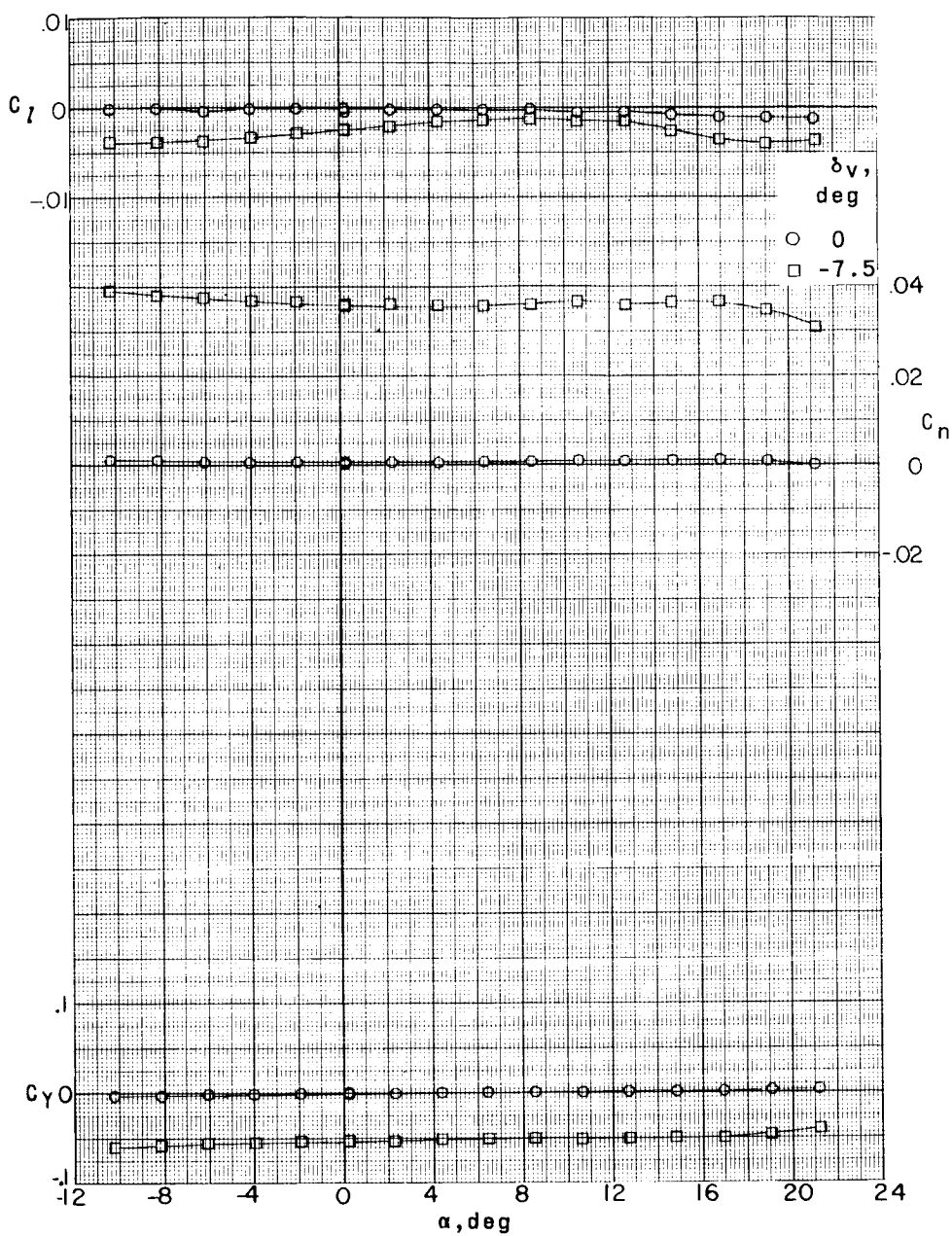
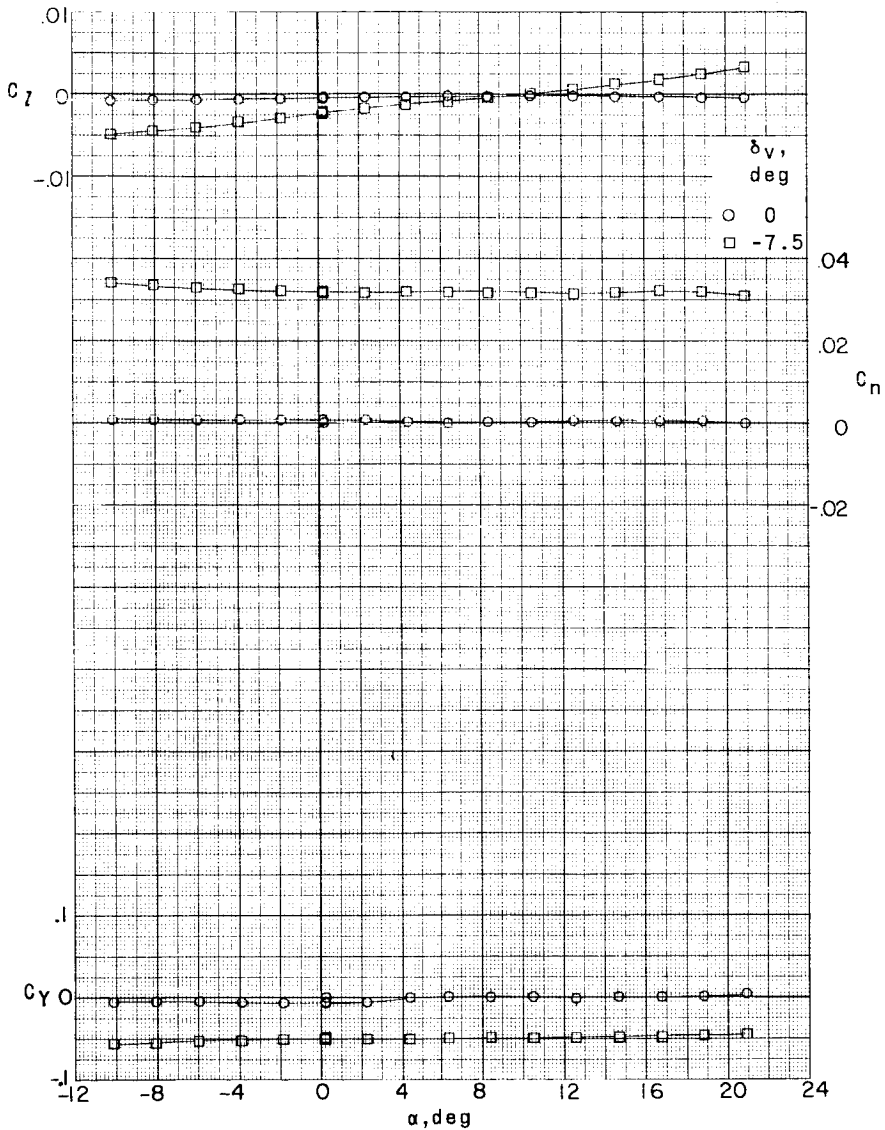
(a) $M = 2.29$.

Figure 31.- Lateral stability characteristics of a 0.067-scale model of the X-15 airplane with various deflections of the vertical tail. Speed brakes retracted; $\delta_H = 0^\circ$.

~~CONFIDENTIAL~~

117



(b) $M = 2.98$.

Figure 31.- Continued.

CONFIDENTIAL

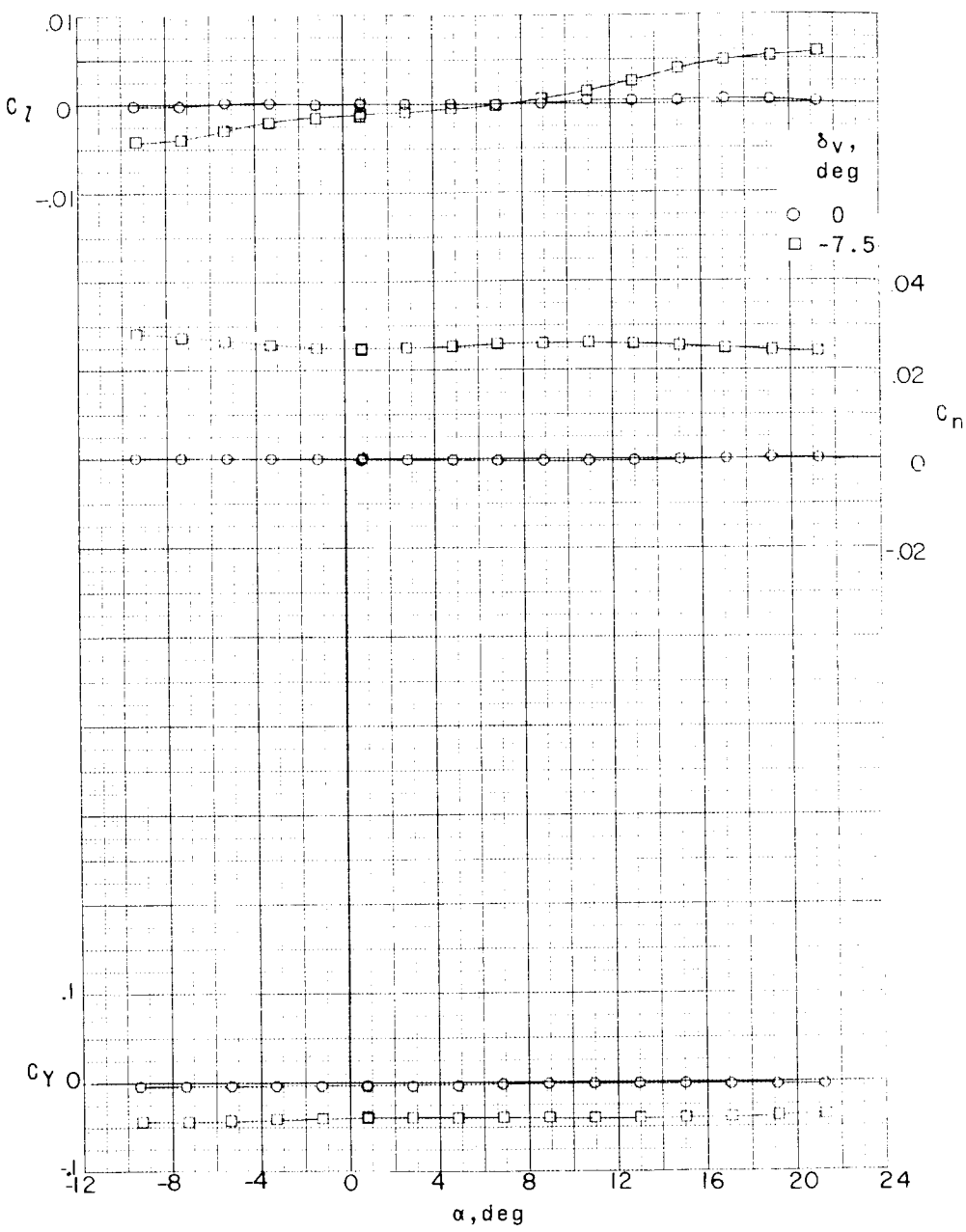
(e) $M = 4.65$.

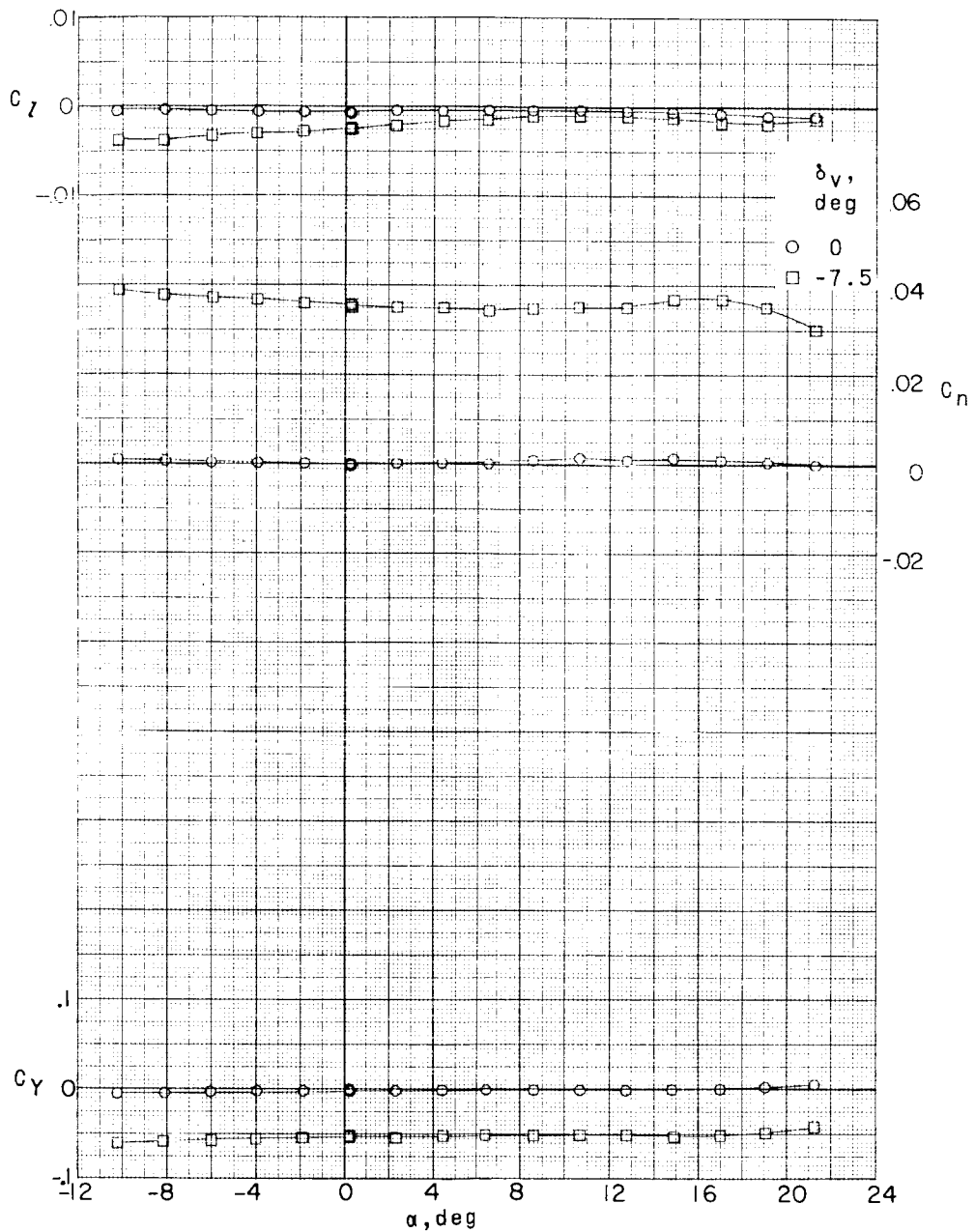
Figure 51.- Concluded.

CONFIDENTIAL

DECLASSIFIED

CONFIDENTIAL

119



(a) $M = 2.29$.

Figure 32.- Lateral stability characteristics of a 0.067-scale model of the X-15 airplane with various deflections of the vertical tail. Speed brakes retracted; $\delta_H = 20^\circ$.

CONFIDENTIAL

001312201030

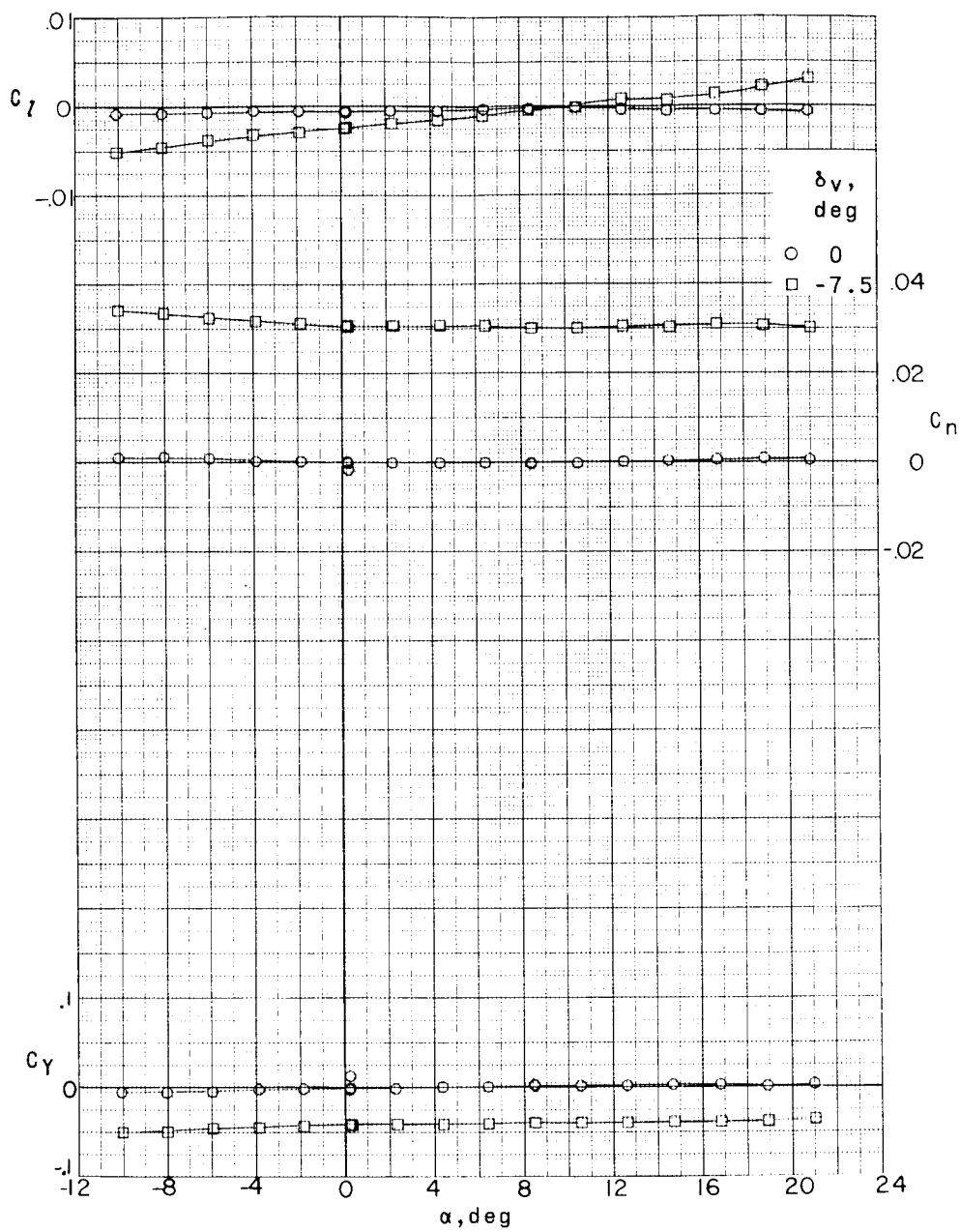
(b) $M = 2.98$.

Figure 32.- Continued.

~~CONFIDENTIAL~~

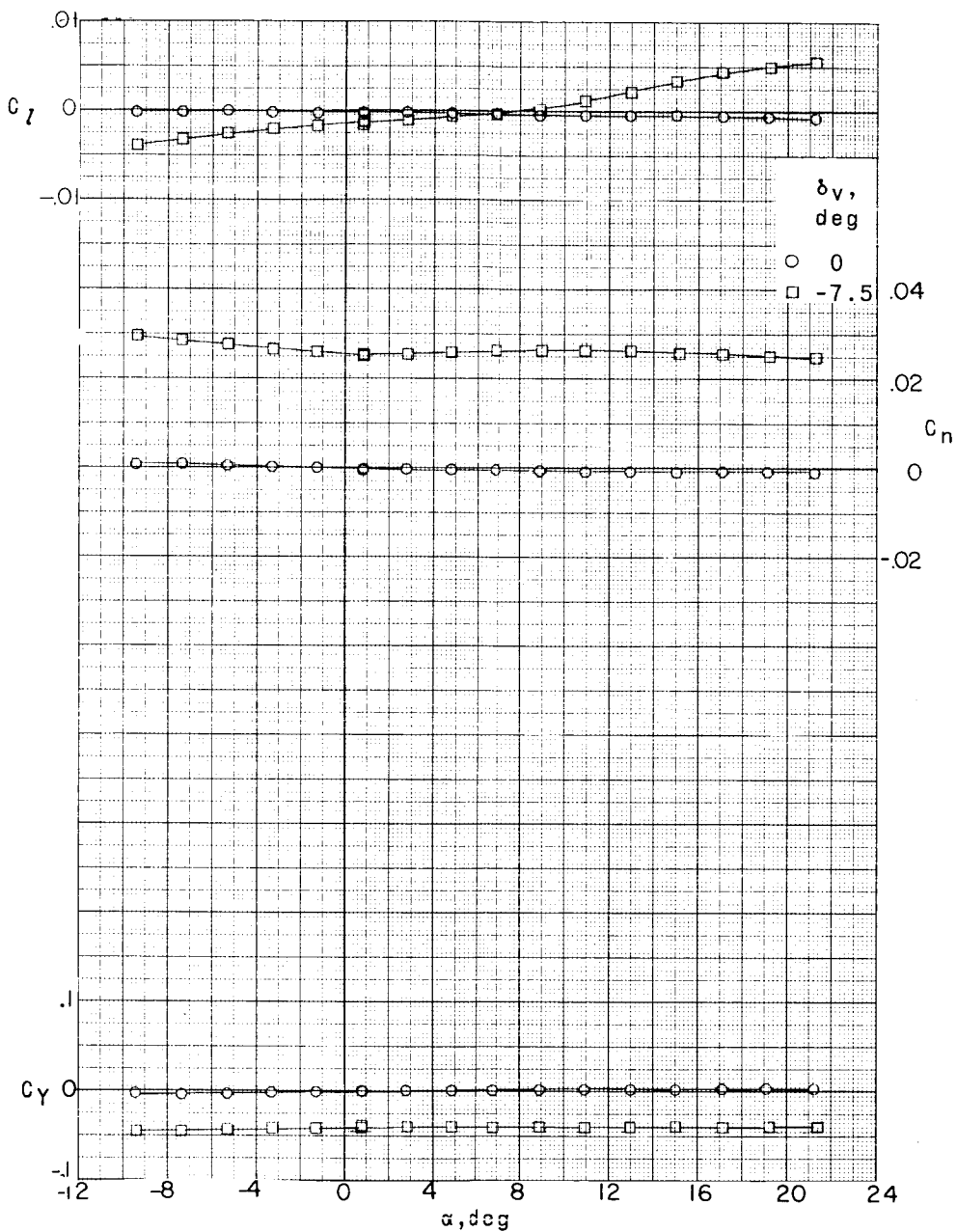
~~CONFIDENTIAL~~(c) $M = 4.65$.

Figure 32.- Concluded.

CONFIDENTIAL

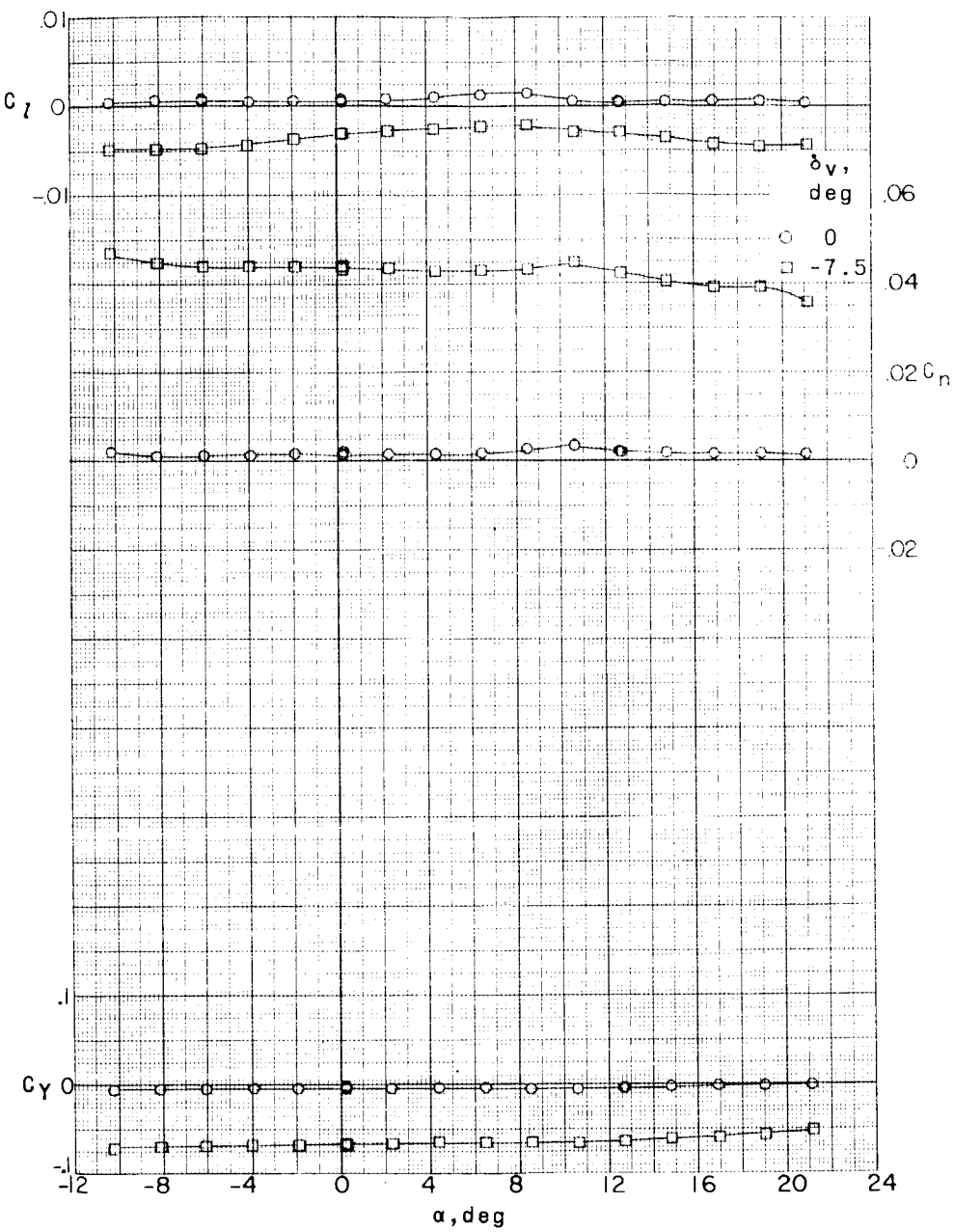
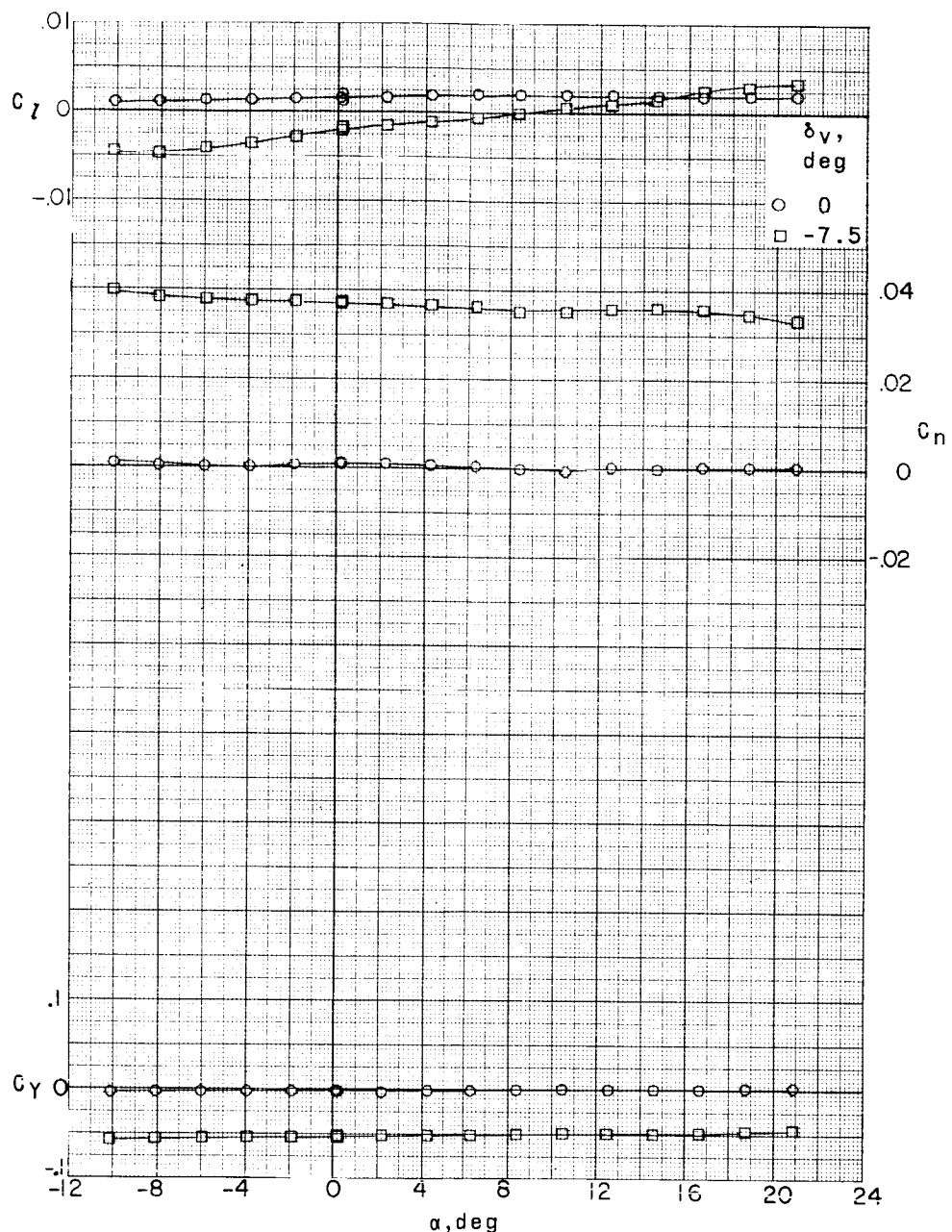
(a) $M = 2.29$.

Figure 33.- Lateral stability characteristics of a 0.067-scale model of the X-15 airplane with various deflections of the vertical tail.
Speed brakes open 45° ; $\delta_H = 0^\circ$.

~~CONFIDENTIAL~~

123



(b) $M = 2.98$.

Figure 33.- Continued.

CONFIDENTIAL

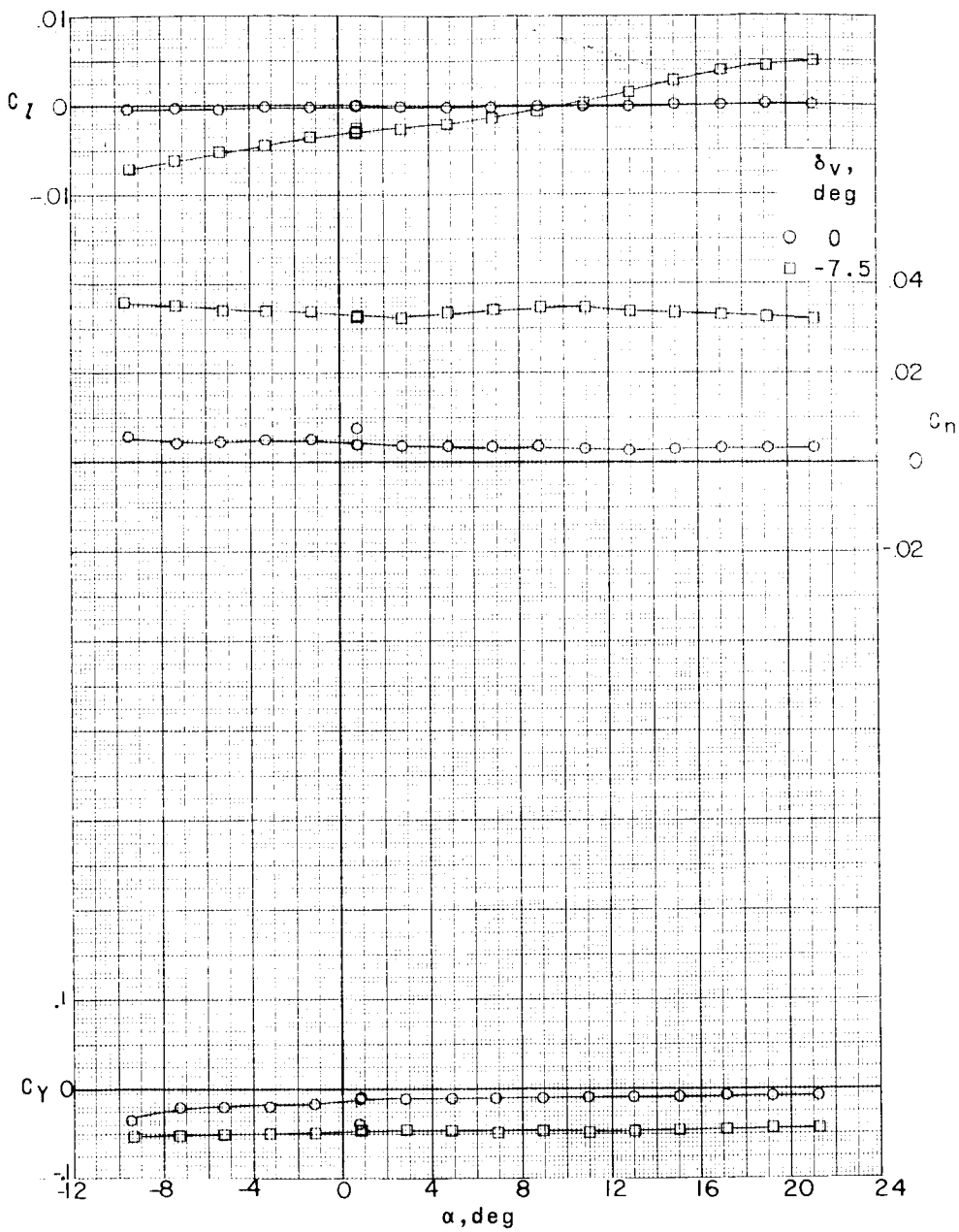
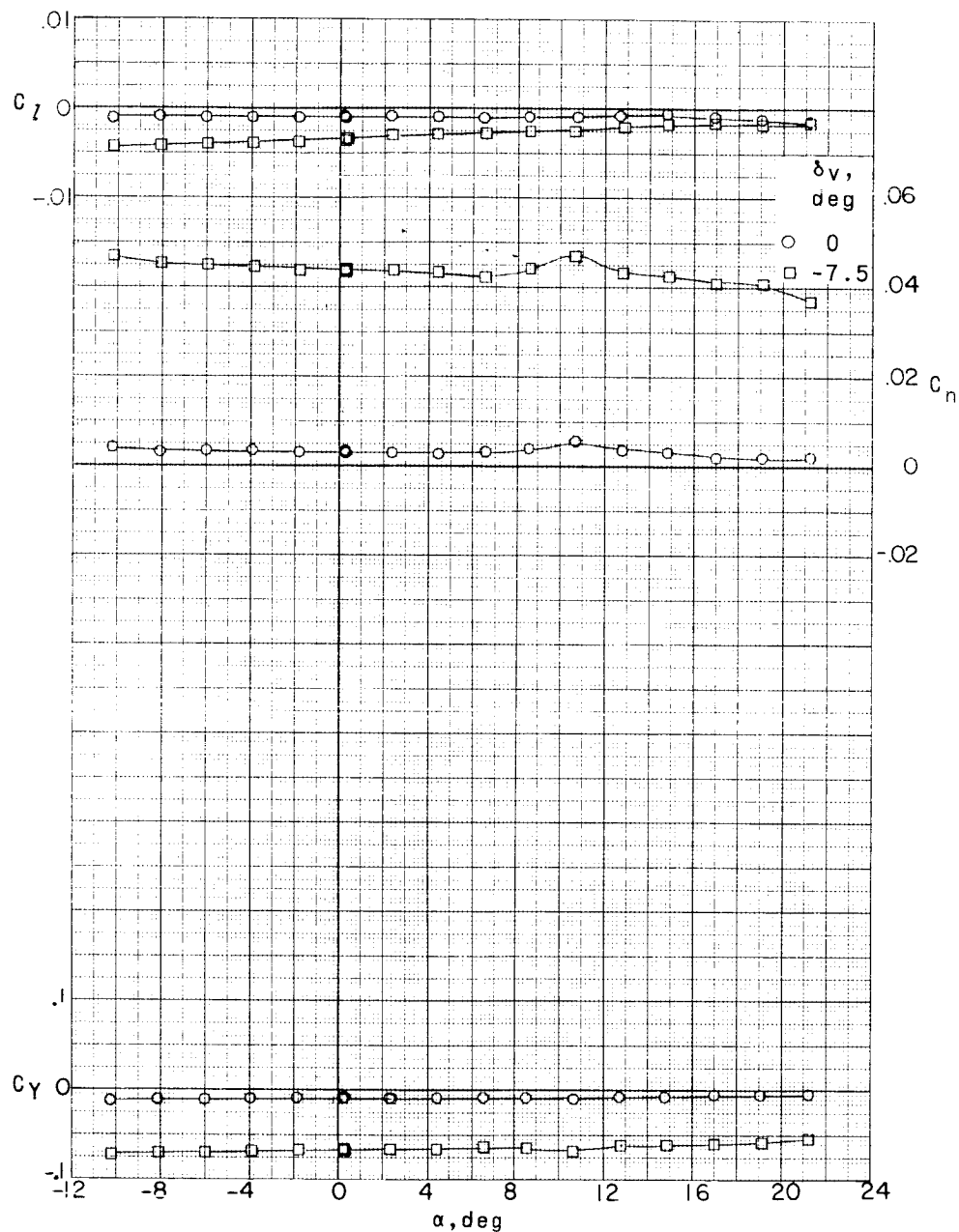
(c) $M = 4.65$.

Figure 33.- Concluded.

CONFIDENTIAL

~~CONFIDENTIAL~~

125



(a) $M = 2.29$.

Figure 34.- Lateral stability characteristics of a 0.067-scale model of the X-15 airplane with various deflections of the vertical tail. Speed brakes open 35° ; $\delta_H = 20^\circ$.

CONFIDENTIAL

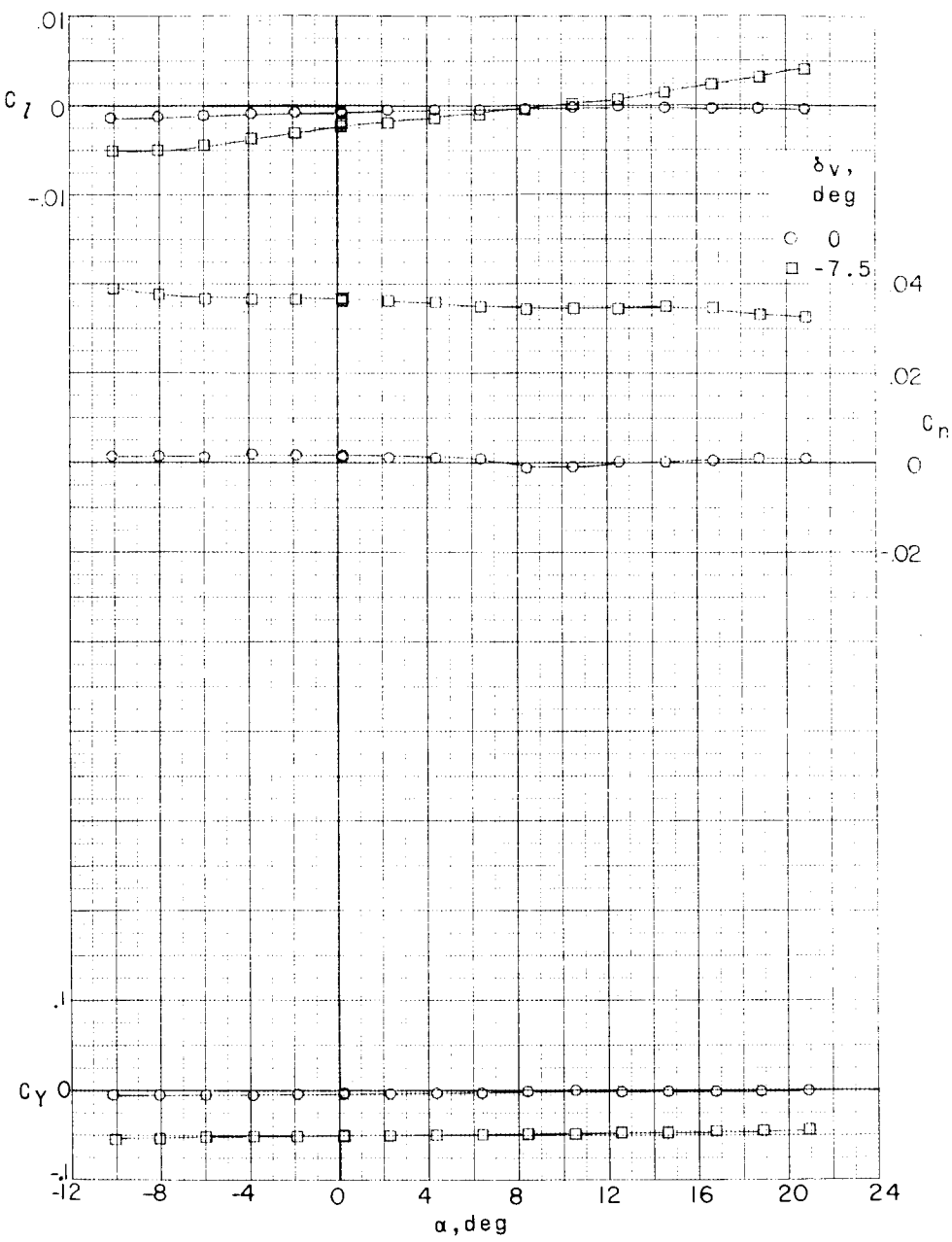
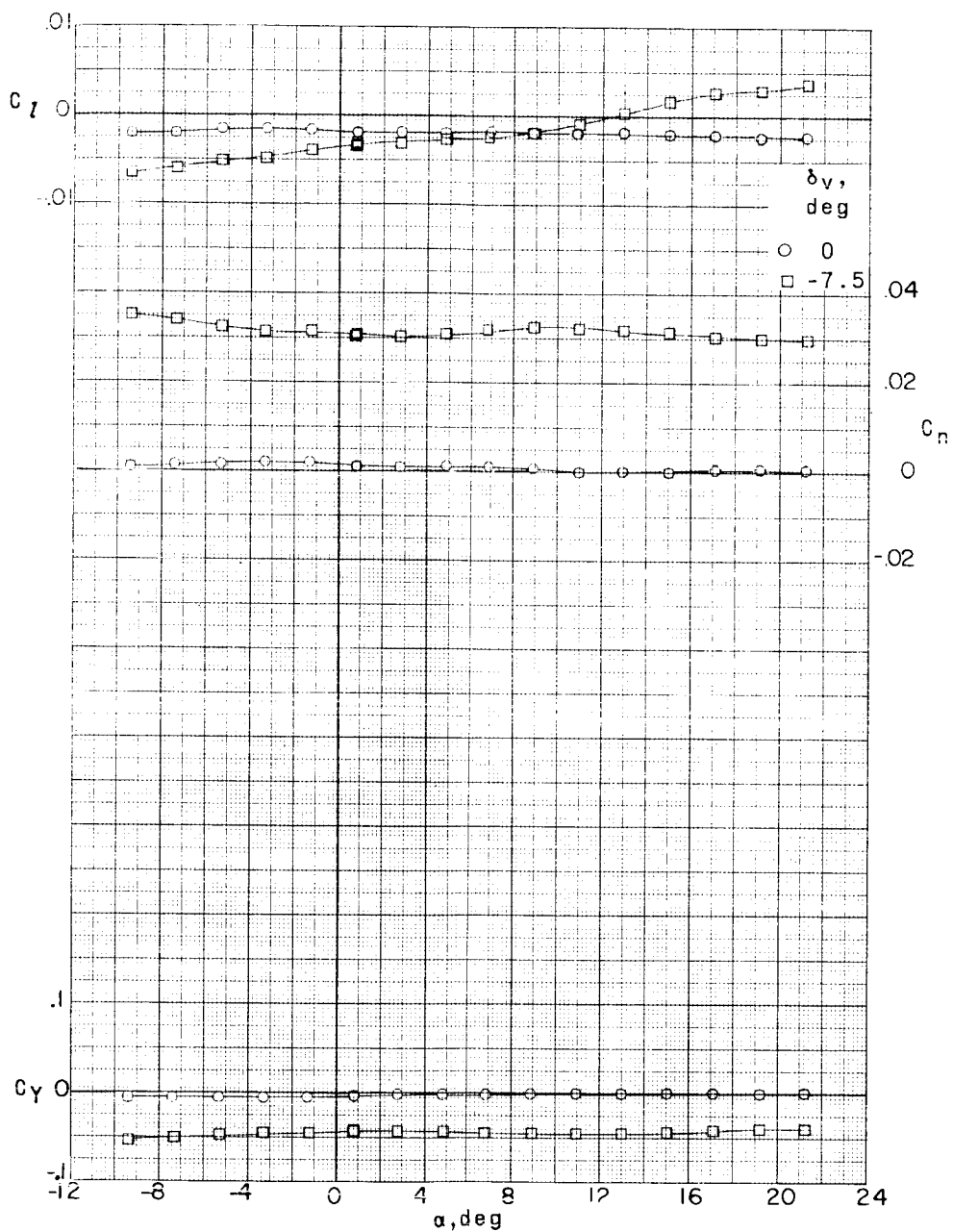
(b) $M = 2.98$.

Figure 34.- Continued.

REF ID: A6572
DECLASSIFIED

127



(c) $M = 4.65$.

Figure 34.- Concluded.

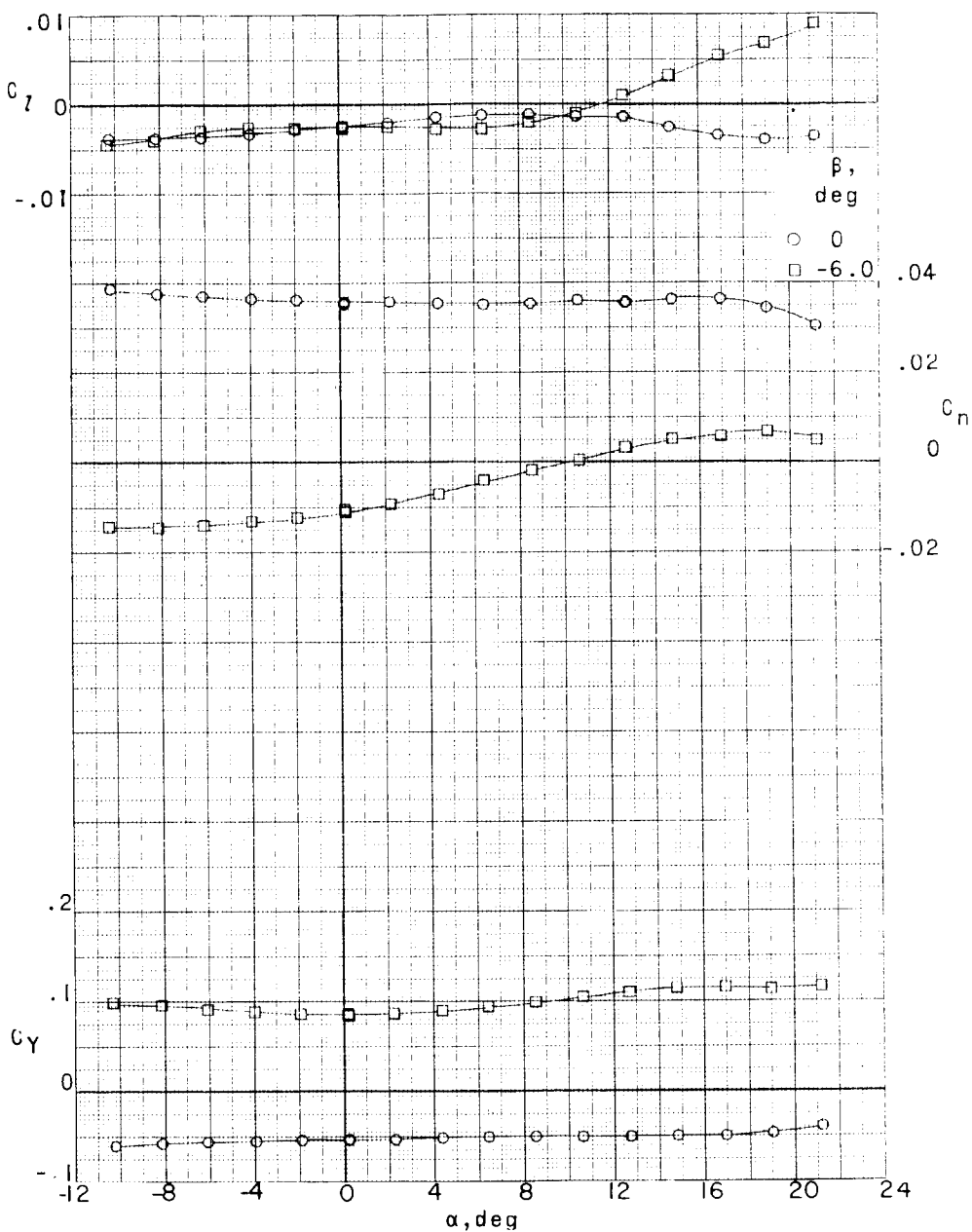
(a) $M = 2.29$.

Figure 35.- Lateral stability characteristics of a 0.067-scale model of the X-15 airplane. Speed brakes retracted; $\delta_v = -7.5^\circ$.

~~CONFIDENTIAL~~

~~CONFIDENTIAL~~

DECLASSIFIED

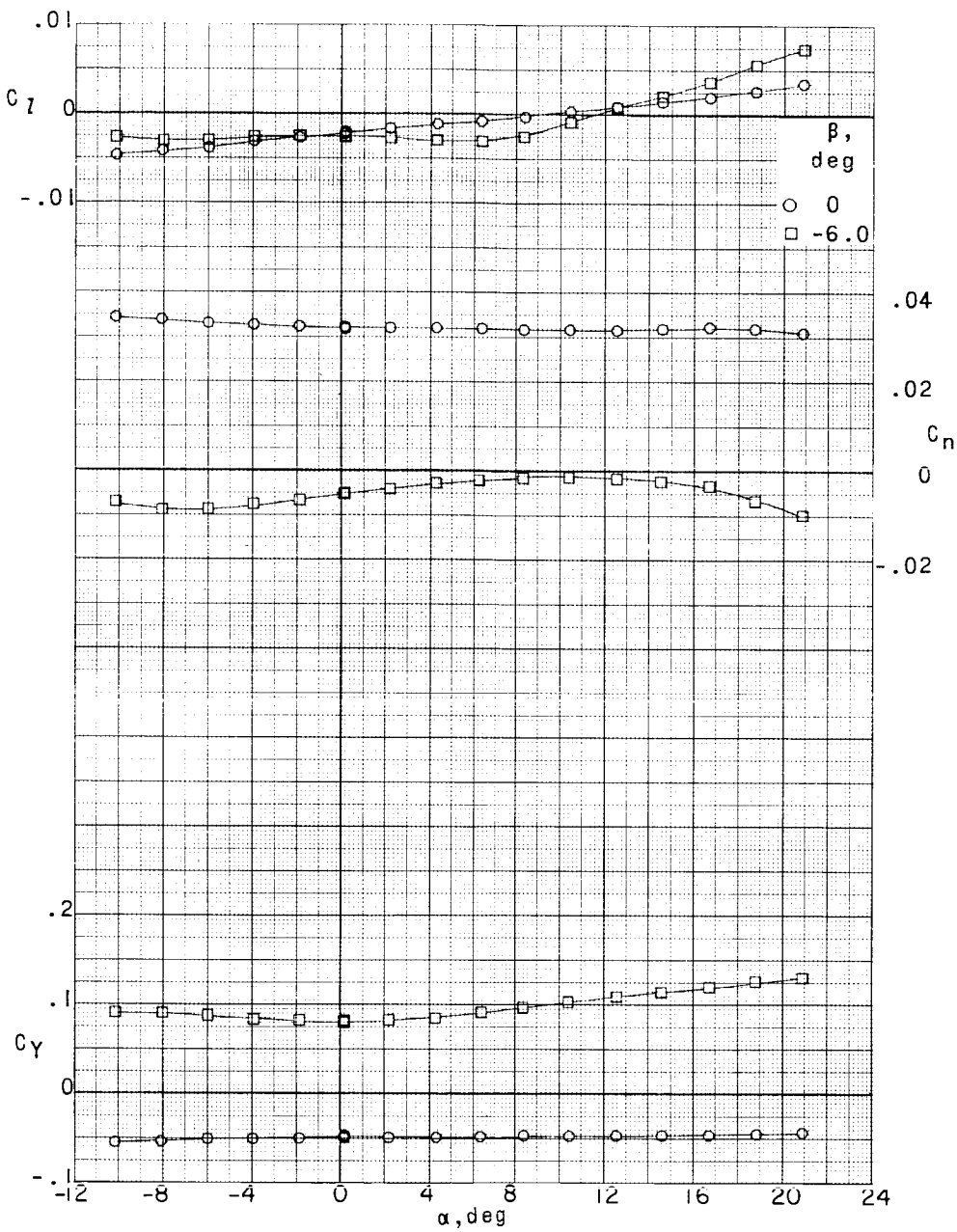
(b) $M = 2.98$.

Figure 35.- Continued.

CONFIDENTIAL

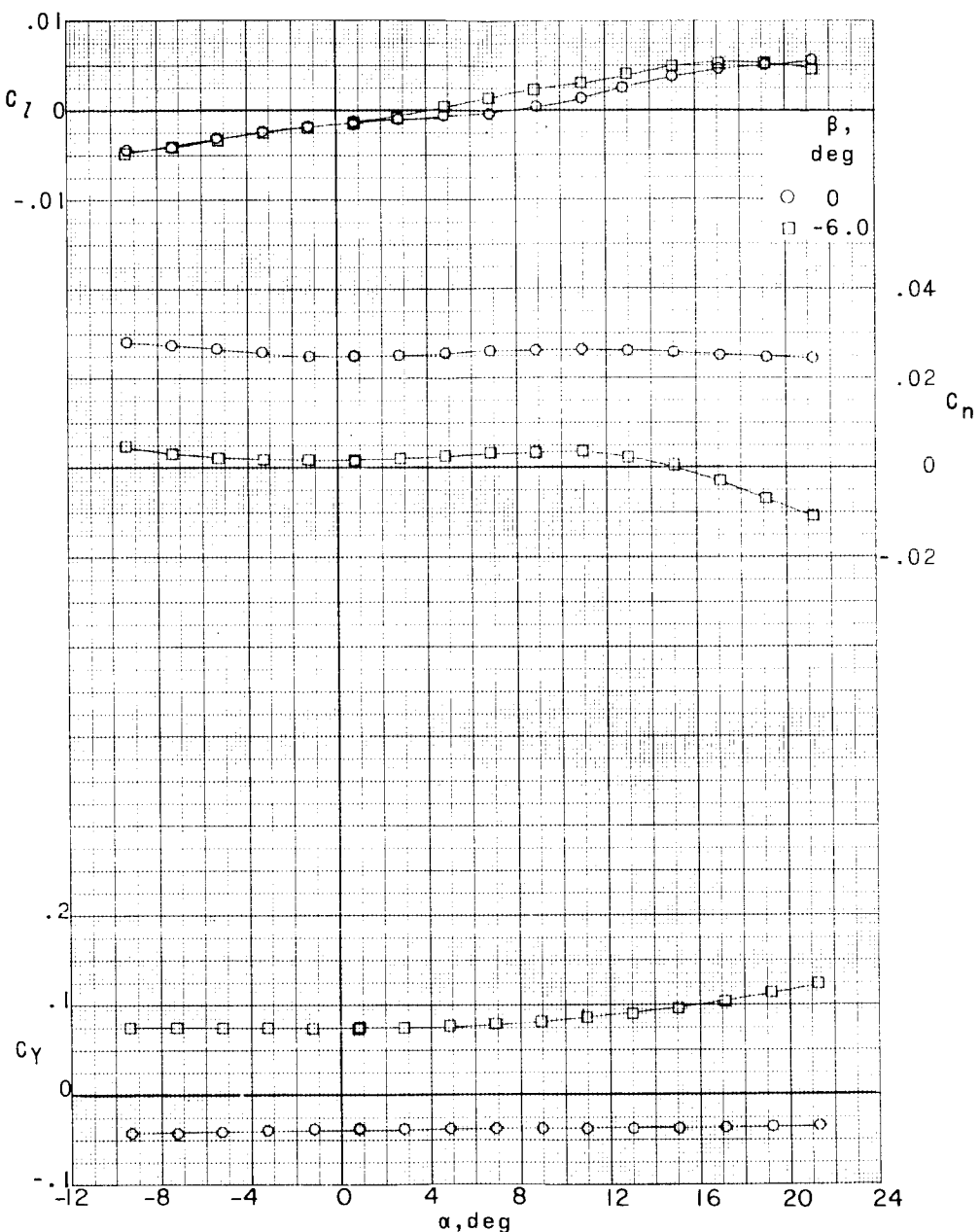
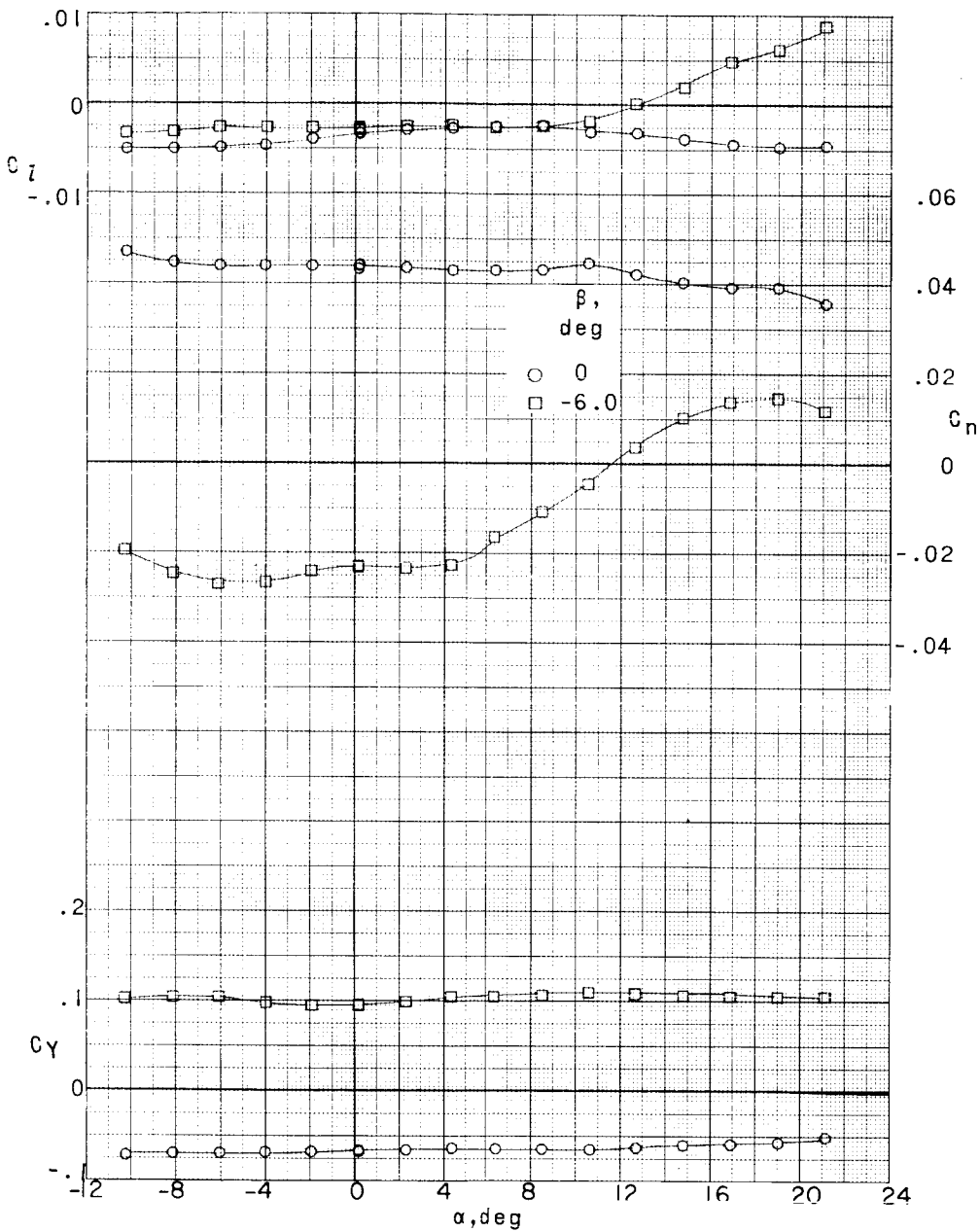
(c) $M = 4.65$.

Figure 35.- Concluded.

DECLASSIFIED

~~CONFIDENTIAL~~

131



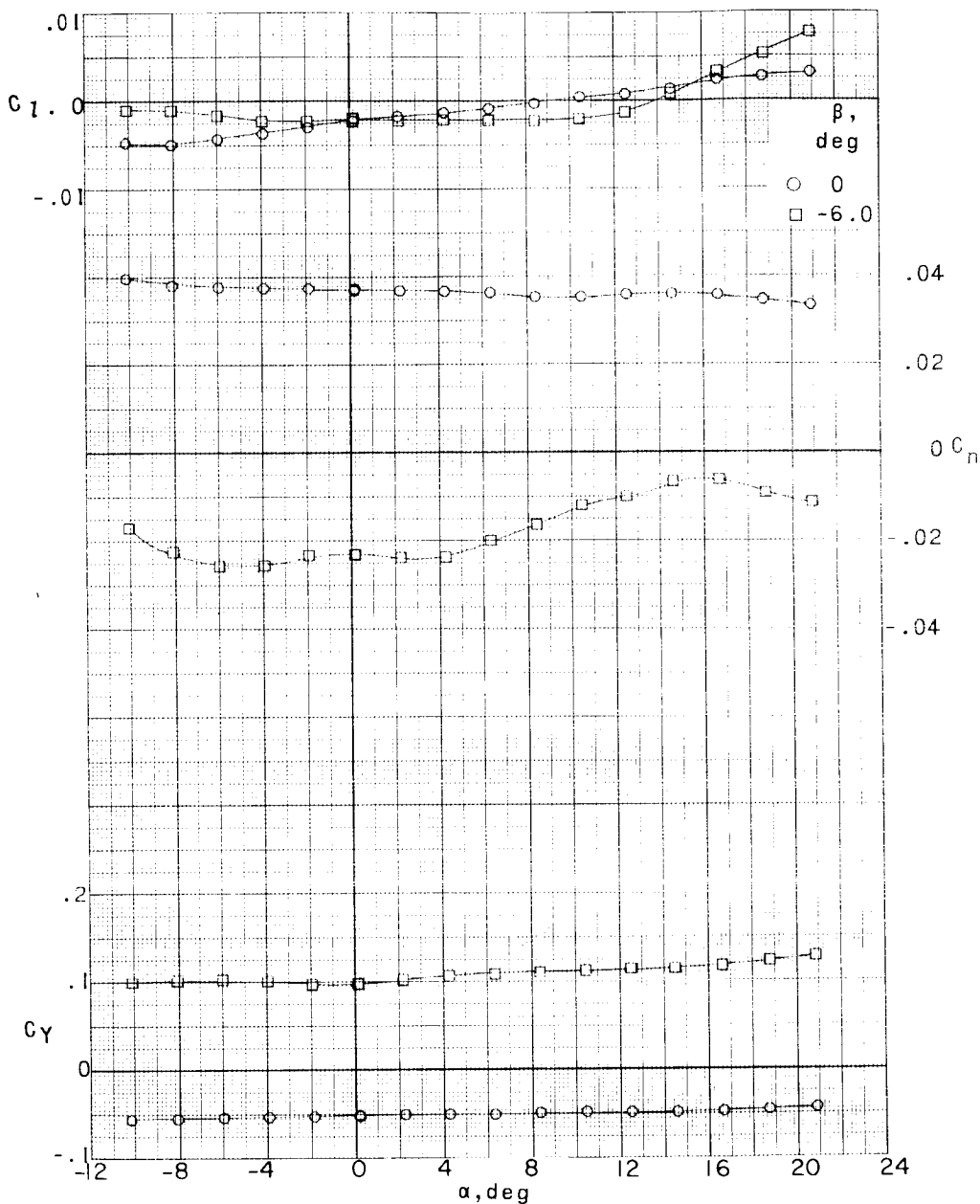
(a) $M = 2.29$.

Figure 36.- Lateral stability characteristics of a 0.067-scale model of the X-15 airplane. Speed brakes open 35° ; $\delta_v = -7.5^\circ$.

001302201030

132

~~CONFIDENTIAL~~



(b) $M = 2.98$.

Figure 36.- Continued.

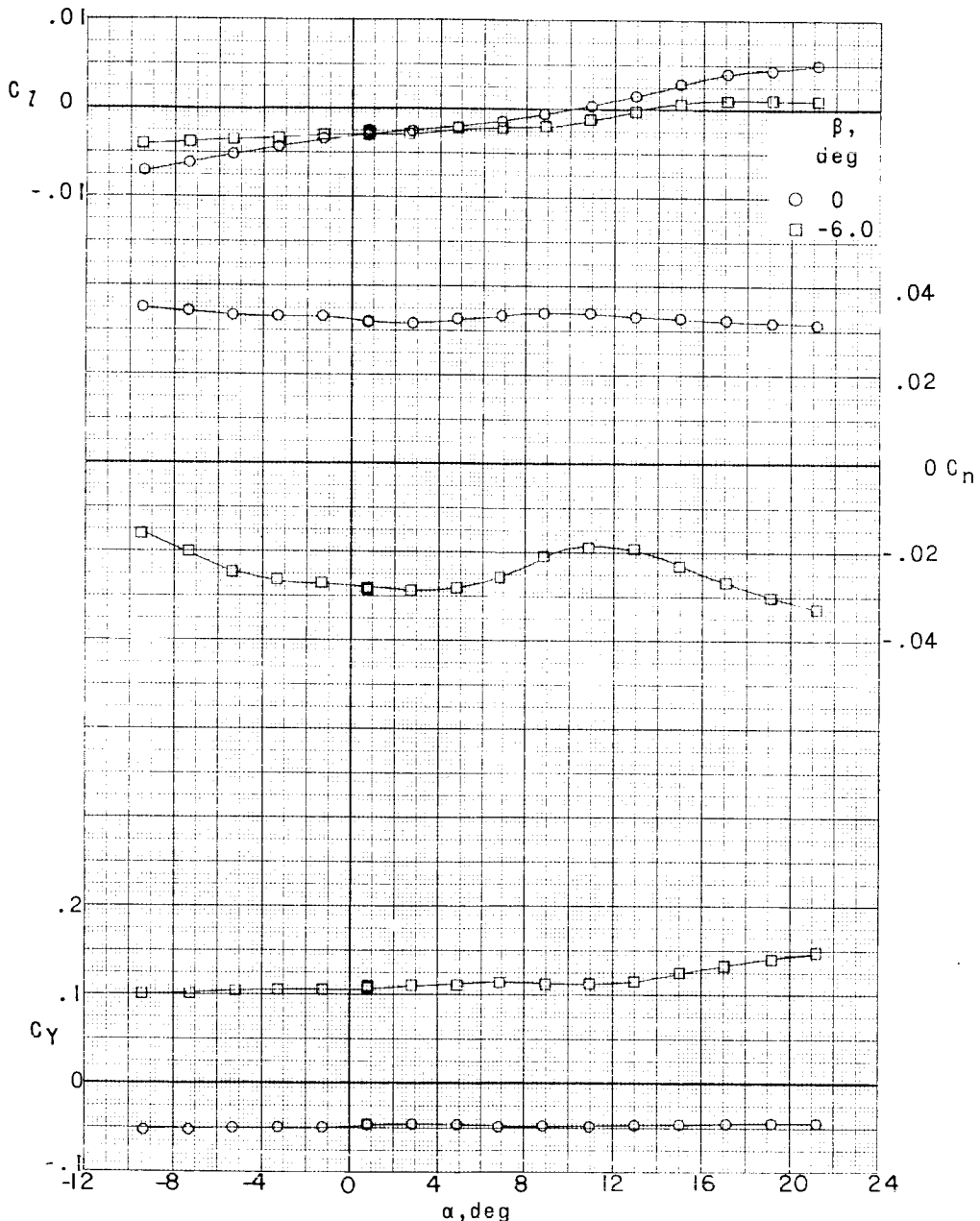
~~CONFIDENTIAL~~

L-351

DECLASSIFIED

~~CONFIDENTIAL~~

133



(c) $M = 4.65$.

Figure 36.- Concluded.

CONFIDENTIAL

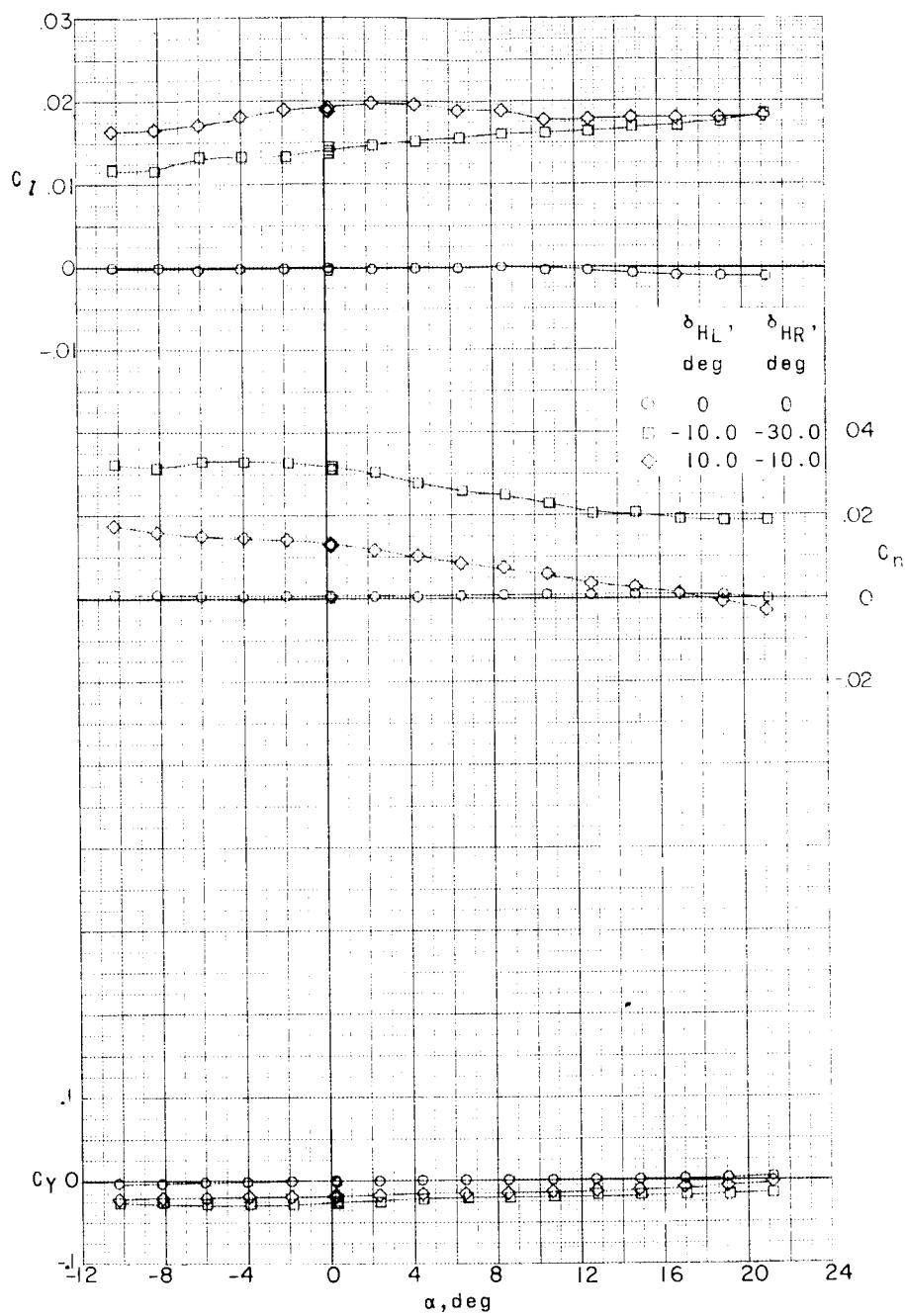
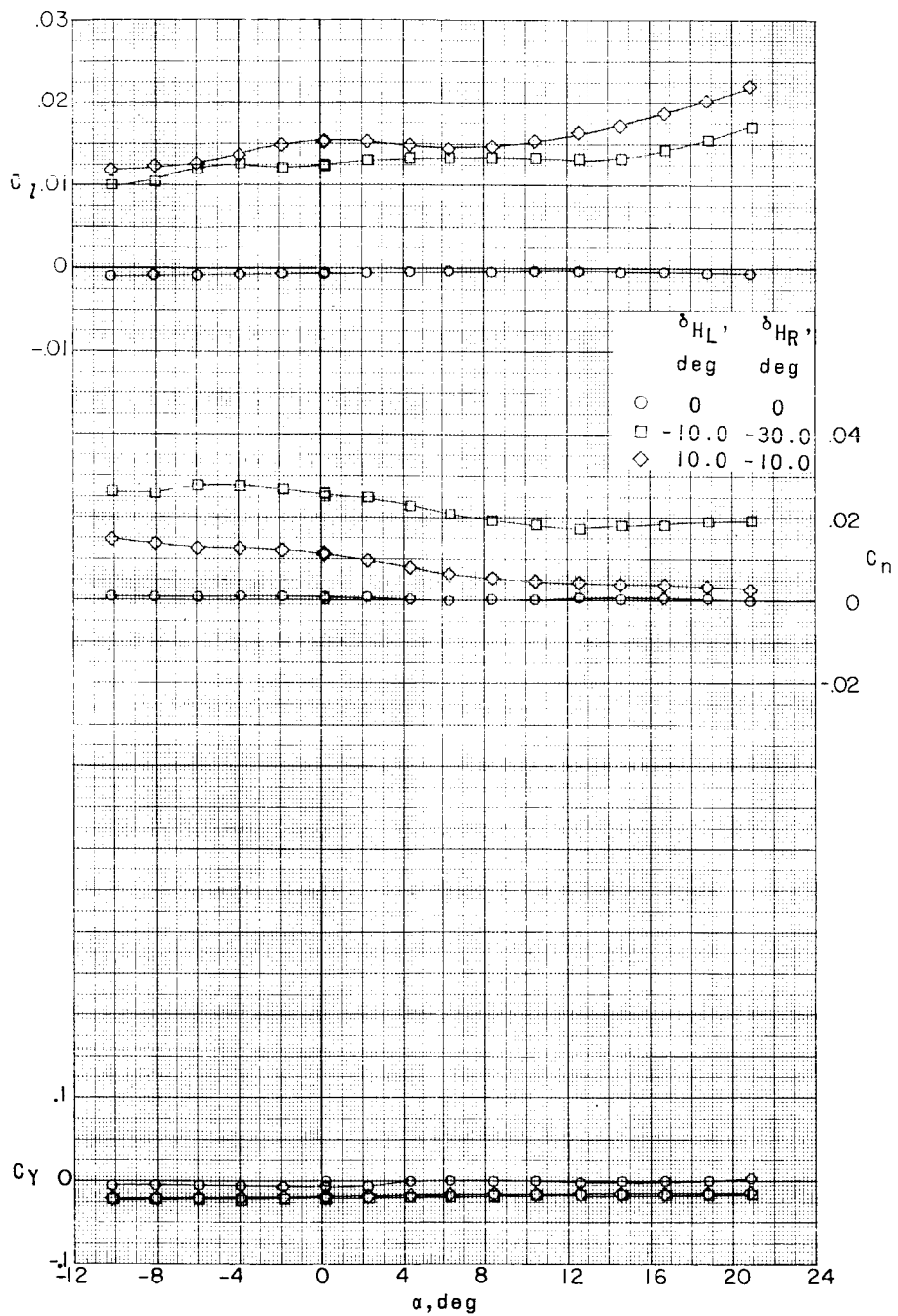
(a) $M = 2.29$.

Figure 37.- Lateral stability characteristics of a 0.067-scale model of the X-15 airplane with various roll-control deflections of the horizontal tail with speed brakes retracted.

CONFIDENTIAL

~~CONFIDENTIAL~~

135



(b) $M = 2.98.$

Figure 37.- Continued.

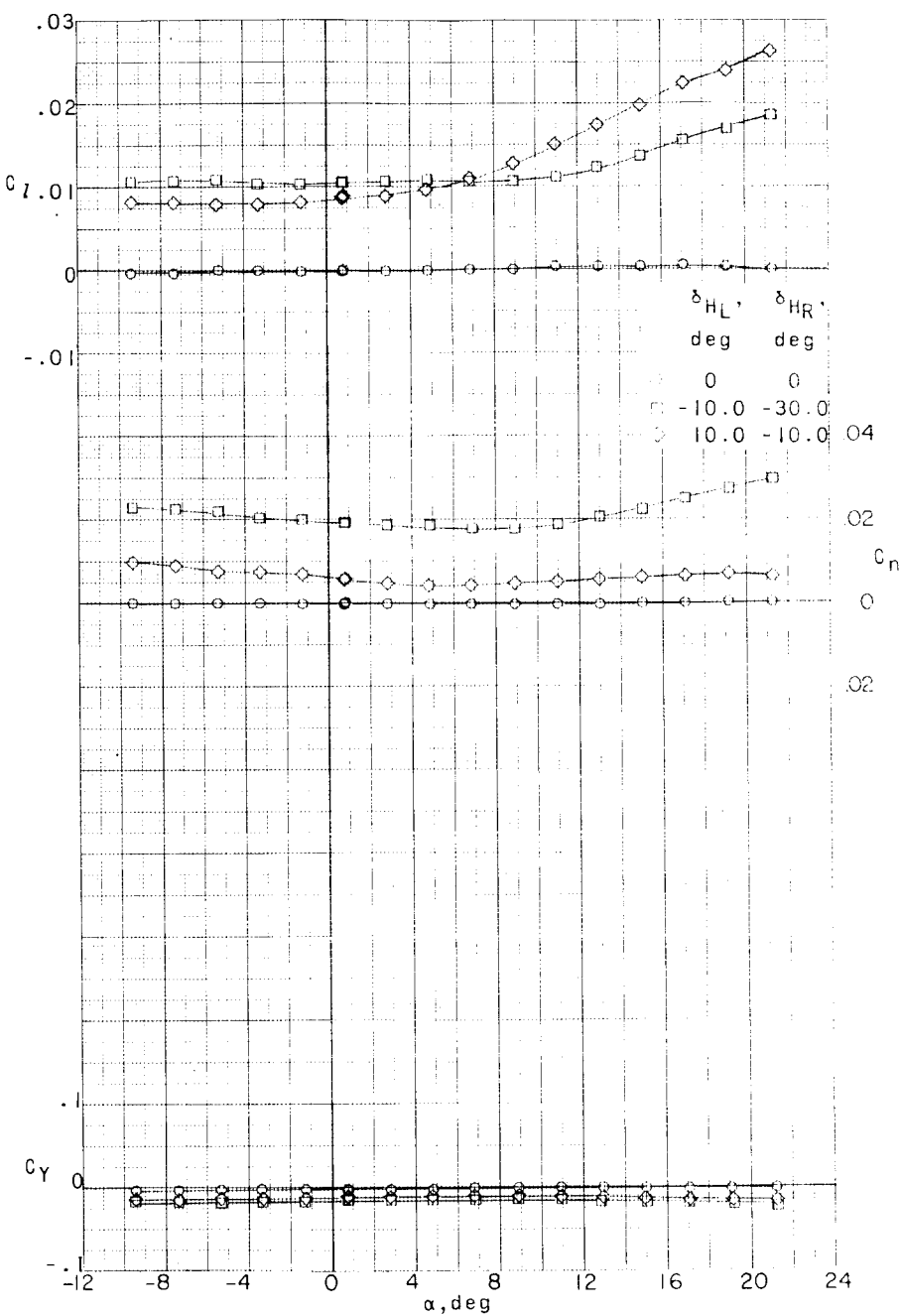
031913201030
CONFIDENTIAL(c) $M = 4.65$.

Figure 37.- Concluded.

DECLASSIFIED

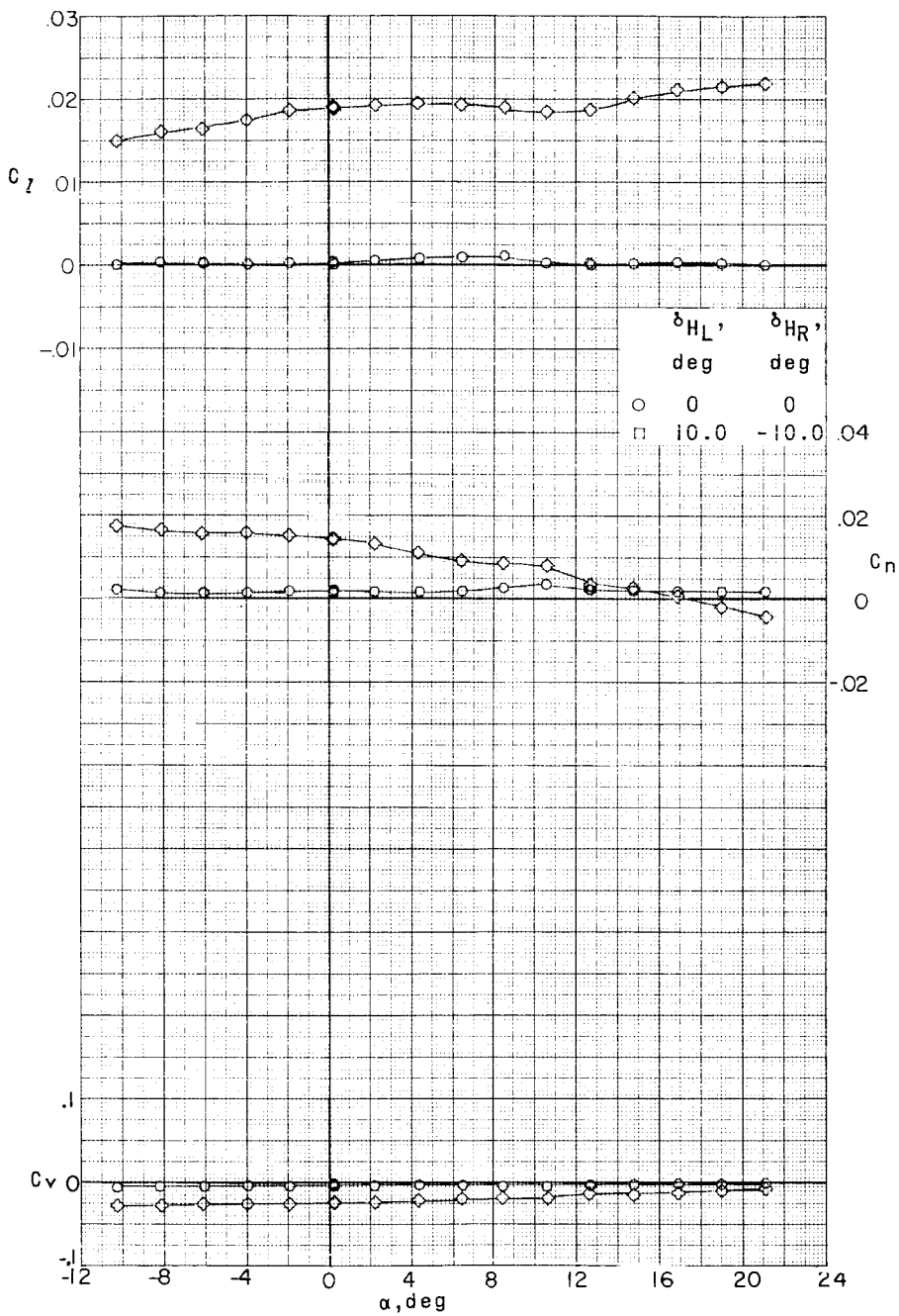
~~CONFIDENTIAL~~(a) $M = 2.29$.

Figure 38.- Lateral stability characteristics of a 0.067-scale model of the X-15 airplane with various roll-control deflections of the horizontal tail with speed brakes open 35° .

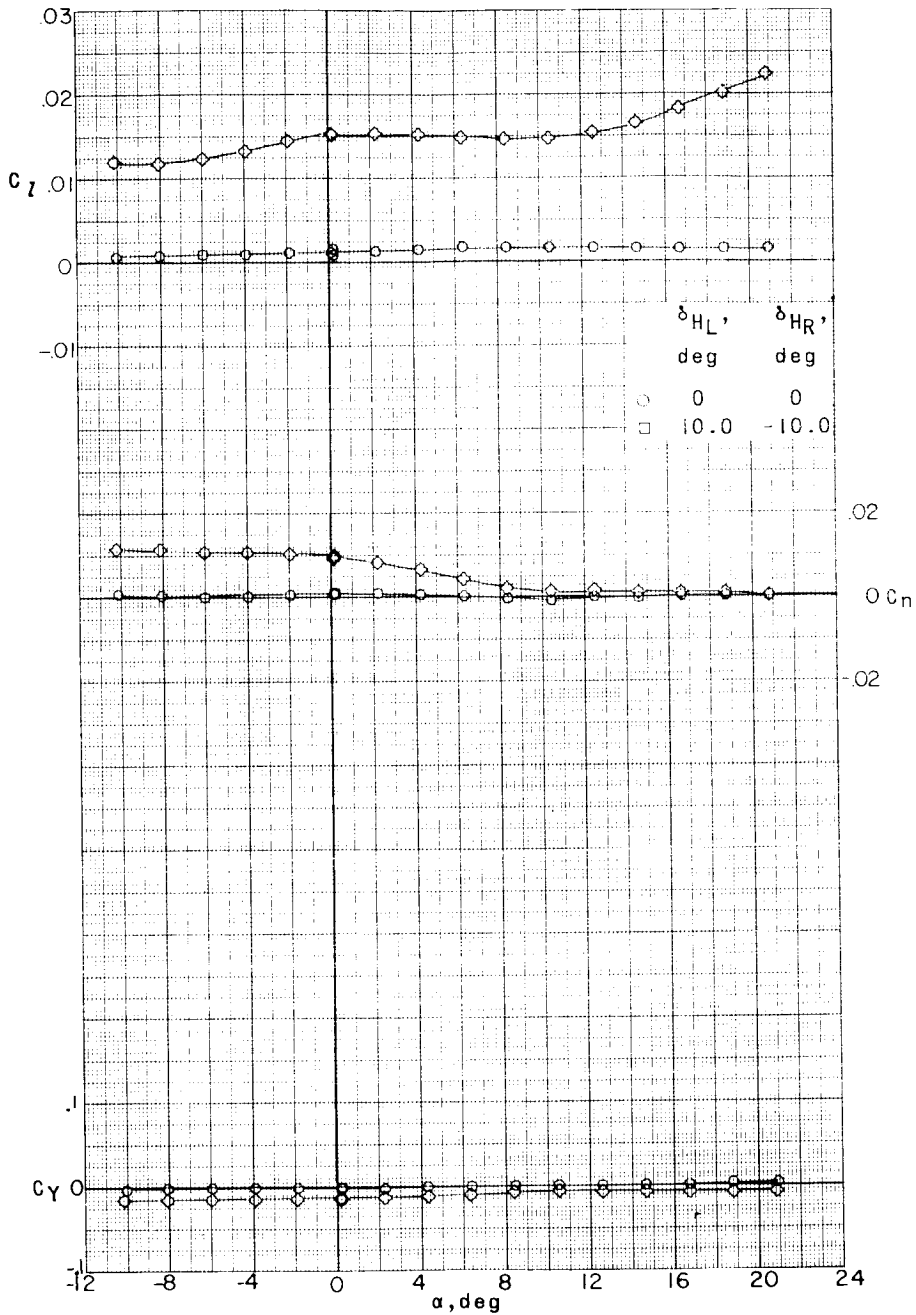
031912201030
~~CONFIDENTIAL~~(b) $M = 2.98.$

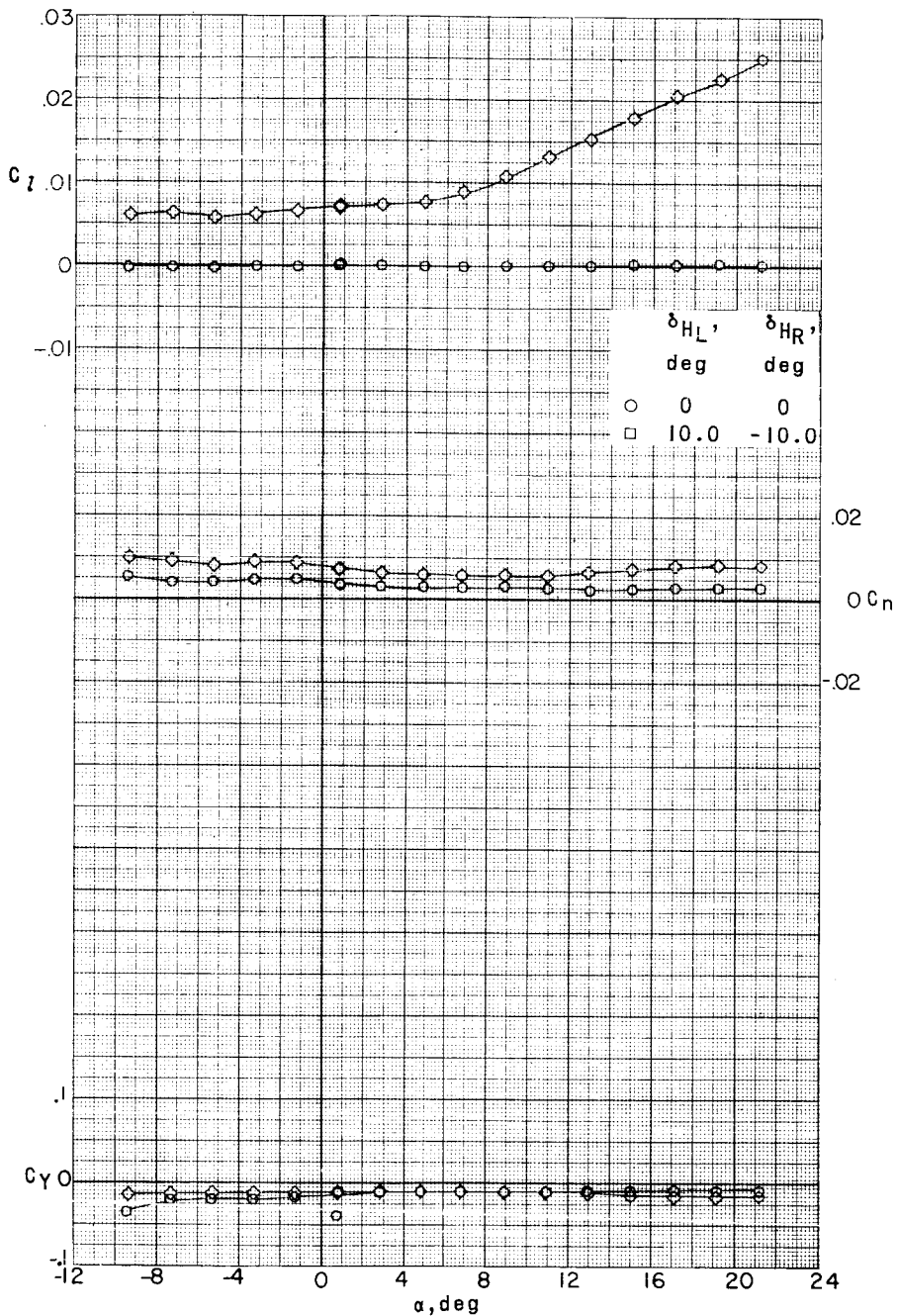
Figure 38.- Continued.

~~CONFIDENTIAL~~

DECLASSIFIED

~~CONFIDENTIAL~~

139



(c) $M = 4.65$.

Figure 38.- Concluded.

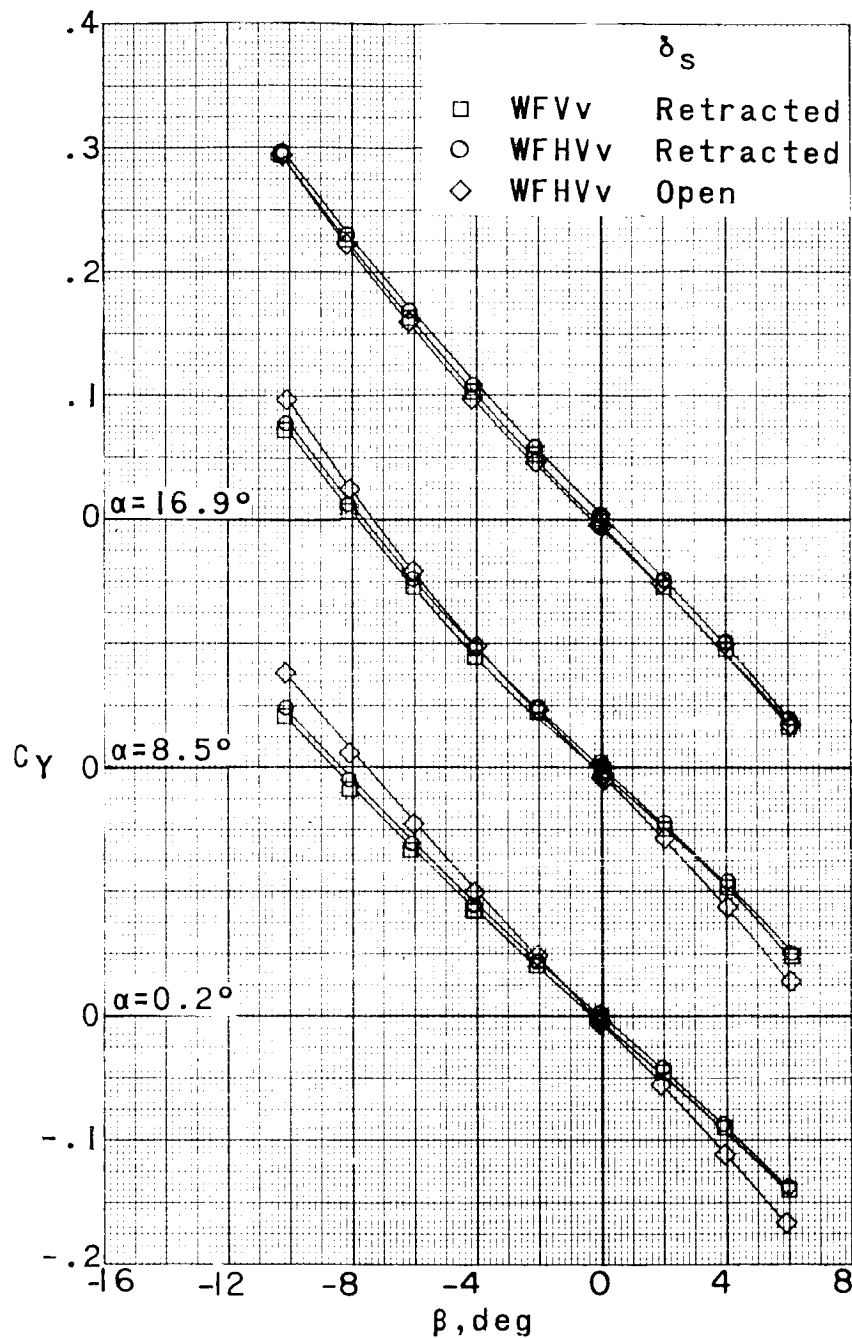
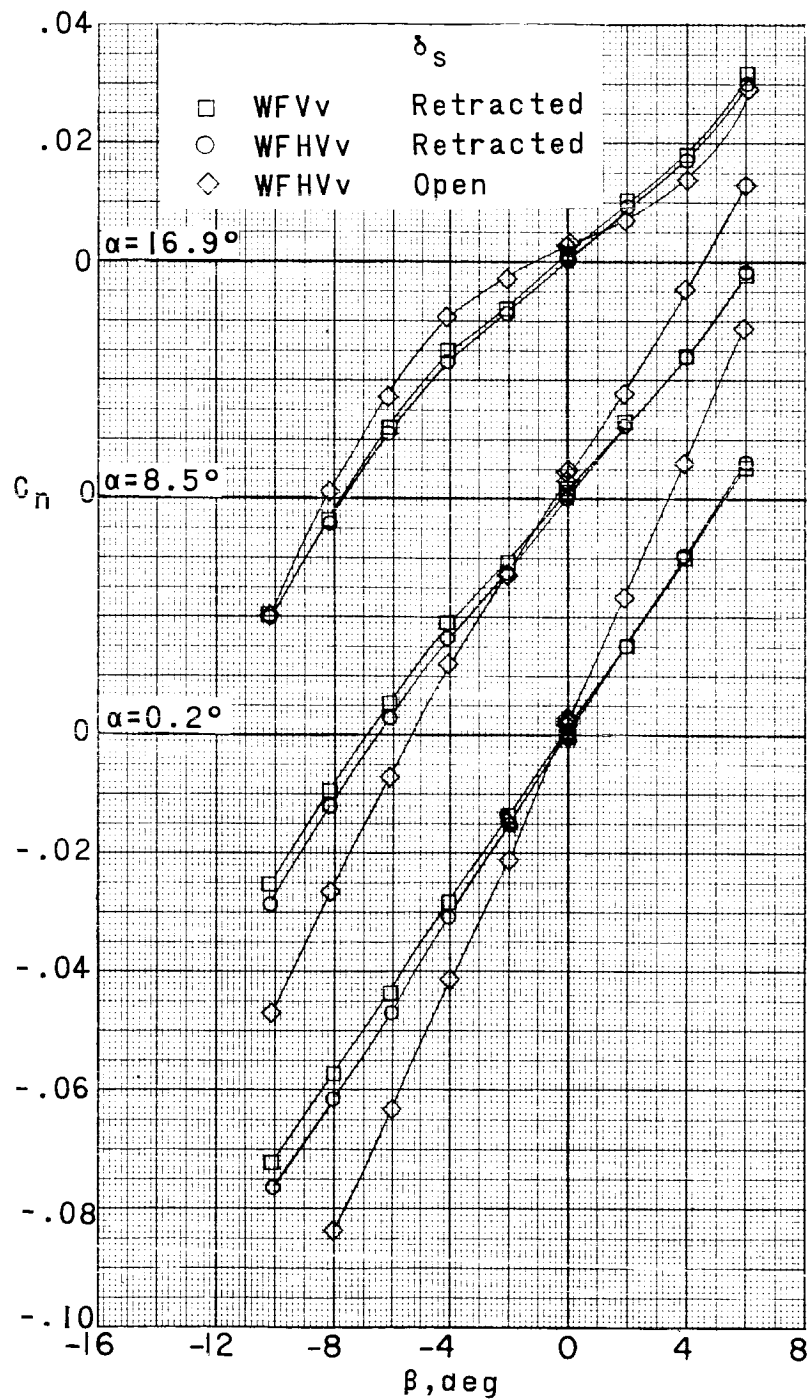
00073020 1030
CONFIDENTIAL(a) $M = 2.29$

Figure 39.- Lateral stability characteristics of a 0.067-scale model of the X-1b airplane at different angles of attack with various configurations.

DECLASSIFIED

CONFIDENTIAL

141



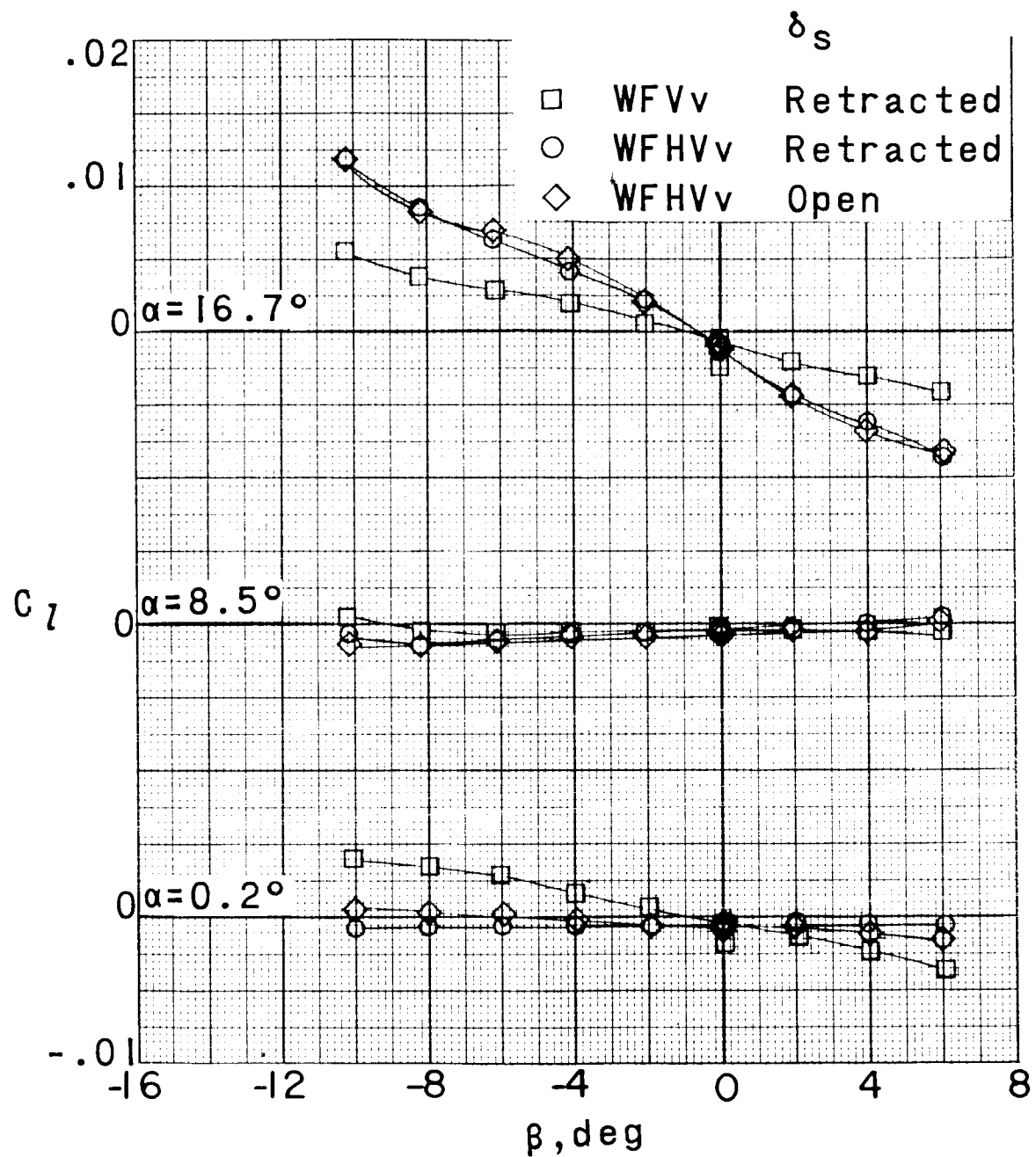
(a) Continued.

Figure 39.- Continued.

03191201030

~~CONFIDENTIAL~~

142



(a) Concluded.

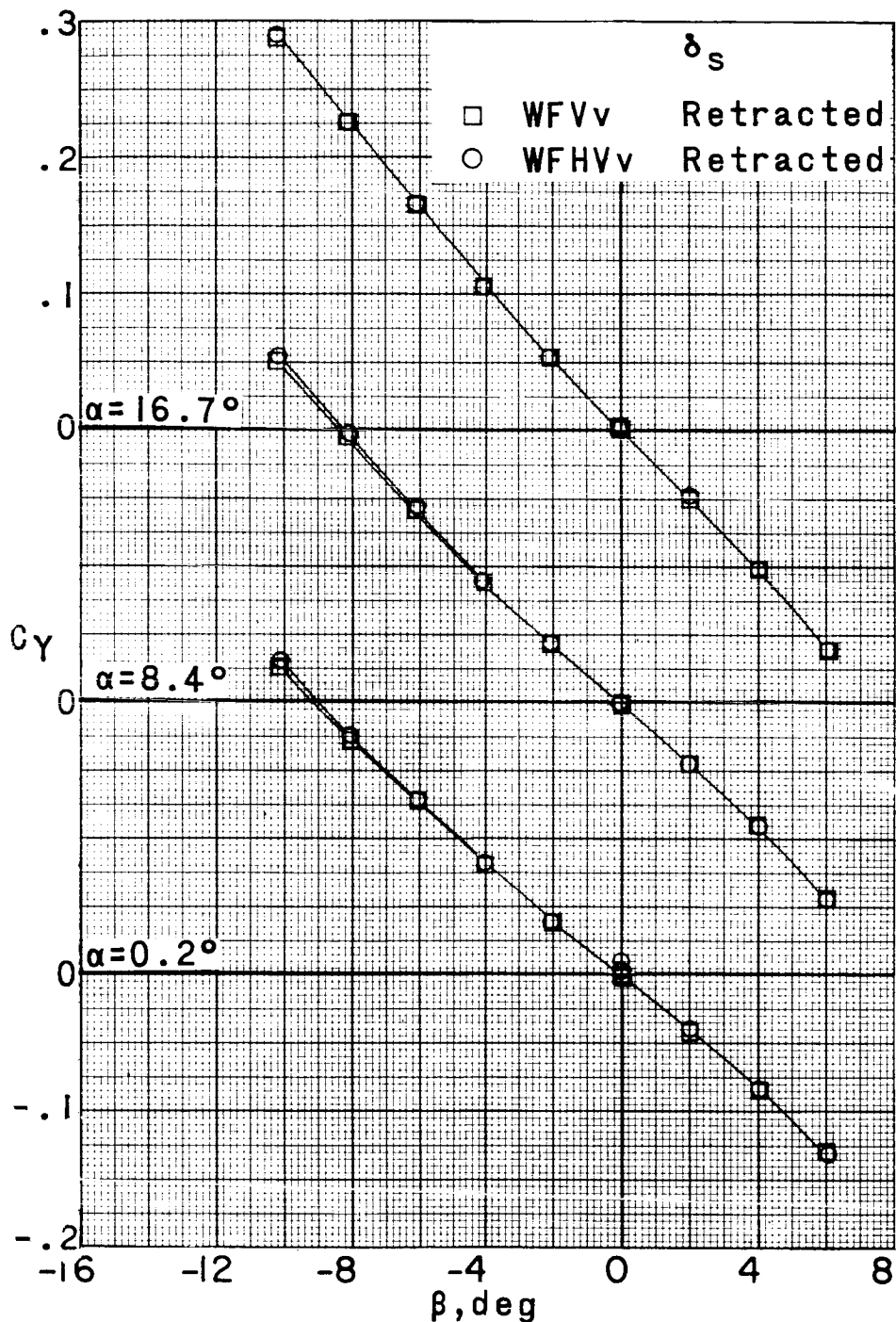
Figure 39.- Continued.

~~CONFIDENTIAL~~

DECLASSIFIED

CONFIDENTIAL

143

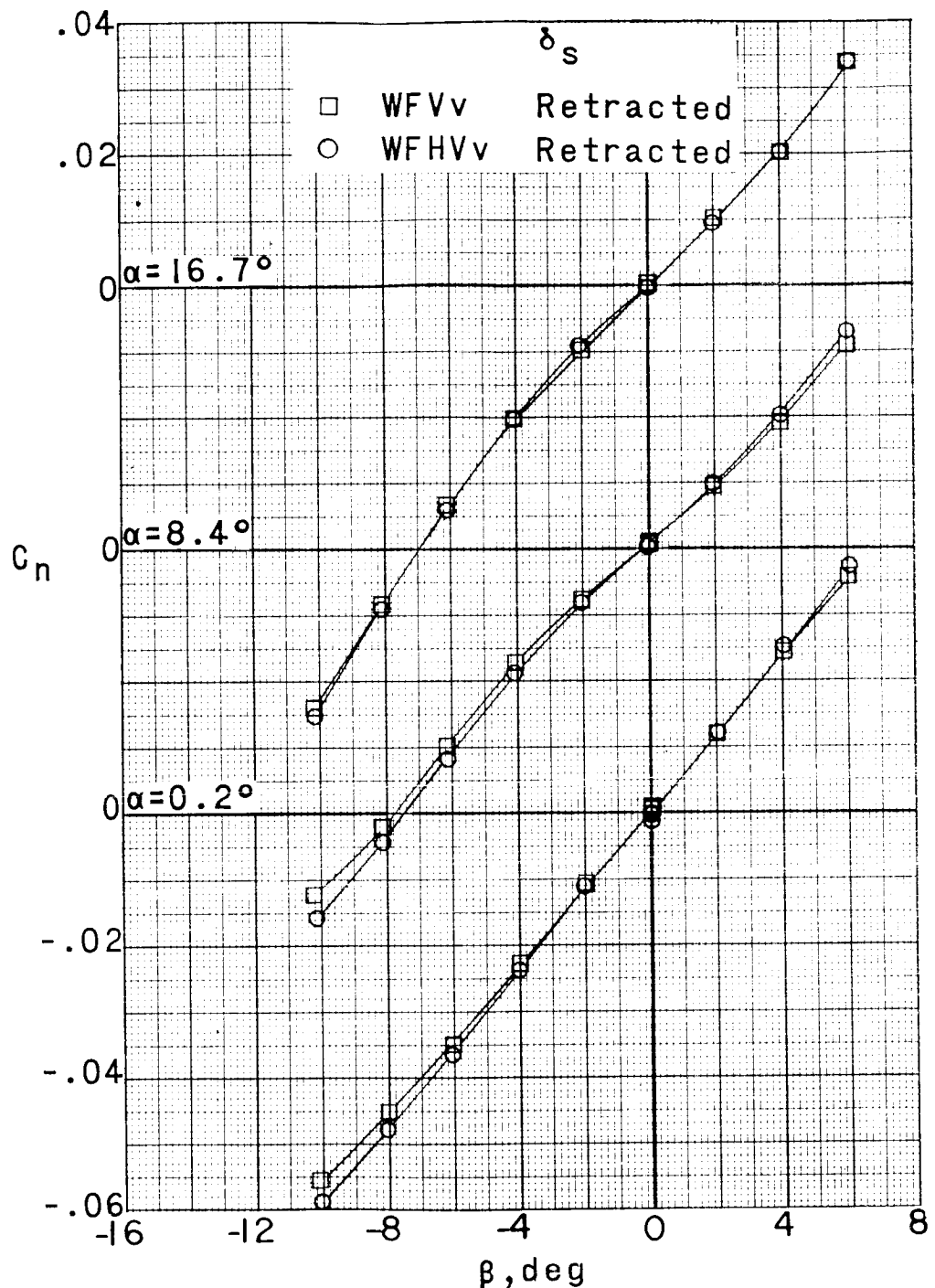


(b) $M = 2.98$.

Figure 39.- Continued.

031912261030

144

~~CONFIDENTIAL~~

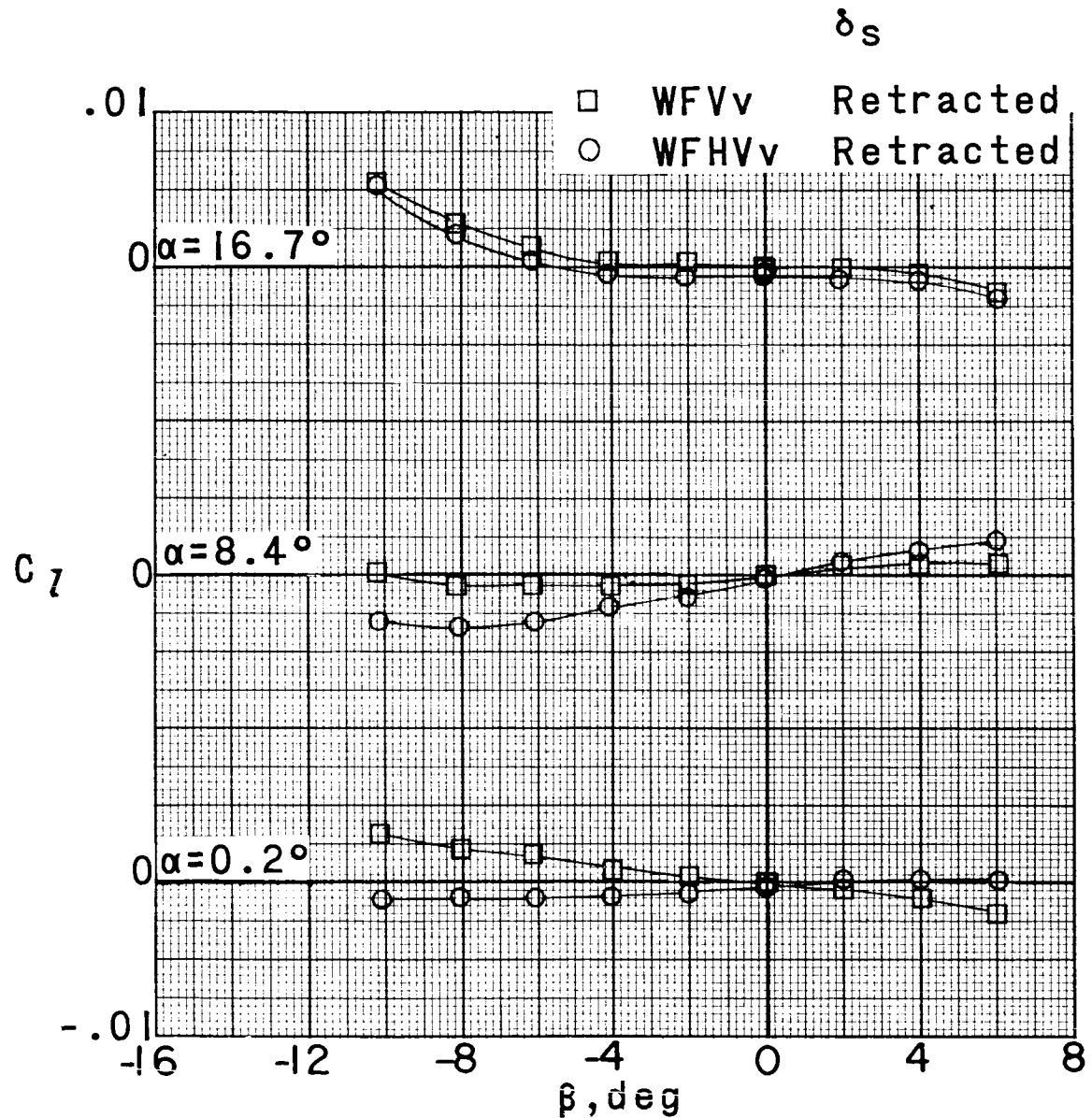
(b) Continued.

Figure 39.- Continued.

~~CONFIDENTIAL~~

DECLASSIFIED
CONFIDENTIAL

145



(b) Concluded.

Figure 39.- Continued.

CONFIDENTIAL

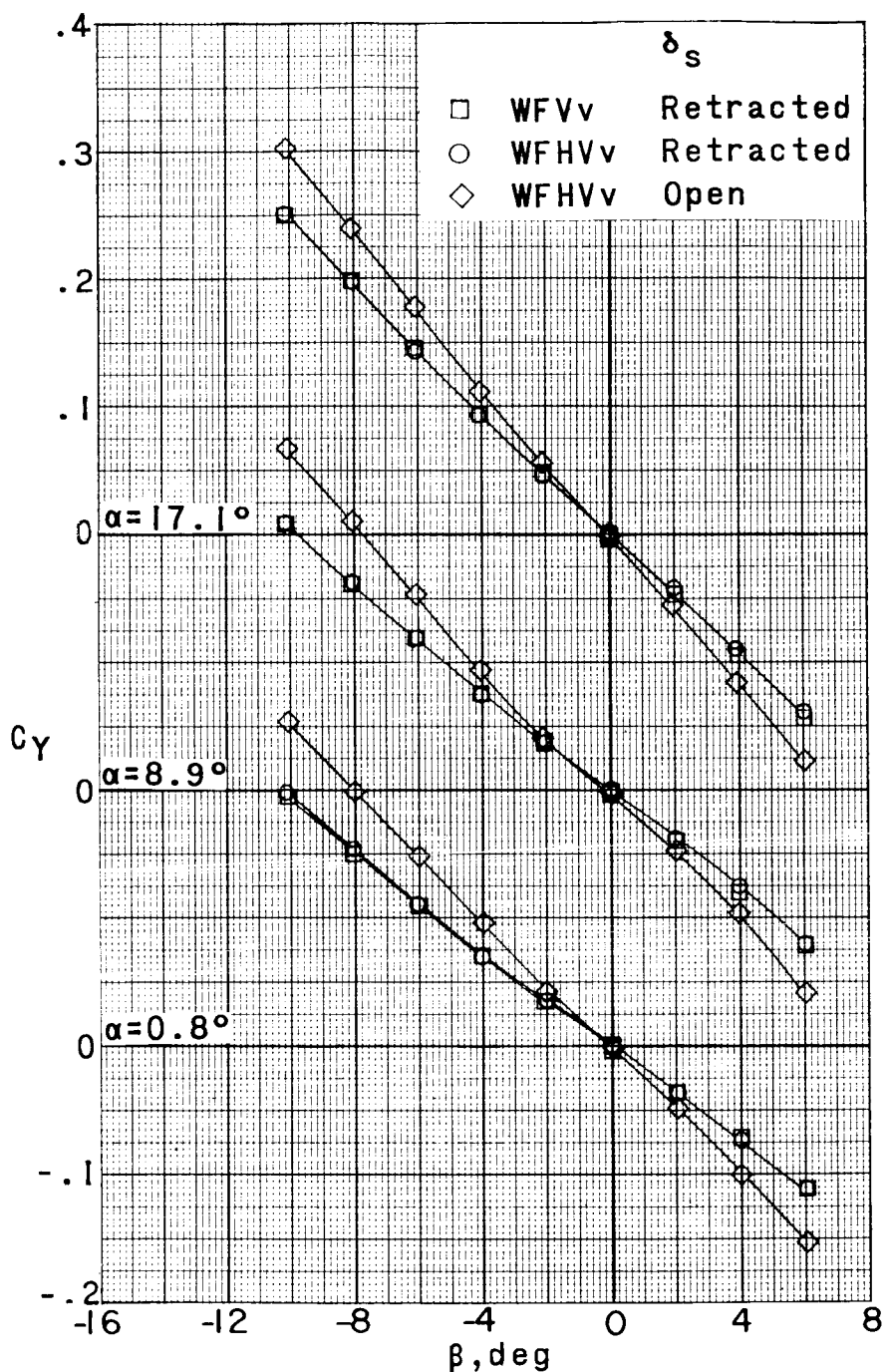
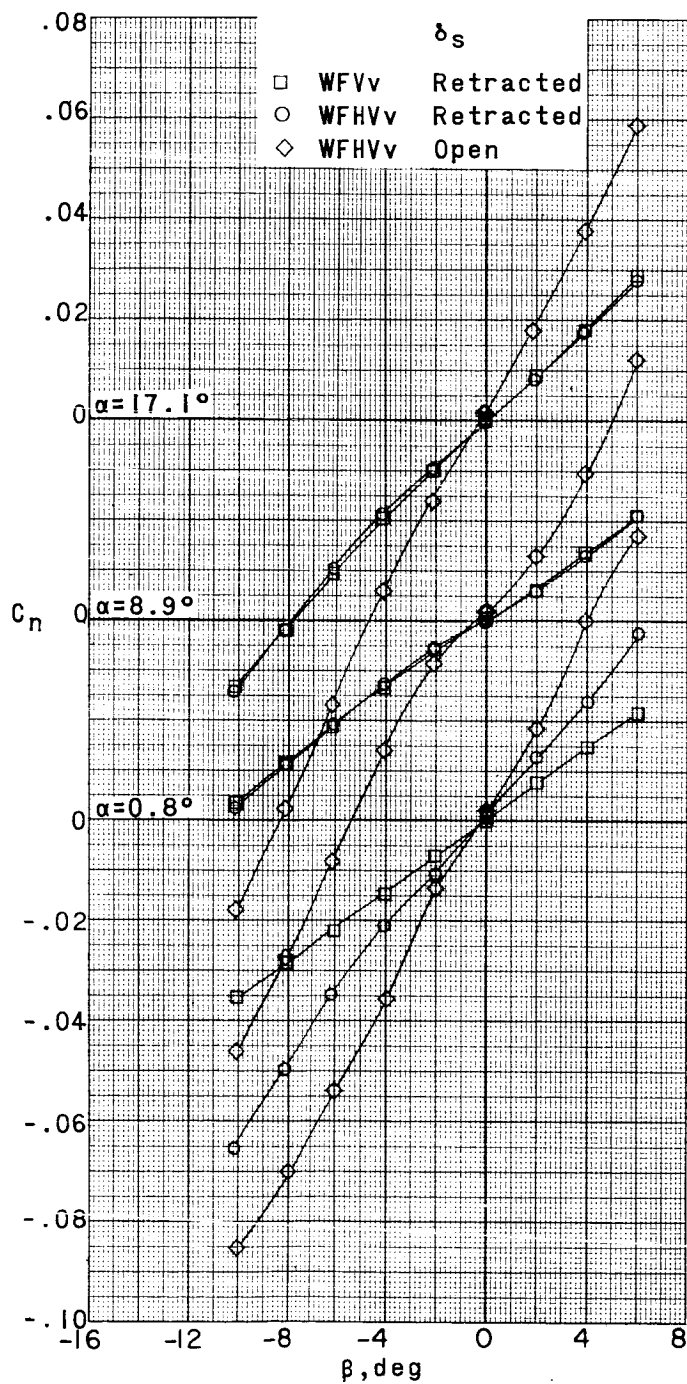
(c) $M = 4.65$.

Figure 39.- Continued.

CONFIDENTIAL

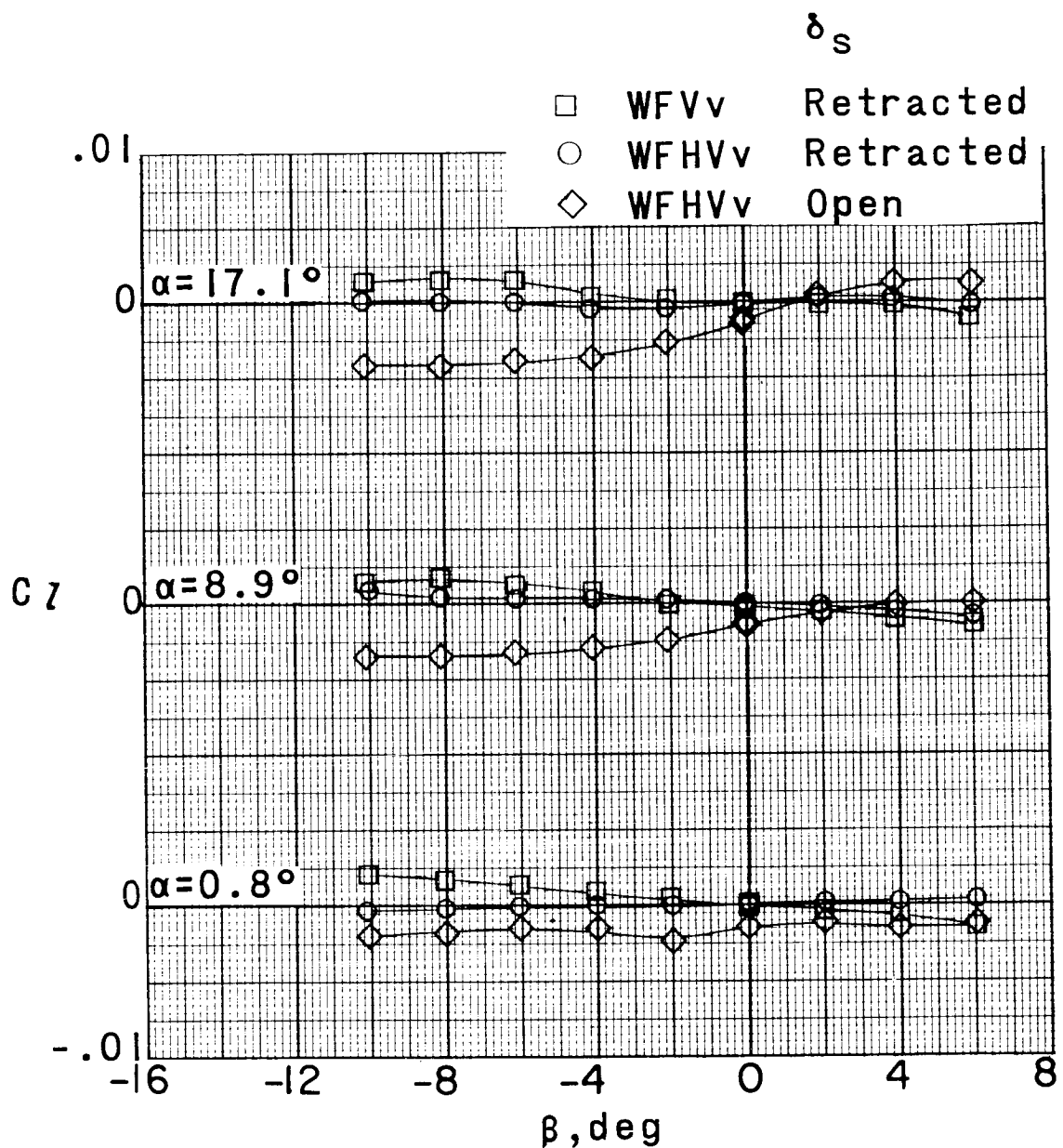
DECLASSIFIED

147



(c) Continued.

Figure 39.- Continued.

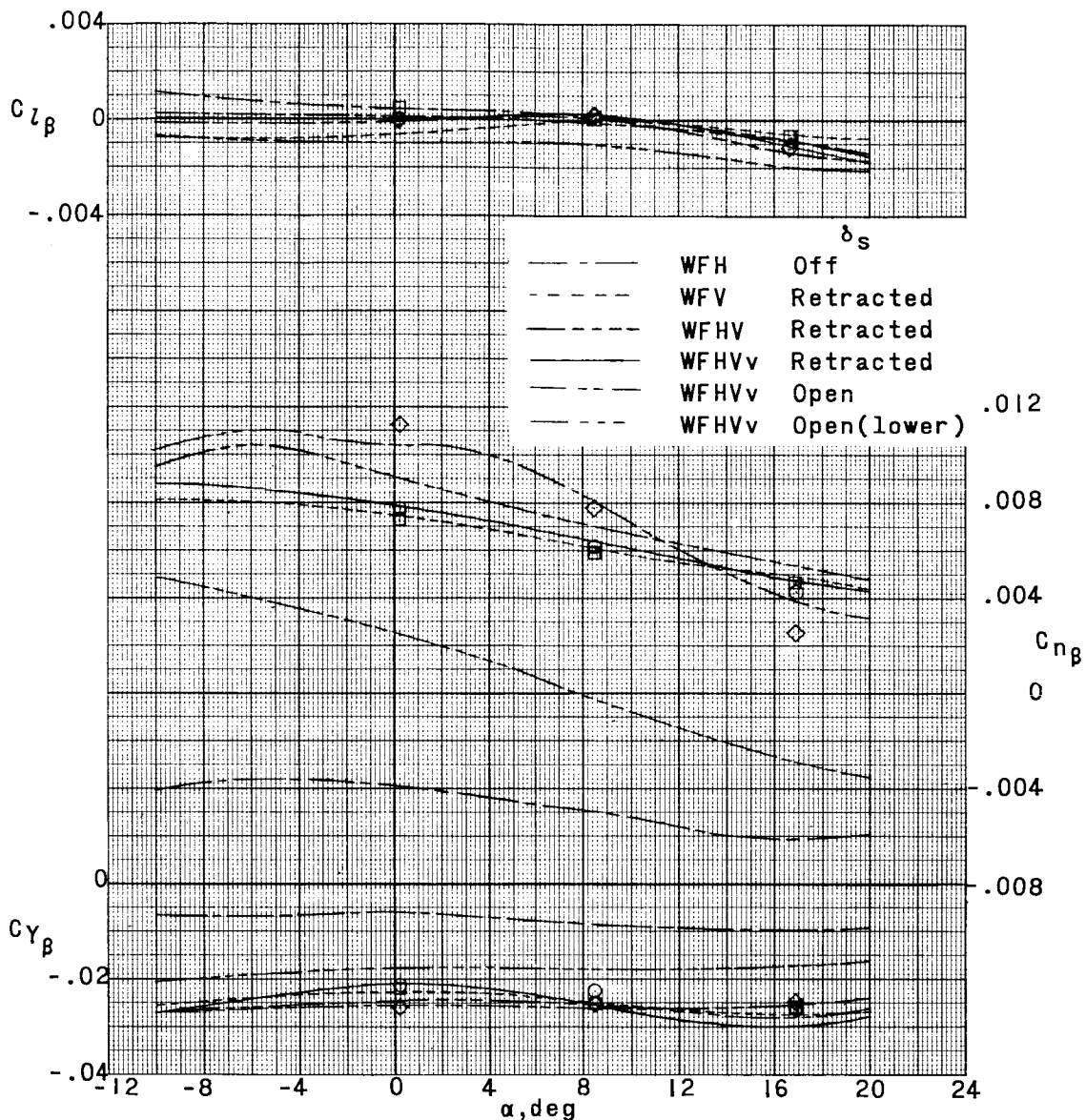


(c) Concluded.

Figure 39.- Concluded.

DECLASSIFIED
CONFIDENTIAL

149



(a) $M = 2.29$.

Figure 40.- Summary of lateral stability characteristics of a 0.067-scale model of the X-15 airplane as affected by various model components.

03130220142000

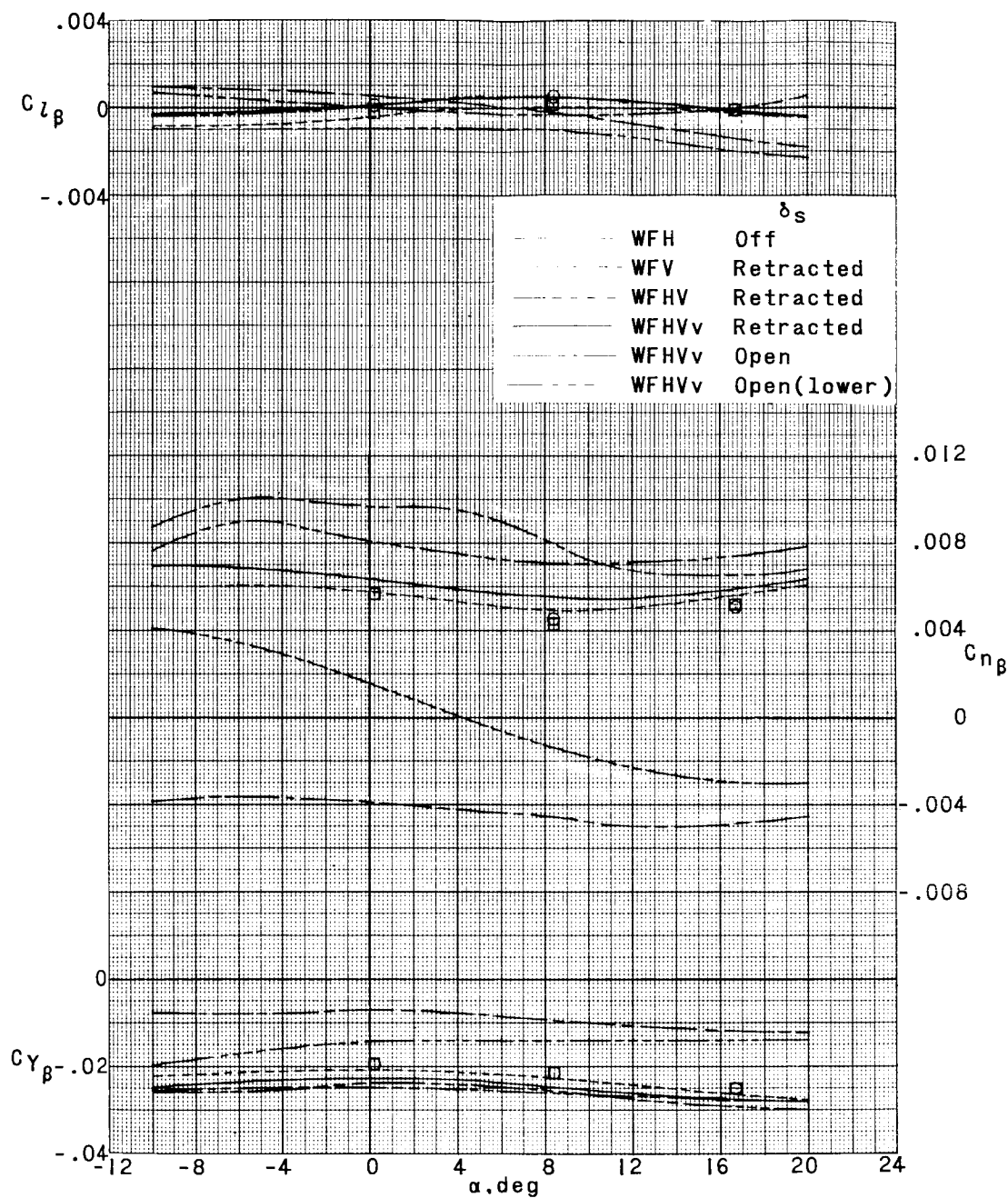
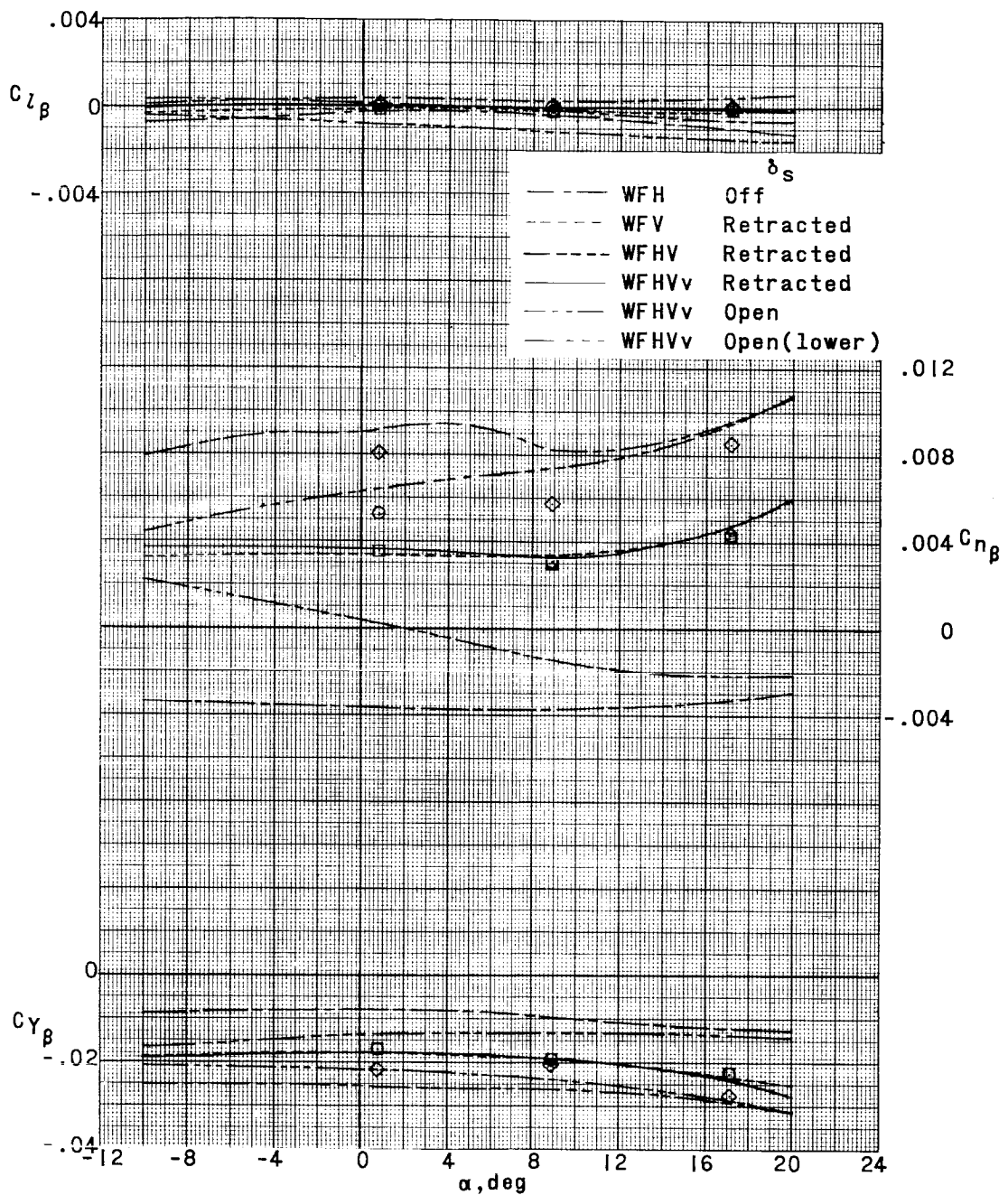
(b) $M = 2.98$.

Figure 40.- Continued.

REF ID: A65125
CONFIDENTIAL

151



(c) $M = 4.65.$

Figure 40.- Concluded.

CONFIDENTIAL

152

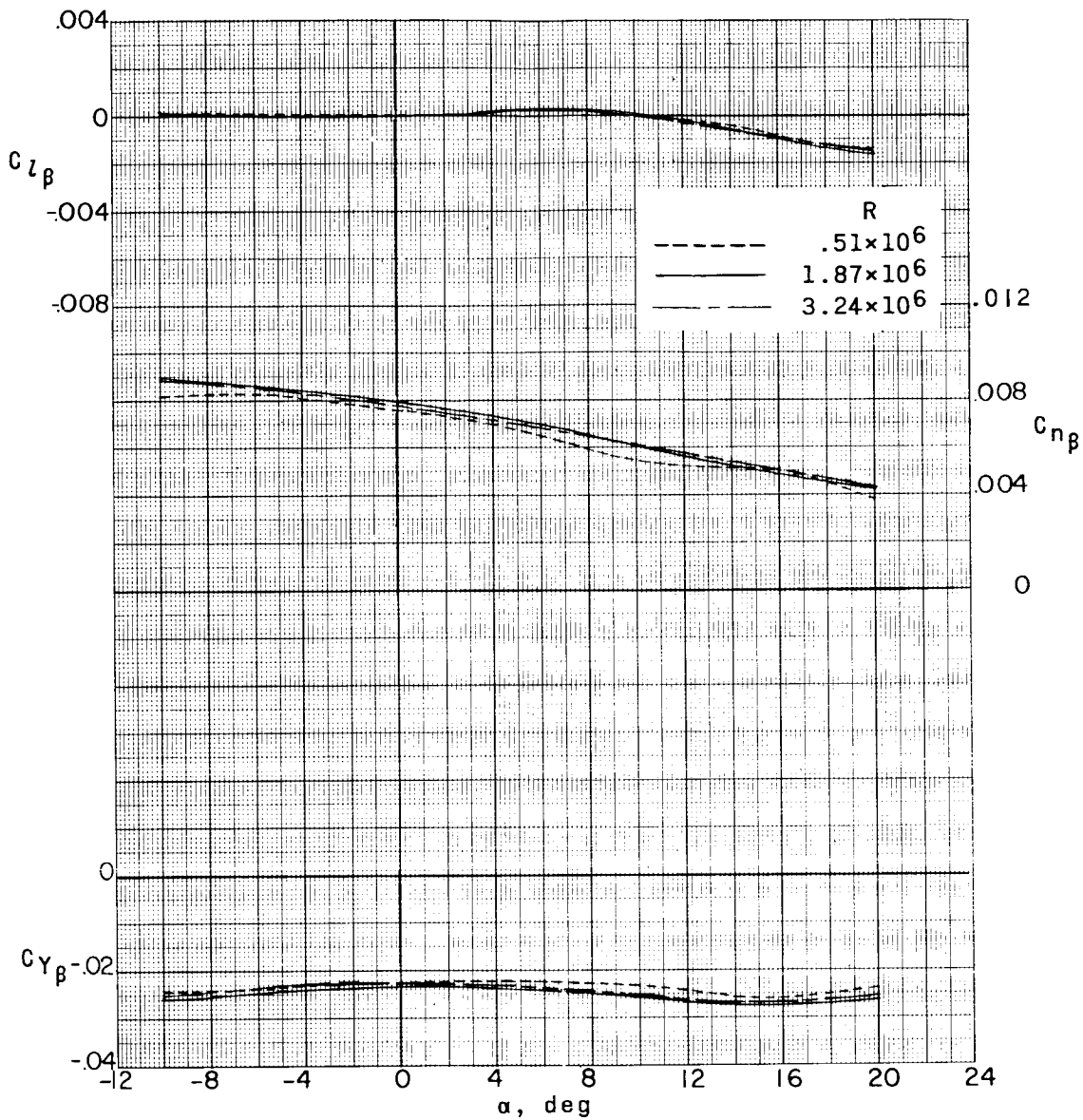
(a) $M = 2.29$.

Figure 41.- Summary of lateral stability characteristics of a 0.067-scale model of the X-15 airplane as affected by Reynolds number with speed brakes retracted.

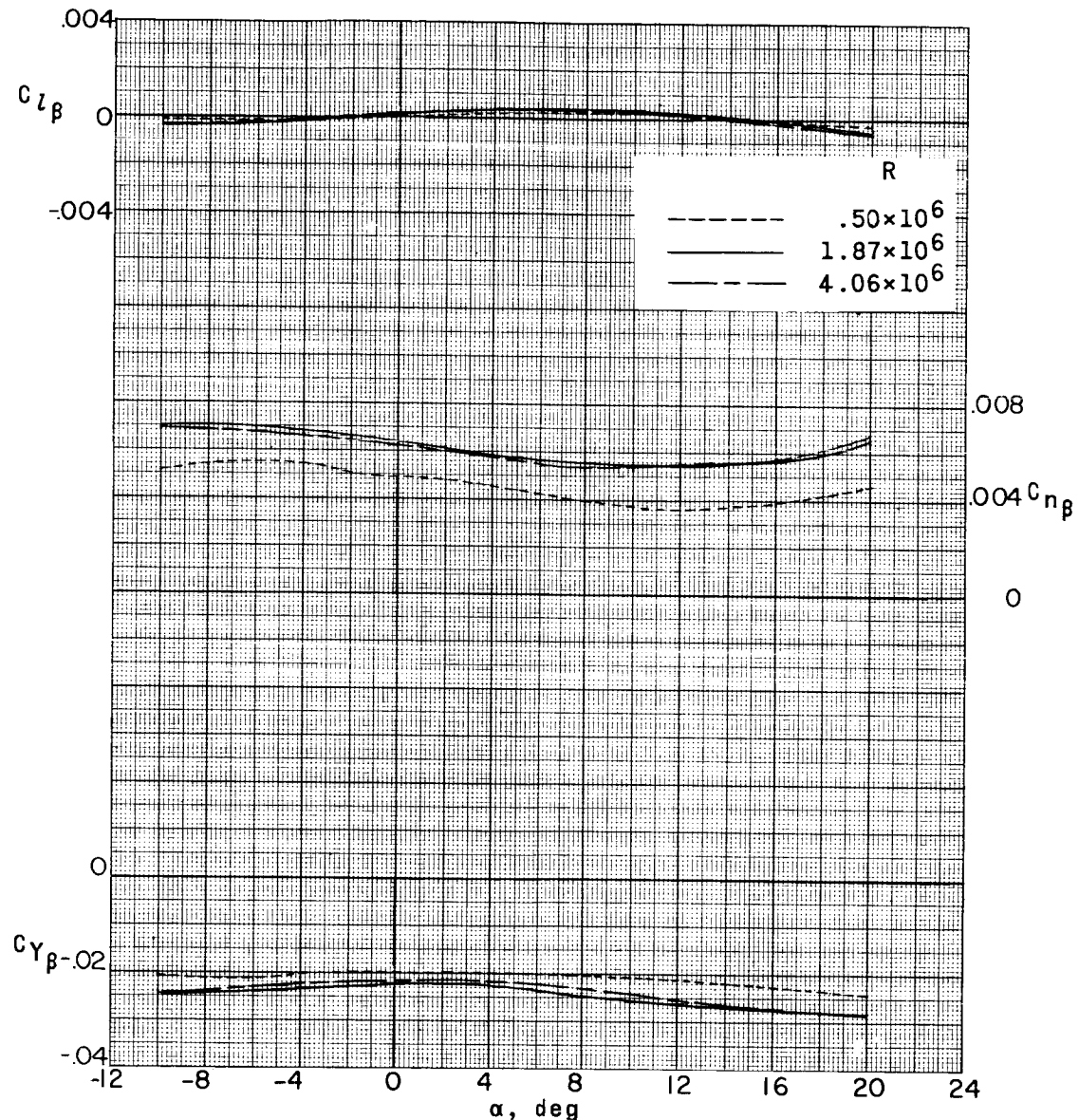
REF ID: A65125
DECLASSIFIED
CONFIDENTIAL(b) $M = 2.98$.

Figure 41.- Continued.

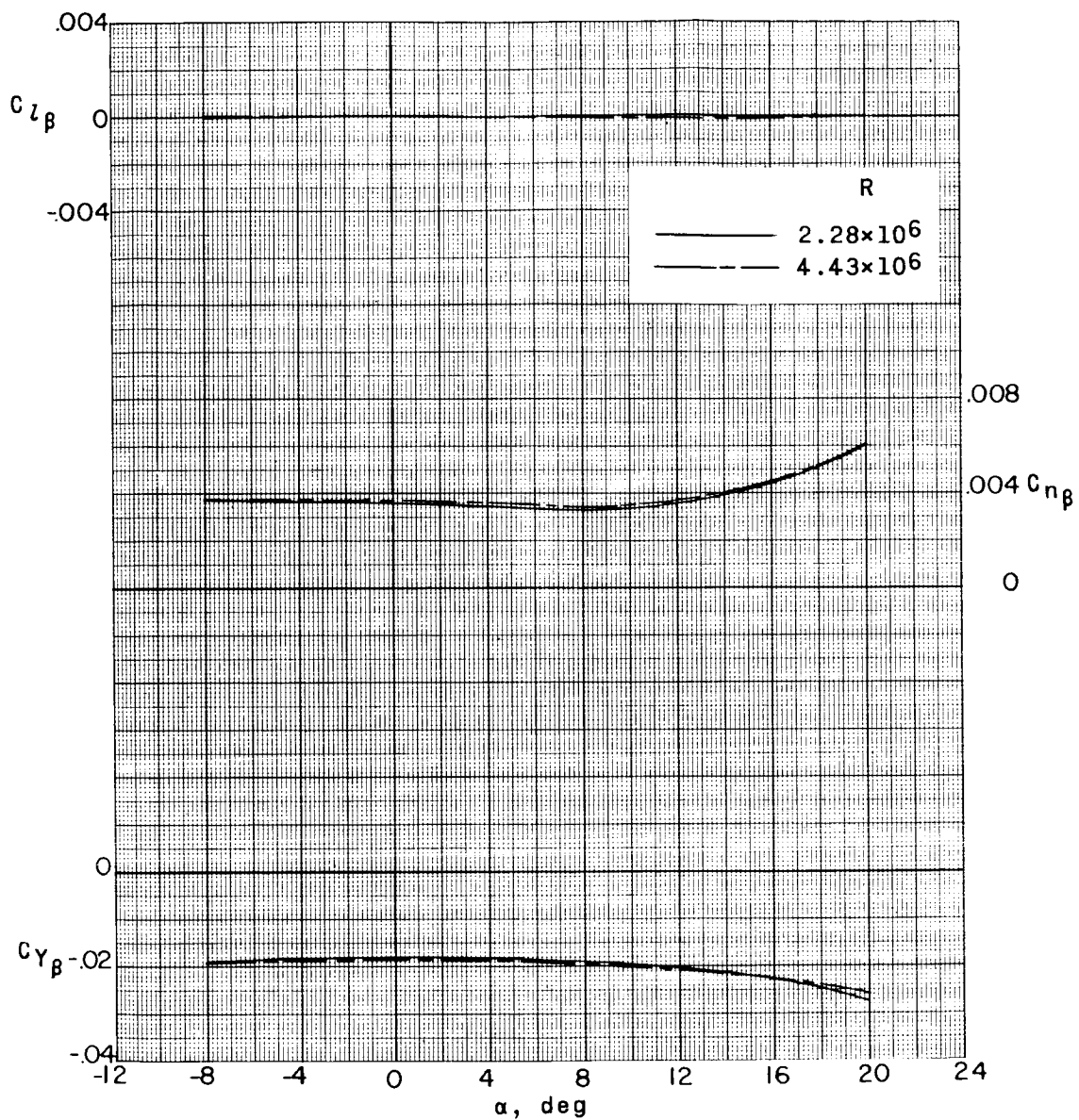
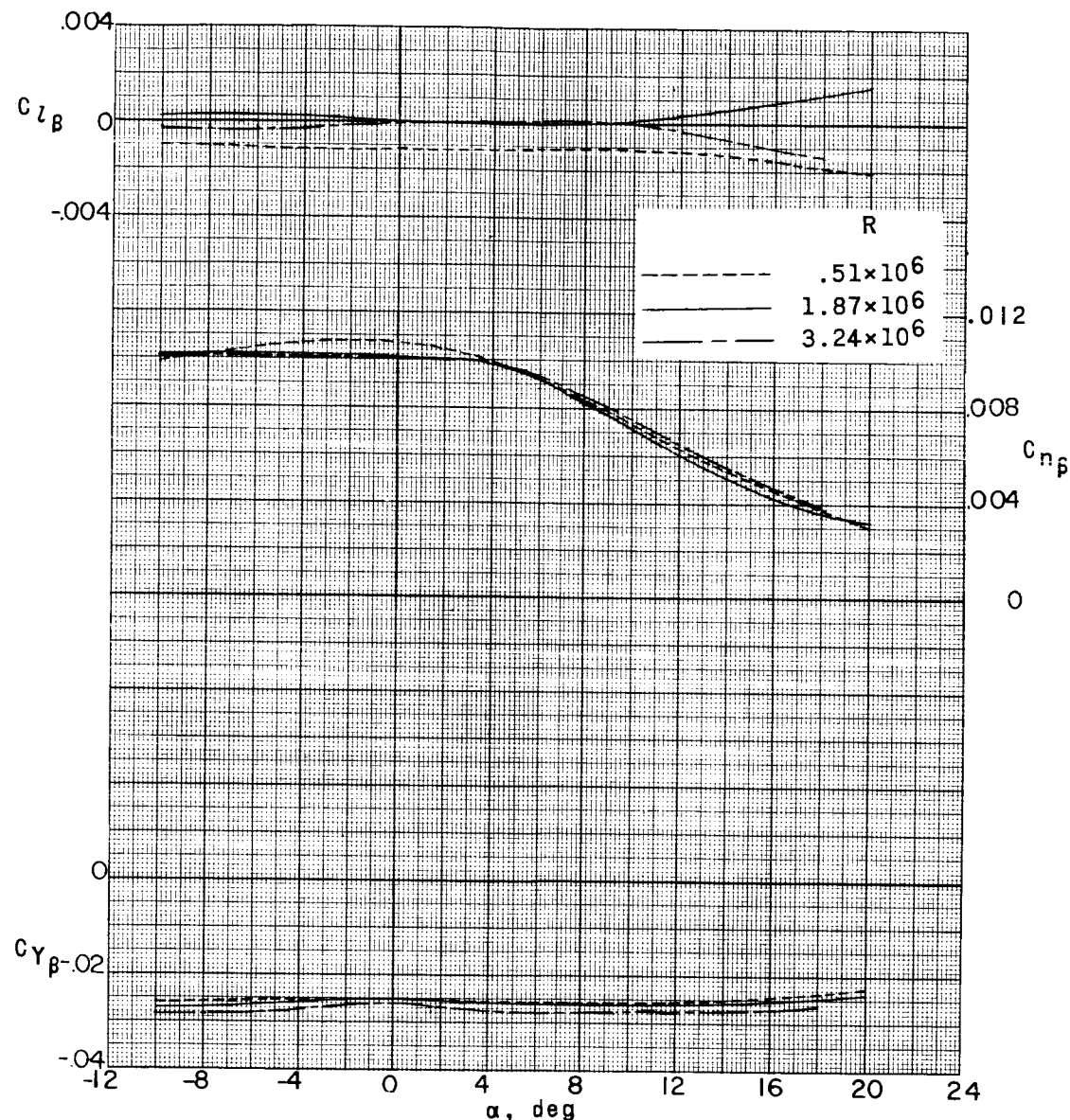
031312201030
CONFIDENTIAL(c) $M = 4.65$.

Figure 41.- Concluded.

DECCLASSIFIED
CONFIDENTIAL

155

L-351



(a) $M = 2.29$.

Figure 42.- Summary of lateral stability characteristics of a 0.067-scale model of the X-15 airplane as affected by Reynolds number with speed brakes open 35° .

CONFIDENTIAL

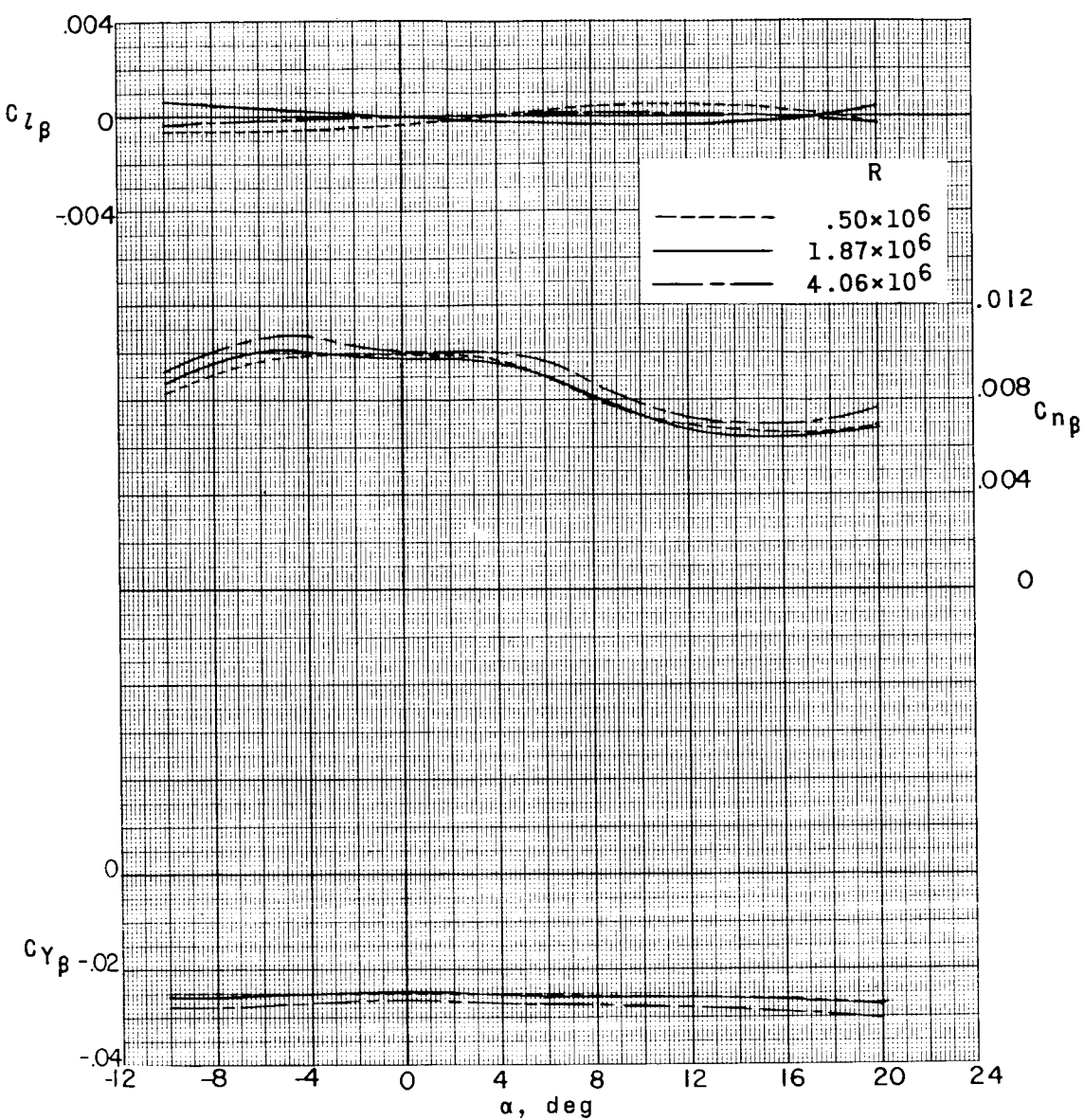
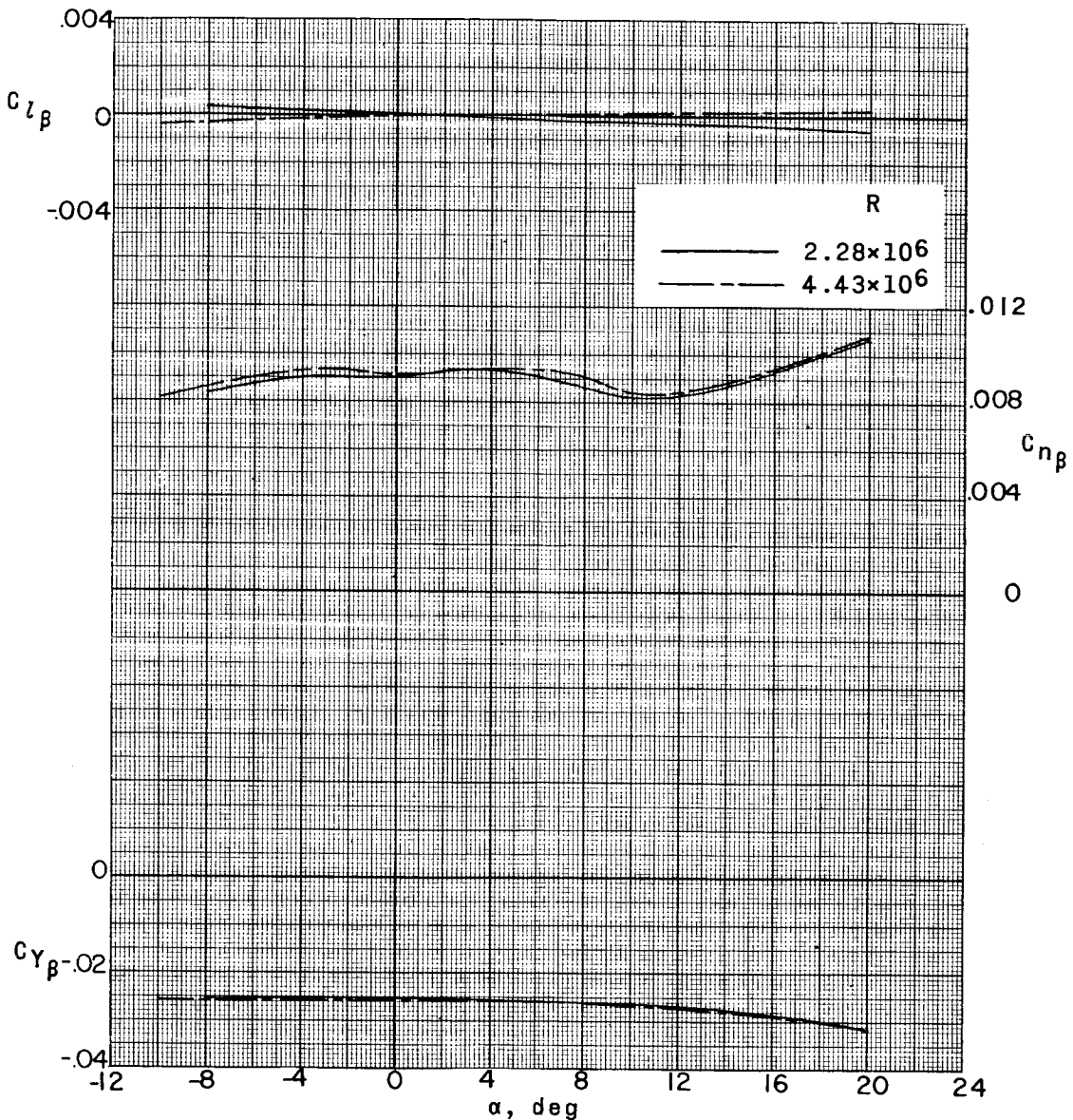
(b) $M = 2.98.$

Figure 42.- Continued.

DECLASSIFIED

CONFIDENTIAL

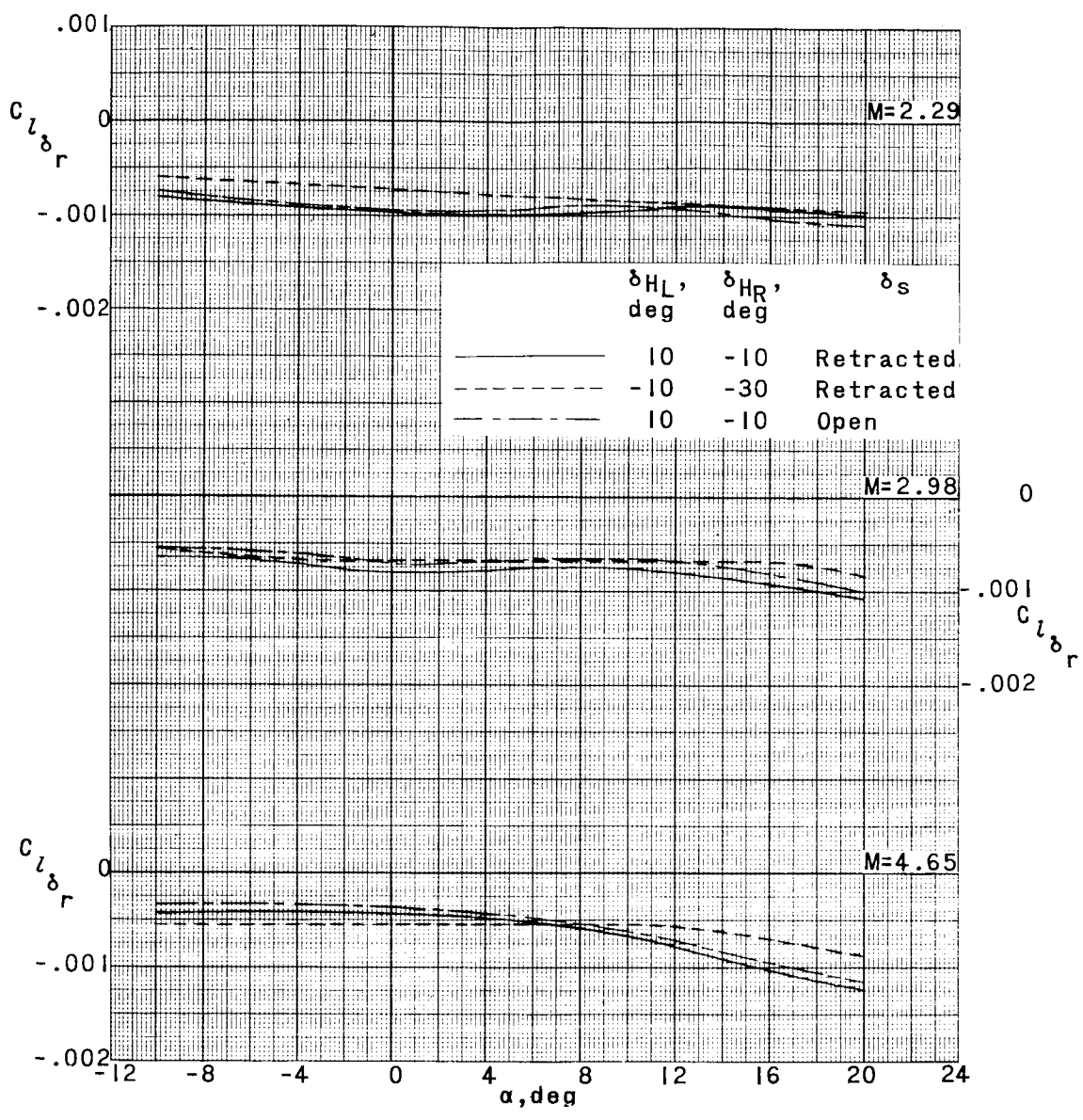
157



(c) $M = 4.65$.

Figure 42.- Concluded.

001912241430
CONFIDENTIAL



(a) $C_{l\delta_r}$ plotted against α .

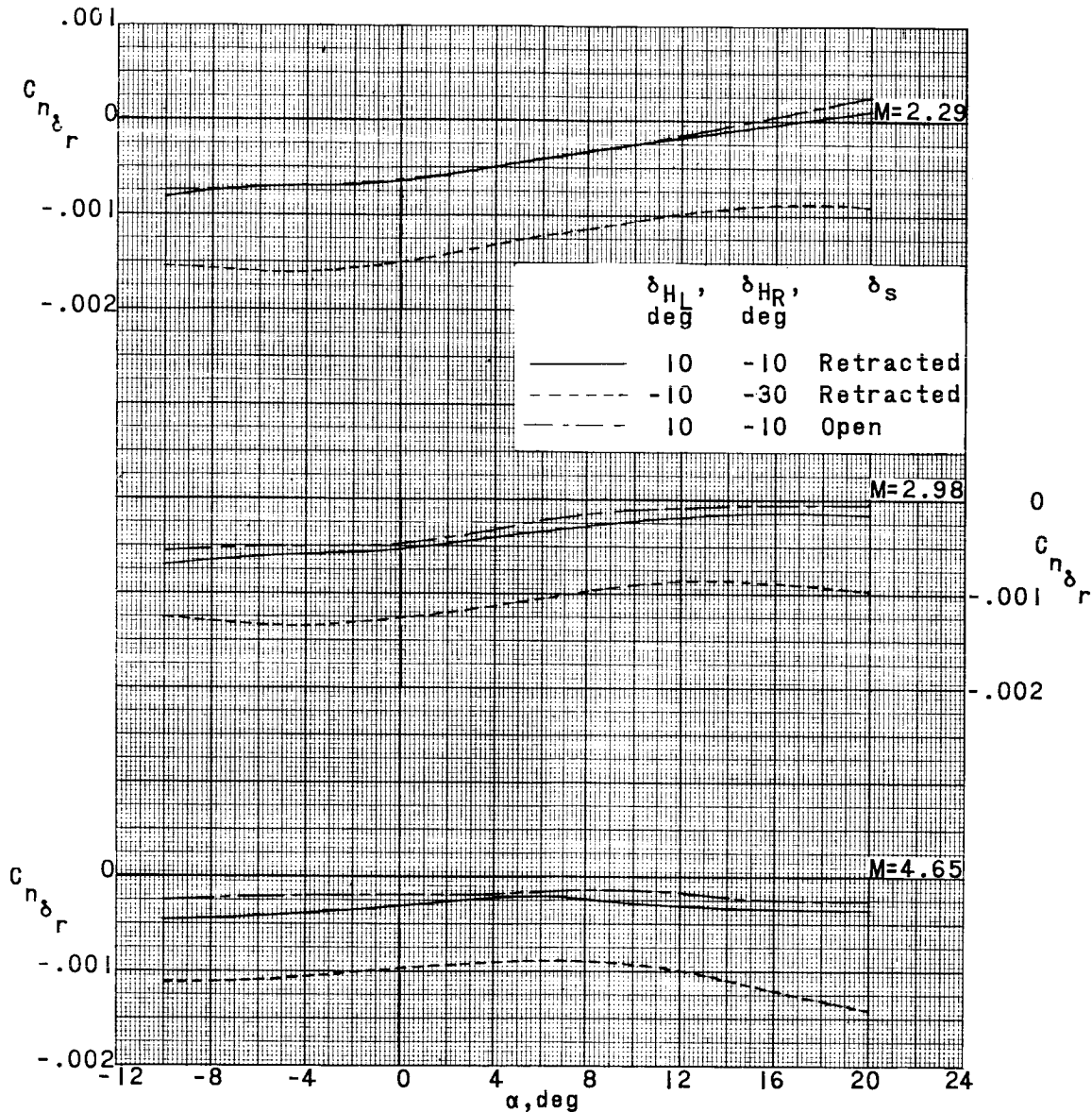
Figure 43.- Summary of roll-control characteristics of a 0.067-scale model of the X-15 airplane as affected by various elevator deflections.

CONFIDENTIAL

DECLASSIFIED

CONFIDENTIAL

159



(b) $C_{n_{\delta_r}}$ plotted against α .

Figure 43.- Concluded.

CONFIDENTIAL

0000000000000000

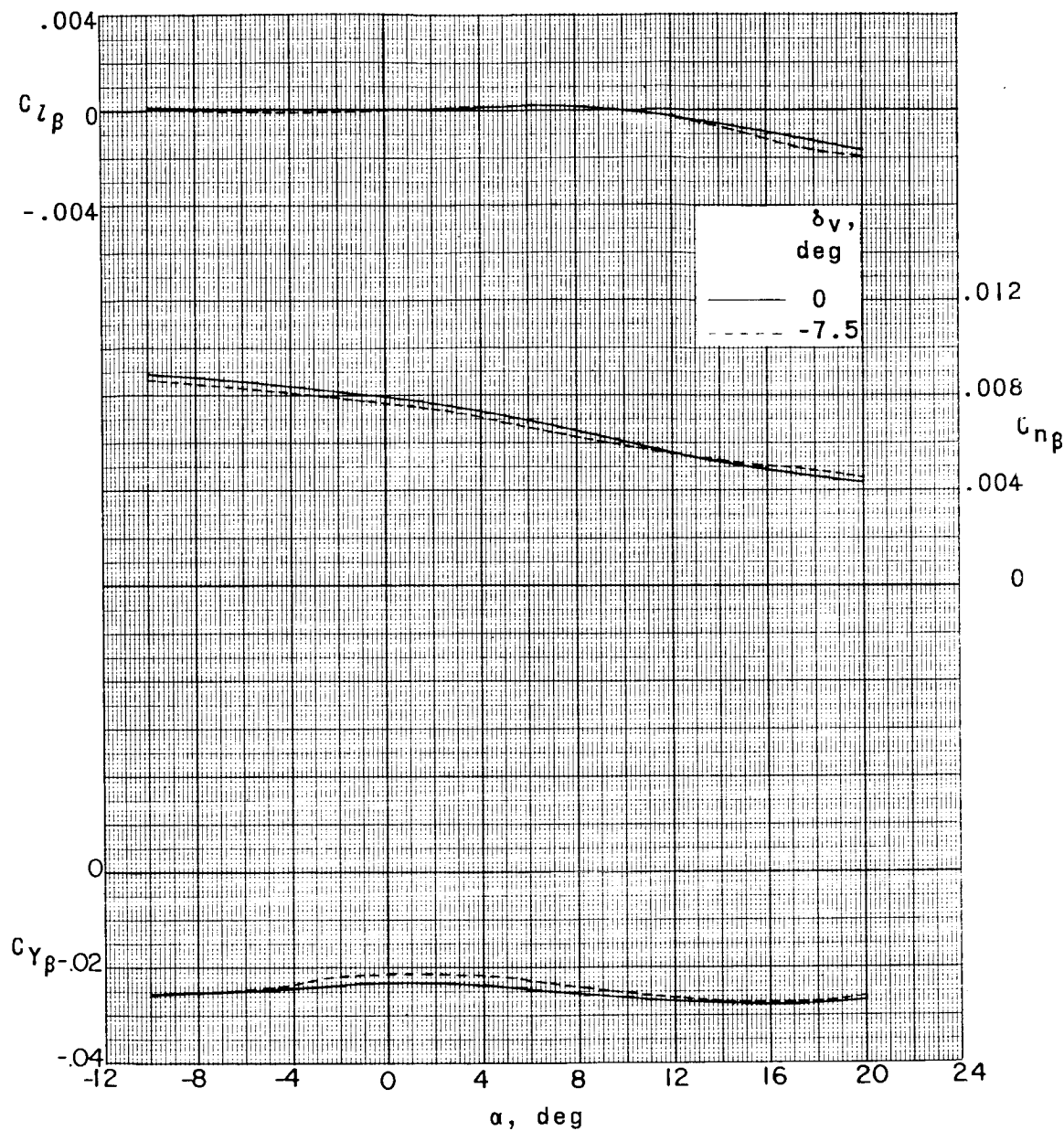
(a) $M = 2.29$.

Figure 44.- Summary of lateral stability characteristics of a 0.067-scale model of the X-15 airplane as affected by deflection of vertical tail with speed brakes retracted.

0000000000000000

REF ID: A65125
DECLASSIFIED

161

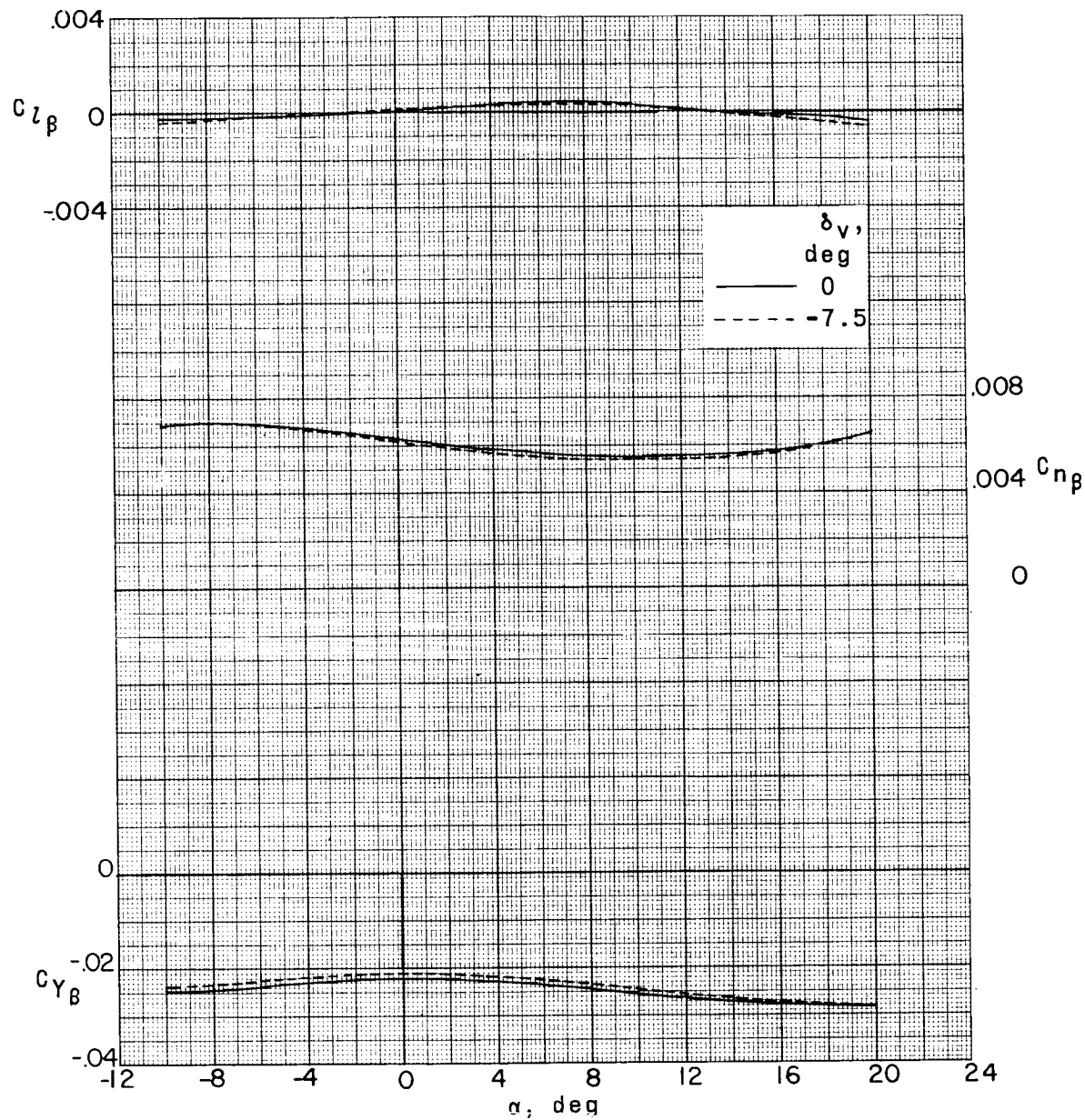
(b) $M = 2.98.$

Figure 44.- Continued.

CONFIDENTIAL

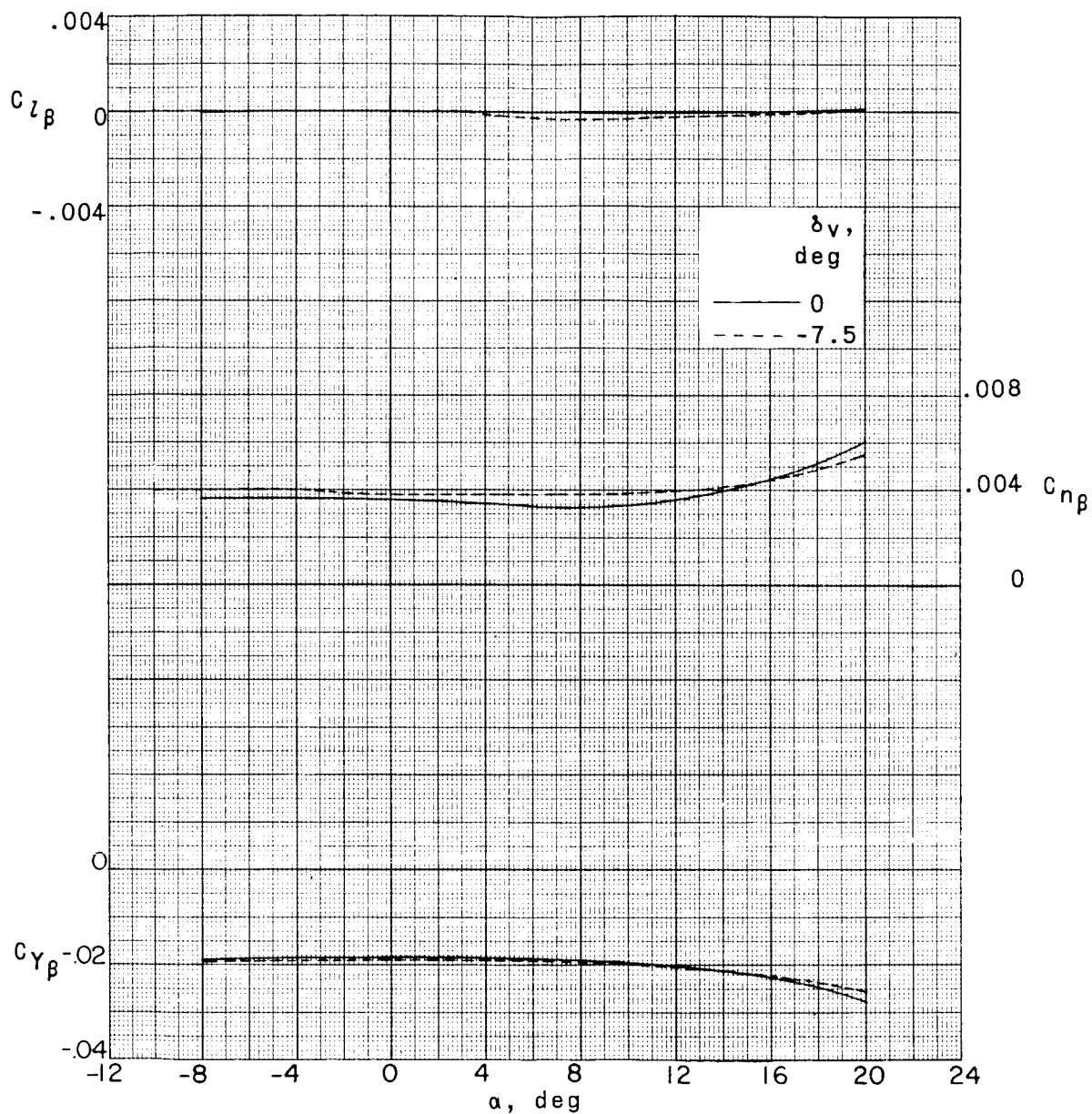
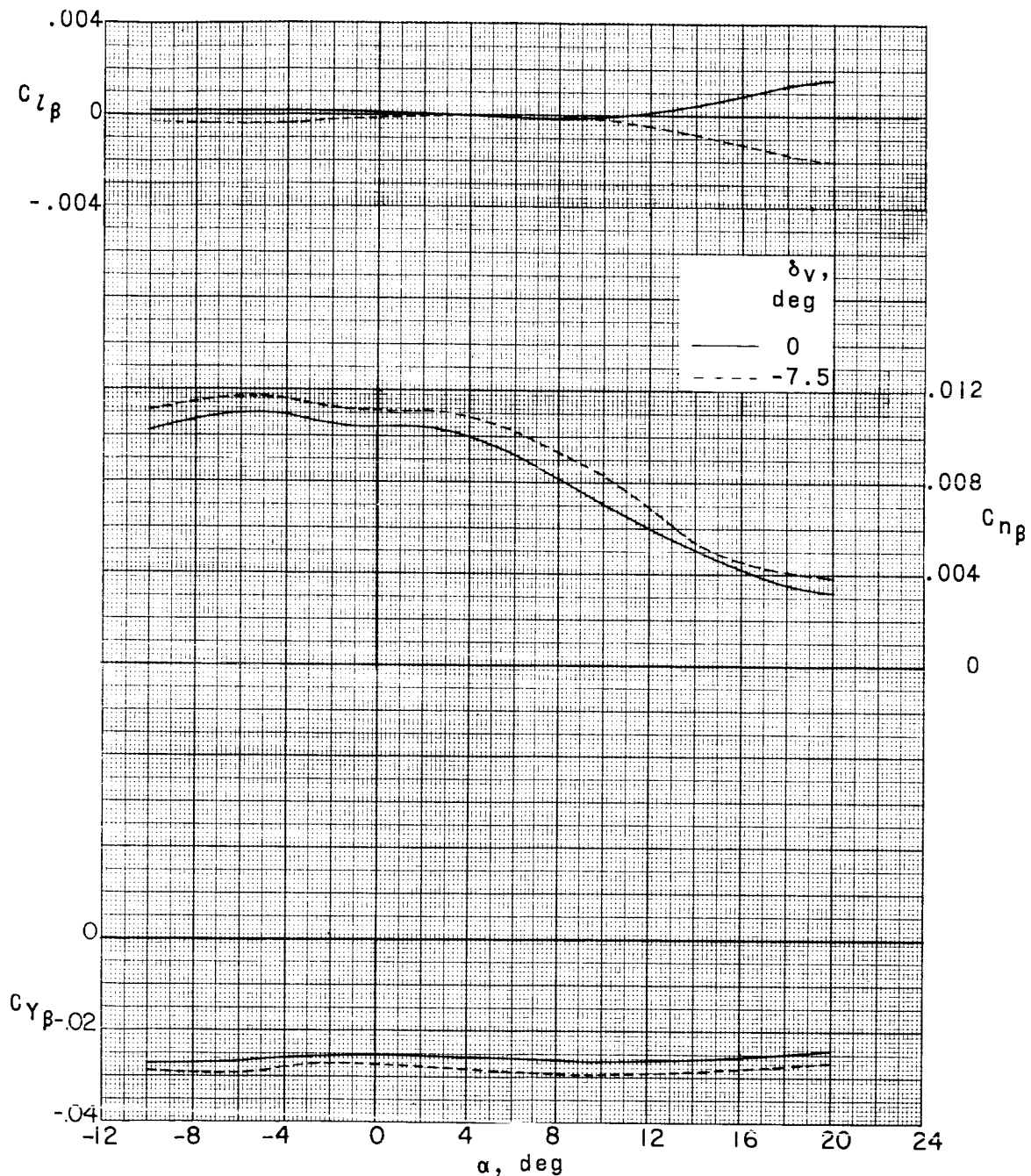
(c) $M = 4.65.$

Figure 44.- Concluded.

DECLASSIFIED

~~CONFIDENTIAL~~

163



(a) $M = 2.29$.

Figure 45.-- Summary of lateral stability characteristics of a 0.067-scale model of the X-15 airplane as affected by deflection of vertical tail with speed brakes open 35° .

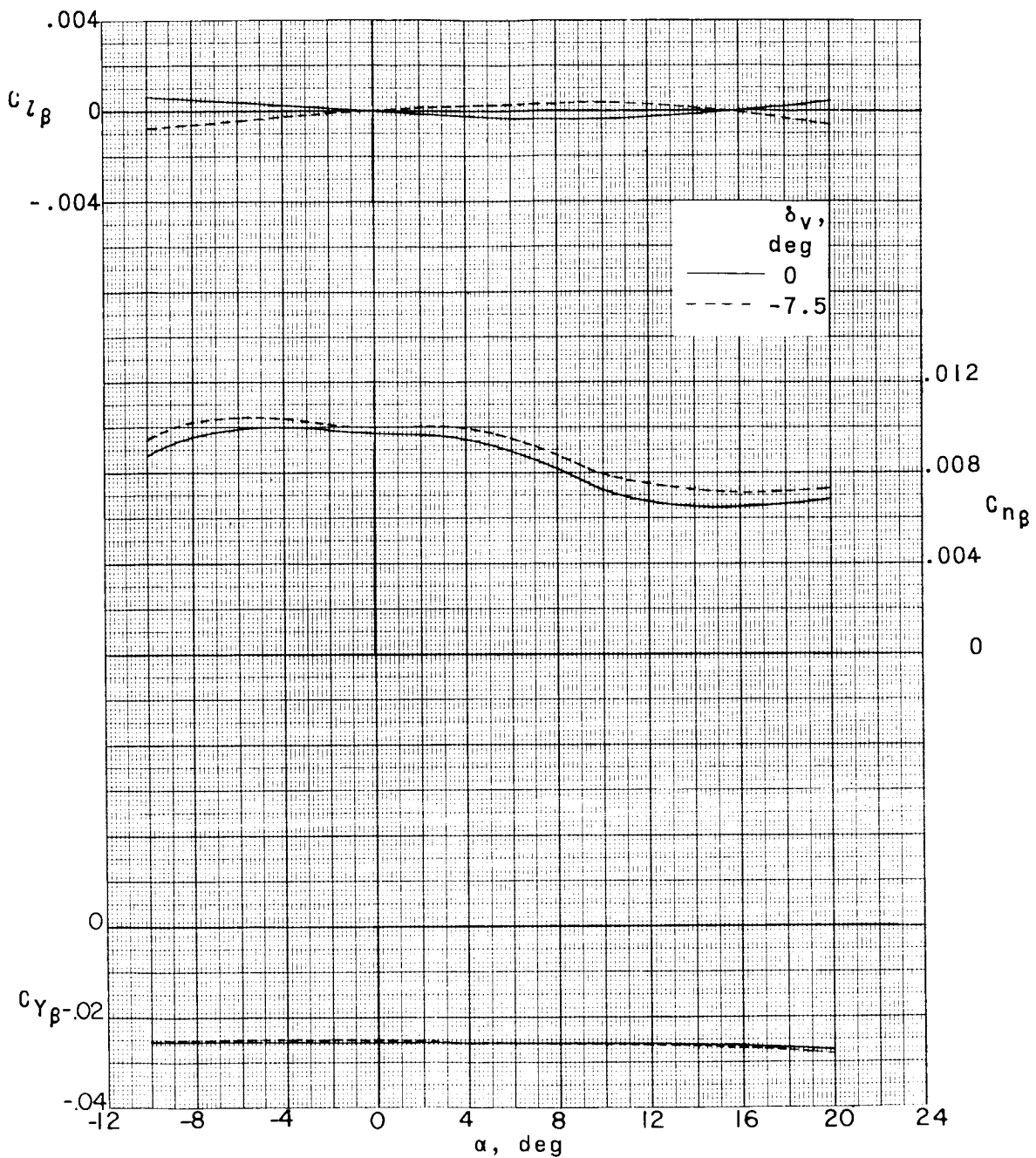
030303060000
CONFIDENTIAL(b) $M = 2.98.$

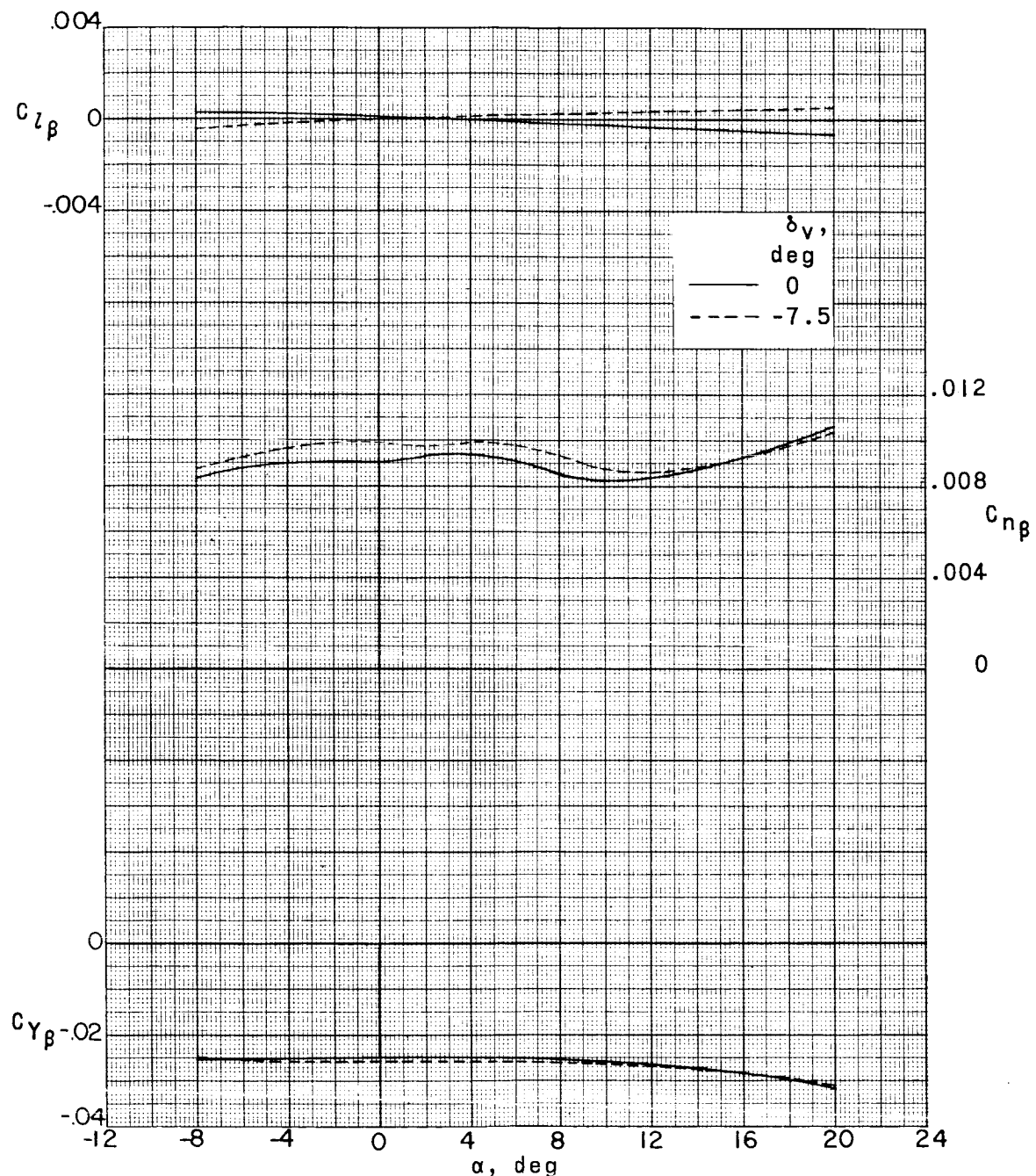
Figure 45.- Continued.

CONFIDENTIAL

DECLASSIFIED

~~CONFIDENTIAL~~

165



(c) $M = 4.65.$

Figure 45.- Concluded.

~~CONFIDENTIAL~~

CONFIDENTIAL

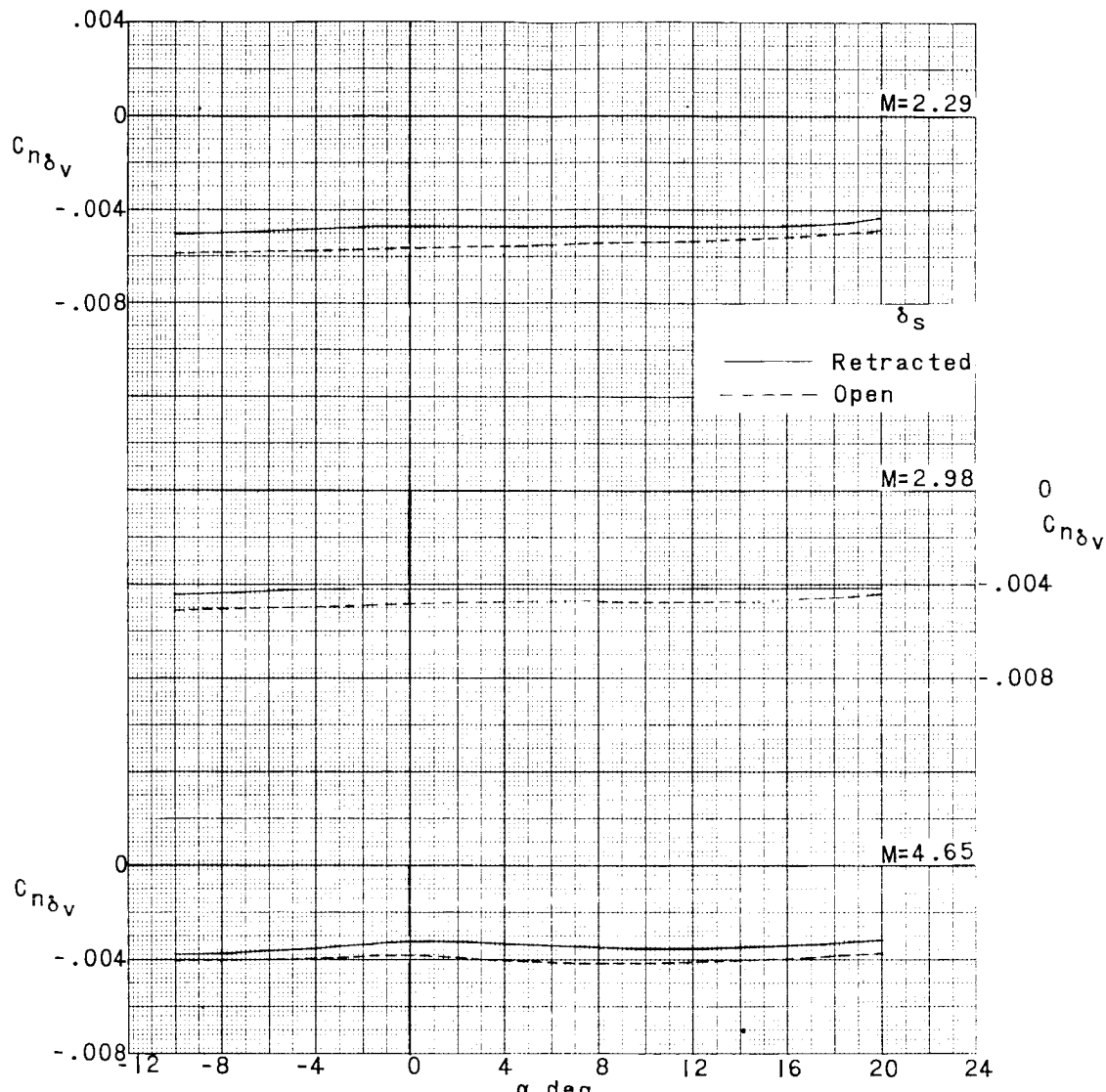
(a) $C_{n\delta_V}$ plotted against α .

Figure 46.- Summary of vertical-tail control characteristics of a 0.067-scale model of the X-15 airplane. $\delta_H = 0^\circ$.

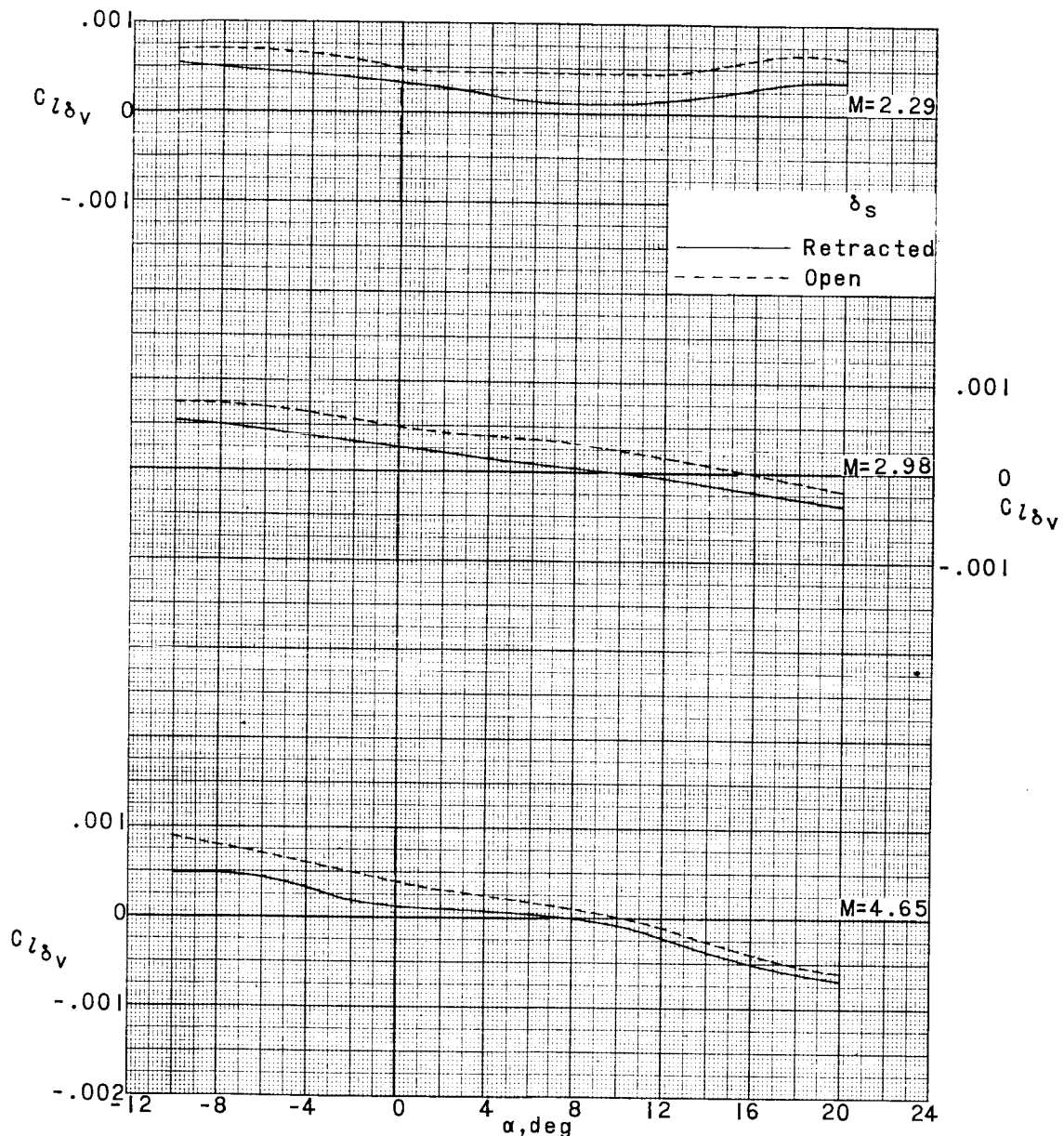
CONFIDENTIAL

L-351

DECLASSIFIED

~~CONFIDENTIAL~~

167



(b) $C_{l\delta_v}$ plotted against α .

Figure 46.- Concluded.

CONFIDENTIAL

168

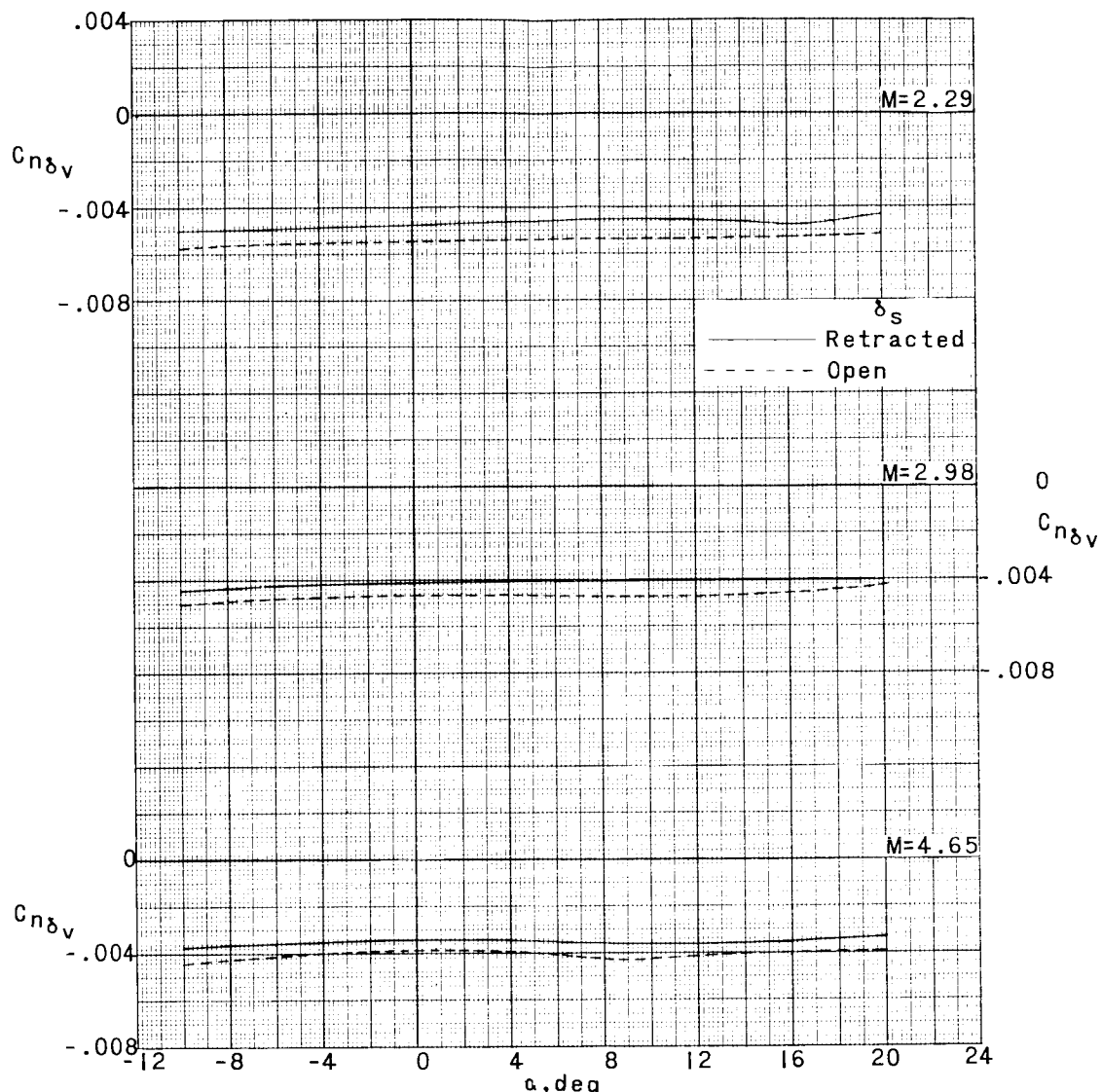
(a) $C_{n\delta_v}$ plotted against α .

Figure 47.- Summary of vertical-tail control characteristics of a 0.067-scale model of the X-15 airplane. $\delta_H = -20^\circ$.

L-351

DECLASSIFIED
CONFIDENTIAL

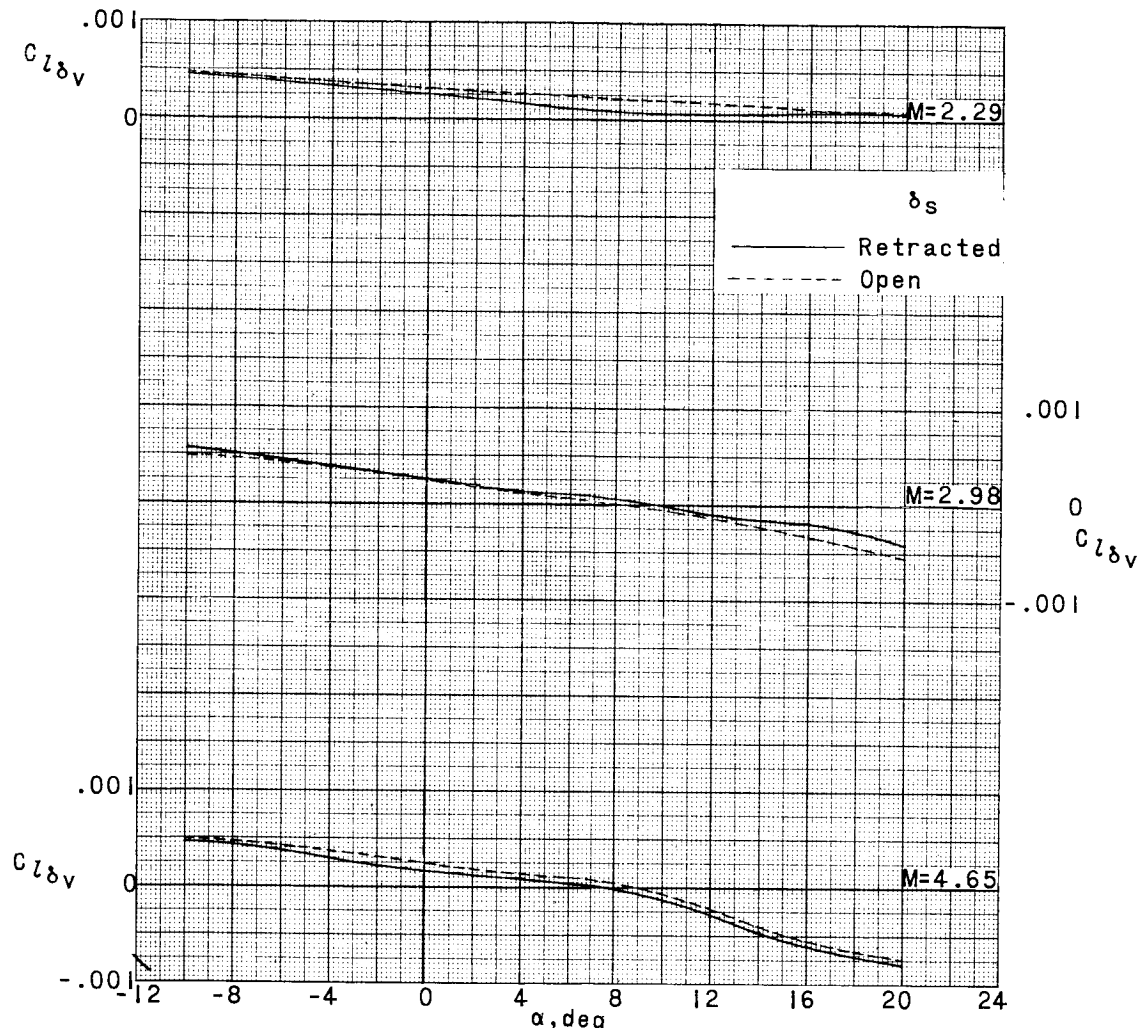
(b) $C_{l_{\delta_V}}$ plotted against α .

Figure 47.- Concluded.